

Characterisation of the protective immune response to Rift Valley fever virus after natural exposure or vaccination with ChAdOx1 RVF

Daniel Wright

Student Number: 1145708

DPhil in Clinical Medicine

Nuffield Department of Medicine

St Cross College

Supervisors:

Prof. George Warimwe

Prof. Thomas Bowden

Word count: Approx. 40,000 excluding figure legends, references and appendix

Abstract

Rift Valley fever virus is a single stranded RNA *Phlebovirus*. Spread by numerous species of mosquito, it is predominantly a disease of livestock including sheep, goats and cattle. Disease is characterised by extremely high mortality in young animals and abortions in pregnant animals, with significant impacts on food security and the wider economy. Spill over into humans results in a wide spectrum of disease from self-limiting febrile illness to haemorrhagic fever and death. RVFV is endemic throughout multiple countries in Africa. Current livestock vaccines have significant drawbacks and due to a lack of licenced human vaccines or therapeutics, RVF is considered a priority pathogen for the development of countermeasures by the WHO and OIE. A safe, effective and cheap vaccine that protects livestock and humans against RVF disease would be invaluable.

This thesis seeks to advance this goal on several fronts by facilitating the development of a leading RVF vaccine candidate, ChAdOx1 RVF, co-developed for use in livestock and humans. Firstly, I provide much needed data on the naturally acquired, and likely protective, immune response towards RVFV in Kenyan adults. Showing long-lasting antibodies target both glycoproteins, Gn and Gc, with the former as the principle target of the long-lived neutralising antibody response. I then analysed the factors influencing successful manufacture of ChAdOx1 RVF which has allowed the vaccine to be produced for critical livestock and human trials, improving our understanding of construct design, genetic- and thermo- stability of this vector. I show that neutralising antibodies, strongly associated with protection, were induced in the first humans vaccinated with ChAdOx1 RVF. Characterisation of the cellular and humoral response in livestock then provides important context for the vaccine's proven ability to elicit protective immunity in multiple target species.

Finally, I explore the possibility of improving the utility of the RVF vaccine in livestock by creating a bivalent vaccine which targets an additional disease, Peste-des-petits ruminants. The extremely high efficacy of ChAdOx1 RVF in livestock, including during pregnancy, and the induction of neutralising antibodies in humans is extremely encouraging. ChAdOx1 RVF has the potential to become a vital countermeasure against RVF outbreaks, significantly improving animal and public health from a disease with pandemic potential.

Acknowledgments

I've genuinely loved doing this DPhil at the Jenner Institute, KEMRI-Wellcome and STRUBI. Firstly, I'm incredibly grateful for the support and expertise of both my supervisors, George Warimwe and Thomas Bowden. I'm indebted to George for initially giving me the opportunity to do a DPhil in his group and for opening my eyes to Rift Valley fever and livestock immunology. I've learned a lot under your supervision. Not only have you been extremely supportive throughout, giving me many opportunities to present some of our work and allow me to improve as a scientist, but also out of the lab, introducing me to Kilifi football and Coastal Kenyan life! And to Thomas for the guidance, advice and feedback throughout my DPhil. Your patience and expertise were invaluable.

I have been extremely fortunate to have worked with so many fantastic colleagues, past and present: Madeleine, John, Henry, James, Doris, Don, Liz, Adam W, Pawan, Sean, Jonathan, Dan, Duncan, Andres, Marta, Marco, Rebecca, Federica, Lisa, Sandra, Sarah, Rachel, Martino, Indra, Guido, Ruben, Rob, Rhys and Adam T among many others. Particularly for all the tennis, squash, rounders, running, cycling, football, coffee trains and Friday BBC quizzes that have made my DPhil so enjoyable. Also, huge thanks to other senior members at the Jenner that have generously shared their knowledge: Alex Spencer, Edd Wee, Sue Morris, Nick Edwards, Tess Lamb, Katie Ewer, Simon Draper and Sarah Gilbert. And to Julie Furze and Mariya Mykhaylyk for keeping the Jenner labs running so efficiently.

I owe a huge amount to my parents for their unwavering support for just about anything I have done. If I'm anywhere near the parent to Louis that you've been to me I'll be doing well. And Cindy, to whom I owe so much. I probably wouldn't even be in academia if it wasn't for your encouragement and support (and job finding skills!). While pandemics are no fun, lockdown with

you has been pretty great. And finally to baby Louis who, to be honest, hasn't helped much with the DPhil but his arrival has been better than I ever imagined.

Table of Contents

Abstract i

List of Figures viii

List of Abbreviations x

1 Introduction 1

1.1 Discovery and Historical Background 2

1.2 Epidemiology 3

1.2.1 Transmission 3

1.2.2 Disease burden and impact 6

1.2.3 Risk factors 8

1.3 Disease manifestations 9

1.3.1 Humans 9

1.3.2 Animals 10

1.4 Virology 12

1.4.1 Structure and host cell entry 12

1.5 Phylogeny 15

1.6 Immunology 16

1.6.1 Naturally acquired immunity 16

1.6.2 Vaccine-induced immunity 18

1.6.3 Immune epitopes 19

1.7 Disease control and treatment 21

1.7.1 Diagnosis 21

1.7.2 Treatment 21

1.8 Vaccines 22

1.9 Thesis Aims: 27

2 Materials and Methods 28

2.1 Molecular Biology 29

2.1.1 Mammalian cell expression of RVFV Gn-Avi 29

2.1.2 Mammalian cell expression of RVFV Gc-Sumo 30

2.1.3 Mouse monoclonal antibody production (4D4 and 5E2) 30

2.1.4 Nanobody expression 31

2.1.5 Nanobody purification 32

2.1.6 SDS-PAGE 32

2.1.7 Western blots 33
2.2 Vaccine construct production 33
2.2.1 ChAdOx1 RVF vaccine production 33
2.2.2 ChAdOx1 RVF-PPR bivalent production 38
2.2.3 ChAdOx1 PPR monovalent production 41
2.2.4 QC of vaccine constructs' genetic sequence 43
2.2.5 QC of vaccine construct antigen expression 44
2.2.6 Genetic stability testing 46
2.3 Serology 46
2.3.1 Human total IgG enzyme-linked immunosorbent assays (ELISAs) 46
2.3.2 Human total IgG avidity ELISAs 47
2.3.3 Human IgG subclass ELISAs 48
2.3.4 Livestock total IgG ELISA 48
2.3.5 Mouse total IgG ELISA 48
2.3.6 RVFV neutralisation assays 49
2.3.7 Gn- and Gc-specific antibody depletion 52
2.4 Mouse vaccinations 52
2.5 Naturally exposed Kenyan adults study population [chapter 3] 53
2.6 RVF001 Clinical trial [chapter 5] 54
2.6.1 Vaccination 54
2.6.2 Ethics and regulatory approval 54
2.6.3 Serum collection 54
2.6.4 PBMC separation and freezing 55
2.7 Ex vivo ELISpots 55
2.7.1 Naturally exposed human PBMC [chapter 3] 55
2.7.2 Human ChAdOx1 RVF clinical trial PBMC [chapter 5] 56
2.7.3 Livestock PBMC 57
2.8 Statistical analysis 57
3 Characterisation of naturally acquired immunity to RVFV among Kenyan adults 58
3.1 Introduction: 59
3.2 Objectives: 59
3.3 Results: 60
3.3.1 Production of RVFV Gn and Gc recombinant proteins 60
3.3.2 Do IgG responses against Gn and Gc correlate with RVFV nAb titres? 62

3.3.3 What is the relative contribution of antibodies targeting Gn and Gc to the RVFV nAb response? 64
3.3.4 What are the long-term kinetics of IgG and RVFV nAb titres after historical infection? 68
3.3.5 Is there a detectable cellular response to RVFV Gn and Gc after historical RVFV infection? 71
3.4 Discussion: 73
4 Determining factors that underlie successful manufacture of ChAdOx1 RVF vaccine 78
4.1 Introduction: 79
4.2 Objectives: 83
4.3 Results: 83
4.3.1 Determining the immunogenicity of mixed batch vs clonal vaccine 83
4.3.2 Resynthesis of ChAdOx1 RVF 84
4.3.3 Determining the factors that contribute to genetic stability of ChAdOx1 RVF production 86
4.3.4 Assessing the thermostability of ChAdOx1 RVF in X48A liquid formulation or lyophilised 92
4.4 Discussion: 95
5 Immunogenicity of ChAdOx1 RVF among adults in Oxford 100
5.1 Introduction: 101
5.2 Objectives: 103
5.3 Results: 103
5.3.1 Neutralising antibody response elicited after vaccination with ChAdOx1 RVF 103
5.3.2 IgG response targeting Gn and Gc elicited after vaccination with ChAdOx1 RVF 104
5.3.3 IFNγ ELISpot response after vaccination with ChAdOx1 RVF 106
5.4 Discussion: 108
6 Immunogenicity of ChAdOx1 RVF in livestock 113
6.1 Introduction: 114
6.2 Objectives: 116
6.3 Results: 116
6.3.1 IgG responses in livestock towards both Gn and Gc after vaccination with ChAdOx1 RVF or Smithburn 116
6.3.2 Harmonizing neutralisation assays using new live-attenuated RVFV strain 120
6.3.3 Investigating the immunogenicity of reduced dosing schedules of ChAdOx1 RVF in cattle and sheep. 121

6.3.4 Comparison of immunogenicity from livestock efficacy trials with immunogenicity from the dose de-escalation study 123
6.3.5 ELISpot optimisation 124
6.3.6 Cellular immunity in pregnant sheep and goats 126
6.3.7 Expression of nanobodies from a vaccinated llama 130
6.3.8 Assessment of the nanobodies ability to bind Gn and Gc and neutralise RVFV in vitro 131
6.4 Discussion: 134
7 Production of monovalent and bivalent vaccines to target an additional livestock disease 141
7.1 Introduction: 142
7.2 Objectives: 144
7.3 Results: 144
7.3.1 Cloning of monovalent ChAdOx1 PPR and bivalent ChAdOx1 RVF-PPR 144
7.3.2 Confirmation of antigen expression 151
7.4 Discussion: 154
8 Contributions to the pandemic response 158
9 Concluding remarks and future work 160
References 173
Appendix 185

List of Figures

Figure 1. RVFV cycle. 4
Figure 2. Schematic of the RVFV genome 13
Figure 3. Schematic surface representation of the pentameric assembly of envelope-displayed RVFV Gn-Gc 14
Figure 4. Replication cycle of RVFV. 15
Figure 5. Recombinant protein production of the RVFV Gn and Gc ecto domain. 61
Figure 6. Total IgG titre towards recombinant Gn and Gc correlate strongly with neutralising antibody titre in 50 adults naturally exposed to RVFV 63
Figure 7. Optimisation of depletion conditions.. 65
Figure 8. Neutralising antibody titres predominantly target RVFV Gn over Gc. 66
Figure 9. FRNT titres also correlate with binding IgG titres towards Gn and Gc 67
Figure 10. Replication of antibody depletion experiment 68
Figure 11. Natural exposure to RVFV elicits a high-titre, long-lived humoral response. 70
Figure 12. IgG subclass response remains stable over many years.. 71
Figure 13. A low but significant Ex vivo IFNγ ELISpot response in naturally exposed individuals. .. 72
Figure 14. Schematic of the RVF polyprotein encoded by ChAdOx1 RVF. 80
Figure 15. Schematic of the 'mixed' batch of ChAdOx1 RVF showing the proportion of incorrect viral clones 81
Figure 16. The ChAdOx1 RVF batch containing the mixed population of virus elicits lower immunogenicity than, otherwise identical, clonal vaccine (from preclinical batch). 84
Figure 17. Comparison of the number of instances of identical consecutive bases between the two versions of ChAdOx1 RVF.. 85
Figure 18. Western blot showing greater expression of Gn and Gc after infection of HeLa cells with resynthesized compared to the mixed batch of ChAdOx1 RVF. 86
Figure 19. Experimental plan to investigate genetic stability. 88
Figure 20. Next-generation sequencing results show manufacture using HEK293 cells results in low read coverage and significant errors. 90
Figure 21. Gel electrophoresis using flank to flank PCR product after each passage in HEK293 cells. 91
Figure 22. ChAdOx1 RVF in X48A liquid formulation remains stable when stored at 4°C or -80°C. 93
Figure 23. Comparison between ChAdOx1 RVF in X48A liquid formulation and lyophilised after 12 and 16 months storage at various temperatures. 94
Figure 24. RVF001 Trial design. 102
Figure 25. Neutralising antibody titres in volunteers vaccinated with ChAdOx1 RVF or after naturally acquired infection.. 104
Figure 26. Binding IgG titres towards RVFV Gn and Gc over time in volunteers vaccinated with ChAdOx1 RVF or after naturally acquired infection. 105
Figure 27. IFNγ ELISpot response after PBMC stimulation of an overlapping peptide library covering the GnGc polyprotein 106
Figure 28. Further breakdown of IFNγ ELISpot response 107
Figure 29. nAb titres correlate with binding IgG titres but not IFNγ response 108

Figure 30. Timecourse of total IgG titres, as measured by standardised ELISA, towards Gn (top) or Gc (bottom), in livestock vaccinated with ChAdOx1 RVF, Smithburn or PBS 117
Figure 31. D28 post-vaccine comparison of anti-Gn (left) and anti-Gc (right) IgG titres 28 days after vaccination with ChAdOx1 RVF or Smithburn. 117
Figure 32. Correlations between neutralisation titre, as measured by VNT assay, and total IgG titre towards Gn (top row) and Gc (bottom row), as measured by ELISA at D28 post-vaccine. 119
Figure 33. Correlations between neutralisation titre, as measured by VNT assay, and IgG avidity towards Gn (top row) and Gc (bottom row), as measured by ELISA at D28 post-vaccine. 119
Figure 34. VNT_{80} is consistent with previous assays 120
Figure 35. Humoral response in sheep after vaccination with different doses of ChAdOx1 RVF.. 122
Figure 36. Humoral response in cattle after vaccination with different doses of ChAdOx1 RVF.. 123
Figure 37. Comparison of neutralisation titres between the dose-escalation trial (D, Table 1) and the challenge trial (B, Table 1) 124
Figure 38. Initial test of cattle PBMC by RVF ELISpot..... 125
Figure 39. ELISpot peptide concentration titration using sheep PBMC pre- and post-ChAdOx1 RVF vaccination. 126
Figure 40. IFNγ ELISpot response in pregnant goats and sheep. 127
Figure 41. IFNγ ELISpot response in pregnant goats..... 128
Figure 42. IFNγ ELISpot response in pregnant sheep..... 129
Figure 43. Correlation between IFNγ response and VNT_{50} in pregnant goats. 130
Figure 44. SDS-PAGE of recombinant nanobodies expressed in E. coli. 131
Figure 45. Optical density (OD) at 405 nm measured by Gn or Gc ELISA for 13 nanobodies..... 132
Figure 46. Viral neutralising titres of 13 nanobodies isolated from a vaccinated llama. 134
Figure 47. Cloning of the bivalent ChAdOx1 RVF-PPR and the monovalent ChAdOx1 PPR vaccine constructs 146
Figure 48. NGS read coverage and error rate of ChAdOx1 RVF-PPR bivalent and ChAdOx1 PPR monovalent BAC plasmids prior to linearisation and virus bulk-up..... 148
Figure 49. NGS read coverage and error rate of ChAdOx1 RVF-PPR bivalent and ChAdOx1 PPR monovalent vaccines after virus rescue..... 150
Figure 50. Western blot on cell lysate from HeLa cells infected with ChAdOx1 RVF, ChAdOx1 RVF-PPR or ChAdOx1 PPR.. 151
Figure 51. Immunofluorescent staining of RVFV Gn and PPRV H in the various constructs.. 152
Figure 52. Test of C77's ability to detect PPRV H by ELISA. 153

List of tables

Table 1. Summary of ChAdOx1 RVF livestock trials. 25
Table 2. Nanobody binding affinity and neutralisation characteristics 133

List of Abbreviations

5E2	Mouse mAb targeting RVFV Gc
4D4	Mouse mAb targeting RVFV Gn
Ad5	Human adenovirus serotype 5
ADCC	Antibody-dependent cellular cytotoxicity.
ALP	Alkaline phosphatase
ALT	Alanine transaminase
AMP	Ampicillin
AST	Aspartate transaminase
AU	Arbitrary Units
AUC	Area under the curve
BAC	Bacterial artificial chromosome
BSA	Bovine serum albumin
C77	Mouse mAb targeting PPRV H
CBPP	Contagious caprine pleuropneumonia
CD3	Cluster of differentiation 3
CDR H3	Third heavy-chain complementarity-determining-region
CDC	Complement-dependent cytotoxicity
CEPI	Coalition of Epidemic Preparedness
ChAdOx1	Chimpanzee Adenovirus Oxford 1
ChAdOx1 nCoV-19	ChAdOx1 novel Coronavirus 2019 vaccine (Oxford/AZ)
CI	Confidence interval
CMP	Chloramphenicol
CMV	Cytomegalovirus
Covid-19	Coronavirus disease 2019
CPE	Cytopathic effect
D0/D2/D5/D10	DMEM + 0%/2%/5%/10% FCS (+1% L-glutamine, 1% penicillin/streptomycin)
DAPI	Diamidino-2-phenylindole
DIVA	Distinguish Infected from Vaccinated Animals
DMEM	Dulbecco's Modified Eagle Medium
DMSO	Dimethyl sulfoxide
DPBS	Dulbecco's Phosphate Buffered Saline
DTT	Dithiothreitol
ECF	East Coast fever
F	Fusion protein (PPRV)
FCS	Foetal Calf Serum
FDA	Food and Drug Administration (US)
FITC	Fluorescein isothiocyanate
FMD	Foot and Mouth Disease
FRNT	Focus reduction neutralisation titre
GMP	Good Manufacturing Practice
GMT	Geometric mean titre
H	Hemagglutinin protein (PPRV)
HEK293	Human embryonic Kidney 293 cells

HIV	Human immunodeficiency Virus
HRP	Horseradish Peroxidase
IEP	Interepidemic periods
IFNγ	Interferon gamma
Ig	Immunoglobulin
IL-10	Interleukin 10
IMAC	Immobilized metal affinity chromatography
IPTG	Isopropyl ß-D-1-thiogalactopyranoside
IU	Infectious Units
KAN	Kanamycin
KHDSS	Kilifi Health and Demographic Surveillance System
LLD	Lower limit of detection
LMIC	Lower and middle income country
mAb	Monoclonal antibody
MERS	Middle Eastern Respiratory Syndrome
MHC	Major Histocompatibility Complex
MOI	Molarity of Infection
MP-12	live-attenuated strain of RVFV
MVA	Modified vaccinia virus Ankara
N	RVFV nucleoprotein
nAb	Neutralising antibody
NaSCN	Sodium thiocyanate
NGS	Next generation Sequencing
NP	SARS-Cov-2 nucleoprotein
NSs	Non-structural protein on the S (short) segment of RVFV
OD	Optical density
P0/P5/P10	Passage 0/5/10
PBMC	Peripheral blood mononuclear cells
PBS/T	Phosphate buffered Saline + 0.05% Tween20
PCR	Polymerase Chain Reaction
PEI	Polyethylonamine
PKR	Protein Kinase R
PPR	Peste-des-petits ruminants
PPRV	Peste-des-petits ruminants virus
QC	Quality Control
R0/R10	RPMI + 0%/10% FCS
RBD	Receptor binding domain (of SARS-CoV-2)
RPM	Revolutions per minute
RPMI	Roswell Park Memorial Institute 1640 media
RPV	Rinderpest Virus
RT	Room temperature
RVF	Rift Valley fever
RVFV	Rift Valley fever virus
RVFV-4s-eGFP	RVFV 4-segmented green fluorescent protein (live-attenuated strain)
saRNA	Self-amplifying RNA
SARS-CoV-2	Severe Acute Respiratory Syndrome Coronavirus 2

SEB	Staphylococcal Enterotoxin B
SEC	Size Exclusion Chromatography
SEM	Standard Error of the Mean
SFC	Spot forming cells
SFTSV	Severe fever with thrombocytopenia syndrome virus
SFV	Sandfly fever virus
TE Buffer	Tris EDTA buffer
TES	Tris, EDTA, Sucrose buffer
TES/4	TES buffer diluted 1:4 in H_2O
TNFα	Tumour Necrosis Factor alpha
tPA	Tissue Plasminogen Activator
TPP	Target Product Profile
T-REx	HEK293-based tetracycline repressor cell line
VHH	Single variable domain of heavy chain
VNT	Virus Neutralisation Titre
VP	Viral Particle
VTLB	Vegitone Lysogeny broth
VVCF	Viral Vector Core Facility
WHO	World Health Organisation
α	anti-

1

Introduction

This chapter is based on the published paper: **Wright, D**., Kortekaas, J., Bowden, T. A, Warimwe, G. M. Rift Valley fever: biology and epidemiology. J Gen Virol, 2019. 100(8): p. 1187-1199. All text and figures included in this chapter were originally written/made by myself. Permission to include all parts from the published paper were obtained from authors.

1.1 Discovery and Historical Background

Rift Valley fever virus (RVFV) was discovered by Daubney et al. in 1930 near Lake Naivasha in the Kenyan Rift Valley after an unexpected increase in lamb mortality [1]. Inoculation of blood from sick animals into healthy animals was shown to be able to induce disease [2]. Attempts to limit the outbreak led to moving affected livestock herds to greater altitude or using mosquito nets. After 5-6 days, new infections abated and mosquitos as vectors were suspected [2, 3]. This was later confirmed when virus was isolated from several naturally infected species of Aedes and Culex mosquitos [4, 5].

After investigation, almost all the herders during the first outbreaks spoke of experiencing fever and severe pains [1]. Anecdotal evidence of a potential human RVFV infection in a farm manager was credited with clearing his recurrent malaria relapses [1]. By this time hundreds of human cases were thought to have occurred in various outbreaks with no reports of mortality. Risk of death from infection was therefore considered low and human susceptibility was confirmed by transfusing filtered blood from an infected lamb into another malaria patient [1]. Unfortunately, in addition to contracting RVF, the patient went on to have their worst malarial relapse to date. In subsequent years, many more animal infection studies were carried out, improving our understanding of the clinical signs and symptoms in a wide range of animal species [2, 6-9]. Much of our early understanding of human disease came from reports of accidental infections in laboratory workers [8, 10, 11]. Symptoms including general malaise, severe headache, fever and aches were common, in addition to seroconversion in the absence of symptoms [10, 11]. One case proved fatal after experiencing thrombophlebitis [12].

1.2 Epidemiology

1.2.1 Transmission

Since its discovery in Kenya numerous outbreaks affecting goats, sheep, cattle, camels and humans have occurred in Africa causing significant suffering [13]. Our understanding of the epidemiology of RVFV, particularly with regards to how it is maintained during inter-epizootic/epidemic periods (IEPs), is incomplete. A single species of Aedes mosquito, later identified as *Aedes mcintoshi*, has shown the ability to pass the virus to their progeny. It is possible, therefore, that virus may remain viable in mosquito eggs during the dry season before hatching once the rains return [14, 15]. Whether this is the only species capable of vertical transmission and the extent it allows RVFV to circulate during IEPs requires further investigation. The virus may also be maintained at a low level in a sylvatic cycle as mosquitoes can transmit RVFV to wild ungulates. Indeed, neutralising antibodies against RVFV have been detected in a diverse range of species, such as African buffalo, giraffe, black rhino, impala and African elephants among many others [16, 17]. Some of these species, such as buffalo and giraffe are susceptible to RVF disease [18], while others such as elephants appear not to be. There is, however, no evidence to suggest these animals develop sufficiently high viraemia to allow transmission to mosquitoes. While low-level viral maintenance in sylvatic cycles during IEPs is plausible, it is likely that only ruminants (e.g. sheep, cattle, goats) and pseudoruminants (e.g. camels) function as amplifying hosts (**Figure 1**).

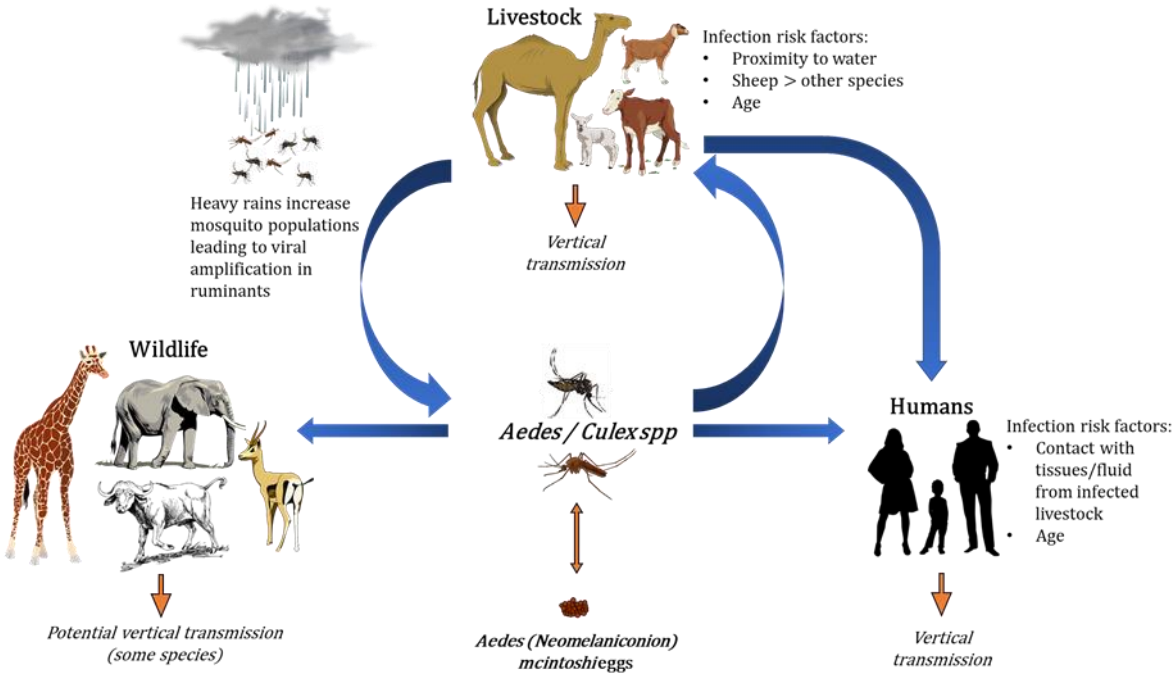


***Figure 1**. RVFV cycle. Between epizootics/epidemics RVFV may be maintained through transovarial transmission in Aedes (Neomelaniconion) mcintoshi eggs. Wild ungulates and livestock can also harbour low-level infection. During heavy rains, a surge in mosquito populations leads to increased infection of livestock and viral amplification between numerous vector species and ruminants occurs. As more livestock become infected, the chances of spill over into humans increases. Human infection can occur via mosquito bite, or more commonly, via contact with infected animal tissue and fluid. From [19]*

During periods of exceptionally heavy rains, subsequent flooding results in large increases in mosquito populations which can lead to RVF epizootics, with large numbers of livestock becoming infected. Significant heavy rains and flooding in East Africa can occur following the arrival of the El Niño/Southern Oscillation (ENSO) climate phenomenon [20]. Because of this correlative link between RVFV infection and weather, rainfall data and changes in vegetation have been used to predict RVF outbreaks [21]. However, integrating climate data with accurate local data on animal and human populations and their movements, where surveillance is often suboptimal leads to variability in the predictive value of these models [21, 22]. Syndromic surveillance of livestock herds during periods when conditions appear to be favourable for RVF outbreaks have also been used as

an early warning system in Kenya [23]. These systems may lead to better awareness of RVF among farmers and uptake of interventions to control disease [23].

Numerous mosquito species are capable of transmitting RVFV [15]. Other arthropods, such as midges, ticks and sandflies can become infected with the virus and could potentially act as mechanical vectors [15]. A study of mosquitoes trapped during an epizootic found more than 53 species caught in the field were positive for RVFV [24], while more than 65 species are described as potential vectors, the vast majority from *Aedes* and *Culex spp* [25]. The degree to which some of these potential RVFV vectors can successfully transmit virus varies between mosquito species [26]. Unlike animals, most human infections are attributed to contact with infected tissues or fluids, rather than mosquito bite [6, 27]. Larger outbreaks, however, such as the Egyptian outbreak of 1977, are unlikely to have all resulted from direct animal contact. Here, *Culex pipiens* was implicated for the first time [28]. There are documented cases of human infections with no direct link to livestock, which were consequently attributed to mosquito bites [29].

Numerous cases of human transmission during the 1930s-50s occurred by way of accidental laboratory infection [7]. Indeed, much of our early knowledge of the disease in humans came from these case reports. To date, direct human-to-human transmission has not been documented. Even during epidemics in hospital settings with sub-optimal personal protective equipment, there is no evidence of nosocomial transmission [30]. In one case, viral RNA was isolated from urine and semen in an immunosuppressed patient 4 months after initial onset of symptoms [31]. Whether RVFV can be transmitted sexually, however, is unknown. Vertical transmission, from mothers to foetus, has been documented in human cases [32, 33] and ex vivo experiments have demonstrated that RVFV can directly infect human placental tissue [34].

For livestock, direct transfer between animals may be rare or non-existent as evidenced by early experiments demonstrating that viraemic sheep fail to transfer the virus to naïve animals [6]. More recently, sheep with acute RVFV infections that were co-housed with highly susceptible immunocompromised naïve lambs failed to transmit any virus [35]. Vertical transmission occurs in all susceptible livestock species; this has been demonstrated even in pregnant sheep with no detectable viremia [36]. In a rodent model of pregnant rats, vertical transmission occurred in both sick and asymptomatic rats, with pregnant animals being more prone to death than their non-pregnant counterparts [34]. The placenta of these animals was shown to be a major site of viral replication [34]. While outbreaks have so far been confined to Africa and the Arabian Peninsula, a wide range of mosquitoes can transmit RVFV and are also present in vast areas covering Europe, Asia and the Americas [24].

1.2.2 Disease burden and impact

After the discovery of RVFV in the 1930s, outbreaks appeared regularly from the 1950s onwards [13]. This began with large outbreaks in Kenya and South Africa in 1950-51 [17]. In 1974-75, another outbreak in South Africa resulted in the country's first human fatalities; 110 human cases were recorded resulting in 7 deaths [37]. The largest RVF outbreak on record occurred in Egypt from 1977-79 where 598 deaths were documented from an estimated 200,000 human cases [38]. Considerable human cases were reported in Mauritania in 1987, with 220 deaths [39]. In 1997-98, after exceptionally heavy rainfall, a large outbreak in East Africa resulted in 478 deaths from an estimated 89,000 human cases [40].

The first outbreak of RVF outside the African continent occurred in the year 2000, where 880 laboratory-confirmed human cases and 123 deaths were recorded in Saudi Arabia over a six-month period [13, 41]. During this time, an additional 1,328 cases and 166 deaths were recorded in Yemen. Evidence suggests the strain of RVFV that emerged on the Arabian Peninsula originated from the

1997-98 East-African outbreak [42]. More recently in 2008, 747 human cases and 230 deaths were reported in Sudan and since 2016, smaller outbreaks in Niger and East Africa have resulted in numerous human deaths [43]. While the high reported case fatality rates from some of these outbreaks reflects the dangers of severe RVF, by only including laboratory-confirmed cases, they do not account for the likely larger population of people experiencing mild illness who remain undiagnosed.

Estimating total animal losses during outbreaks is difficult as these numbers are generally poorly documented. The first recorded outbreak in Kenya resulted in an estimated 5,000 animal deaths [6], while the much larger outbreaks in Kenya and South Africa in 1950-51 resulted in over 100,000 sheep dying and approximately half a million abortions [17]. Even more were estimated to have died in the South African 1975 outbreak [37]. In Saudi Arabia, the outbreak resulted in widespread livestock deaths and up to 10,000 abortions in cattle, sheep, goats and camels [44]. In the 2006-7 outbreak in Tanzania, livestock mortality was estimated at 50,000 [13].

RVF outbreaks can have dire socio-economic consequences at both local and national levels [45, 46]. In addition to the direct cost of human morbidity and death, livestock deaths and subsequent reduction in production has cost producers millions of dollars. These animal losses can have knock-on effects altering herd dynamics. For example, when significant proportions of young animals are killed, there are fewer to breed the following generation resulting in further, potentially long-term, production losses [45]. In addition to the direct losses of livestock, embargoes are placed on the exportation of livestock during outbreaks which can have crippling impacts on economies heavily dependent on animal trade. In Somalia, for example, livestock exporters lost approximately US$330M between 1998-2003 as a result of the ban on livestock imports, with further losses from producers and the subsequent reduction in tax intake for the government [47]. Overall, losses in Somalia due to the 2006-2007 outbreak have been estimated at US$471M, representing 5% of the

total GDP. The same outbreak caused US$66M losses in Kenya [45]. Saudi Arabia and Yemen suffered economic losses of US$10M and US$107M, respectively. The impact of human cases on household incomes was estimated at US$120 per RVF case in the 2007-08 Kenyan outbreak, a significant sum considering the low average incomes in some of the affected countries [48].

1.2.3 Risk factors

Numerous seroprevalence studies in human populations have been carried out, which shed light on those most at risk of infection [49]. The most significant risk factor is having contact with livestock [50, 51]. Adults are more likely to be seropositive than children, either as a function of their age allowing them more time to come into contact with RVFV, or due to the increased occupational risk [52]. Heavy rainfall often precedes RVF outbreaks, where an increase in vector population may increase transmission potential. While it is not considered the primary cause of human infection, any behavioural factors that increase the frequency of mosquito bites, such as sleeping outdoors in RVFV-endemic areas, may also increase the chance of becoming infected [53].

It is currently poorly understood why some people remain asymptomatic or have only mild symptoms before recovering while others develop more severe disease with lasting problems. There is some evidence that coinfection with other pathogens may increase susceptibility. For example, HIV-1 coinfection was found to increase the likelihood of severe disease and death due to RVF, with case fatality estimated at 75% [54]. This was largely due to encephalitis with all showing signs of neurological illness and fits with the important role CD4+ T cells play in protection against encephalitis in animal models [55]. Higher levels of the anti-inflammatory cytokine IL-10 in acutely ill patients has also been associated with fatal disease [56]. Other studies have shown a role of host genetic factors on susceptibility, identifying an association between SNPs in genes involved in immunological pathways and severe disease [57].

Risk factors for livestock infections are less well understood and often contradictory [49]. For instance, numerous studies have associated either males or females with increased chance of seropositivity [49]. The relationship between animal type (sheep or goats) and risk of infection is also not always clear. While no association was found in certain herds, in others, sheep seemed significantly more at risk [58-60]. Differences in host-genetic factors, environmental factors such as feeding preferences of vectors or differences in animal husbandry may explain why sheep could have a higher chance of infection. Proximity to water has also been identified as a risk factor, most likely linked to the number of mosquitoes present [61]. As with humans, older animals are more likely to be seropositive [49].

1.3 Disease manifestations

1.3.1 Humans

Human infections can result in a wide spectrum of clinical outcomes [38]. While most cases induce a self-limiting febrile illness, an estimated 1-2% of infections result in much more severe disease, often with high mortality rates [26]. Following an incubation period of 2-6 days, clinical symptoms of RVF include fever, headache, backache, vertigo, anorexia and photophobia [62, 63]. The fever may last several days with a convalescent period ranging from a few days to a month. Some patients experience a biphasic febrile illness, where a reduction of symptoms occurs around the 3rd day before recrudescence 1-3 days later [62]. Severe RVF disease can encompass a wide range of manifestations, summarised below.

Hepatitis, jaundice and haemorrhagic disease: As the major site of RVFV replication, the liver becomes damaged which can lead to jaundice and haemorrhagic disease. Elevation of liver enzymes aspartate transaminase (AST) and alanine transaminase (ALT) occurs, with highest levels occurring in fatal cases [56]. Haemoglobin and platelet counts are reduced with clotting time increased. Other manifestations may include thrombosis [63]. Patients with haemorrhagic fever

have a very high fatality rate and usually succumb within a week or two after the onset of symptoms [63, 64].

Ocular disease: Ocular disease is estimated to occur in 2-5% of RVFV infections, while prevalence among those experiencing severe disease can be >10% [65, 66]. It usually develops 1-3 weeks after initial onset of symptoms and most commonly involves macular and paramacular oedema [65-67]. Other symptoms may include photophobia, reduced vision, blind spots, uveitis, retinitis, and retinal haemorrhage [13, 63]. Disease duration varies from being permanent to resolving in a matter of weeks [13].

Encephalitis and neurological disease: In addition to the symptoms of mild disease, severe and lasting problems can occur shortly after initial symptoms subside, including: reduced consciousness, hallucinations, confusion, vertigo, excessive salivation, weakness, paralysis, decerebrate posturing, hemiparesis and pleocytosis [13, 63].

Abortions/Miscarriage: The link between RVFV infection and human abortion is less clear than in ruminants. A study looking into the incidence of abortion during the 1977 outbreak in Egypt found no increase above the normal frequency of abortions [68]. However, a study in 2016 showed for the first time a significantly increased risk of miscarriage after laboratory confirmed RVFV infection during pregnancy [69]. The risk of abortion in humans, however, appears to be lower than that in livestock. Further studies on the mechanisms underlying pregnancy loss due to RVF are warranted.

1.3.2 Animals

RVFV affects a wide range of animals in an age-dependent manner, where young animals are significantly more at risk of disease and death. However, the various species are not equally susceptible to disease [63]. As in human disease, the major site of RVFV replication is the liver and

it is this organ which bears the brunt of disease in all species. Liver lesions generally result in elevated expression of liver enzymes. Animals with severe RVF disease exhibit leukopenia [26] and while tropism is mostly limited to hepatocytes and monocytes, virus is disseminated to other tissues through circulation in blood [70]. Severe disease can also occur suddenly, causing death in the absence of any other signs [71].

Sheep are the most susceptible of livestock species. The incubation period of the disease is 24-36 hours with signs including fever, listlessness, loss of appetite, disinclination to move, abdominal pain and bloody diarrhoea [63]. Post-mortem analysis reveals multi-focal liver necrosis and occasional mild splenomegaly [72]. The breed of sheep can influence the severity of clinical manifestations [72]. Adult sheep mortality after experimental infection is between 20%-30% [7]. Mortality in new-born lambs is much greater at 95-100% [7] and acutely infected pregnant ewes have almost 100% chance of abortion [63].

Goats are also highly susceptible with similar symptoms to sheep. However, the course of disease can be somewhat more variable, with viremia and symptoms inconsistent after infection [7]. Peak viremia in the blood of goats is also significantly lower than in lambs of identical age after experimental infection [7]. Also, unlike lambs, goats do not always experience febrile illness [7]. When disease does occur, the formation of hepatic lesions is followed by necrotic hepatitis. In adults, hepatic lesions are more focal.

Cattle are less susceptible to disease than sheep and goats. RVFV infections in adults are usually asymptomatic but can also manifest as acute disease with mortality between 0-5% [63]. As with the other livestock species, younger animals are more susceptible and calves usually develop acute disease with mortality of approximately 10% [63, 73], although experimental infections have resulted in significantly higher rates [7]. A more recent study has demonstrated that the onset and

duration of fever, in addition to other aspects of disease including viraemia and liver pathology, are less consistent when compared with sheep [73].

There are few examples describing clinical disease in camels suggesting that these pseudoruminants are less susceptible than cattle, with the vast majority experiencing asymptomatic infection. However, acute RVFV infection may still result in severe disease and death. Symptoms can include ocular discharge, haemorrhages and foot lesions [74]. The first human deaths from RVF in an outbreak in Mauritania, in 2010, were associated with contact with an infected dromedary camel [74]. Abortions in pregnant camels during outbreaks have also been documented [74].

1.4 Virology

1.4.1 Structure and host cell entry

RVFV is a negative-sense single-stranded RNA phlebovirus in the phenuviridae family (formally bunyaviridae). The *Phenuviridae* family includes other viruses of biomedical significance (e.g. Severe fever with thrombocytopenia syndrome virus [SFTSV] and Sandfly fever virus [SFV] which encompasses sandfly Naples virus, sandfly Sicilian virus and Toscana virus]). RVFV is comprised of a tripartite, predominantly negative-sense genome consisting of a small (S), medium (M) and large (L) segment [25] (**Figure 2**).

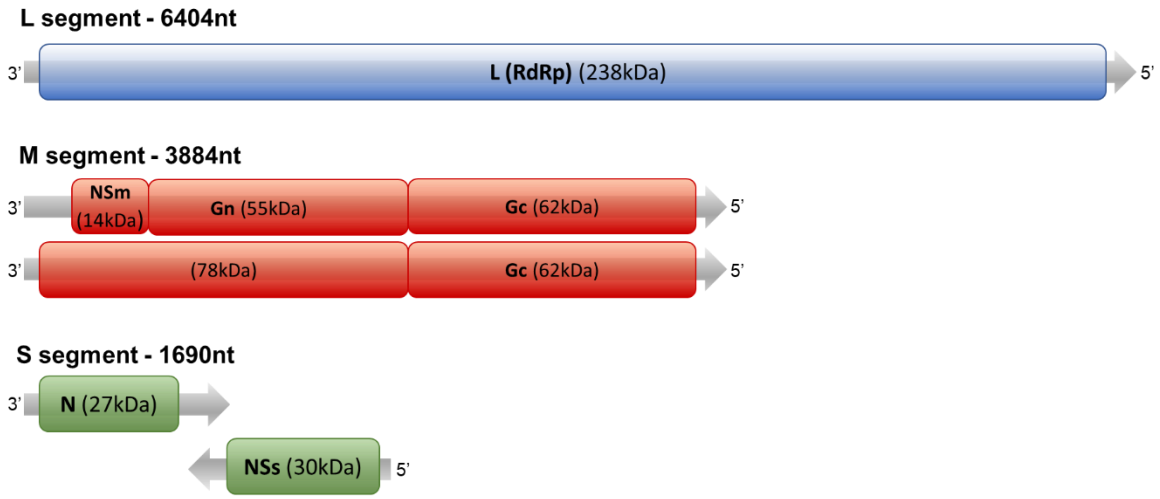


Figure 2. *Schematic of the RVFV genome consisting of three single-stranded RNA segments; small (S), medium (M) and large (L). L segment contains the RNA-dependant RNA polymerase. The M segment encodes the Gn and Gc structural proteins along with a non-structural protein (NSm). Depending on the initiation site, a 78 kDa protein including NSm and Gn can also be expressed. The Gn and Gc polyprotein is then post-translationally cleaved. The ambi-sense S segment encodes the nucleoprotein and a non-structural (NSs) protein, the key virulence factor. From [19]*

The S segment encodes the nucleoprotein (N) and a non-structural protein (NSs) and is the only segment that employs an ambi-sense strategy (**Figure 2**). The L segment encodes the viral polymerase. The M segment encodes another non-structural protein (NSm) and a 78 kDa precursor glycoprotein which is post translationally cleaved into the two glycoproteins, Gn and Gc. Gn and Gc interact to form heterodimers which are then arranged into higher order pentamers and hexamers covering the surface of the mature virion (***Figure* 3**). Both are targets of neutralising antibodies and facilitate host cell entry, Gc is a class II fusion protein responsible for membrane fusion while Gn appears to shield Gc preventing premature fusion [75-78]. The function of the 78 kDa protein is not fully understood but appears to play a structural role in mosquito-cell derived virions but not those expressed in mammalian cells [79, 80].

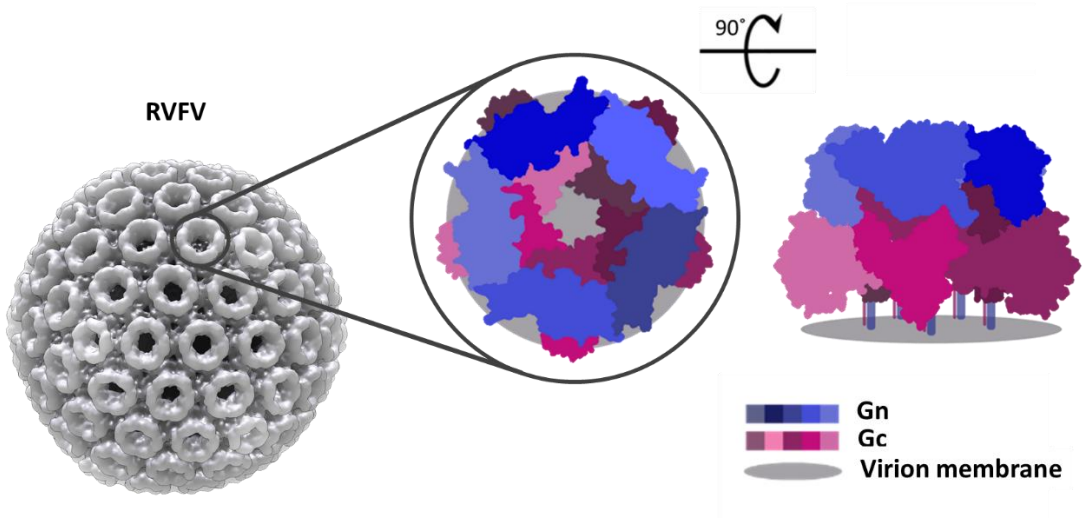


Figure 3. *Schematic surface representation of the pentameric assembly of RVFV Gn-Gc heterodimers based upon integrative cryoEM and X-ray crystallography (PDB ID: 6F9F) [75]. Pentamers and hexamers of Gn-Gc heterodimers encapsulate RVFV with T=12 icosahedral symmetry. Each membrane-distally located RVFV Gn is rendered in a shade of blue and each membrane-proximally located RVFV Gc is rendered in a shade of purple. The C-terminal regions of RVFV Gn and Gc are shown as lines due to the lack of high resolution structural information and are anchored to the virion membrane (grey). Figure adapted from [81], with Gn/Gc schematic originally adapted from Ruben Hulswit with permission.*

RVFV can gain entry into cells via interaction with C-type lectins, DC-SIGN and L-SIGN [82-84]. DC-SIGN is highly expressed on dermal dendritic cells where RVFV can replicate productively [82] Heparan sulfate proteoglycans have also been identified as an important host-cell attachment factor [85, 86]. Recently, the ubiquitous and highly conserved low-density lipoprotein receptor-related protein 1 (LRP1) was identified as an essential host factor for RVFV infection [87]. The replication cycle of RVFV is illustrated below (**Figure 4**).

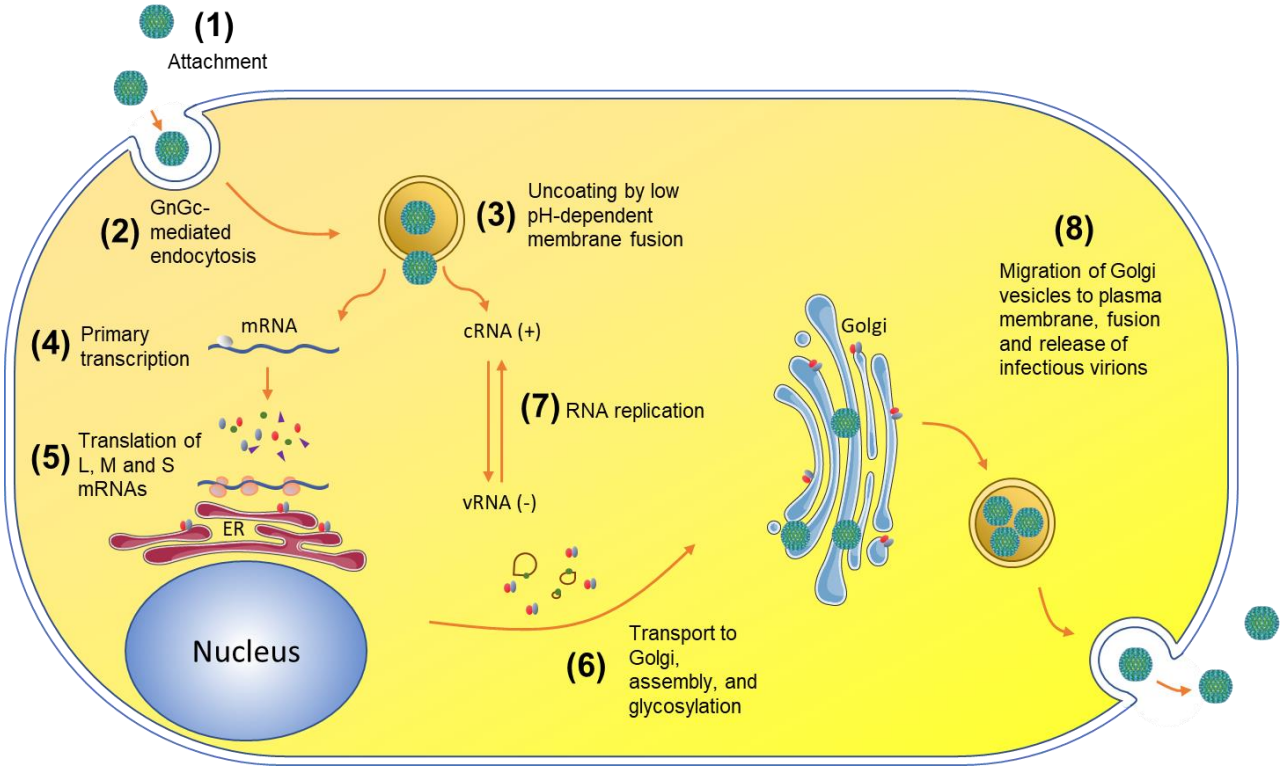


***Figure 4**. Replication cycle of RVFV. (1) Viral attachment to host membrane. (2) GnGc-mediated endocytosis. (3) Uncoating by acidification of endocytic vesicles, fusion of viral and endosomal membranes. (4) Primary transcription of mRNA by viral RNA polymerase. (5) Translation of viral proteins, cleavage of M-segment polyprotein and dimerization of GnGc in the endoplasmic reticulum (ER). (6) Transportation of GnGc hetrerodimers to the Golgi, glycosylation of Gn and Gc and budding into the Golgi cisternae. (7) RNA replication into positive-sense complimentary RNA (cRNA), which serves as a template for negative-sense viral RNA (or in the case of the ambisense S segment, templates for sub-genomic mRNA). (8) Migration of Golgi vesicles containing viruses to cell surface, fusion of vesicular membranes with plasma membrane, release of infectious virions. This figure is from [19] and was originally adapted from [88] with permission from the authors and the copyright holder.*

1.5 Phylogeny

It is estimated that RVFV diverged from a recent common ancestor during the 1880s-90s [89, 90]. The virus circulates throughout East Africa, with outbreaks in other regions often the result of a single introduction [42]. Several studies conducting sequence analysis of RVFV isolates throughout Africa and Saudi Arabia have shown limited genetic diversity of ~5% at the nucleotide level and ~2% at the amino-acid level [89-91]. A large study of 198 isolates obtained over a 67-year period from numerous countries categorized sequences into 15 lineages (A-O) [89]. These individual RVFV

lineages are not unique to specific regions and many have been isolated from multiple geographical settings [92]. Sequence analysis has demonstrated that numerous lineages can circulate concurrently during outbreaks [92] and there is evidence of previous genetic reassortment between them [89, 91]. Data regarding the virulence of different RVFV strains is limited. While all isolates belong to a single serotype [93], importantly, and despite the limited diversity, individual strains of RVFV can cause differential disease severity in natural host species [72, 73]. Challenge trials in sheep and calves, respectively, showed a strain isolated during the 2006/07 Kenyan outbreak (Kenya-128B-15) led to higher viremia and increased liver damage compared to those challenged with a strain isolated during the 2000/01 Saudi Arabia outbreak (SA01-1322) [72, 73].

Domain-specific analysis of the glycoproteins demonstrated that the most membrane distal region of Gn undergoes the greatest level of non-synonymous mutations, suggestive that this region of the molecule is under comparatively strong selection pressure and is subject to fewer structural constraints [94]. The relatively conserved nature of the antigenic RVFV Gn-Gc surface bodes well for efforts to develop broadly efficacious vaccines capable of protecting against any strain.

1.6 Immunology

1.6.1 Naturally acquired immunity

Protection against RVFV in all species is associated with neutralising antibodies (nAbs), which can be detected within the first week post-infection [26, 95]. Sheep and cattle exposed to RVFV have been shown to be completely resistant to disease upon re-infection [6]. Passive serum transfer experiments in non-human primate and rodent models have confirmed the role of antibodies in protection against RVFV infection [96, 97]. Administration of convalescent human sera to naïve lambs can also confer protection from challenge [6]. The response can be long-lived, with neutralising antibodies detected in two people 12 and 25 years post-infection, respectively, in the absence of subsequent exposure [62, 98].

The only identified targets of nAbs are the surface glycoproteins, Gn and Gc [99-104]. The N protein is the immunodominant protein of many bunyaviruses, where IgG and IgM specific to N are abundant after natural infection in all species evaluated [26, 105, 106]. However, there is no evidence that anti-N antibodies exhibit virus neutralising activity. Experimental challenge in animals has revealed measurable IgM levels targeting the glycoproteins and N, and to a lesser extent NSs, in the first few days after infection [26]. This drops to <10% prevalence in animals after 50 days. Positivity for RVFV-specific IgG begins to appear shortly after IgM with animals generally becoming IgG positive within 3 weeks [26].

The production of anti-RVFV neutralising antibodies is likely the primary mechanism of protection in all species. It is possible that the diversity of known IgG structures amongst species, such as the ultralong loop in the third heavy-chain complementarity-determining-region (CDR H3) of cattle antibodies and the heavy-chain only antibodies of camels may allow the recognition of species-specific epitopes [107, 108]. The single domain antibodies of camelids, for example, are only ~90kDa in size, significantly smaller than conventional IgG and may have access to epitopes that larger antibodies do not. A more detailed understanding of the humoral immune response to RVFV could help to guide future vaccine strategies. Identification of neutralising epitopes may allow the omission of parts of the RVFV proteins which do not contribute to protection, leaving the immune response to focus on those that do [109]. The possibility of reducing the antigen size while maintaining or increasing immunity could potentially be exploited by allowing the combination of additional antigens in vaccines. Furthermore, vaccine development can be guided by a detailed characterization of naturally acquired immunity, likely to provide long-lived protection. The degree to which virus-host interactions differ between species is an area in need of future research.

In comparison to antibodies, relatively little is known about T cell responses against RVFV, particularly after natural exposure. Dendritic cells and macrophages are among the first immune

cells encountered after infection and replication of RVFV has been demonstrated in both [110, 111]. African green monkeys exposed to RVFV via aerosolized droplets develop neurological disease similar to that seen in humans [112]. In these animals challenged with RVFV, early proliferation of CD4+ and CD8+ T cells and expression of Th1 cytokines was associated with non-lethal outcomes [112]. This is in line with findings that higher concentrations of IL-10, a cytokine that suppresses Th1 response, is associated with fatal cases compared to non-fatal cases in humans [56]. The same study also found that B cell and neutrophil activators were elevated in non-fatal compared to fatal cases [56].

Innate immunity plays a critical role in RVF disease progression [56]. The NSs protein, an interferon antagonist, is the major virulence determinant of RVFV. RVFV lacking NSs induces strong type-I interferon responses, which explains its attenuation in livestock and humans [113-116]. Counteracting the innate immune response by RVFV is achieved through various mechanisms [117]. YY1, a host protein involved in modifying IFN-β transcription, is bound by NSs and another host protein, SAP30. Together this complex serves to suppress IFN-β at the transcriptional level, occurring very early on in the first few hours post-infection [26, 118]. After this, NSs interacts with components of the transcription factor TFIIH, preventing their assembly and thereby causing a rapid general decrease in host cellular RNA synthesis [119]. Alongside transcriptional shutoff, NSs promotes viral replication via degradation of Protein Kinase R (PKR) [117, 120, 121]. PKR plays a key function in antiviral defence by inhibiting protein synthesis and thus its degradation blocks host translational shutoff.

1.6.2 Vaccine-induced immunity

As with natural exposure, protection through vaccination is likely primarily conferred via induction of nAbs towards the viral glycoproteins. Hence, the aim of RVF vaccine programmes is to elicit high titre RVFV nAbs. Previous inoculations with RVFV candidate vaccines in humans have shown their

potential to induce long-lived nAbs [122, 123]. Although none are licenced and potential safety concerns or requirements for multiple doses for these live-attenuated and inactivated candidate vaccines, respectively, limit their utility.

In livestock, immunisation can induce detectable nAbs in as early as 4-5 days in some animals and in all animals by 2-4 weeks [103, 124, 125]; nAb titres can be further boosted following challenge [103, 124]. In some areas there have been questions about the efficacy of live-attenuated livestock vaccines. In Egypt, for example, despite 70% of cattle being vaccinated some studies have found significantly lower seropositivity [126, 127]. Whether this is directly related to the vaccine rather than issues with implementing the vaccination programme requires further investigation. Some widely used livestock vaccines, such as the inactivated RVF ZH501 and RVF Menya require multiple doses in order to generate protective immunity [128], increasing the costs and logistics involved in vaccination.

There are examples of challenge studies carried out in mice showing partial protection in the absence of detectable nAbs [104, 129]. This is the case when vaccinating mice with the N protein [104, 129]. The mechanism of this protection is poorly understood but cellular immunity has been implicated [104]. Indeed, there is evidence that the N protein is a potent human CD8+ T cell antigen [130]. This protection may also come from non-neutralising antibodies via cell-mediated cytotoxicity (ADCC) or complement-dependent cytotoxicity (CDC) [129].

1.6.3 Immune epitopes

Wang *et al.* recently isolated RVFV monoclonal antibodies (mAbs) from a convalescent human returning from Angola [131], and found that Gn-specific mAbs were protective and function by blocking virus binding to cells. Another study in which rabbits were vaccinated with the ectodomain of the Gn identified a class of mAbs which protects against RVFV infection in a mouse model by

targeting the membrane-distal domain of Gn (domain B [residues 366–439]) [94]. This class of antibodies recognizes a region that is spatially distinct from that targeted by the characterised human-derived mAbs, supportive of the possibility of a potent mAb cocktail targeting multiple epitopes for therapeutic use. Another panel of mAbs recently isolated from humans identified neutralising epitopes on monomeric Gn and Gc, together with mAbs that bind the tertiary GnGc structure [132]. The mAbs targeting the monomeric glycoproteins recognised two major sites on Gn domain A (residues 164 to 186 and 270 to 294). Another two major sites on Gc identified neutralising mAbs primarily bound domain I and the fusion loop of domain II. The identified mAbs appear to either block binding to cell receptors or prevent cell fusion by inhibiting rearrangement of GnGc, thus preventing engagement of Gc's fusion loop [132]. To date, no epitopes have yet been characterised in target livestock species.

In mice, both B and T cell epitopes have been identified in the viral glycoproteins Gn and Gc. A widely used commercially available mouse mAb recognises a linear B cell epitope on Gn [133], while CD8+ T cell epitopes have been identified on both Gn and Gc [104]. More broadly, a study in the 1990s investigated mAbs raised in vaccinated mice and found examples targeting either Gn or Gc that were capable of neutralising RVFV [100]. A later study in mice vaccinated with cDNA containing Gn or Gc, showed only Gn-vaccinated mice developed neutralising antibodies, while Gc-vaccinated mice did not [101]. A limitation of identifying epitopes using individual glycoproteins, however, is that the conformation of Gc or Gn alone will be different than they appear when presented as pentamers and hexamers of Gn/Gc heterodimers on the mature virion surface. Important epitopes may therefore be missed, particularly at the interface between Gn and Gc. While a low-resolution reconstruction of the RVFV envelope has allowed the positions of the Gn and Gc glycoproteins to be revealed [75], higher resolution structural information of the Gn/Gc assembly is needed to guide our understanding of the mature, antigenic surface of the virus.

1.7 Disease control and treatment

1.7.1 Diagnosis

Often the first sign of an RVF outbreak is the near simultaneous abortions in herds of pregnant sheep termed 'abortion storms'. There are several methods to diagnose acute RVFV infection in livestock and humans, but all must be carried out in laboratory settings [25]. One method of diagnosing very recent infection is to use enzyme-linked immunosorbent assays (ELISA) detecting IgM towards RVFV antigens [134]. Molecular methods using real-time reverse transcriptase (RT)-PCR to detect viral RNA can be used to detect acute infection and are highly sensitive and specific. Virus can also be isolated by cell culture from blood samples taken during the febrile stage (or from organ samples collected post-mortem). Lastly, histopathological methods can be used; i.e. post-mortem examination of liver for hepatic lesions.

Viral neutralisation assays are the gold standard in detecting previous exposure to RVFV due to their high sensitivity and specificity. However, these require specialist laboratory facilities capable of working safely with live RVFV. Commercial ELISA kits that detect antibody against the N protein are also available (ID-VET, Montpellier, France).

1.7.2 Treatment

Most human cases of RVF do not require treatment, as evidenced by individual case reports and seroprevalence studies showing much higher levels of infection than confirmed acute cases [62, 135, 136]. For those with severe RVF disease there is no specific treatment other than general supportive therapy. Several groups are investigating potential RVF therapeutics, and some, such as Ribavirin and Favipiravir have shown efficacy in rodent models (reviewed in [137]). During the 2000 outbreak in Saudi Arabia, intravenous administration of Ribavirin to RVF patients was stopped due to the apparent increase of neurological disease in these patients [71]. The development of an

effective treatment for RVF disease is of considerable importance and continued research is warranted.

1.8 Vaccines

At present, vaccination is regarded as the only practical method to prevent RVFV infections in livestock. However, there is significant room for improvement of existing livestock vaccines, particularly regarding safety and their inability to distinguish infected from vaccinated animals (DIVA). In addition, tools to limit spillover into humans are hampered by the absence of any licensed human vaccines [138]. Replicating the seemingly long-lived nAb response resulting from natural exposure is an attractive goal. For humans, there are two vaccines currently defined as Investigational New Drugs in the USA; MP-12 and TSI-GSD-200 [139]. MP-12 was created in the 1980s, the strain contains 23 nucleotide mutations distributed over all 3 genome segments [140]. It has been conditionally licensed for animal vaccination [139] and is safe and immunogenic in both animals and humans although some teratogenic effects have occurred in pregnant ruminants [25, 122]. TSI-GSD-200 is a formalin-inactivated vaccine created by the US army to protect those whose work may put them at risk of infection. It has an excellent safety profile but requires multiple boosters to achieve efficacy, and even then almost 10% of vaccinees tend to have low nAb titres or fail to seroconvert [123].

For livestock, RVF vaccine use is inconsistent across Africa and the Arabian Peninsula with most countries having no implementation due to the sporadic nature of outbreaks or lack of reported cases [139]. The frequency of vaccination in countries that do vaccinate, such as Kenya, South Africa and Egypt among others, using a handful of licensed vaccines, varies based on the ecological setting [139]. For livestock, the most widely used commercial vaccine, named after its developer Smithburn (and also known as RIFTVAX™), is live-attenuated and induces long-lasting protection after a single dose [138]. However, the Smithburn vaccine cannot be administered to pregnant

animals as residual virulence results in a high risk of abortion [141]. In addition, there is a possibility of reversion to virulence as may have occurred previously with this vaccine [142]. There is also the prospect of genetic reassortment with wild-type RVFV, however, this is unlikely to result in an increase in pathogenicity beyond that of the wildtype virus. DIVA compliance would be an attractive bonus for a novel RVFV vaccine. When using live-attenuated RVFV as a vaccine, such as Smithburn, the antibody profile generated is similar to natural infection, rendering the mapping of outbreaks difficult in the face of vaccination. Subunit vaccines have the advantage of not including all the RVFV antigens. By measuring responses to the N protein, if not present in the vaccine, it is possible to differentiate animals that have been naturally exposed from those that have been vaccinated using commercially available kits.

Another livestock vaccine, Clone 13, was one of a number of viral clones isolated from a human patient infected with the 74HB59 strain in the Central African Republic [143]. It was found to be naturally attenuated due to a large deletion in the NSs gene, the primary virulence factor, with subsequent infection in mice showing it did not cause disease [143]. Clone 13 has proven safe and immunogenic after a single dose in cattle, sheep and goats [113, 114, 116]. Overdose studies in pregnant ewes, however, have found Clone 13 able to cross the placental barrier and cause teratogenic effects [144]. A thermostabilized version, selected from viable clones after incubation at 56°C, has been used to vaccinate livestock in Senegal and Mali [139].

There are several promising vaccine candidates currently under development which aim to address the shortfalls of current vaccines, namely single-dose efficacy or safety concerns. A subunit vaccine using the GnGc glycoproteins has shown 100% efficacy in sheep [145]. Another, RVFV-4s, where the M segment is split into 2 parts separately encoding Gn and Gc, has conferred sterile immunity in lambs after a single vaccination [146]. In addition, vaccinated pregnant sheep

showed no teratogenic affects with no presence of RVFV-4s virus in the blood or organs of their foetuses [147].

Another candidate is ChAdOx1 RVF, which forms the basis of this thesis. ChAdOx1 RVF is a replication deficient chimpanzee adenovirus encoding the RVFV structural glycoproteins Gn and Gc. Developed for use in both livestock and humans, ChAdOx1 RVF has shown 100% efficacy against RVF viral challenge in sheep, goats and cattle [103]. More recently it was found to be extremely protective against disease and foetal loss in pregnant animals [148]. A summary of the ChAdOx1 RVF livestock trials carried out to date are presented in **Table 1.** A first-in-human clinical trial of ChAdOx1 RVF began in July 2021 and forms the basis of chapter 5. This thesis seeks to advance our understanding of RVF immunology and continue the development of ChAdOx1 RVF, a vaccine candidate with significant potential to improve animal and public health.

Table 1. Summary of ChAdOx1 RVF livestock trials.
[a] Cattle vaccinated with thermostabalised vaccine stored between -80°C and +55°C (*n* = 4 per temperature)
[b] Combined data from ChAdOx1 RVF with and without Matrix Q™ adjuvant
[c] RIFTVAX™ is also referred to as the Smithburn vaccine

Trial ID	Livestock trials	Trial location	Ref	Species	Challenge?	*n*	Vaccine/ dose (IU)	Efficacy results
A	Cattle thermostability	Compton, UK	[149]	Cattle	NO	*20* [a]	1x10^9 IU ChAdOx1 RVF	*n/a*
B	multi species efficacy	ILRI, Kenya	[103]	Sheep	YES	14 [b]	1x10^9 IU ChAdOx1 RVF	100% sterile protection
						5	RIFTVAX™ [c]	100% sterile protection
						7	PBS	0% protection
				Goats	YES	13[b]	1x10^9 IU ChAdOx1 RVF	100% sterile protection
						4	RIFTVAX™	86% sterile protection
						6	PBS	0% protection
				Cattle	YES	11[b]	1x10^9 IU ChAdOx1 RVF	100% sterile protection
						4	RIFTVAX™	80% sterile protection
						6	PBS	0% protection
				Camels	NO	7	1x10^9 IU ChAdOx1 RVF	*n/a*
						4	PBS	
C	pregnant livestock	Lelystad, The Netherlands	[148]	Pregnant Sheep	YES	8	1x10^9 IU ChAdOx1 RVF	100% sterile protection for adults and foetuses
						8	PBS	0% protection
				Pregnant Goats	YES	8	1x10^9 IU ChAdOx1 RVF	100% protection against disease (adults only). 94% protection against foetal loss
						8	PBS	0% protection

(Table continued)

Table 1 (continued).

Trial ID	Livestock trials	Trial location	Ref	Species	Challenge?	*n*	Vaccine/ dose (IU)	Efficacy results
D	dose de-escalation trial	Pirbright, UK	*n/a*	sheep	NO	5	$5x10^8$ IU ChAdOx1 RVF	*n/a*
						5	$5x10^7$ IU ChAdOx1 RVF	
						5	$5x10^6$ IU ChAdOx1 RVF	
				Cattle	NO	7	$5x10^8$ IU ChAdOx1 RVF	
						7	$5x10^7$ IU ChAdOx1 RVF	
						7	$5x10^6$ IU ChAdOx1 RVF	
E	Field trial	Kapiti, Kenya	*n/a*	sheep	NO	80	$5x10^8$ IU ChAdOx1 RVF	*n/a*
						80	RIFTVAX™	
						20	PBS	
				Goats	NO	80	$5x10^8$ IU ChAdOx1 RVF	
						80	RIFTVAX™	
						20	PBS	
				Cattle	NO	80	$5x10^8$ IU ChAdOx1 RVF	
						80	RIFTVAX™	
						20	PBS	
				Camels	NO	80	$5x10^8$ IU ChAdOx1 RVF	
						80	RIFTVAX™	
						20	PBS	

1.9 Thesis Aims:

1. To characterise naturally acquired immunity to RVF among Kenyan adults
2. To determine factors that underlie successful manufacture of ChAdOx1 RVF vaccine
3. To characterize the immunogenicity of ChAdOx1 RVF among adults in Oxford
4. To characterize the immunogenicity of ChAdOx1 RVF in livestock
5. To assess the potency of nanobodies raised after vaccination with ChAdOx1 RVF and recombinant Gn and Gc proteins
6. To explore the possibility of including an additional Peste-des-petits ruminants antigen in ChAdOx1 RVF to create a bivalent RVF / PPR vaccine with more utility in improving livestock health.

2

Materials and Methods

2.1 Molecular Biology

2.1.1 Mammalian cell expression of RVFV Gn-Avi

cDNA of the Gn ectodomain (UniProt accession number P21401, residues 154-560) was previously cloned into pHLSec mammalian expression vector, which encodes a C-terminal hexa-histidine tag by Dr Elizabeth Allen [150]. I transformed this plasmid into *E. coli* and bulked it up. cDNA was purified using a Gigaprep (Qiagen) following manufacturer's instructions. After ethanol precipitation, DNA was resuspended in 7 mL dH_2O and quantified by Nanodrop.

6x T175 flasks of >80% confluent Human Embryonic Kidney cells (HEK293T, ATCC CRL-1573) in Dulbecco's modified eagle media (DMEM, Sigma Aldrich) containing 10% Foetal Calf Serum (FCS, Sigma), 1% L-glutamine and 2% non-essential amino acids (D10, Life Technologies) were prepared. Cell monolayer in T175 flasks were washed briefly in Dulbecco's Phosphate buffered saline (DPBS, Sigma Aldrich). 3 mL Trypsin-EDTA (Life Technologies) was added for 5 minutes before addition of 50 mL D10. Each flask's cells were split between 2 roller bottles, ~25 mL each and topped up to 200 mL with D10. Roller bottles were incubated at 37°C for 4 days. Media was aspirated and replaced with 200 mL D2 (identical to D10 but with 2% FCS rather than 10%).

6 mg of Gn-AviTag plasmid DNA was added to 300 µL chloroform, mixed thoroughly and spun at 13,000 g for 5 minutes. 6 mL Polyethylenimine (PEI) and 6 mg DNA was added to 600 mL D2 and inverted to thoroughly mix. 50mL of this was added to each of the 12 roller bottles (now containing ~250 mL media total). Roller bottles were incubated at 37°C for 4-5 days. Supernatant was transferred to 250 mL bottles and spun at 5000 g for 20 minutes. Supernatant was filtered using 0.22µm filter (Sigma Aldrich) and pellet was discarded. Supernatent containing Gn-AviTag protein was buffer exchanged into Tris Buffered Saline (TBS) pH 8 using the AKTAflux (GE Healthcare) before purification by immobilised nickel-affinity chromatography (IMAC), using 5 mL HisTrap FF crude column and AKTA FPLC system (GE Healthcare). Fractions covering the peak were collected and

concentrated using 4 mL, 3,000 molecular weight cut off (MWCO) Amicon ultra centrifugal filters (Millipore) to a final volume of ~400 µL. Gn-AviTag was further purified by Size Exclusion Chromatography (SEC). Using a Superdex 200 10/300 Increase column (GE Healthcare) into 10 mM Tris-HCl, 150mM NaCl, pH 8.0. Sample was loaded into the loop and run at 0.5 mL min^{-1}. Fractions covering the UV peak at ~15 mL were collected. Final Gn-AviTag concentration was quantified by nanodrop.

2.1.2 Mammalian cell expression of RVFV Gc-Sumo

cDNA of the Gc ectodomain (UniProt accession number P21401, residues 691-1120) linked to an N-terminal SUMO tag, which also encodes a hexa-histidine tag, was previously subcloned into the pURD expression vector to generate a stable cell line in HEK293T cells by Dr Elizabeth Allen [151]. I thawed a single vial of cells in a 37°C water bath until a small ball of ice remained. D10, warmed to 37°C was added to the vial and the entire contents aspirated into a tube containing 9 mL D10. This was spun at 400 g for 5 minutes. The pellet was resuspended in a T75 flask containing 30 mL D10 and incubated at 37°C. I harvested the cells after 5 days and RVFV Gc was purified from clarified cell supernatant by IMAC in an identical way to RVFV Gn-AviTag above. Once purified, the SUMO-tag was cleaved with 3C protease (Pearsons) overnight at 37°C [940 µL of Gc protein at 8.8 mg/mL, 50 µL 3C protease, 110 µL 10x buffer]. Cleaved RVFV Gc was purified from the SUMO-tag by IMAC again. The flowthrough containing Gc was further purified by SEC using a Superdex 200 10/300 Increase column (GE Healthcare) into 10 mM Tris-HCl, 150 mM NaCl, pH 8.0.

2.1.3 Mouse monoclonal antibody production (4D4 and 5E2)

4D4 and 5E2 hybridomas (obtained from USAMRIID) were thawed and cultured in DMEM containing 20% ultra-low IgG FBS (culture medium, Life Technologies). Every 4 days, cells were harvested by aspirating media, washing with DPBS, adding 5 mL Trypsin-EDTA (Life Technologies) and incubating at 37°C for 5 minutes. 10 mL culture medium was added to the flask and transferred

to a 50 mL falcon tube which was spun at 400 g for 5 minutes. Supernatant was collected and stored at -20˚C until purification. Cells were resuspended in 10 mL culture media and 5 mL seeded back into the flask and topped up with 45 mL fresh culture medium, incubating at 37°C until the next harvest. Purification: All the supernatants from each passage of the same antibody were pooled and filtered using 0.22 µm filter. Monoclonal antibodies (mAbs) were purified using protein G affinity chromatography following the manufacturer's instructions (GE Healthcare). mAbs were further purified by Size Exclusion Chromatography (SEC). Using a Superdex 200 10/300 Increase column (GE Healthcare) into 10 mM Tris-HCl, 150mM NaCl, pH 8.0. mAbs were buffer exchanged in DPBS and concentrated using a 15 mL, 10,000 molecular weight cut off (MWCO) Amicon ultra centrifugal filter. Final mAb concentration for both 4D4 and 5E2 was quantified by nanodrop.

2.1.4 Nanobody expression

A single llama was vaccinated with ChAdOx1 RVF followed by boosting with another dose 8 months later (1x 10^9 IU / dose). The llama was boosted with recombinant Gn and Gc 6 weeks later. Plasmids containing the VHH were provided by Dr Jan Steyaert's lab in Brussels. These were transfected into WK6 (Su-) *E. coli* by Dr Elizabeth Allen and glycerol stocks created. These plasmids direct the encoded nanobody to the periplasmic fraction space and carry a HIS tag at the C- terminus for purification.

I picked bacteria from glycerol stocks and placed into a starter culture containing 20 mL LB broth (Sigma) + 0.05 µg Carbenicillin, 1 mM $MgCl_2$, and 2% glucose and incubated overnight at 37°C at 190 rpm. In the morning, after ~16hours, cultures were placed on ice. In the afternoon, 3 mL of this culture was seeded into 2x 495 mL Terrific Broth (TB, Sigma) cultures and incubated at 37°C 190 rpm. Once the cultures reached an OD600 of 0.6 after ~2-3 hours, expression was induced by addition of 500 µL of 1M Isopropyl ß-D-1-thiogalactopyranoside (IPTG) per flask (0.1 mM IPTG per flask final concentration). Cultures were incubated overnight at 28°C, 190 rpm. Cultures were

transferred to 500 mL containers and centrifuged at 5000 g, 4°C for 30 minutes. Pellets from identical nanobodies were combined and resuspended in 15 mL TES buffer (0.2 M Tris pH 8.0, 0.5 mM EDTA, 0.5 M sucrose), sample was rocked on ice for >1 h. 30 mL TES/4 (TES buffer diluted 1:4 with H_2O) was then added. Sample was rocked on ice for >45 minutes before being centrifuged at 6000g, 4°C for 30 minutes. The supernatant was collected (~100 mL per nanobody) and filtered through a 0.22 µm filter (Sigma Aldrich) before storing at 4°C until purification.

2.1.5 Nanobody purification

500 µL of Ni-NTA Agarose nickel beads (Qiagen) were spun at 200 rpm for 2 minutes in a microfuge. Supernatant was discarded and beads were resuspended in 700 µL TBS + 20mM Imidazole (TBS/I) before being transferred to a 50 mL tube and topped up to 25 mL TBS/I. Beads were incubated at room temperature for 10 minutes before centrifuging at 2000 rpm for 10 minutes. Supernatant was discarded and 50 mL of nanobody supernatant was added to the tube containing beads. Tubes were rotated at room temperature for 1 h. Meanwhile, Poly-Prep Chromatography columns (Bio-Rad) were calibrated with 2 mL TBS/I. The nanobody/beads mixtures were then added to the column until all ~100 mL nanobody had run through. Columns were washed with 10 mL TBS + 2% Imidazole. TBS + 5% Imidazole was then added to columns with flow through collected in fresh labelled tubes. A final wash of TBS + 30% imidazole was run through and collected. The 5% imidazole fraction was concentrated in a 3,000 molecular weight cut off (MWCO) Amicon ultra centrifugal filter and buffer exchanged into TBS to a final volume of ~1 mL. Nanodrop was used to calculated concentration, taking into account the extinction coefficient as determined by its amino acid sequence.

2.1.6 SDS-PAGE

14 µL protein, 1 µL Dithiothreitol (DTT) and 5 µL 4x Loading Dye (ThermoFisher) were incubated for 10 minutes at 95°C before loading on a NuPAGE 4-12 % Mini polyacrylamide gel (ThermoFisher).

Gel was ran at 200 Volts for 40 minutes. Gels were stained with Quick Coomassie Stain (Generon) for 2 h followed by destaining in dH_2O overnight.

2.1.7 Western blots

2.1.7.1 RVFV Gn/Gc proteins:

After SDS-PAGE, gels were turbo blotted for 8 minutes. Western blots were carried out using the iBind system (Life Technologies) according to manufacturer's instructions. Mouse mAbs 4D4 (Gn) and 5E2 (Gc) diluted 1:1000 were used as primary antibodies. Goat anti-mouse IgG conjugated to ALP (Sigma Aldrich) was used as the secondary antibody, diluted 1:5000. Gels were developed using SIGMAFAST BCIP/NBT (Sigma Aldrich) in H_2O buffer for approximately 5 minutes before rinsing in dH_2O.

2.1.7.2 Nanobodies

After SDS-PAGE, gels were turbo blotted for 8 minutes. Blots were then blocked in 10% skimmed milk in PBS (blocking buffer) for 1 h. blots were washed 5x in PBS/T. Mouse anti-penta His antibody (34660, Qiagen), diluted 1:5000 in blocking buffer was added for 2 hours. Blot was washed again and horse radish peroxidase-conjugated goat anti-mouse IgG (Sigma Aldrich) was diluted 1:5000 in blocking buffer and incubated for 1 h. Blot was washed a final time as before and developed with Clarity Western ECL substrate (Bio-Rad) and imaged with the Chemi-Doc (Bio-Rad) imaging system.

2.2 Vaccine construct production

2.2.1 ChAdOx1 RVF vaccine production

Initial manufacture of ChAdOx1 RVF for clinical trials and large-scale livestock trials failed QC due to the introduction of a single base pair deletion in the GnGc region. The GnGc transgene insert was resynthesized (GeneArt) to remove instances of >3 identical consecutive bases. This sequence was cloned into an entry plasmid followed by Gateway® recombination with the ChAdOx1 plasmid,

as previously described [103]. Because the GnGc sequence was not ordered with the flanking restriction sites, these were added by carrying out a PCR of the GnGc region using primers containing the restriction sites.

Fwd primer (Acc65I)	0.5 µL (of 10 µM stock)
Rev primer (NotI)	0.5 µL (of 10 µM stock)
Phusion MM	25 µL
H_2O	22 µL
DMSO	1 µL
GeneArt plasmid	1 µL (10 ng)

Fwd primer (Acc65I)	5’ TCAATGGGTACCATGGACGCCATGAAGCGCGGA 3’
Rev primer (NotI)	5’ TGAGCGGCCGC TCAGCTGGCCTTCTTGGTAGC 3’

This was run under the following PCR conditions:

1.	98 °C	2 minutes
2.	98 °C	15 s
3.	67.5 °C	30 s
4.	72 °C	1.5 minutes
5.	Repeat steps 2-4	x 25
6.	72 °C	10 minutes

PCR clean-up kit (Qiagen) was used on the PCR product according to manufacturer’s instructions. The PCR product was then digested with Acc65I and NotI and incubated at 37 °C for 2 h:

Acc65I	1 µL
NotI	1 µL
3.1 buffer	3 µL
H_2O	5 µL
Cleaned up PCR product	20 µL (142 ng/µL)

I added 6 µL of 6x loading dye (New England Biolabs) and ran on a 0.8% agarose gel at 95 V for 30 minutes, over two wells. Extracted 3.3 Kb bands and purified DNA using Qiagen Gel Extraction Kit according to manufacturer's instructions. ChAdOx1 entry plasmid (p1990) was also digested with Acc65I and NotI, followed by incubation at 37°C for 2h:

Acc65I	1 µL
NotI	1 µL
3.1 buffer	3 µL
H_2O	23.48 µL
p1990	1.52 µL (500 ng)

Cleaned up digestion using QIAgen PCR Purification kit according to manufacturer's instructions. The digested entry plasmid and digested GnGc insert were then ligated together at room temperature for 15 minutes.

digested GnGc	16 µL
Digested p1990	1 µL (16 ng)
T4 ligase buffer	2 µL
T4 ligase	1 µL

I then transformed 5 µL of ligation reaction into 50 µL competent cells (C2988) and incubated on ice for 30 minutes. This was heat shocked for 30 seconds at 42 °C and further incubated on ice for 5 minutes. 300 µL Vegitone LB (VTLB) broth (Sigma) was added and incubated at 37 °C shaking 225 rpm for 50 minutes. I then streaked out 20 µL, 100 µl and 250 µL volumes onto separate Kanamycin VTLB agar plates and incubated overnight at 37 °C. The next day I picked 6 colonies using a p10 tip, swirled in PCR tubes containing 10 µL molecular biology grade H_2O before dropping into 5 mL VTLB broth containing 1:2000 kanamycin. Cultures were left at RT until their corresponding H_2O tubes had confirmed the presence or absence of the GnGc insert by PCR. PCR tubes containing H_2O and DNA were heated to 95 °C for 10 minutes. PCR reaction:

Forward primer (J1170)	0.5 µL (of 10 µM stock)
Reverse primer (J1210)	0.5 µL (of 10 µM stock)
Phusion MM	5 µL
H_2O	3 µL
Template DNA	1 µL

PCR conditions:

1.	98 °C	2 minutes
2.	98 °C	15 s
3.	62°C	30 s
4.	72 °C	2 minutes
5.	Repeat steps 2-4	x 30
6.	72 °C	10 minutes

The PCR product was ran on a gel as described previously. For PCRs confirmed to contain the GnGc insert by having a 3.3 Kb band, their corresponding 5 mL culture prepared earlier was incubated overnight at 37 °C, shaking at 225rpm. These were then miniprepped (Qiagen) according to manufacturer's instructions. Restriction digest on all plasmids were carried out for further confirmation of correct cloning:

Acc65I	1 µL
NotI	1 µL
3.1 buffer	3 µL
H_2O	23.6 µL
plasmid	1.4 µL (500 ng)

Restriction digests were incubated for 2 h at 37 °C. 6 µL Loading dye was added and 20 µL run on a gel as described earlier in 2.2.1. After confirmation of correct size bands, one of the plasmids was kept and hereafter referred to as p5351. p5351 entry plasmid was cloned into p2563 ChAdOx1 destination plasmid by LR-clonase recombination:

p5351	0.40 µL
p2563	0.43 µL (350 ng/µL)

TE buffer	7.17 µL
LR Clonase	2 µL

Ligation reaction was incubated at 25 °C for 6 h before being transformed into Stellar™ competent cells as described on previously. Cells were streaked out onto chloramphenicol (CMP) VTLB agar plates and incubated overnight at 37 °C. 9 colonies were then picked from the CMP plate and streaked sequentially onto a fresh CMP plate, followed by a kanamycin (KAN) plate, followed by swirling in 2 mL VTLB broth containing 1:1000 CMP. Plates and VTLB cultures were incubated overnight at 37 °C. Plates were then inspected for colonies that grew on CMP plates but not KAN plates. For a single colony that satisfied these requirements, their equivalent 2 mL culture was added to 498 mL VTLB and incubated overnight at 37°C shaking 225rpm. Bacterial cells were harvested by centrifugation at 6000g for 15 minutes at 4 °C. Pellet was resuspended in 12 mL of P1 (Qiagen) and transferred to a 50 mL falcon tube. 12 mL P2 (Qiagen) was added and after mixing, incubated at RT for 5 minutes. 12 mL of chilled P3 (Qiagen) was added, mixed, and incubated for 10 minutes at RT. Tube was centrifuged at 15,000 g for 30 minutes at 4° C. Supernatent was filtered in a Maxi-prep Qiafilter (Qiagen) and added to a Tip 100 (Qiagen), previously equilibrated with 4 mL of buffer QBT (Qiagen). Once all supernatant had run through, column was washed twice with 10 mL buffer QC (Qiagen). DNA was eluted with 3 mL QF at 65 °C into a fresh tube. Eluted DNA was transferred to 3x 2 mL tubes (1 mL each). 700 µL isopropanol was added to each tube, mixed and centrifuged at 15,000 g, 4 °C for 30 minutes. Supernataent was aspirated and pellets pooled using 500 µL 70% EtOH. Tube was centrifuged at 15,000 g, 4 °C for 15 minutes. Supernatant was aspirated and after 15 minutes of air drying pellet, DNA was resuspended in 100 µL TE buffer (Qiagen), quantified by nanodrop, and stored at 4 °C until needed. The purified BAC was then linearised with PmeI:

plasmid DNA (6 µg)	75 µL
PmeI	2 µL
cutsmart buffer	3 µL
TE buffer	10 µL

This was handed to VVCF to transfect into T-REx cells and bulked up.

2.2.2 ChAdOx1 RVF-PPR bivalent production

2.2.2.1 RVFV GnGc shuttle vector production (short promoter)

p2022 shuttle vector was digested with Acc65I and NotI:

Acc65I	1 µL
NotI	1 µL
3.1 buffer	3 µL
H_2O	5 µL
Digested p2022 plasmid	1.4 µL (~500 ng)

PCR cleanup kit (Qiagen) was used on the digested plasmid according to manufacturer's instructions. RVFV GnGc previously digested with Acc65I and NotI was then ligated with digested p2022 and incubated overnight at 16 °C:

digested GnGc	16 µL
p2022	1 µL (350 ng/uL)
T4 ligase buffer	2 µL
T4 ligase	1 µL

I transformed 8 µL of ligation reaction into 50 µL competent cells (C2987). Colony was picked, swirled in 10 µL H_2O for PCR, then ejected the same tip into identically labelled 5 mL LB + KAN. This was done for 5 colonies. PCR tubes were heated for 10 minute at 95 °C. Flank to flank PCR was carried out as described in 2.2.1 to check for correct band size. 2 µL loading dye was added to each 10 µL PCR product and ran on gel as previously described. 4 out of 5 colonies contained the

correct size transgene band, one of which was taken forward and their respective 5 mL culture was incubated at 37 °C, 225 rpm overnight. Miniprepped (Qiagen) culture according to manufacturer's instructions. The resulting plasmid was p5879.

2.2.2.2 PPRV H shuttle vector production (short promoter)

The Peste des petits ruminants virus (PPRV) Hemagglutinin antigen was synthesised in a pMA vector containing an ampicillin resistance gene from GeneArt (sequence in appendix). Using an earlier template of an Ad5 H vaccine (p2464), the sequence was amended to remove 21 instances of >3 identical consecutive base runs, whilst maintaining the identical amino acid sequence. The PmeI sites were removed and KpnI and NotI restriction sites at the 5' and 3' ends, respectively, were added (while ensuring that these restriction sites were not present within the antigen sequence).

The 5 µg pMA vector was resuspended in 50 µL molecular biology grade H_2O to 100 µg/mL. 1 µL was diluted 1:10 in H_2O, 2 µL of this (10 µg/mL) was transformed into 50 µL competent cells and incubated on ice for 30 minutes. Heatshocked for 30 seconds at 42 °C and further incubated on ice for 5 minutes. 300 µL SOC solution was added and incubated at 37 °C shaking 225 rpm for 1 h. I streaked out 50 µL and 250 µL volumes onto carbenicillin plates and incubated overnight at 37 °C. I Picked a single colony into 5 mL LB broth (Sigma) and incubated at 37 °C, 225 rpm overnight. The following day, I took 700 µL culture and added to 300 µL glycerol (50% final concentration) and stored as a glycerol stock. The remaining culture was Miniprepped (Qiagen) according to manufacturer's instructions.

KpnI and NotI digested p3665 (shuttle vector destined for the E4 loci of ChAdOx1) was provided by Susan Morris. I digested the PPRV H GeneArt plasmid DNA with KpnI-HF and NotI-HF:

plasmid DNA	20 µL (100 µg / mL)
H_2O	5 µL
Cutsmart buffer	3 µL
NotI-HF	1 µL
KpnI-HF	1 µL

Incubated for 2 h at 37°C. Added 6 µL Loading Dye and ran entire volume over 2 wells of a 0.8% agarose gel at 95 V for 30 minutes. I extracted vector band of 1.8 Kb representing PPRV H and cleaned-up the gel extraction using gel extraction kit (Qiagen) according to manufacturer's instructions. I then ligated PPRV H with p3665 to make p5880 PPRV H shuttle vector:

digested PPRV H	16 µL
p3665	1 µL
T4 ligase buffer	2 µL
T4 ligase	1 µL

Incubated overnight at 16 °C. Transformed 8 µL of ligation reaction into 50 µL competent cells (C2987) as described previously. Grew 5x colonies in 5 mL LB broth overnight at 37 °C, 225rpm. Miniprepped (Qiagen) cultures according to manufacturer's instructions. The resulting plasmid was p5880.

2.2.2.3 ChAdOx1 RVF-PPR BAC plasmid

Ligated the shuttle vectors p5879 and p5880 containing RVFV GnGc and PPRV H, respectively, with the ChAdOx1 bivalent destination vector, p4771:

p5879	1.1 µL
p5880	0.63 µL
p4771	2.1 µL (225 ng/µL)
TE buffer	4.2 µL
LR clonase	2 µL

Incubated at 20 °C overnight. Added 1 µL proteinase K and incubated for 10 minutes at 37 °C. Transformed as previously described (C2987 cells) and streaked onto CMP plates and incubated overnight at 37 °C. Two colonies grew. Picked each and streaked onto fresh CMP, followed by KAN followed by AMP plates. A colony that grew only on CMP and not the other two was picked and added to 5 mL LB broth containing CMP and incubated for 8 h at 37 °C, 225rpm. The 5 mL culture was seeded into 495 mL LB broth + CMP and incubated overnight at 37 °C, 225rpm. The BAC plasmid was purified as described in 2.2.1and labelled p5881. The purified BAC was then linearised with PmeI:

plasmid DNA (6 µg)	75 µL
PmeI	2 µL
cutsmart buffer	3 µL
TE buffer	10 µL

This was handed to VVCF to transfect into T-REx cells and bulked up.

2.2.3 ChAdOx1 PPR monovalent production

The same PPRV H insert, synthesised by GeneArt, was used to make a monovalent ChAdOx1 PPR vaccine. ChAdOx1 entry plasmid (p1990) was digested with NotI-HF and KpnI-HF and incubated for 2 h at 37°C:

p1990	1.4 µL (~500ng)
H_2O	18.6 µL
3.1 buffer	3 µL
NotI-HF	1 µL
KpnI-HF	1 µL

PCR cleanup kit (Qiagen) was used on the digested plasmid according to manufacturer's instructions. PPRV H, already digested with NotI-HF and KpnI-HF, and cleaned-up for the bivalent vaccine, was then ligated with digested p1990

Digested H	16 µL
Digested p1990	1 µL
T4 ligase buffer	2 µL
T4 ligase	1 µL

Ligation reaction was incubated overnight at 16°C. I then transformed 8 µL of ligation reaction into 50 µL competent cells (C2987) and incubated on ice for 30 minutes. This was heatshocked for 30 seconds at 42°C and further incubated on ice for 5 minutes. 300 µL SOC solution was added and incubated at 37°C shaking 225 rpm for 1 h. I then streaked out 50 µL and 250 µL volumes onto separate AMP agar plates and incubated overnight at 37°C. I then picked 5 colonies and grew up in 5 mL LB broth (containing AMP) overnight at 37°C 225 rpm. Aliquots were taken for glycerol stocks, with the remaining cultures miniprepped (Qiagen) according to manufacturer's instructions. Confirmation of plasmid containing H was carried out by restriction digest for 2 h at 37°C:

NotI-HF	1 µL
KpnI-HF	1 µL
Cutsmart buffer	3 µL
H_2O	12 µL
Template plasmid	13 µL (~500ng)

I then added 6 µL loading dye and ran on a gel to confirm correct band sizes. A single correct plasmid then taken forward and labelled p5882. The p5882 shuttle plasmid was then ligated with p2563 ChAdOx1 BAC:

p5882	0.63 µL
P2563	1.2 µL (225 ng/µL)
TE buffer	6.2 µL
LR clonase	2 µL

Transformation and purification of the resulting ChAdOx1 PPR H BAC plasmid (labelled p5883) was carried out exactly as described for the ChAdOx1 RVF plasmid.

2.2.4 QC of vaccine constructs' genetic sequence

Upon receiving the bulked up virus from VVCF I carried out QC on the sequence. 5 µL virus was added to 15 µL DNAreleasy™ (Anachem) and the following protocol run:

1.	65 °C	15 minutes
2.	96 °C	2 minutes
3.	65 °C	4 minutes
4.	96 °C	1 minute
5.	65 °C	1 minute
6.	96 °C	30 seconds

Flank to flank PCR on this material was carried out to confirm antigen was present and of correct size for downstream sequencing:

Forward primer (J1170)	5 µL (of 10 µM stock)
Reverse primer (J1210)	5 µL (of 10 µM stock)
Phusion MM	25 µL
H_2O	10 µL
Template DNA	5 µL

DNA was sent to Frederic Jackson at the CBF for NGS. After confirmation of correct sequence, plasmid was linearised with PmeI as described earlier and handed to VVCF for bulking up. DNA was then purified from virus for further NGS using QIAamp DNA Blood Mini Kit (Qiagen) according to manufacturer's instructions. DNA was eluted in 150 µL H_2O and passed again to Frederic Jackson at the CBF for NGS. NGS data in excel format was then sent to me for analysis.

For ChAdOx1 RVF, the same PCR conditions as described for the flank to flank PCR in 2.2.1 were used to provide additional verification of the correct GnGc sequence (at this point, NGS was not fully validated for vaccines destined for clinical trials). PCR product was cleaned-up according to manufacturer's instructions and sent to Source Bioscience for Sanger sequencing along with the following primers:

Primer ID	Sequence (5' – 3')
fwd1_newinsert	CACTGTCCTAACAACTACCAG
fwd2_newinsert	GGCTCTAAGAAATGTACAGG
fwd3_newinsert	GCCCACGGACTGATCAATTAC
fwd4_newinsert	GGCGTGAAAGAGGATCAGACC
fwd5_newinsert	GCCGAGGGCATCAGCGGCAGC
fwd6_newinsert	GCCGGCGCTAGAGTGTGCCTG
rev1_newinsert	GTCGTTGTTCAGATGGTGGGC
rev2_newinsert	CCGCCGATCTTAGGACACTGG
rev3_newinsert	CACCAGGCAAGGGTCTTGTGG
rev4_newinsert	GGGCAGTGCCAGACAGTCTGC
rev5_newinsert	GGAGCTGCTGGCGCCCAGATC
rev6_newinsert	CGGTCAGATTCAGAAAGGCGG
J1170	GGAGTATTTACGGTAAACTGCCCACTTG
J1210	CAGGAGCTCTAGCATTTAGG

2.2.5 QC of vaccine construct antigen expression

$5x10^5$ HeLa cells per well were seeded into a 6-well plate and incubated at 37 °C overnight. Media was aspirated, wells washed twice with DPBS and 3 mL of vaccine diluted in D2 was added to each

well (10 MOI). Plate was incubated for 24 h at 37 °C. Virus was aspirated, wells washed 3x with 2 mL DPBS. 1 mL DBPS was added to each well followed by cell scraping and collection into a 2 mL tube. 1 mL DPBS was added to each well again and aspirated into the corresponding 2 mL tube. Tubes were centrifuged at 13,000 g for 5 minutes. Supernatant was discarded and cell pellets lysed with 300 µL M-PER Mammalian Protein Extraction reagent (Thermo Scientific) and 3 µL HALT 100x Protease Inhibitor (Thermoscientific) and incubated at RT for 5 minutes. Tubes were centrifuged as before and the supernatant collected and stored at -80°C until required. The lysate was tested by Western blot as described on page 31.

For detection of antigens by fluorescent microscopy. HeLa cells were seeded and infected exactly as described above, except a coverslip was added to each well prior to addition of cells. 24 h post-infection with vaccine constructs, virus was aspirated. Wells were washed twice with 3 mL DPBS and aspirated. 800 µL of neutral buffered 10% formalin, 4% formaldehyde was added for 10 minutes on ice followed by 20 minutes at RT. Wells were washed 3x with 3 mL PBS and aspirated. Cells were permeablised with 1 mL/well of 0.2% Triton™ X-100 in PBS (Sigma) and placed on a plate rocker for 10 minutes at RT. Wells were washed as before and blocked with 2 mL/well of 1% BSA in DPBS (blocking buffer, Sigma) and placed on a plate rocker for 30 minutes at RT. Wells were washed again before addition of 800 µL/well of C77 mAb (PPRV H) or 4D4 mAb (RVFV Gn) diluted 1:200 in blocking buffer and incubated for 2.5 h at RT on the plate rocker. Wells were washed and 800 µL/well of secondary anti-mouse AF488 (Life Technologies) diluted 1:1000 in blocking buffer was added and incubated for 1.5h at RT on the plate rocker. Wells were washed a final time. 40 µL of Hardset Vectorshield with DAPI (2BScientific) was placed onto a glass slide. The coverslips at the bottom of the 6 well plates were then picked off using a needle and carfully placed face down on top of the slide containing the Vectorshield drop. Slides were assessed using a Leica DMI3000 B fluorescent microscope.

2.2.6 Genetic stability testing

HEK293 cells or T-REx cells were seeded in six well plates overnight ($0.5x10^6$/well). The following day, at >80% confluency, 10 MOI of ChAdOx1 RVF was added. 24 h later cells were checked for cytopathic effect (CPE). 48 h post-infection, cells were harvested. The media was aspirated and the cells scraped and collected into a 15 mL tube by rinsing the well with 2 mL DPBS twice. Cells were centrifuged at 1800 rpm for 5 minutes. Cells were resuspended in 1 mL PBS and transferred to a 1.25 mL Apex tube. Vials were snap frozen and thawed 3x in ethanol and dry ice to break open the cells. Lysates were centrifuged again at 1800 rpm and supernatant harvested and stored at -80°C until required for the next passage. For the next passage, duplicate wells were infected by adding 5, 20 or 100 µL of the previous lysate. The concentration of virus that resulted in similar CPE after 24 h was then harvested 48 h post-infection as above. This was repeated for 10 passages.

For NGS sequencing, DNA was prepared as described above using QIAamp DNA Blood Mini Kit (Qiagen).

2.3 Serology

2.3.1 Human total IgG enzyme-linked immunosorbent assays (ELISAs)

A positive reference serum was made by pooling samples from naturally exposed Kenyan adults previously identified as having high titres of neutralising antibodies against RVFV. This was included on each plate as a standard curve and was serially diluted in 2-fold steps from 1:100 to 1:51,200 in 1% casein in PBS (ThermoFisher). Each dilution was added to the plate in duplicate, with the 1:100 dilutions given an arbitrary value of 10 RVFV antibody units (AU).

96 well NUNC flat bottom plates (ThermoFisher) were coated with 50 µL/well of Gc or Gn protein at a concentration of 1 µg/mL in DPBS (Sigma) before covering and incubating overnight at 4°C. Plates were washed 6x with phosphate buffered saline containing 0.05% Tween20 (PBS/T) followed

by blocking with 100 µL/well of casein for 1 hour at RT. Plates were then tapped dry and Test Sera were diluted 1:100 in casein. 50 µl/well was added to triplicate wells and incubated for 2 hours at RT. Plates were washed again as before and 50 µL/well of secondary antibody (goat anti-human whole IgG conjugated to HRP, Insight Biotechnology) was diluted 1:1000 in casein and added to the plate for 1h at RT. Plates were washed a final time and developed by adding 50 µL/well of TMB developer (Abcam). After 8 minutes incubating in the dark at RT, 100 µL TMB stop solution (Abcam) was added. The optical density (OD) was read at 450 nm using a Varioskan flash reader. For the clinical trial chapter, a different secondary antibody was used (goat anti-human whole IgG-ALP (Sigma Aldrich). Plates were developed by adding 50 µl/well of 4-nitrophenyl phosphate in diethanolamine buffer (Pierce). OD was read at 405 nm when the internal control reached an OD of 1.0. OD values were then fitted to a 4-parameter standard curve using Gen5 software (BioTek). An internal control was included on every plate, made up from a 1:800 dilution of the positive standard. Test sera antibody units were calculated from their OD values using the parameters estimated from the standard curve. Any Test Serum sample giving an OD of >2.0 was repeated by diluting the sample further.

2.3.2 Human total IgG avidity ELISAs

Total IgG avidity was determined by sodium thiocyanate (NaSCN) displacement as described previously [152]. Using the total IgG ELISA data, sera were individually diluted in casein according to their AU values to normalise titres (e.g. a 300 AU sample was diluted 1:300 etc.). The assay was carried out as described for total IgG with the following exceptions: Each sample was added to 12 wells of a 96 well plate. An additional step, directly after the wash following 2h incubation of Test Sera, was carried out where 50 µL of PBS or NaSCN (in 1M increments from 1M to 5M was added in duplicate for each sample and incubated at RT for 15 minutes. Plates were washed, secondary antibody was added and plates developed exactly as per the total IgG assay. The IC50, determining

the concentration of NaSCN that results in a 50% reduction in ELISA OD compared to their PBS duplicates was calculated.

2.3.3 Human IgG subclass ELISAs

These were performed as per the total IgG ELISAs with the following exceptions: Secondary antibodies (biotin conjugated mouse anti-human IgG1, IgG2, IgG3 or IgG4, Bio-Rad) were incubated for 1h. After washing, 50 µL/well of eXtravidin-ALP (Sigma), diluted 1:5000 in casein was added for 1h. Plates were developed by adding 50 µl/well of 4-nitrophenyl phosphate in diethanolamine buffer (Pierce). OD was read at 405 nm.

2.3.4 Livestock total IgG ELISA

Plates were coated with 50µl/well of monoclonal antibody towards RVFV Gc (5E2) or Gn (4D4) at a concentration of 1 µg/mL in DPBS and incubated overnight at RT. Plates were washed and blocked as described above. Plates were then tapped dry and 50 µL/well of Gc protein or Gn protein (1 µg/ml), diluted in casein was added for 1 hour. Plates were washed as before and Test Sera were diluted 1:100 (pre-challenge time points) or 1:800 (post-challenge time points). 50 µL/well was added to duplicate wells and incubated for 2 hours at RT. ELISAs were then completed as per the human protocol, with the exception of the secondary antibodies used (Goat/sheep: donkey anti-sheep/goat IgG HRP, 1:15,000, Bio-Rad. Cattle: mouse anti-bovine IgG HRP, 1:500, Bio-Rad). Any Test Sera with OD >2.0 was repeated at higher dilutions. Any Test Sera with OD <0.25 was repeated at lower dilutions (with a minimum dilution of 1:100).

2.3.5 Mouse total IgG ELISA

A positive reference serum made from a pool of high responding mice was included on each plate as a standard curve. This was serially diluted in 2-fold steps from 1:200 to 1:102,400 in PBS/T. Each

dilution was added to the plate in duplicate, with the 1:100 dilutions given an arbitrary value of 16 RVFV antibody units (AU).

96 well NUNC flat bottom plates (ThermoFisher) were coated with 50 µL/well of Gc or Gn protein at a concentration of 1 µg/mL in PBS (Sigma) and incubated overnight at RT. Plates were washed 6x with PBS/T followed by blocking with 100 µL/well of PBS containing 10% skimmed milk (Sigma) for 1 hour at RT. Plates were washed and Test Sera was diluted 1:100 in PBS/T. 50 µL/well was added to duplicate wells and incubated for 2 hours at RT. Plates were washed again as before and 50 µL/well of secondary antibody (goat anti-mouse IgG conjugated to ALP, Sigma Aldrich) was diluted 1:1000 in PBS/T and added to the plate for 1h at RT. Plates were washed a final time and developed by adding 50 µL/well of 4-nitrophenyl phosphate in diethanolamine buffer (Pierce). OD was read at 405 nm until an internal control made up from a 1:800 dilution of the positive standard reached an OD value of 1.0. OD values were then fitted to a 4-parameter standard curve using Gen5 software (BioTek). Test sera antibody units were calculated from their OD values using the parameters estimated from the standard curve. Any Test Serum sample giving an OD of >2.0 was repeated by diluting the sample further.

2.3.6 RVFV neutralisation assays

2.3.6.1 MP-12 virus neutralisation titre (VNT)

The 50% neutralising titre (VNT_{50}) was calculated as described previously [104]. Briefly, serum pools were diluted in DMEM containing 10% FCS, 1% L-glutamine and 1% penicillin/streptomycin (D10) across a 96-well plate (100 µL/well) in quadruplicate before addition of 100 $TCID_{50}$ of RVFV MP-12 strain (100 µL/well). Sera and virus were incubated at 37°C for 1 h before being added to a 96 well tissue culture (TC) plate containing 50 µL a confluent monolayer of Vero E6 cells (10^5 cells in 50 µL per well were seeded the day before). Plates were incubated at 37°C for 72h before cells were fixed by adding 50 µL/well of PBS containing 10% formaldehyde for 1h. Plates were aspirated and stained

with PBS containing 1% crystal violet (Sigma) for 10 minutes. Plates were washed with water and left to dry before being scored by eye. The Spearman-Karber method was used to determine the VNT_{50} of each sample.

2.3.6.2 RVFV-4s-eGFP VNT

Test sera were diluted in D5 in triplicate starting at 1:40 followed by 7 serial titrations of 1:2 with a final volume of 50 µL per well in 96 well TC plates. 50 µL of RVFV-4s eGFP, diluted in D5 media to $1x10^{3.6}$ $TCID_{50}$, was added to each well and incubated at RT for 2 h. 50 µL of Vero E6 cells, diluted to $4x10^5$ / mL in D5 was then added to each well before plates were incubated for 48 hours at 37 °C with 5% CO_2. A virus-only control plate (identical to the test sera plates, only with 50 µL media added in place of serum [48 wells]) was incubated with the other plates.

Plates were aspirated and then fixed by adding 100 µL of 4% formaldehyde for 20 minutes. Formaldehyde was aspirated and plates were washed 3x with PBS. Plates containing 300 µL PBS per well were then left in the CL3 hood while fumigation took place overnight. The following day, once the hoods were purged, the plates were removed from CL3 and read on a fluorescent AID ELISpot reader. Wells were considered positive if they showed an 80% reduction in spots compared to the average spot count of the 48 virus-only wells. VNT_{80} was calculated by taking the log2 of the maximum dilution showing at least an 80% reduction in spots. Where replicates had different maximum dilutions showing an 80% reduction, an average of the log2 dilutions was taken.

2.3.6.3 MP-12 Focus-reduction neutralising titre assay (FRNT) [Chapter 3]

FRNT neutralisation assay was conducted as previously described [153] with some alterations. Briefly, serum was diluted in D10 in 2-fold steps in triplicate using 96 well U-bottom plates from a starting dilution of 1:20. MP-12 RVFV was diluted to give approximately 100 focus-forming units in the absence of serum. This was added to each well and incubated for 1h at 37 °C before transferring

mixture to 96-well TC plates containing Vero E6 monolayers at >80% confluence (seeded the day before at $2x10^5$ cells/mL in D10, 50 µL/well). After 2h at 37 °C, virus/serum was removed and replaced with D10 media. Plates were incubated a further 48h at 37 °C. Virus foci were detected by adding 1:1000 dilution of Anti-Gn 4D4 mouse mAb in D10 for 2h followed by 1:1000 dilution of horseradish peroxidase (HRP)-conjugated goat anti-mouse IgG antibody in D10 for 1h (Abcam, Cat. No. ab6789). After addition of 3,3'-diaminobenzidine (Sigma) substrate for 10 minutes at room temperature, the plates were washed a final time and air dried. Foci were counted using an AID ELISpot reader. Serum dilution required to reduce virus foci by 50% compared to virus-only control wells (6 replicates) was calculated from a 4 parameter standard curve using GraphPad Prism version 8 (GraphPad Software Inc., California, USA). Initial screening of Kilifi samples to identify positives was undertaken by myself, HK, JG, and MC.

2.3.6.4 RVFV-4s-eGFP FRNT [Chapter 5]

A very similar method to the MP-12 FRNT was carried out with the following changes. Serum was diluted in 2-fold steps in duplicate from a starting dilution of 1:80, 100 µL/well. 100 µL of 10,000 $TCID_{50}$/mL RVFV-4s-eGFP was added to each well and incubated at 37 °C for 1h. Each plate contained a negative control serum and a positive control serum in duplicate. Each plate also contained media-only wells in duplicate (200 µL media, no virus) in addition to 10 wells of virus-only (100 µL media + 100 µL virus).

After the 1 h incubation, 100 µL/well of the serum/virus U-bottom plates was then transferred to 96-well TC plates containing Vero E6 monolayers at >80% confluence (seeded the day before at $2x10^5$ cells/mL in D10, 50 µL/well). TC plates were incubated for 15-18h in 37 °C, 5% CO_2. Plates were then developed in exactly the same way as for the MP-12 FRNT assay. Serum dilution required to reduce virus foci by 50% compared to virus-only control wells (10 replicates) was calculated from

a 4 parameter standard curve using GraphPad Prism version 9 (GraphPad Software Inc., California, USA).

2.3.7 Gn- and Gc-specific antibody depletion

6 serum samples collected in 2018 from Kenyan adults that previously tested positive by FRNT were pooled. In order to deplete αGc and/or αGn antibodies, 96-well NUNC ELISA plates were coated with 5 µg/mL of recombinant Gn, Gc, or DPBS alone. Plates were incubated overnight at 4 °C. After washing with PBS/T as previously described, plates were blocked with 200 µL/well of 1% casein in PBS (Sigma) for 2h. Neat pooled human sera was diluted 1:50 in D0 (DMEM containing 2% L-glutamine and 1% penicillin/streptomycin) with subsequent 1:2 titrations. Diluted sera was added to each antigen coated plate (including uncoated) and incubated on a plate rocker for 4h at room temperature. Serum was then removed and added to another freshly coated and blocked plate containing the same antigen. For duel depletion, these steps were repeated on freshly coated and blocked plates containing the heterologous antigen. Reduction of antigen-specific IgG was confirmed by ELISA. The remaining serum was added directly to the MP-12 FRNT assay. $FRNT_{50}$ was calculated as described above.

2.4 Mouse vaccinations

All mouse vaccinations and blood collections, apart from chapter 4, were carried out by Alex Spencer and Marta Ulaszewska, both at the Jenner Institute. Female BALB/c mice between 6-12 weeks old were vaccinated with $5x10^7$, $1x10^8$ or $4x10^8$ IU of ChAdOx1 RVF. Mouse work in chapter 4 was carried out by Sandy Douglas and Adam Berg. Female BALB/c mice between 6-8 weeks old were vaccinated with $1x10^5$, $1x10^6$ or $1x10^7$ IU ChAdOx1 RVF. For all mouse work, serum was collected by cardiac bleed 28 days post vaccination.

2.5 Naturally exposed Kenyan adults study population [chapter 3]

Volunteers were enrolled as part of a previous study estimating RVFV exposure by Bernard Bett *et al* [154]. I had no part in sample collection or processing. Briefly, a cross-section of randomly selected households in Tana River County, Kenya (2013-2014) were enrolled after consenting and all human subjects within that household were sampled. For this analysis, serum samples from 50 adults ≥18 years old (n = 26 male, n = 24 female) were selected at random for antibody characterization from those identified as RVFV-exposed on the basis of seropositivity by both RVFV neutralization assay (VNT50 >10) and a diagnostic ELISA kit (BDSL, National Institute for Communicable Diseases, Centre for Emerging and Zoonotic Diseases, Johannesburg, South Africa) undertaken by Bernard Bett *et al*. [155]. A further 6 RVFV-exposed individuals from the same study were assessed in the antibody depletion assays. Serum and peripheral blood mononuclear cells (PBMCs) were available from 200 adults ≥18 years old (n = 72 male, n = 128 female) under longitudinal surveillance for malaria studies in Kilifi County in 2018. Blood samples were collected in plain vacutainers and serum harvested after centrifugation at 1,000 RCF for 5 minutes, before storage at -80°C until use. For some of these adults, serum samples were available dating back to 1998 when they were enrolled into the longitudinal cohort. Additional screening of the serum samples collected in 2013-2014 identified positive individuals not sampled in 2018 (this was undertaken by me, J.N.G, H.K.K, and M.H.A.C. Heparinised blood was used for PBMC isolation using standard protocols [156] and were resuspended in FCS containing 10% DMSO prior to freezing. Vials containing ~$5x10^6$ PBMC in 1mL were slowly cooled to -80°C in Mr Frosty's before being transferred to liquid nitrogen until use. Ethical approval for this study was provided by the Kenya Medical Research Institute Scientific and Ethics Review Unit (SSC 3296), and the African Medical Research Foundation's Ethics and Scientific Review Committee (approval number P65-2013).

2.6 RVF001 Clinical trial [chapter 5]

A phase I study to determine the safety and immunogenicity of the candidate Rift Valley Fever Virus (RVFV) vaccine ChAdOx1 RVF in UK healthy adult volunteers. ClinicalTrials.gov Identifier: NCT04754776

2.6.1 Vaccination

ChAdOx1 RVF was manufactured by Advent S.r.l., Pomezia, Italy. Volunteers were vaccinated by intramuscular route with $5x10^9$ vp (Group 1, n = 3), $2.5x10^{10}$ vp (Group 2, n = 6) or $5x10^{10}$ vp (Group 3, n = 6).

2.6.2 Ethics and regulatory approval

This trial was undertaken with ethical approval granted by the Research Ethics Committee (REC). The trial fully complies with Good Clinical Practice (GCP) and complies with the Medicines for Human Use (Clinical Trial) Regulations 2004, the Declaration of Helsinki, and all other applicable regulatory requirements. All volunteers have signed the informed consent form. At the screening visit, the volunteers were fully informed of all aspects of the trial, the potential risks and their obligations.

2.6.3 Serum collection

All clinical trial blood samples were processed at BSL2 under Good Clinical Practice. Red-top vacutainers containing ~9 mL blood were centrifuged at 1800 rpm for 5 minutes. Approximately 4 mL of serum was transferred into two cryovials using a pastette pipette and stored at -80°C until required.

2.6.4 PBMC separation and freezing

Blood samples in 4x green-top lithium heparin tubes from each volunteer (~40 mL total) were poured into two Leucocep tubes (previously prepared and already containing 15 mL lymphoprep). Tubes were spun at 1000 g for 13 minutes with no brake. ~4 mL Plasma was taken from the top layer using a pastette and stored in two cryovials at -80°C. Everything else above the membrane in each of the two leucocep tubes, including the PBMC layer, was poured into separate 50 mL tubes and each topped up to 40 mL with RPMI + 1% L-glutamine and 1% penicillin/streptomycin (R0). Tubes containing PBMCs were spun at 1800 rpm for 5 minutes. Supernatant was discarded and both tubes from the same volunteer were resuspended and combined into a single 50 mL tube and topped up to 30 mL with R0. Cells were again spun at 1800 rpm for 5 minutes. Supernatant was discarded and cells were resuspended in 10 mL R10 (identical to R0 but also containing 10% FCS) and incubated at 37°C prior to counting. Cells were counted using a Casy Counter and resuspended in R10 to a concentration of $5x10^6$ / mL for ELISpot plating (described below).

After using the required number of cells for ELISpot, the remaining cells were centrifuged at 1800 rpm for 5 minutes. Cells were resuspended in cold FCS, between ~$10\text{-}16x10^6$ / mL and incubated at 4 °C for 20 minutes. The same volume again of chilled 20% DMSO was added making ~$5\text{-}8x10^6$ / mL of 10% DMSO final concentration. This was transferred into cryovials, 1mL per vial and placed in Cool Cells before storage at -80 °C overnight. The following day, PBMC vials were transferred to liquid nitrogen for long-term storage.

2.7 Ex vivo ELISpots

2.7.1 Naturally exposed human PBMC [chapter 3]

264 15mer peptides overlapping by 11 amino acids, covering the Gn-Gc polyprotein (Genbank accession number DQ380208, bases 411–3614) were synthesised (Mimotopes) with crude purity. Peptides were reconstituted to 100 mg/mL in DMSO. Peptides were further diluted and split into 5

pools of 52/53 peptides each at 1.25 µg/mL final concentration in RPMI containing 10% FCS, 1% L-glutamine and 1% penicillin/streptomycin (R10). ELISpots were carried out as previously described [157]. Briefly, ELISpot plates were coated with capture mAb, 1-D1K (Mabtech) diluted 1:100 in carbonate-bicarbonate buffer (coating buffer), 50 µL per well, wrapped in cling film and incubated 16-72 overnight at 4°C. Plates were washed 3x with sterile PBS and blocked with 100 µL of R10 for 1-5 hours. R10 was flicked off and 50 µL peptides (2.5 µg/mL concentration) were added according to the plate layout, 50 µL per well (1.25 µg/mL peptide final concentration). Positive control wells were stimulated with SEB at 0.02 µg/mL. PBMC were diluted to $4x10^6$ / mL and 50 µL added to each well ($2x10^5$ PBMC/well). Plates were incubated at 37 °C, 5% CO_2 for 16-20 hours. Plates were then washed 6x with PBS/T before addition of 50 µL/well biotinylated detection mAb, 7-B6-1 (Mabtech), diluted 1:1000 in PBS and incubated at RT for 2-4 h. Plates were washed as before and 50 µL/well Streptavidin-ALP (Mabtech) diluted 1:1000 in PBS was added and incubated at RT for 1-2 h. Plates were washed and developed by addition of 50 µL/well BCIP/NBT-plus substrate (Mabtech). After ~3 minutes plates were washed under tap water and dried before reading on an AID ELISpot plate reader. Responses from unstimulated wells were subtracted before quantifying the response to the 5 pools and summing them.

2.7.2 Human ChAdOx1 RVF clinical trial PBMC [chapter 5]

Clinical trial ELISpots were carried out in a very similar way to above with the following exceptions. 264 15mer peptides overlapping by 11 amino acids, covering the Gn-Gc polyprotein (Genbank accession number DQ380208, bases 411–3614) were synthesised (ProImmune) with >80% purity. After reconstituted to 100 mg/mL in DMSO, peptides were further diluted and split into 10 pools of 25/26 peptides each at 5 µg/mL final concentration. PBMC were diluted to $5x10^6$ / mL and 50 µL added to each well in triplicate ($2.5x10^5$ PBMC/well). Positive control wells were stimulated with 50 µL/well anti-human CD3 mAb, CD3-2 (Mabtech) diluted to 0.04 µg/mL in R10. Responses from

unstimulated wells were subtracted before quantifying the response to the 10 pools and summing them.

2.7.3 Livestock PBMC

ELISpots were carried out in the same way as for the clinical trial human ELISpots with the following differences: Antibody kit used was for Bovine which also cross-reacts with sheep and goat IFNγ (mAbtech). PBMC were assayed from frozen rather than fresh. Cells were thawed as previously described and resuspended to $4x10^6$ (200,000 cells per well). Each pool was assayed in duplicate. PMA/Ionomycin without Brefeldin A (BioLegend) dilluted 1:500 in R10 was used as a positive control. All Antibody development steps were diluted in PBS containing 0.5% FCS.

2.8 Statistical analysis

Normality tests were carried out using D'Agostino & Pearsan test. Correlations were calculated using (mostly non-parametric) Spearman tests. Unpaired T test (parametric) or Mann Whitney test (non-parametric) were used to compare two groups. Paired T test (parametric) or Wilcoxon matched-pairs signed rank test (non-parametric) were used to compare a single pre- and post-vaccine timepoint. RM one way ANOVA (or if some values were missing, then Mixed-effects analysis) with Geisser-Greenhouse correction and Dunnett's multiple comparisons test were used to compare between pre-vaccine and multiple post-vaccine timepoints from the same individuals. Kruskal Wallace with Dunn's multiple comparisons (non-parametric) was used to compare multiple groups. Unpaired T test was used to compare two area under the curves (AUC). EC50s were compared by Extra sum-of-squares F test. All statistics were calculated using GraphPad Prism version 8 or 9 (GraphPad Software Inc., California, USA).

3

Characterisation of naturally acquired immunity to RVFV among Kenyan adults

This Chapter is based on the published paper: ***Wright D.****, Allen, E. R., Clark, M. H. A., Gitonga, J. N., Karanja, H. K., Hulswit, R. J. G., Taylor, I., Biswas, S., Marshall, J., Mwololo, D., et al. Naturally Acquired Rift Valley Fever Virus Neutralising Antibodies Predominantly Target the Gn Glycoprotein. iScience. 2020;23(11). All text included in this chapter was originally written by myself. All figures were made by myself.*

Contributions: DW + ERA: expressed Gn/Gc proteins. G.M.W: VNTs in Figure 1. D.W: Depletion assay, VNTs, FRNTs, ELISAs, ELISpots. I.T + S.B + D.M. + J.M: Tana River County sample collection. D.W + J.N.G + H.K.K + M.H.A.C: Screened naturally exposed individuals from Kilifi County to identify positives (data not included). G.M.W + T.A.B: Supervision

3.1 Introduction:

Historical studies have demonstrated that livestock and non-human primates that recover from RVFV infection are protected upon re-exposure, and this can be passively transferred to susceptible animals through administration of convalescent sera [6, 96]. Neutralising antibodies elicited post-infection, that target RVFV Gn and Gc, are correlated with this protection [7]. A correlate of protection may either be mechanistic; directly causing the protection, or non-mechanistic whereby it simply correlates with another immune measure that is causing the protection [158]. While passive transfer of serum shows protection can be achieved in the absence of cellular immunity, ruling out the impact of non-neutralising antibodies or Fc functions of neutralising antibodies is difficult. Neutralising mAbs have, however, provided protection in vivo using animal models [94, 99, 100, 132, 133]. Identifying the minimal nAb titre associated with protection would be extremely beneficial. In humans, occupational exposure to RVFV infection during the decades following the discovery of RVFV provided the first evidence of naturally acquired RVFV nAbs and these could be long-lived, being readily detectable in two individuals 12 and 25 years post-infection, respectively, despite no further exposure [98, 159]. However, beyond these case studies, naturally acquired immunity to RVFV in humans is poorly described. Here, I sought to address this paucity of information by characterizing the humoral and cellular response to RVFV among naturally exposed adults in Kenya, including an investigation of the longevity and kinetics of RVFV nAbs in this population. Additional qualitative attributes of the humoral response to RVFV, such as avidity and the IgG subclasses predominantly involved, may also be important factors contributing to protection and these too have been assessed.

3.2 Objectives:

1. Produce RVFV Gn and Gc recombinant glycoproteins to enable assays measuring the immune response towards them.

2. To characterize the total IgG titre, avidity and subclass response towards the two glycoproteins, Gn and Gc.
3. To investigate the relative importance of antibodies towards Gn and Gc by measuring the impact on RVFV neutralisation in vitro after depleting pooled human sera of antibodies towards one or both glycoproteins.
4. To investigate the kinetics and longevity of the humoral response over multiple years in historically infected individuals.
5. To investigate the cellular immune response after historical infection by measuring IFNγ production after PBMC stimulation with peptides spanning the Gn-Gc polyprotein and nucleoprotein.

3.3 Results:

Stored samples from two adult populations in coastal Kenya were used for this study (see Methods). One population comprised a random selection of fifty RVFV-exposed individuals included in a previous cross-sectional survey investigating the risk factors for RVFV exposure in Tana River county [154]. The second population was composed of adults under longitudinal surveillance for malaria within the Kilifi Health and Demographic Surveillance System (KHDSS) [160] in Kilifi county and had previously not been screened for RVFV exposure (see Methods).

3.3.1 Production of RVFV Gn and Gc recombinant proteins

I first expressed the recombinant ecto domains of Gn and Gc using the mammalian HEK293 cell line as described in Materials and Methods. Proteins were initially purified using their HIS tag and further purified by size exclusion chromatography, with resulting fractions run on a gel to confirm correct size band (**Figure 5**).

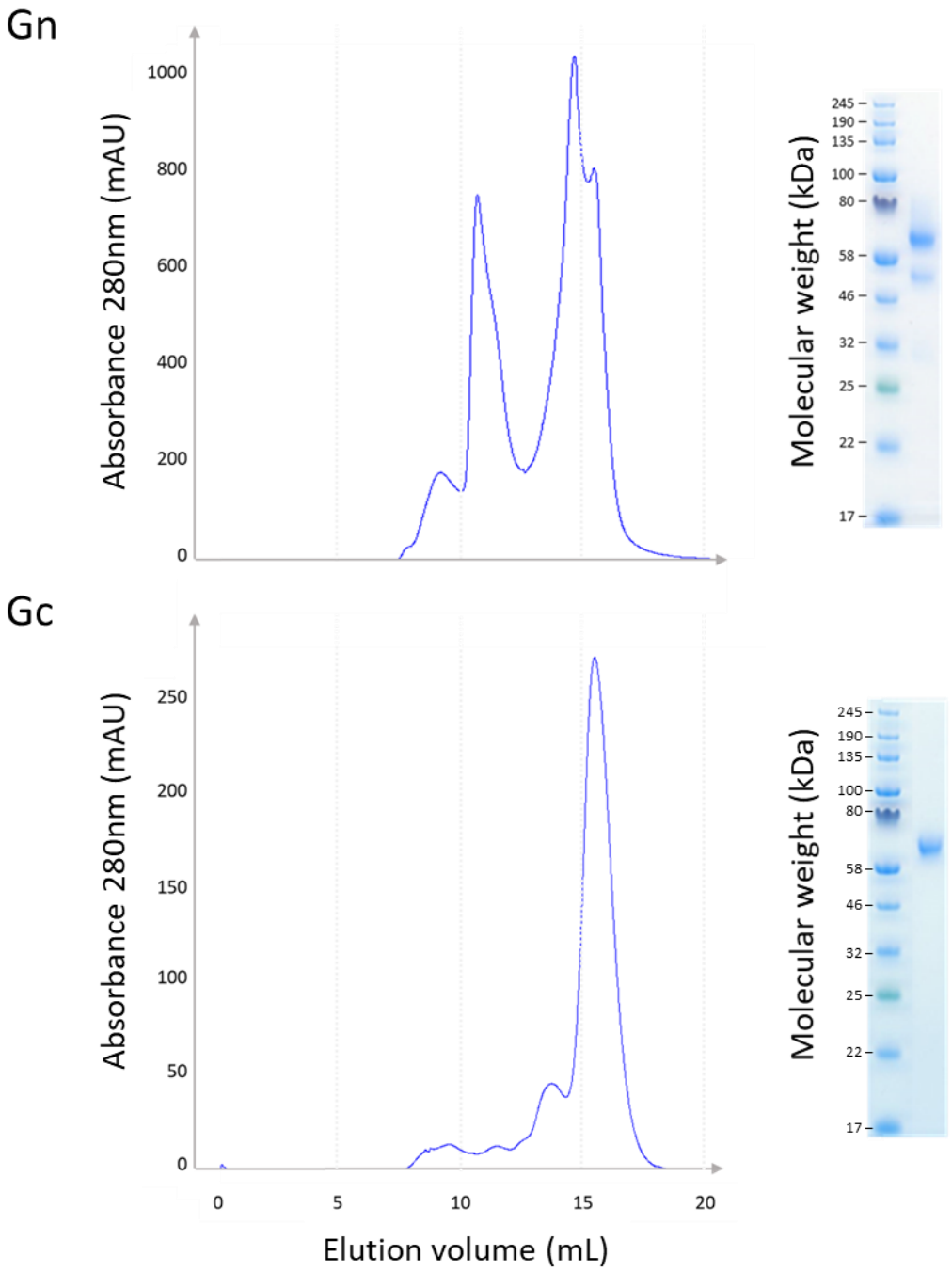


Figure 5. *Recombinant protein production of the RVFV Gn and Gc ecto domain. Histag purified RVFV Gn (top) and RVFV Gc (bottom) purified by size exclusion chromatography. 13-17 mL fraction (Gn) and 14.5-18 mL fraction (Gc) was collected and run on SDS-PAGE. Samples were loaded with reducing buffer on a NuPAGE 4-12 % Mini polyacrylamide gel and stained with Quick Coomassie Stain. Expected molecular weight for both Gn and Gc is ~60 kDa*

3.3.2 Do IgG responses against Gn and Gc correlate with RVFV nAb titres?

To address this, I measured IgG antibody responses against Gn and Gc in fifty RVFV-exposed adults from Tana River county and assessed their relationship with the RVFV nAb response, previously measured by George Warimwe. The geometic mean titre (GMT) of RVFV nAb as measured by virus neutralising assay (VNT_{50}) in these fifty adults was approximately 2100 (95% CI 1543-2792), and ranged between ~160 to >14000 (**Figure 6**). Total IgG titres against Gn (ELISA GMT of 67.3) and Gc (ELISA GMT of 66.9) were highly correlated (r = 0.77, p <0.001, Spearman's correlation). A strong correlation was observed between the RVFV nAb titre and IgG response against Gn (r = 0.76, p <0.0001) and Gc (r = 0.68, p <0.0001) (**Figure 6a**). IgG1 subclass predominated the antibody response against both Gn and Gc (**Figure 6c**).

I also measured the avidity of the antibody response to each glycoprotein, expressing this as the concentration of NaSCN, a chaotropic agent, required to reduce ELISA signal by 50% (NaSCN IC_{50}). Anti-Gc antibody avidity was significantly higher than that for anti-Gn antibodies (**Figure 6b**); however, a correlation between antibody avidity and nAb titre was only observed for Gn (r = 0.37, p = 0.009) and not Gc (r = 0.08, p = 0.57).

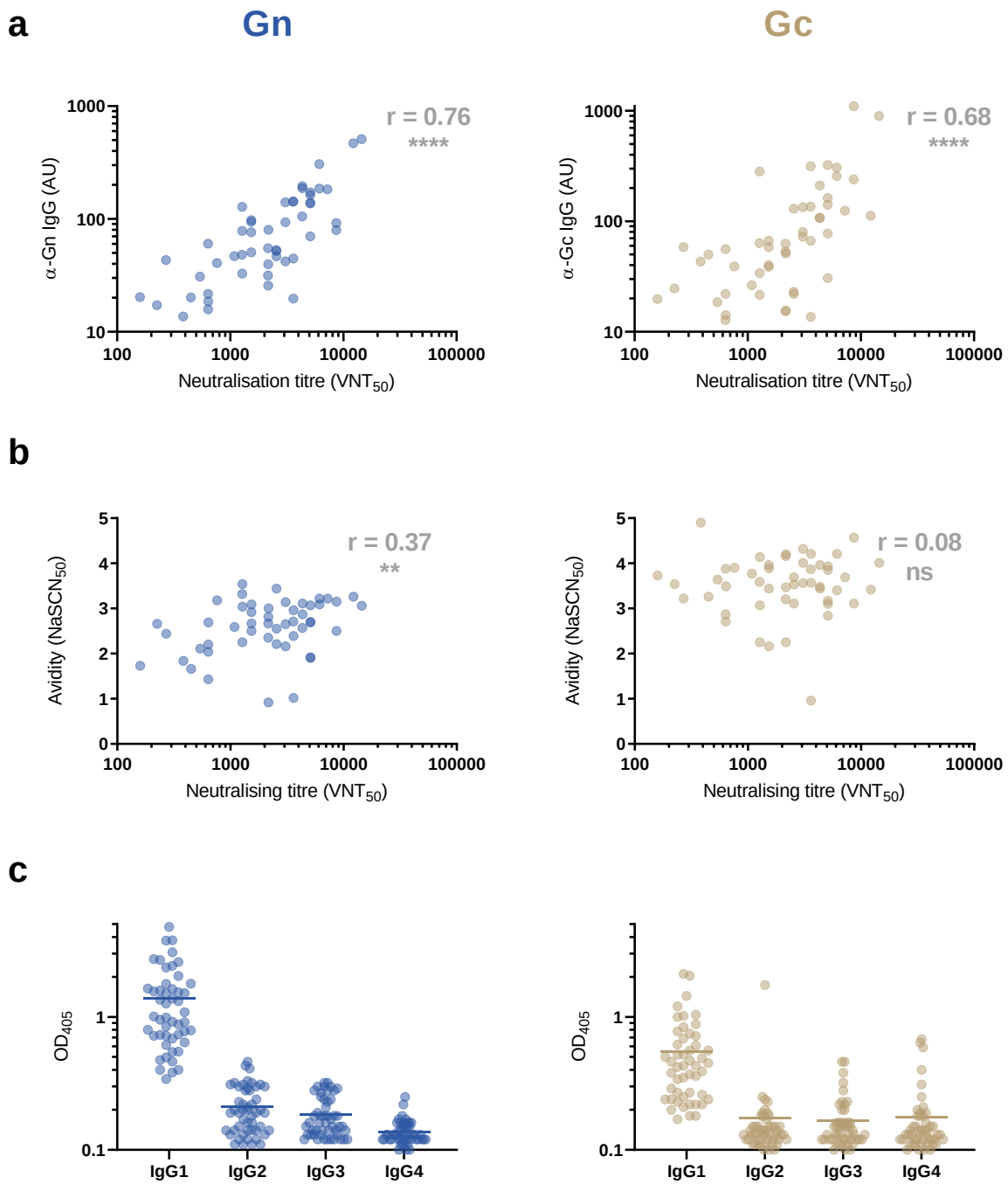
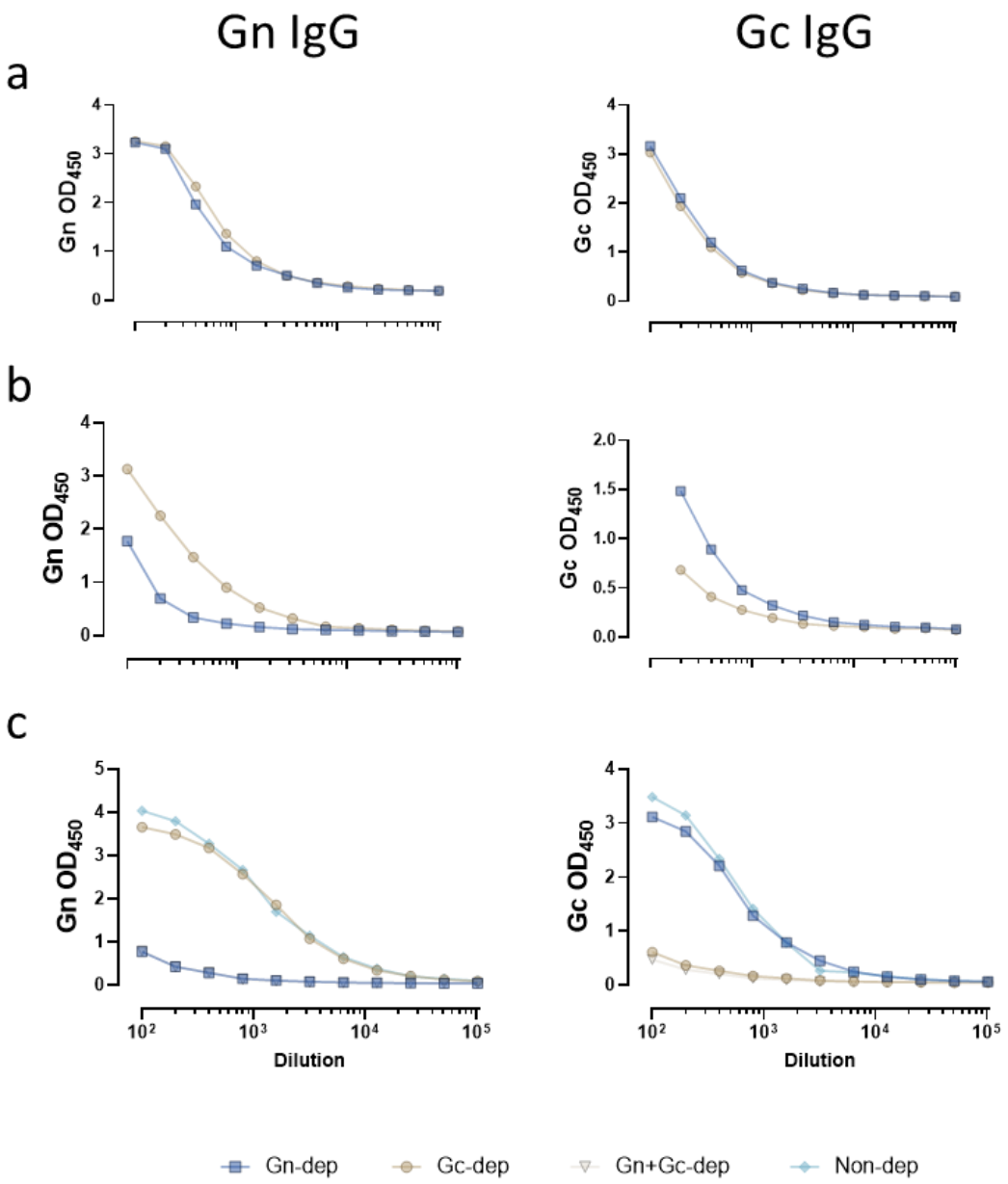


Figure 6. *Total IgG titre towards recombinant Gn and Gc correlate strongly with neutralising antibody titre in 50 adults naturally exposed to RVFV. (a) Correlations between neutralisation titre, as measured by VNT_{50} assay, and total IgG titre towards Gn and Gc, as measured by ELISA (Gn: r = 0.76, 95% CI: 0.60-0.86,****. Gc; r=0.68, 95%CI: 0.49- 0.81,****. Spearman correlation,**** = p < 0.0001. (b) Correlations between neutralisation titre and avidity of total IgG towards Gn and Gc (Gn: r = 0.37, 95% CI: 0.09-0.59, **; Gc: r= 0.08, 95%CI: -0.21-0.36, p=0.57).** = p=0.009. (c) IgG subclass response towards Gn and Gc. Lines represent geometric means. VNTs in (a) and (b) carried out previously by G.W.*

3.3.3 What is the relative contribution of antibodies targeting Gn and Gc to the RVFV nAb response?

To investigate this, I pooled available sera from 6 RVFV-exposed adults from Tana River county that had high titres (>300 anti-Gn and anti-Gc AU). I then depleted the pooled serum of antibodies specific for one or both of the recombinant RVFV glycoproteins (see Methods). Initial attempts involved a coating antigen concentration of 1 µg/mL but antigen-specific depletion was minimal (**Figure 7a**). This was improved by increasing the coating antibody concentration to 5 µg/mL, although antibody depletion was still not particularly effective (**Figure 7b**). Finally, increasing the incubation time and performing two incubation steps, consecutively, using a second freshly coated and blocked plate, resulted in significantly reducing antigen-specific antibody titres (**Figure 7c**).



	Endpoint titre (% of non-depleted pool)	
	Gn ELISA	Gc ELISA
Non-depleted	48,026 (100%)	15,215 (100%)
Gn Ab depleted	784 (2%)	13,434 (88%)
Gc Ab depleted	44,156 (92%)	1,091 (7%)
Gn+Gc Ab depleted	758 (2%)	680 (4%)

Figure 7. *Optimisation of depletion conditions.* ***(a),*** *plates were coated with 1 µg/mL of protein and serum incubated for 2h.* ***(b)*** *plates coated with 5 µg/mL and serum incubated for 2h.* ***c,*** *plates were coated with 5 µg/mL and serum incubated for 3h, repeated twice, consecutively on a freshly coated and blocked plate. Duel-depletion and non-depletion were only carried out in* ***(c).*** *Table represents endpoint ELISA titres from* ***c.*** *anti-human IgG conjugated to alkaline phosphatase was used to detect the antibodies binding to Gn and Gc.*

ELISA was used to confirm the depletion, showing a reduction in IgG endpoint titre of 98% and 93% for Gn and Gc, respectively, compared to non-depleted serum (**Figure 8**). I then measured the impact of this antigen-specific antibody depletion on the ability of the pooled serum to neutralize RVFV in vitro by VNT. Anti-Gn antibody depletion resulted in a 79% reduction in nAb titre compared to the non-depleted serum (**Figure 8**). In contrast, depletion of anti-Gc antibodies from sera showed a modest 29% reduction compared to the non-depleted serum (**Figure 8**). Depletion of both Gn and Gc antibodies showed a 79% reduction in nAb titre, highly similar to the pool depleted of anti-Gn antibodies alone (**Figure 8**).

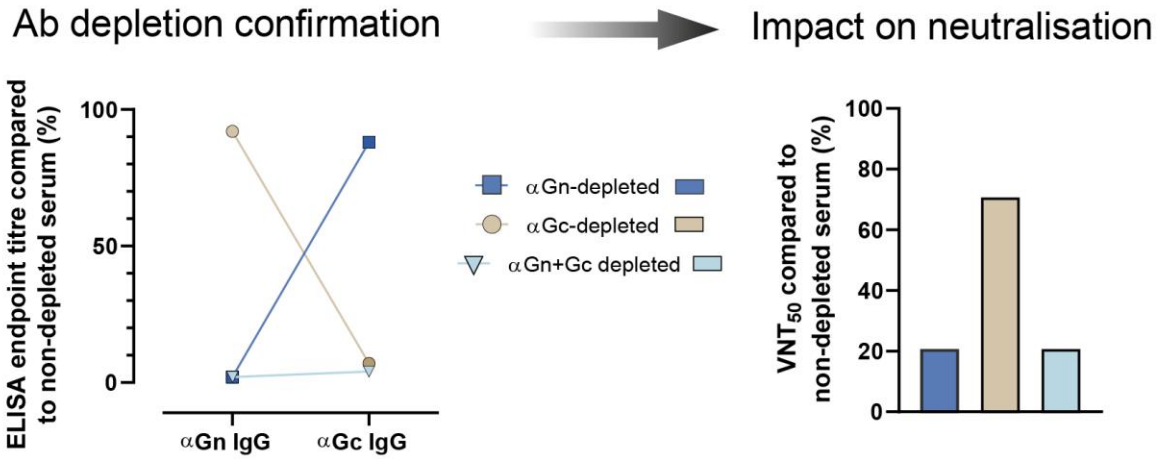


***Figure 8**. Neutralising antibody titres predominantly target RVFV Gn over Gc. Individual sera were pooled from individuals in Tana River county (n = 6) and depleted of anti-Gn antibodies, anti-Gc antibodies, both or neither. (Left) confirmation by endpoint ELISA titre of serum pools after the depletion. Depletion of Gn and Gc antibodies reduced their titres by 98% and 93%, respectively, with minimal impact on titres towards the opposite antigen. Duel depleted serum reduced Gn and Gc titres by 98% and 96%, respectively. (right) Neutralisation titre (VNT_{50}) of each depleted pool as a percentage of non-depleted serum (VNT_{50} of Gn antibody depletion, 1600; Gc antibody depletion, 5344; Gn+Gc antibody depletion, 1600; non-depleted, 7557). ELISA signal was detected using an anti-human IgG secondary antibody conjugated to alkaline phosphatase. Endpoint titres were defined as the dilution required to reduce OD_{405} to background levels (0.150)*

Using sera collected as part of the longitudinal surveillance for malaria studies in Kilifi county, 6/200 (3%) in 2018 had previous RVFV exposure as determined by the presence of RVFV nAbs. To confirm

the predominance of Gn as a target of the RVFV nAb response, I pooled sera from these 6 individuals and repeated the depletion experiment described above using a different assay to measure RVFV nAbs, focus reduction neutralisation assay ($FRNT_{50}$; see Methods). Neutralisation titres determined using this assay also correlate with Gn and Gc binding IgG titres, although the relationship is stronger for Gn than Gc, perhaps reflecting their comparatively greater role in neutralisation (**Figure 9**).

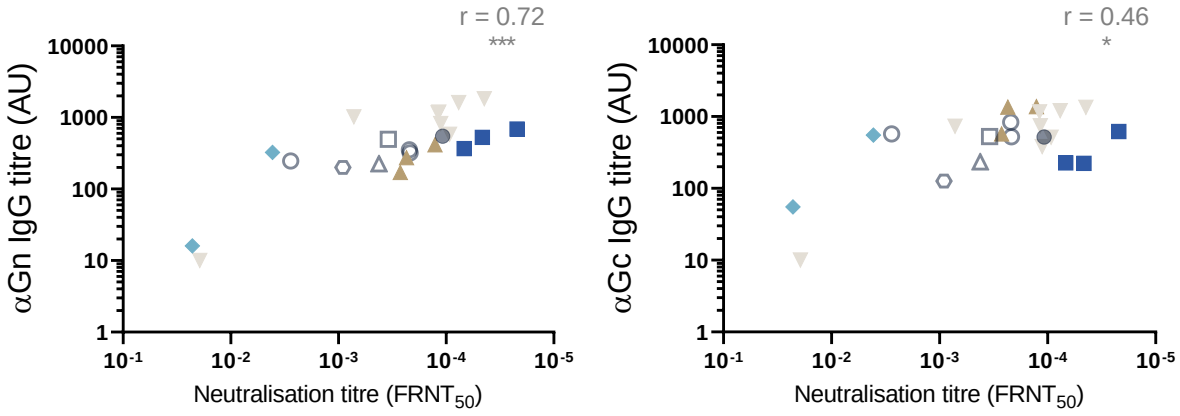


Figure 9. *FRNT titres also correlate with binding IgG titres towards Gn and Gc. 22 serum samples from nine individuals in Kilifi county with serum samples spanning 1-11 years were assayed. Identical symbols are from the same individual over different years (left) Gn: r = 0.72 [95% CI: 0.43 - 0.88]. (right) Gc; r = 0.46 [0.06 - 0.74]. Identical symbols are from the same individual during different years). ***, p = 0.0001; *, p = 0.03, non-parametric spearman correlations*

Depleting a pool of these sera was consistent with the previous data, showing a relative reduction in $FRNT_{50}$ of approximately 71%, 0% and 65% in sera depleted of antibodies to Gn, Gc or both, respectively (**Figure 10**). Variable slope, 4 parameter non-linear regression models of each depleted pool's ability to neutralise RVFV show a statistically significant difference between $FRNT_{50}$ of pools depleted of anti-Gn and anti-Gc ($p < 0.0001$, $F = 17.03$) (**Figure 10**).

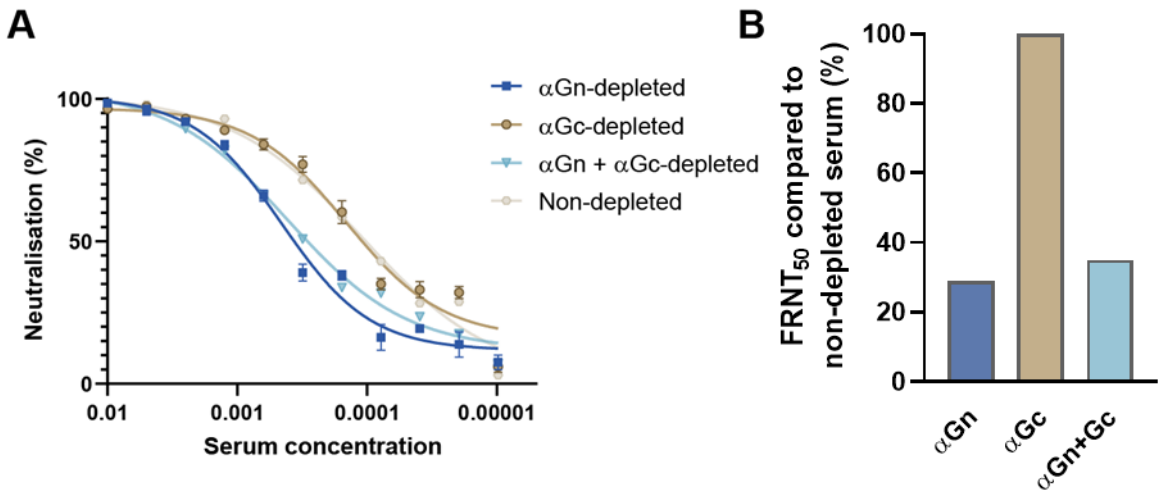


***Figure 10**. Replication of antibody depletion experiment using different serum and different neutralisation assay finds the same result. Serum was pooled from individuals in Kilifi county (n = 6). (left) neutralisation (FRNT) of the depleted or non-depleted pools. 4p non-linear regression, error bars represent SEM of triplicates. (right) $FRNT_{50}$ of the depleted pools in comparison to the non-depleted pool (Gn-depleted $FRNT_{50}$ [reciprocal dilution] = 2,815; Gc-depleted $FRNT_{50}$ = 9,601; Gn+Gc-depleted $FRNT_{50}$ = 3,343)*

As expected from previous studies [99, 100, 131], both Gn and Gc are targeted by neutralising antibodies. These data support RVFV Gn as the major target of the nAb response arising during natural RVFV infection.

3.3.4 What are the long-term kinetics of IgG and RVFV nAb titres after historical infection?

To address this question, I used three of the six RVFV-exposed adults from Kilifi County that had corresponding stored serum samples spanning multiple years between 1998 and 2018. Two additional individuals from earlier years of the same surveillance study, identified as having previous RVFV exposure, were also included. Each of these 5 RVFV-exposed individuals had sera samples spanning between 3-11 years, although it remains unknown when they became exposed (**Figure 11**). Both RVFV nAbs and binding IgG titres were readily detected over the period of follow up (**Figure 11**). Consistent with the two historical case studies on the durability of RVFV nAb titres [62, 98], demonstrating the continued presence of nAbs up to 25 years post-exposure, the

individual from whom I had the highest number of samples, JA0073 (*n* = 8), demonstrated high nAb titres over an 11-year period (**Figure 11a**).

RVFV nAb titres were generally stable with only slight reductions observed (average fold change per year of 0.88-0.95 from peak nAb titres) (**Figure 11**). Individual JA0073 was seronegative when sampled in 2007 but was strongly seropositive in 2008 suggesting they may have been exposed during 2007, when there was a major RVF epidemic in Kenya [161]. JA0193's nAb titre increased >12 fold, possibly as a result of boosting from interepidemic RVFV exposure as no RVF epidemics were reported in the country during their follow up period (**Figure 11**). JA0176 was RVFV naïve in year 0 as evidenced by their lack of nAbs, exposure sometime in the following 4 years induced moderate nAb titers although comparatively lower than the others. Total binding IgG titres towards both Gn and Gc glycoproteins were also long-lasting in all individuals, remaining high despite a gradual decline over the years, while avidity remained stable (**Figure 11b, c**).

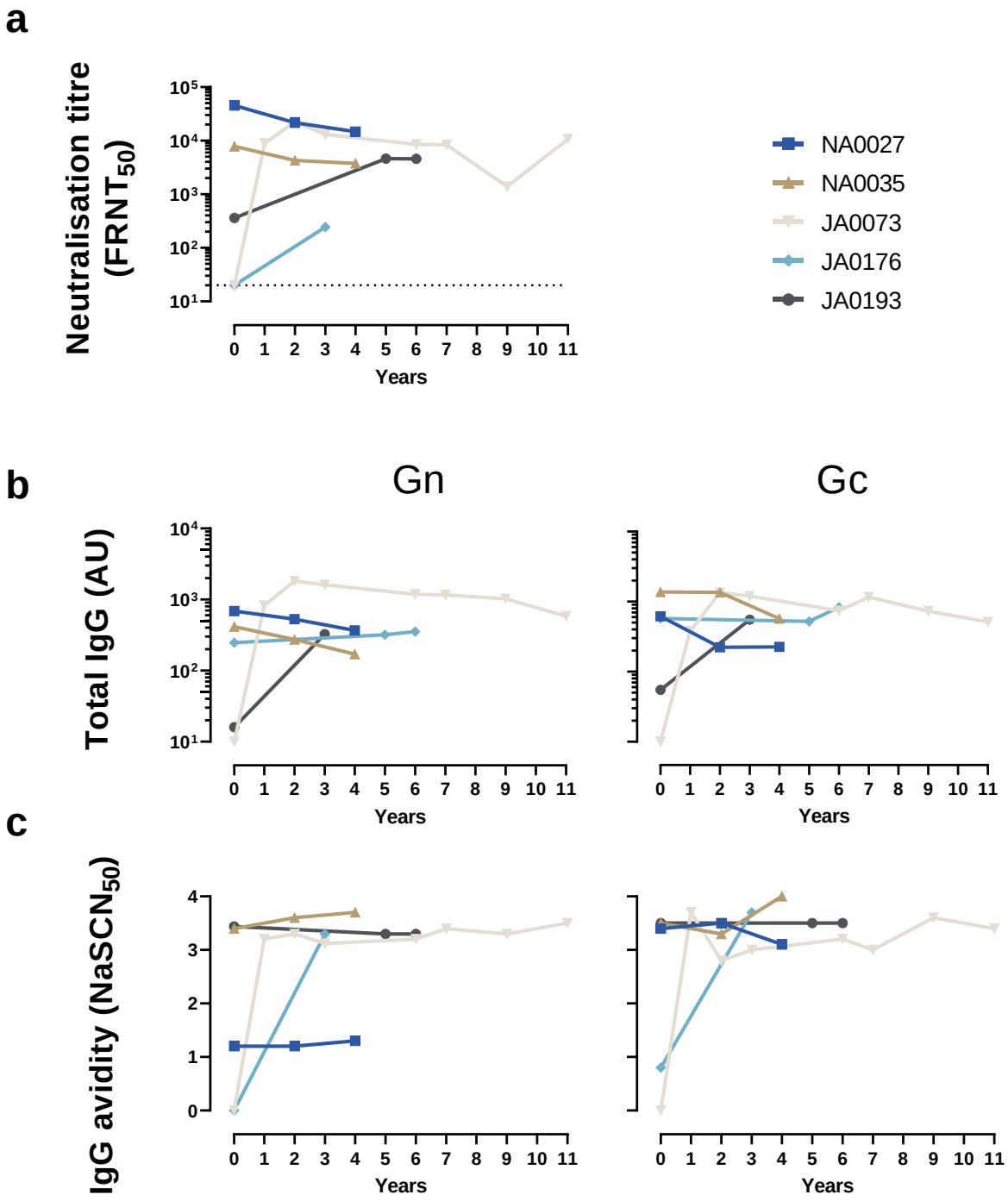


Figure 11. *Natural exposure to RVFV elicits a high-titre, long-lived humoral response. Five individuals from Kilifi county with serum samples spanning 3-11 years were assayed for (a) Neutralisation titre, (b) IgG titre of anti-Gn (left) and anti-Gc (right), (c) Avidity of anti-Gn IgG (left) and anti-Gc IgG (right). Year 0 is their earliest available sample (not necessarily the year of exposure), with subsequent samples plotted relative to that. Individuals' serum samples were collected between the following years: NA0027, 2014-2018; NA0035, 2014-2018; JA0073, 2007-2018; JA0176, 2011-2014; JA0193, 2007-2013.*

The IgG subclass response over time in this population provides further evidence that the IgG response to RVFV is dominated by IgG1 and this remains long-lasting (**Figure 12**). There is also a moderate IgG3 response that remains stable, particularly towards Gn, while little IgG2 and IgG4 are detected towards either antigen.

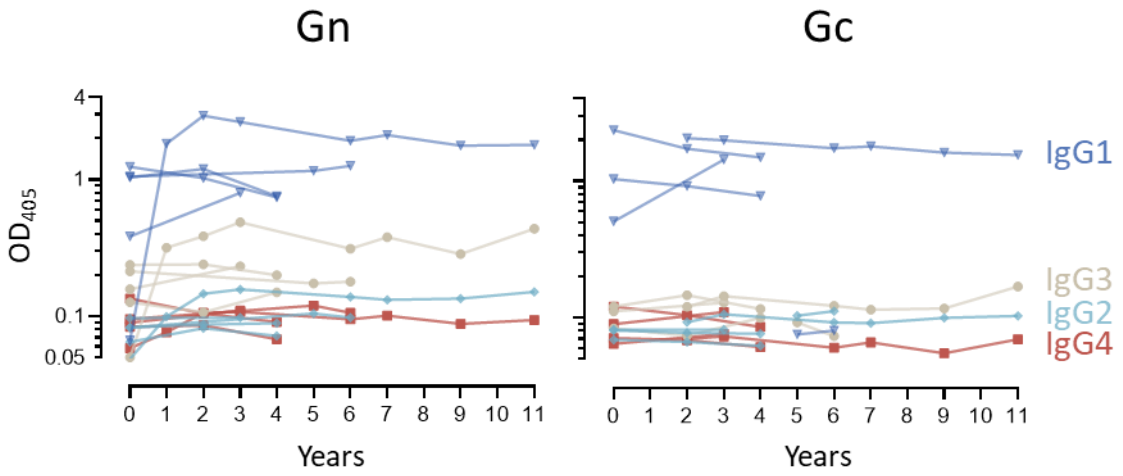


Figure 12. *IgG subclass response remains stable over many years. IgG subclass response towards Gn (left) and Gc (right). Connected lines within each subclass represent the same individual. The IgG subclass response towards Gc was not measured for 3 samples due to insufficient serum quantity.*

3.3.5 Is there a detectable cellular response to RVFV Gn and Gc after historical RVFV infection?

Cryopreserved PBMCs from 5 of the individuals enrolled in the Kilifi County surveillance study (2018), with previous evidence of RVFV exposure, as measured by the presence of RVFV nAbs, were assessed by ELISpot. The responses were compared to five randomly selected samples from the same population sampled at the same time with no evidence of previous RVF exposure, as determined by a lack of detectable RVFV nAbs. Overall, the IFNγ response was moderately low in the five RVFV-exposed individuals with a mean response of 67.4 spot-forming cells (SFC)/10^6 PBMC [95% CI 6.8-128] but this was significantly higher than non-exposed controls (mean response 8.4 SFC/10^6 PBMC [0-21.7]) (**Figure 13**). Responses among RVFV-exposed individuals were comparable across individual peptide pools (**Figure 13**). There was no significant difference in ELISpot response

to N between exposed (mean response 31.6 SFC/10^6 PBMC [95% CI 0-67.6]) and non-exposed controls (mean response 16.8 SFC/10^6 PBMC [0-34.8]) (**Figure 13**). Staphylococcal enterotoxin B (SEB) was used as a positive control for PBMC stimulation and all unexposed and RVFV-exposed individuals had a response >1900 SFC/10^6 PBMC, as expected.

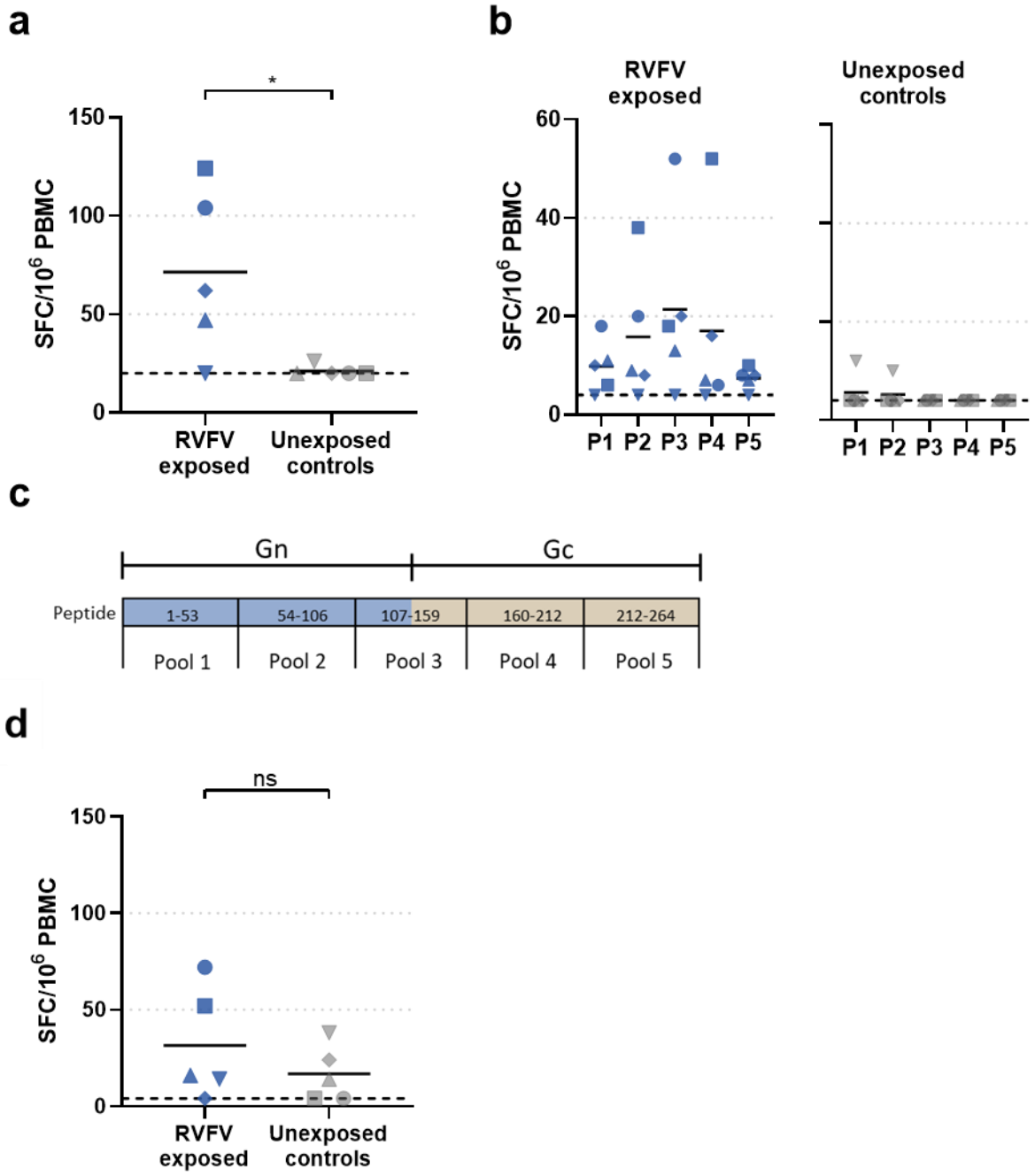


Figure 13. *A low but significant Ex vivo IFNγ ELISpot response in naturally exposed individuals. PBMC from five RVFV-exposed individuals along with 5 case-matched, non-exposed controls were*

*stimulated with an overlapping peptide library spanning the GnGc polyprotein. (**a**) Summed responses from the five peptide pools showing significantly higher response in the naturally exposed group compared to naïve controls (*p < 0.05, unpaired t test). (**b**) Responses to individual peptide pools (**c**) Schematic of the overlapping GnGc peptide library used for stimulation. 264 peptides (15mers, overlapping by 11 amino acids) spanning GnGc were combined into 5 pools (**d**) Responses to separate nucleoprotein (N) pool, p = 0.3, unpaired t test. Solid lines represent means. Dashed lines represent the lower limit of detection of 4 spot-forming cells (SFC)/10^6 PBMC for individual pools and 20 SFC/10^6 PBMC for summed responses. SEB stimulated cells for each volunteer gave >1900 SFC/10^6 PBMC.*

These data indicate that natural RVFV exposure elicits a durable T cell response towards both Gn and Gc.

3.4 Discussion:

The protective role antibodies play against RVFV infection is well documented [96, 97, 162]. The structural glycoproteins displayed on the surface of RVFV, Gn and Gc, are key targets of this protective immune response and monoclonal antibodies have been identified targeting both [99, 100, 131]. Studies of the live-attenuated MP-12 vaccine have shown detectable neutralising antibodies in a majority of individuals at least 5 years post-vaccination [163]. However, relatively little is known about the nature and longevity of the immune response after natural RVFV exposure.

Studies in mice and rabbits have identified monoclonal antibodies targeting either Gn or Gc that are able to neutralize virus and confer protection against RVFV challenge [94, 99, 100, 133]. A study in mice, this time involving vaccination with Gn- or Gc-coding DNA, showed that all those vaccinated with Gn seroconverted, but only half of those vaccinated with Gc [101]. A more recent study isolating mAbs from a convalescent human patient returning to China found that mAbs specific to Gn exhibited much higher neutralisation titres than those that bind Gc [131]. This provides some evidence, perhaps, that the larger negative impact on neutralisation titre seen in this study after depleting antibodies targeting Gn, compared to Gc, reflects a greater neutralising potential of anti-Gn antibodies rather than merely increased abundance over anti-Gc antibodies. Indeed, since this

work was undertaken, a large number of monoclonal antibodies were isolated from Kenyan adults after natural exposure or live-attenuated vaccination; those targeting Gn were much more potent than those targeting Gc [132]. Increased potency of nAbs targeting Gn over Gc may explain our measurement of IgG avidity. Higher avidity antibodies can bind antigen more efficiently, and only the higher avidity of anti-Gn antibodies was associated with increased nAb titre. However, the relationship, while significant, was relatively weak and there are individuals with comparatively low avidity of Gn antibodies yet high neutralising titre. A potential explanation for the lack of correlation between avidity and Gc titres is due to the way neutralisation assays are carried out, by preincubating virus with serum for an hour, prior to transferring the virus/serum mixture to a monolayer of cells. It is possible that having this one hour window reduces the importance of avidity by allowing relatively lower affinity antibodies enough time to bind and block infection. In vivo, when speed of nAb binding may be more critical, avidity may play a greater role than that shown here. While avidity was very stable over many years, it is typically lower in acute or recent infection. However, due to the sparse sampling (no more than once a year), initial changes in the weeks and months post-exposure are not visible.

Protein expression in mammalian cells are subject to various quality control checkpoints to ensure correct folding [164]. Our recombinantly-derived RVFV Gn and Gc were expressed in HEK 293T cells. Similar constructs and protein production methods have been used to successfully produce and crystallize phleboviral Gn [75] and Gc glycoproteins [165], as well as the Gn and Gc from related hantaviruses [166-168] and their native-like fold architectures have been shown to be compatible with cryoEM-derived reconstructions of purified virions and virus-like particles [75]. These combined observations indicate that these recombinantly produced RVFV proteins can serve as 'native-like' mimetics of RVFV Gn and Gc. However, it is important to acknowledge that recombinant material will not completely match the native form of the virus. For example, the recombinant and putatively monomeric RVFV Gn and Gc used in these assays does not replicate

their native higher-order, membrane-bound pentameric and hexameric Gn-Gc assemblies on the virion surface [84, 111]. While these data show that dual depletion of both Gn and Gc antibodies reduces nAb titres to identical levels seen in sera depleted of Gn antibodies alone, even dual-depleted sera can neutralize live virus at the highest concentration (**Figure 8**, **Figure 10**). While this is likely due, at least in part, to the incomplete nature of the depletion (corresponding ELISA signal post-depletion was not entirely eliminated at high serum concentrations), it is also likely that a subset of antibodies recognize epitopes constituting higher-order quaternary assemblies formed on the native virion surface. These antibodies may be capable of neutralising whole virus but may not bind the recombinant Gn or Gc and therefore would not have been depleted. In fact, a study of monoclonal antibodies isolated from Kenyan adults characterised two potent mAbs that target Gn-Gc heterodimers but not individual monomeric Gn or Gc [132]. Nevertheless, we were still able to assess the relative contribution antibodies targeting each individual glycoprotein have on neutralisation, demonstrating reproducibility of the effect in two different populations within Kenya, using two different measures of nAb. While both glycoproteins are clearly immunogenic and targeted by the nAb response, our data suggest that after naturally-acquired human infection, antibodies targeting Gn, rather than Gc, play a larger role in RVFV neutralisation. This is perhaps not surprising considering that the N-terminal component of Gn occupies the most membrane-distal region of the virus, which plays a role in shielding the cognate Gc (***Figure* 3**) [75, 94], and therefore may be more easily accessible to the host immune system.

While protection against RVFV infection has long been associated with the induction of nAbs targeting Gn and Gc [55, 96, 97], it can also arise from other mechanisms. Mice vaccinated with the immunodominant N, for example, show partial protection from RVFV challenge despite the absence of detectable nAbs [104, 129]. Another study showed the cooperative effect of a non-neutralising antibody improving protection in a mouse model [169]. Perhaps more surprisingly, mice vaccinated with modified Vaccinia Ankara (MVA) expressing both Gn and Gc failed to elicit

nAbs but were still protected from viral challenge [170]. IgG1, the predominant subclass recognising the RVFV glycoproteins identified here, can efficiently trigger the classical route of complement [171]. While the contribution that non-neutralising antibodies and cellular immunity have on protection against RVFV is less well characterized, numerous components of the immune response function together during acute infection (including experimental challenge in animals) to provide protection. Studies on the immune response during acute RVFV infections in humans are needed to determine the role of other immune mechanisms in disease pathogenesis and protection.

Due to its extensive anti-viral properties, I have used IFNγ as a broad measure of the cellular response to RVFV in these individuals. The ex vivo ELISpot carried out here is a measure of effector memory T cells that are able to secrete IFNγ within hours of re-exposure to antigen [172]. I have shown that these cells, circulating in the peripheral blood, are relatively low in number in humans with historical RVFV infection. However, those targeting Gn and Gc are still detectable in the majority of individuals many years after exposure and they may potentially play an important role in protection. While responses to N were similar to individual pools of GnGc peptides, they were not significantly higher than in RVF-naïve individuals.

Recently, the T cell responses in human volunteers vaccinated with multiple doses of a formalin-inactivated RVF vaccine were characterized [173]. Despite also showing a generally low cellular response, IFNγ expression post-stimulation with Gn, Gc and N peptides were detected by ELISpot many years post vaccination. A previous study exploring the cellular response to RVFV in a non-human primate model have shown that non-lethal challenge was associated with early proliferation of $CD4^+$ and $CD8^+$ T cells in addition to early Th1 cytokine production, including IFNγ [112]. Another study in humans showed higher expression of IL-10, an anti-inflammatory cytokine, was associated

with fatal cases [56]. These findings, together with the critical role CD4+ T cells play in generating strong antibody responses [55], indicate the importance and benefit of a robust cellular response.

Due to the presence of high-titre, long-lived nAbs, it is plausible that the naturally acquired immune response to RVFV may be sufficient for long-lasting protection, particularly as nAbs are associated with protection in animals. The observation that antibodies targeting Gn play a comparatively larger role in neutralisation than those that target Gc has potential implications for vaccine design and is suggestive that the Gn may be the most critical antigen to include in RVFV candidate vaccines. These data can provide a useful benchmark for immune responses elicited in future clinical trials of candidate vaccines.

To my knowledge this is the first time the humoral response targeting the individual RVFV glycoproteins has been described in naturally exposed humans. While these immunological assessments provide useful data on immunity to infection, there is a lot that we do not know regarding their previous RVFV exposure. Precise dates on when the RVFV infections occurred were unknown, making it difficult to ascribe any acute febrile illnesses encountered by the individuals in the years preceding this study. Further, given that RVFV can also cause self-limiting illness, active surveillance for the incidence of such infections would be the best approach to relate particular acute illnesses to a corresponding boost in immune responses. Additional unknowns include: the route of exposure (mosquito bite vs contact with infected animal tissue), presence of co-infections, and their clinical manifestations. All of these factors will have likely influenced their subsequent response to RVFV and further work with larger sample sizes is needed to connect immunological attributes with clinical outcomes and disease severity.

4

Determining factors that underlie successful manufacture of ChAdOx1 RVF vaccine

The ELISA data that I produced in this chapter is included in the following publication: Berg, A., **Wright, D.***, Dulal, P.*, Stedman, A., Fedosyuk, S., Francis, M. J., Charleston, B., Warimwe, G. M. & Douglas, A. D. 2021. Stability of Chimpanzee Adenovirus Vectored Vaccines (ChAdOx1 and ChAdOx2) in Liquid and Lyophilised Formulations. Vaccines, 9, 1249.*

** Equal contributions*

Chapter contributions: D.W: vaccine construct cloning, virus passaging, NGS analysis, ELISAs. A.B. + S.D.D: mouse work for stability experiments. F.J: NGS. G.M.W + T.A.B: Supervision

4.1 Introduction:

ChAdOx1-vectored vaccines are in development for numerous viral and bacterial pathogens [174-176]. The COVID-19 vaccine, ChAdOx1 nCov-19 (AZ1222), became the first ChAdOx1-vectored vaccine to be granted emergency use licence by the EU and W.H.O and continues to be used globally. The ChAdOx1 vaccine platform involves ligating an antigen cassette of interest into the deleted E1 locus of a bacterial artificial chromosome (BAC), a ~40kb plasmid that encodes the ChAdOx1 genome [177]. The transgene insert coding for the antigen of interest is synthetically produced and, due to the large size of the BAC plasmid, is first cloned into a smaller, more easily manipulated entry plasmid. The antigen cassette is then cloned out of the entry plasmid into the BAC by Gateway™ recombination with the transgene insert under control of the CMV promoter. Recombinant clones of the final BAC plasmid are bulked up in *E. coli*, purified and linearised by PmeI restriction enzyme, excising out an ~8.6 Kb fraction to reveal the inverted terminal repeats, the origins of replication. Linearised virus is then transiently transfected into cell lines that provide the E1 protein *in trans* thereby allowing the otherwise replication-deficient virus to be manufactured. This cell line has historically been HEK293, however, more recently a T-REx cell line which is derived from HEK293 cells but expresses the tetracycline repressor protein have been used. The ChAdOx1 backbone contains the Tet operon which binds the Tet repressor protein. This allows ChAdOx1-vectored vaccines grown up in T-REx cells to avoid expressing the transgene protein while replicating. Errors in the transgene insert can lead to problems of protein expression, potentially resulting in reduced vaccine efficacy. Determining the optimal conditions for manufacture of ChAdOx1-vectored vaccines to ensure the genetic stability of transgene inserts is therefore crucial.

The GnGc transgene encoded in ChAdOx1 RVF is a 3,300 bp DNA sequence producing a 1099 amino acid polyprotein. The sequence is based on the M segment from the MP-12 strain of RVFV. After RVFV infection, the M segment comprised of NSm, Gn and Gc is expressed as a polyprotein. However, this vaccine construct does not contain the first 131 amino acids of the MP-12 M

segment, removing the native leader sequence and most of NSm, and replacing it with a tissue plasminogen activator (tPA) sequence which traffics the protein to the secretory pathway (**Figure 14**). As with RVFV infection, the expressed polyprotein is post-translationally cleaved at host signal peptidase sites into Gn and Gc proteins of ~58kD each. With RVFV, the subsequent Gn and Gc glycoproteins form a complex which is trafficked to the Golgi apparatus by way of a localisation signal in Gn, where budding occurs [178]. For the ChAdOx1 RVF construct, it is likely Gn and Gc behave similarly, C-terminal transmembrane domains likely result in membrane-bound Gn/Gc complexes, while budding and secretion of virus like particles may also be a possibility.

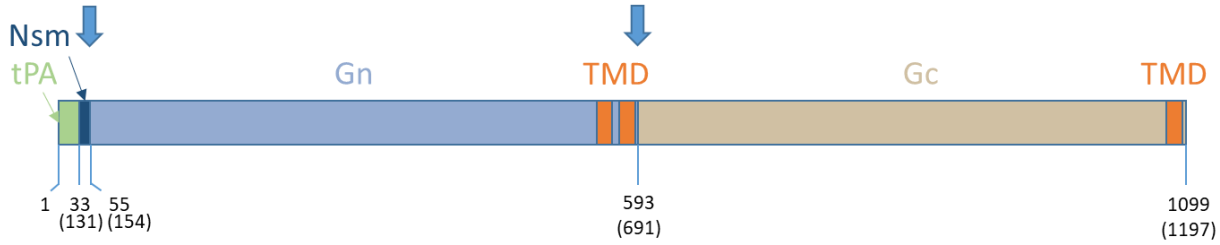


Figure 14. *Schematic of the RVF polyprotein encoded by ChAdOx1 RVF. A tPA signal sequence is encoded upstream of the polyprotein comprising the C-terminus of NSm and full length Gn and Gc. Once expressed, signal peptidase sites (large arrows) result in cleavage of Gn and Gc. TMD = transmembrane domains. The numbers below represent the amino acid position of the antigen expressed by ChAdOx1 RVF. Numbers in brackets represent the position according to the M segment of RVFV [UNIPROT P21401])*

Prior to the availability of a Good Manufacturing Practice (GMP)-approved T-REx cell-line that represses transgene expression, ChAdOx1 RVF was grown in HEK293 cells, resulting in the expression of GnGc as the virus replicates. After the initial manufacture, the batch was shown to contain a mixed population of virus; a significant proportion of the clones was shown to have acquired a single mutation at bp306-310, resulting in a run of 4C's (CCCC) rather than 5 (CCCCC). This deletion, at the N-terminus of the GnGc polyprotein, caused a frameshift resulting in only a fraction of Gn being produced as part of a 141aa truncated protein. As Gc lies downstream of Gn, it was not expressed at all. Previous sequencing of viral clones from this GMP batch estimated that

~90% of the viral sequences had this deletion. The remaining ~10% of the virus was clonal and correct, expressing the full-length Gn and Gc proteins (**Figure 15**).

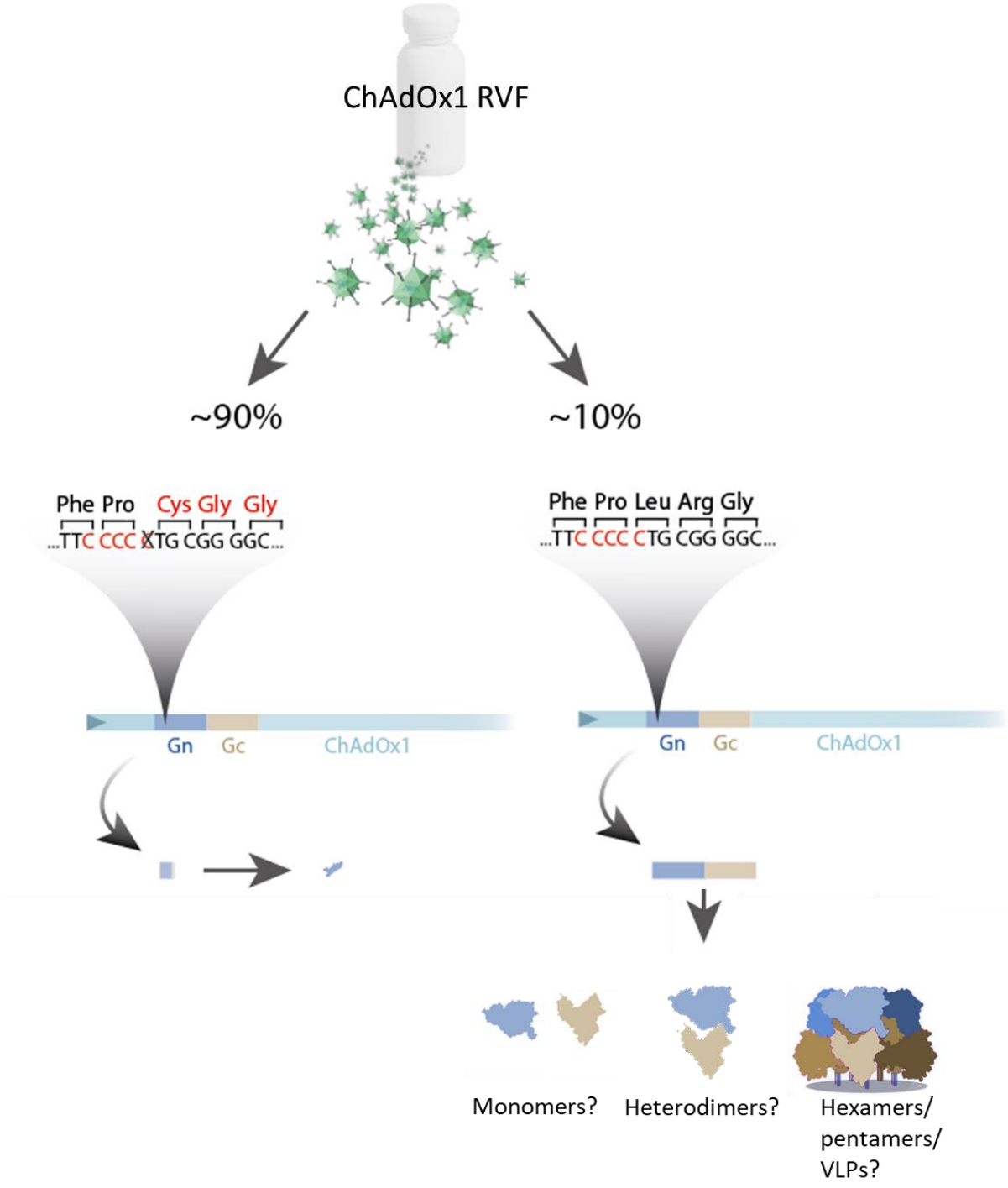


Figure 15. *Schematic of the 'mixed' batch of ChAdOx1 RVF showing the proportion of incorrect viral clones. Genetic stability issues in the initial batch of ChAdOx1 RVF led to a single deletion of a cysteine towards the N terminus of Gn (aa306-311 [as illustrated] or aa381-389) in 90% of viral clones (bases in red). This led to a frameshift (amino acids in red) and only a small portion of Gn as part of a truncated protein being expressed. 10% of the viral clones in this batch did not contain the deletion and correctly expressed full-length Gn and Gc, as assessed by Sanger sequencing >100*

individual viral clones and, later, NGS. How the correctly-expressed Gn and Gc proteins in the ChAdOx1 RVF construct interact has not yet been experimentally determined.

Two potential contributing factors for the genetic stability issues were considered: 1) removing the presence of multiple identical consecutive bases in the transgene sequence, and 2) repression of transgene expression during manufacture. The single deletions always occurred in a run of cytosine residues. Other adenovirus vaccine programmes have also encountered issues with deletions or insertions, always in a run of identical consecutive bases. Errors in regions of consecutive identical bases can occur commonly due to DNA polymerase slippage [179]. Repression of the transgene (e.g. by growing up in T-REx cells rather than HEK293 cells) will allow the virus to replicate in the absence of possible selection pressure that may otherwise be exerted on viruses expressing foreign antigens. Here, I have resynthesised the vaccine construct, modifying the transgene sequence to remove all instances, where possible, of >3 identical consecutive bases while leaving the amino acid sequence unchanged and investigated the impact that both of these features have on the genetic stability of ChAdOx1 RVF. In addition to genetic stability, storage stability of the vaccine at -80°C and thermostability of vaccine exposed to higher temperatures are also crucial to demonstrate. The storage stability of ChAdOx1 RVF at -80 °C was contracted out as part of GMP manufacture at Advent. The latter part of this chapter deals with thermostability of the vaccine, which significantly influences the cost and feasibility of rolling it out, particularly in hotter climates with potentially less access to cold-chain infrastructure.

Previously, thermostabilising ChAdOx1 RVF by drying onto sugar membranes has been shown to maintain its potency at 45^{o}C for up to 6 months [149]. Work led by Sandy Douglas has investigated the thermostability of ChAdOx1 RVF and a ChAdOx2 Rabies vaccine [180]. This involved measuring the potency of the vaccine by in vitro infectivity assay in addition to in vivo immunogencicity in mice. As part of that project, I have measured the IgG titres towards RVFV Gn and Gc in mice

vaccinated with ChAdOx1 RVF that was stored at various temperatures for up to sixteen months in liquid formulation or lyophilised.

4.2 Objectives:

1. To determine the immunogenicity of the mixed batch of ChAdOx1 RVF and how it compares to clonal vaccine.
2. To resynthesize ChAdOx1 RVF to obtain correct and clonal vaccine for future use.
3. To determine the factors that contribute to genetic stability of ChAdOx1 RVF production.
4. To assess the thermostability of ChAdOx1 RVF in X48A liquid formulation or lyophilized after storage at various temperatures for up to 16 months.

4.3 Results:

4.3.1 Determining the immunogenicity of mixed batch vs clonal vaccine

To determine the immunogenicity of the mixed vaccine batch, BALB/c mice (*n* = 5 per group) were vaccinated by Alex Spencer/Marta Ulaszewska at $5x10^7$, $1x10^8$, or $4x10^8$ infectious units (IU) and compared with a pre-clinical, 'correct' clonal vaccine (with the same underlying sequence but without the deletion). I assessed the binding IgG titres against Gc in addition to RVFV nAb titres (**Figure 16**). While only ~10% of the virus was correct and able to express the full-length GnGc polyprotein, the vaccine remained immunogenic. However, binding antibodies towards Gc were higher in the clonal vaccine at all doses tested, significantly so after a low or high dose of vaccine (**Figure 16**). Neutralising antibodies were also higher after the clonal vaccine, significantly so after the highest dose. Results for the mixed vaccine are broadly in line with what would be expected if we gave 10% of the stated dose of 'correct', clonal vaccine.

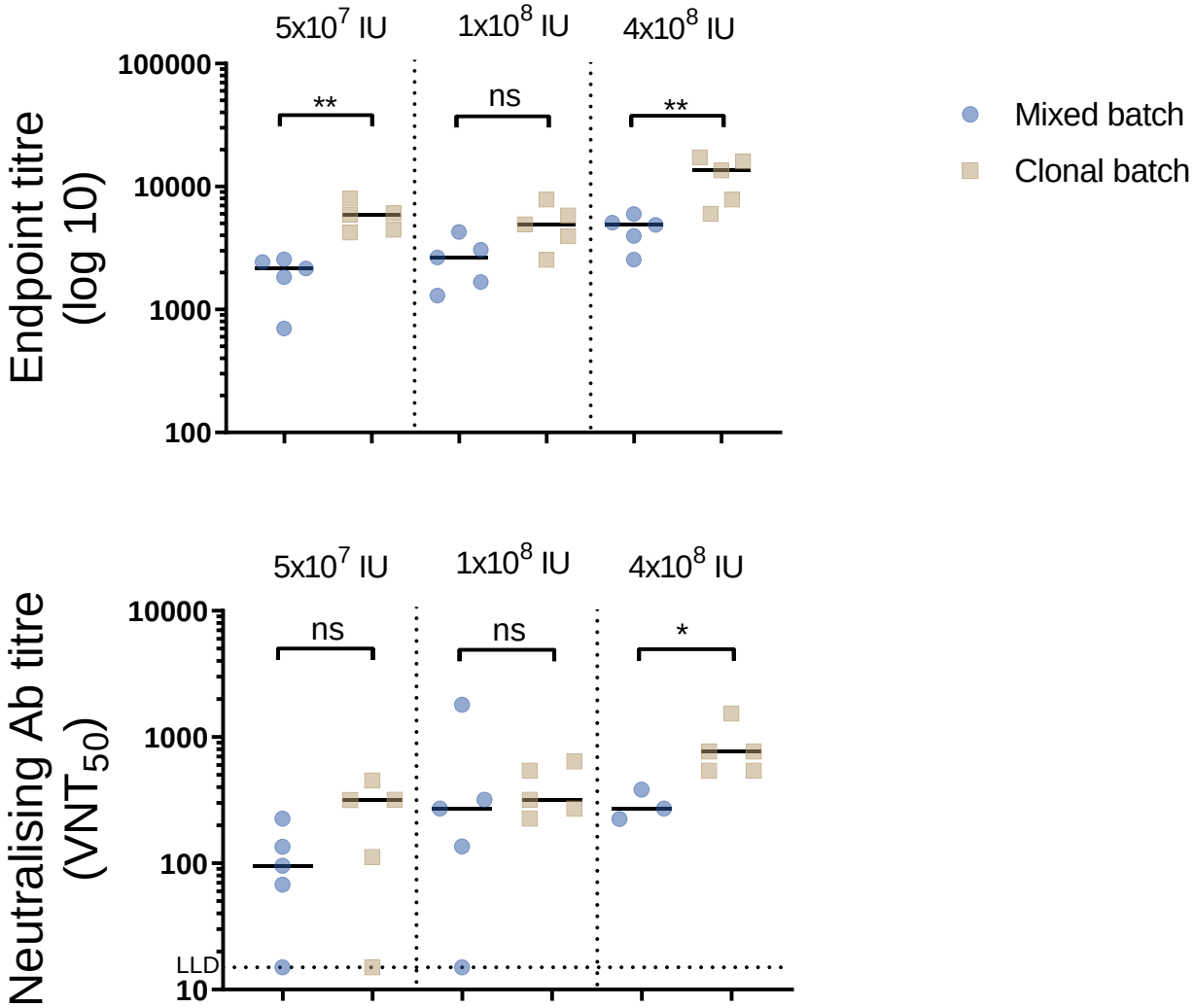


Figure 16. *The ChAdOx1 RVF batch containing the mixed population of virus elicits lower immunogenicity than, otherwise identical, clonal vaccine (from preclinical batch). Top, anti-Gc IgG endpoint ELISA titres. Bottom, VNT_{50} neutralisation titres using the MP-12 strain of RVFV on Vero E6 cells. Plaques were counted by eye and titres were assessed using Spearman-Karber method from quadruplicate wells at each serum dilution. Bars represent medians. Two mice in the high dose 'mixed batch' group did not have enough serum for the VNT assay. * $p < 0.05$; ** $p < 0.01$, Mann Whitney Test. Vaccine preparation, ELISA and VNT was done by myself, animal work was done by Alex Spencer and Marta Ulaszewska.*

4.3.2 Resynthesis of ChAdOx1 RVF

ChAdOx1 RVF was resynthesized to remove all instance, where possible, of >3 consecutive identical base runs within the GnGc transgene. This was done by altering specific codons while ensuring the amino acid sequence remained identical (**Figure 17a**). This was successfully achieved at all instances

of >3 identical bases except for two instances of GGGG, where the amino acid sequence required Tryptophan and Glycine following one another (TGG-GGx), thus in these instances the four consecutive Gs remained (**Figure 17b**).

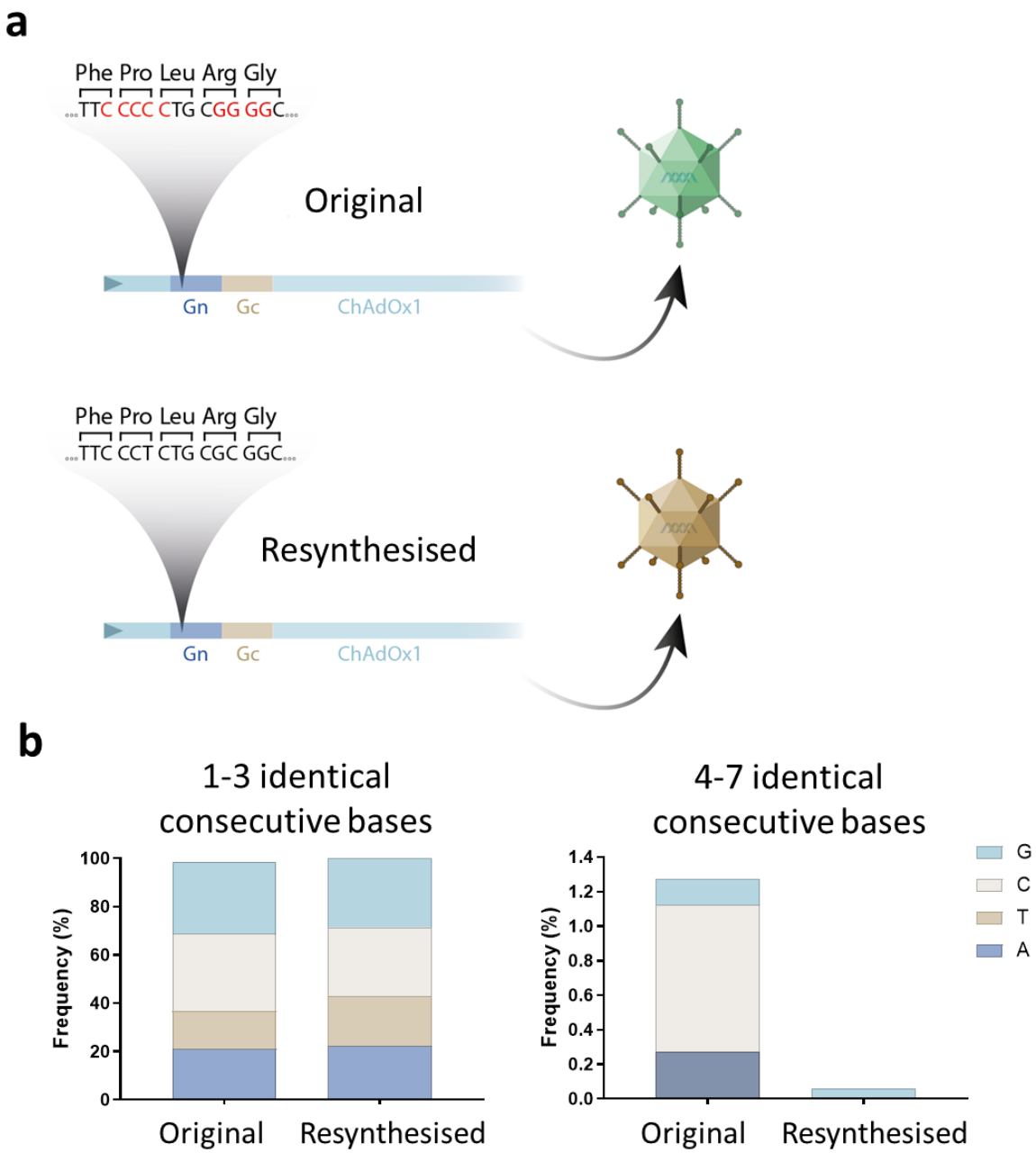


Figure 17. *Comparison of the number of instances of identical consecutive bases between the two versions of ChAdOx1 RVF. (**a**), Schematic of original and resynthesized vaccines, bases in red demonstrate example of sequences that were altered to remove identical base runs. (**b**) Comparison between the frequency of 1-3 or 4-7 identical consecutive base runs in the original and resynthesized vaccines.*

Expression of RVFV Gn and Gc from the resynthesized vaccine was confirmed by infecting HeLA cells and running a Western blot of the cell lysate (**Figure 18**). Expression of Gn and Gc from the resynthesized vaccine was higher than expression from the mixed vaccine batch (**Figure 18**).

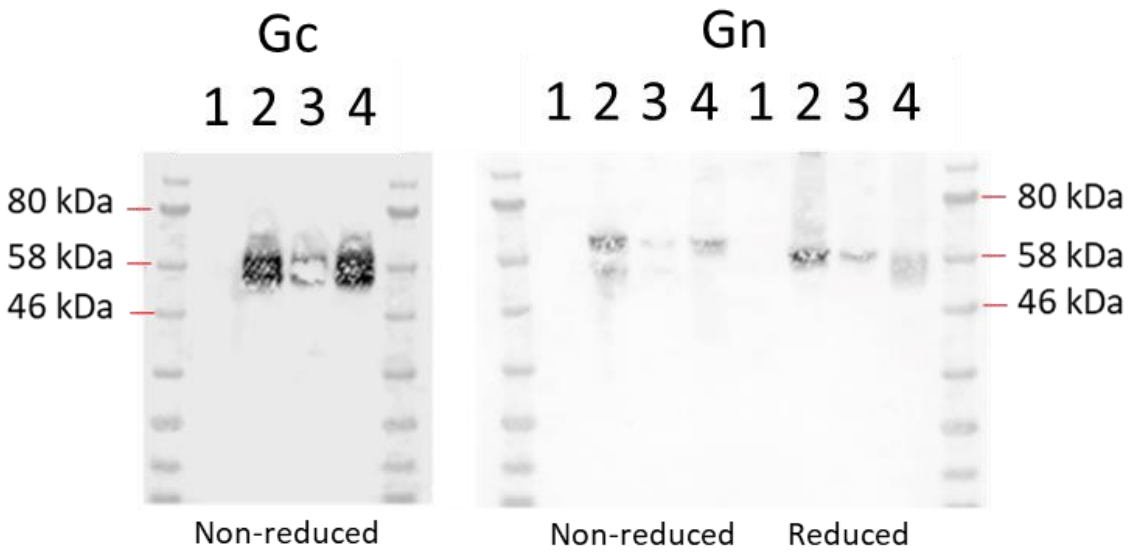


Figure 18. *Western blot showing greater expression of Gn and Gc after infection of HeLa cells with resynthesized compared to the mixed batch of ChAdOx1 RVF. 1: Negative control (uninfected); 2: Resynthesised ChAdOx1 RVF; 3: Mixed batch of ChAdOx1 RVF; 4: Positive control (cell lysate from previous ChAdOx1 RVF infection). The mAb used for Gc (5E2 [NR-43192]) detection binds an epitope that is not present if protein is run in reducing buffer. The mAb used for Gn detection binds a linear epitope (4D4 [NR-43190]). Expected size of both Gn and Gc proteins is ~58 kDa.*

4.3.3 Determining the factors that contribute to genetic stability of ChAdOx1 RVF production

In order to separate the effects of reducing the occurrence of identical consecutive base runs and expression/repression of the transgene during manufacture, a pre-clinical version of the vaccine, known to be clonal and correct but containing the same sequence as the original vaccine was used as a comparator. Both resynthesized and original viruses were then passaged ten times in either HEK293 (allowing protein expression) or T-REx (repression of protein expression). NGS was carried

out to evaluate genetic stability before passaging (P0), after 5 (P5) and after 10 (P10) passages in their respective cell lines (**Figure 19**).

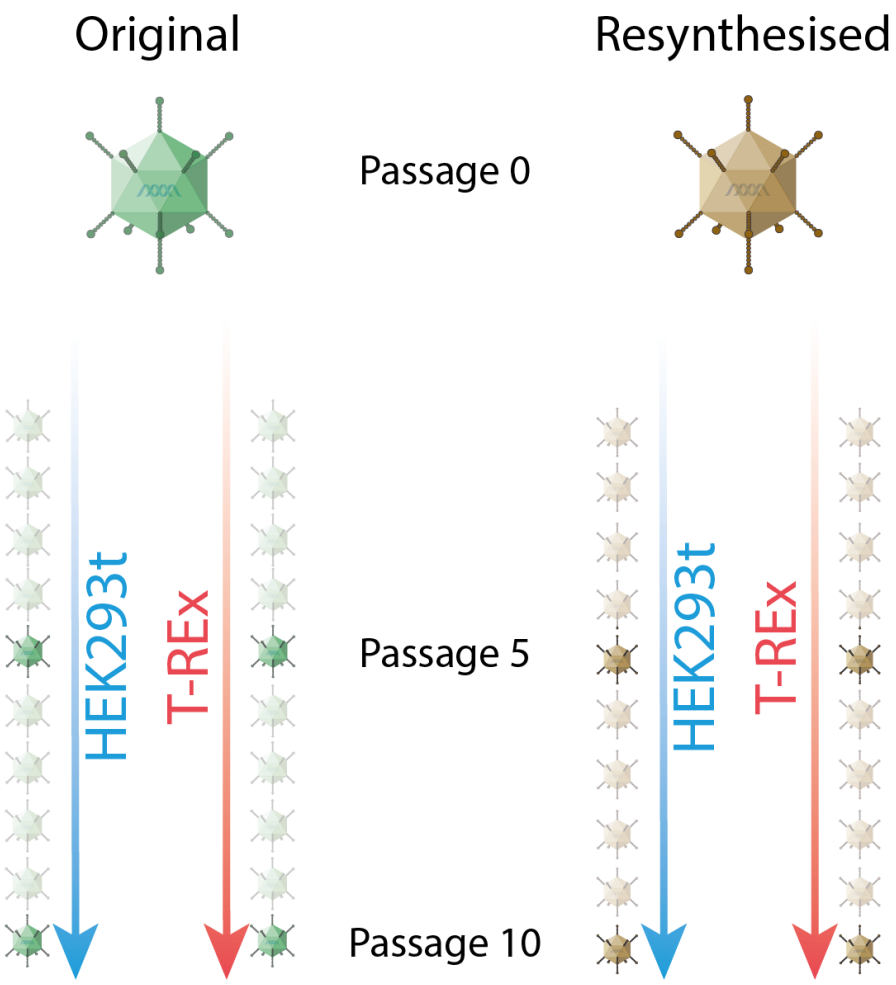


Figure 19. Experimental plan to investigate genetic stability of original (green) and resynthesized (brown) virus passaged in either HEK293 or T-REx cells. Next gen sequencing was carried out on both P0 viruses, and all four P5 and P10 viruses.

NGS data shows that total read coverage over the transgene insert was significantly lower in virus passaged in HEK293 than for virus passaged in T-REx cells, regardless of sequence (**Figure 20b**). This suggests that either many of the viruses lack the GnGc inserts entirely, or the GnGc inserts contain mutations too numerous for the algorithms to be able to combine the read fragments. In addition, of the sequences that were read for the original virus, they acquired the same deletion of a C at bp 306-311 seen during the original manufacture. By passage 5, ~40% had the deletion, by passage 10 ~50% had the deletion (**Figure 20b**). In contrast, the resynthesized vaccine, while still suffering significantly lower read coverage when passaged in HEK293 cells, of the sequences that were read,

showed no significant errors at P5. By P10, however, there were very large numbers of errors throughout the insert, resulting from extremely low read coverage (**Figure 20b**). Regardless of whether the transgene sequence was optimised to remove multiple runs of identical consecutive bases or not, if grown up in T-REx cells with repression of the transgene protein, read coverage was consistently >2000 reads per position with no errors >3% at any base (**Figure 20b**). Read coverage over the transgene region dropped very significantly for both viruses grown in HEK293 cells compared to the rest of the BAC (**Figure 20c**). These data suggest a significant majority of ChAdOx1 RVF virus, regardless of codon optimisation, excised out large fragments of the transgene when grown in HEK293 cells. This was particular to the GnGc transgene; there were no significant errors in the ChAdOx1 backbone regardless of the cell line they were grown up in.

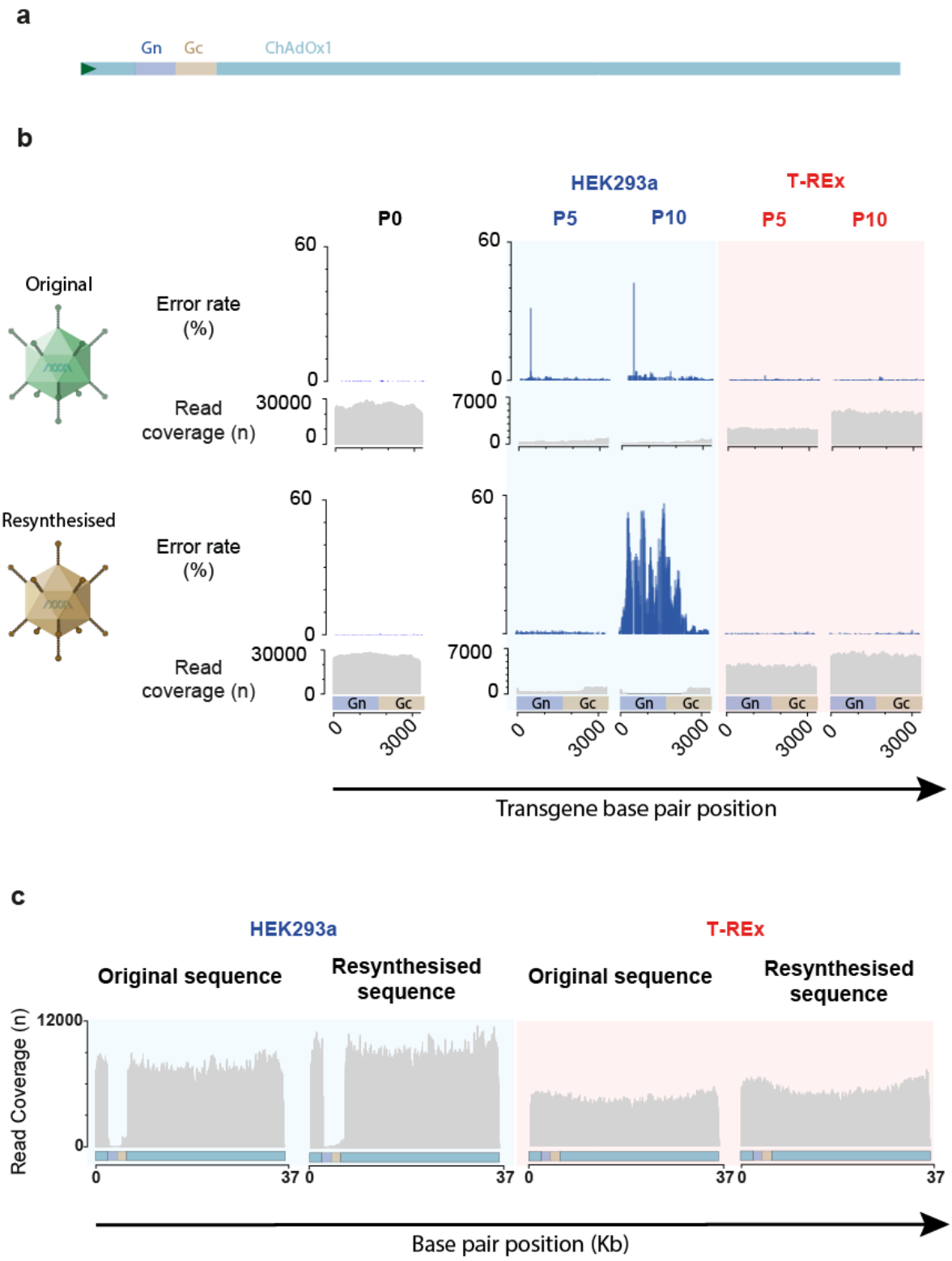


Figure 20. *Next-generation sequencing results show manufacture using HEK293 cells results in low read coverage and significant errors. (**a**), Schematic of ChAdOx1 RVF genome. (**b**), The error rate and read coverage of each base position in the GnGc transgene at passage 0 (P0), 5 (P5) and 10 (P10) in either HEK293 or T-REx cells for the original or resynthesized virus. (**c**), Read coverage of the entire genome after 10 passages in either HEK293 or T-REx cells for the original or resynthesised virus. Samples were prepared by DW and Frederick Jackson (FJ). NGS was carried out by FJ with results provided in excel format. Analysis carried out by DW.*

In an attempt to understand at what point the GnGc insert begins to breakdown when grown in HEK293 cells, flank to flank PCR, covering the GnGc insert from the promoter to the polyA tail, was carried out on cell lysate after each passage (**Figure 21**)**.** The correct size band containing the GnGc insert is rapidly lost in both virus batches. In the case of the original sequence, it is significantly reduced by P2. The correct size band is replaced by multiple smaller bands as the viruses are passaged confirming what the NGS shows, that large sections of the insert are being excised. All studies involving ChAdOx1 RVF from this point onwards have used the resynthesized vaccine construct.

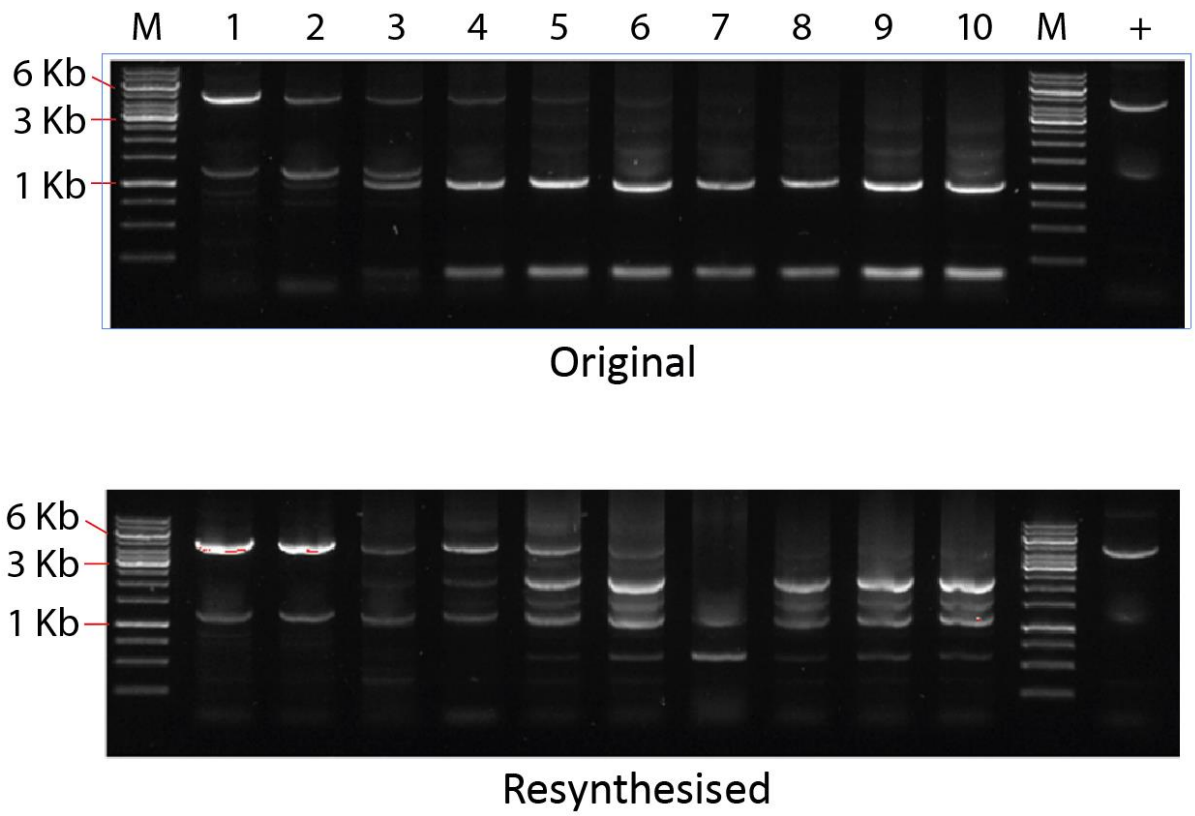


Figure 21. *Gel electrophoresis using flank to flank PCR product after each passage in HEK293 cells. Virus from cell lysate after each passage was treated with DNAreleasy to release the DNA, the product was then used as the template for PCR. Top: PCR product from resynthesized batch. Bottom: PCR product from original batch. P1-10 are the passage number. + is a positive control using the original BAC plasmid. Expected size of the PCR product containing the complete GnGc sequence is 4.79 Kb*

4.3.4 Assessing the thermostability of ChAdOx1 RVF in X48A liquid formulation or lyophilised

The thermostability of ChAdOx1 in X48A liquid formulation was tested after 1 month and 12 months at various temperatures. Due to disruptions caused by the COVID-19 pandemic, the lyophilised vaccine was tested after 16 months rather than 12 months. To investigate the thermostability, mice were vaccinated with ChAdOx1 RVF that had been stored at various temperatures for the appropriate time. 28 days later, the mice were bled and I determined the anti-Gn and anti-Gc titres by standardised ELISA. The vaccine storage, vaccine formulation and mouse work were carried out by Sandy Douglas and Adam Burg.

Vaccination of ChAdOx1 RVF after storage at -80°C and 4°C elicited similar titres after 1 month (**Figure 22a**). It is only when administering the minimal dose of $1x10^5$ IU that there is a significant reduction at 4°C compared to -80°C of approximately -0.4 log difference for Gc titres (**Figure 22a**). Storage at 20°C reduced anti-Gc titres significantly at the high and low dose, but not the middle dose. Due to the drop off in response elicited by vaccine stored at 30°C, this temperature was not tested for the 12 months vaccinations. After 12 months, there was no significant difference between vaccine stored at -80°C and 4°C (**Figure 22a**). While vaccine stored at 20°C elicited lower responses compared to -80°C storage, this was only significantly lower at the lowest dose for both Gn and Gc titres (**Figure 22a**). Lyophilised ChAdOx1 RVF was tested after 16 months at 4°C, 20°C or 30°C. IgG titres were lower after storage at 30°C, although due to the low titres induced by the lower doses, this drop off was significant only at the dose of $1x10^7$ IU (**Figure 22b**). Gc titres in this group also showed a significant reduction at 20°C (**Figure 22b**)

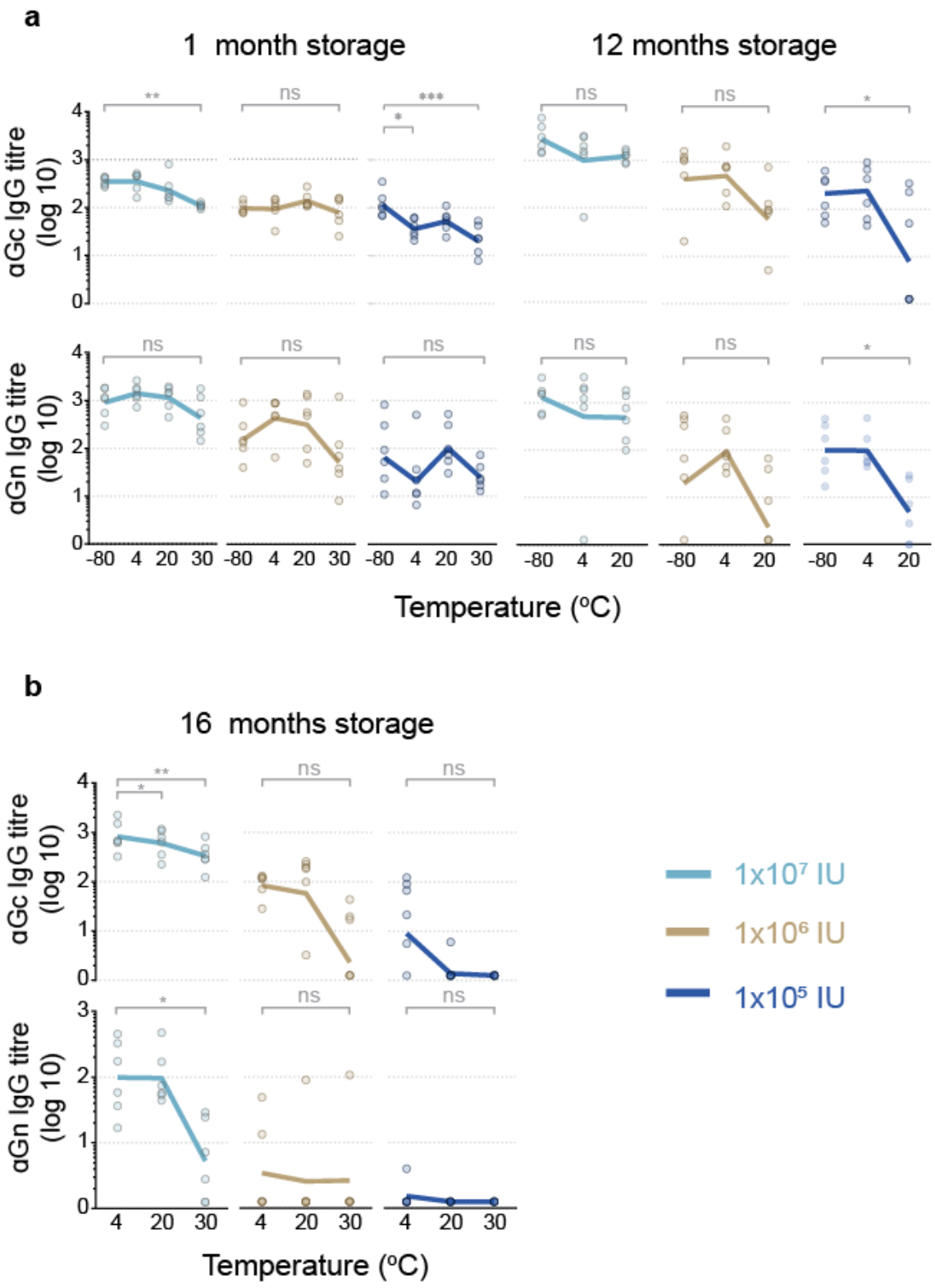


Figure 22. *ChAdOx1 RVF in X48A liquid formulation remains stable when stored at 4°C or -80°C. Mice were vaccinated with ChAdOx1 RVF in liquid formulation or lyophilised after storage between 1-16 months at various temperatures. (**a**) anti-Gc IgG titre (top) and anti-Gn IgG titre (bottom) as measured by standardised ELISA after storage of X48A liquid formulation for 1 or 12 months. (**b**) anti-Gc IgG titre (top) and anti-Gn IgG titre (bottom), as measured by standardised ELISA after storage of lyophilised vaccine for 16 months. Kruskal Wallace with Dunn's multiple comparison. **

*p<0.05, **p<0.01, *** p>0.001. n=6 mice per group. Animal work was carried out by SD and AB. ELISAs carried out by DW.*

Comparisons between 12 months storage in X48A buffer and 16 months lyophilised resulted in significantly reduced immunogenicity at some doses and similar immunogenicity at others (**Figure 23**).

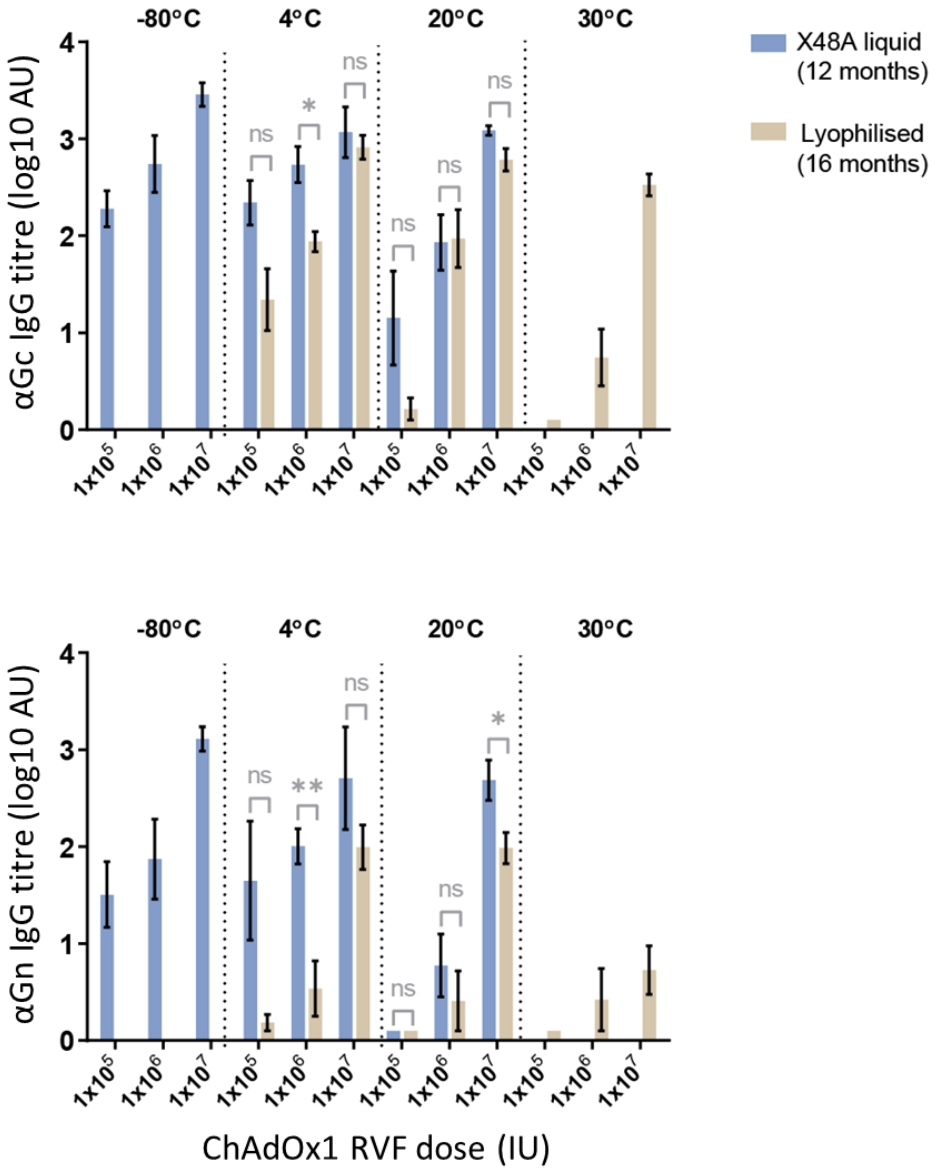


***Figure 23**. Comparison between ChAdOx1 RVF in X48A liquid formulation and lyophilised after 12 and 16 months storage at various temperatures, respectively. Bars represent mean log10 values, error bars represent SEM. Vaccine formulated in liquid X48A buffer was tested after storage at -80°C, 4°C and 20°C. Lyophilised was tested at 4°C, 20°C and 30°C. * p < 0.05; ** p <0.01, Mann Whitney Test.*

4.4 Discussion:

For safety and quality reasons, manufacture of adenovirus-vectored vaccines destined for clinical use require the use of a Good Manufacturing Practice (GMP)-approved cell line. A One Health approach takes a holistic view of RVF vaccine development (reviewed in [181]) and for ChAdOx1 RVF, intended for veterinary and human use, we are able to use the same starting material for both. Vaccine for clinical use can then undergo additional purification beyond the veterinary batch.

When ChAdOx1 RVF was first manufactured, the only GMP-approved cell line available was HEK293, which had been previously used to produce numerous adenoviral-vectored vaccines. However, initial manufacture of ChAdOx1 RVF resulted in a mixed population of virus. I first attempted to find out what impact the mixed batch had on immunogenicity. Vaccinating mice with a high dose ($4x10^8$ IU) of the mixed batch induced a similar immune response to vaccinating with a low dose ($5x10^7$ IU) of clonal vaccine. So while the total dose of viral particles and infectious units is similar between vaccines, the immune response is equivalent to administering only ~10% of the stated dose, the percentage of the vaccine correctly expressing Gn and Gc.

From previous experience with adenoviral-vectored vaccines, including ChAdOx1-vectored vaccines, we know they tend to elicit a dose-dependent antigen-specific response, regardless of antigen [174-176, 182]. Because these viral-vectored vaccines rely on expressing the target antigen in vivo, this dose response is a function of the infectious units rather than viral particle count administered [183]. Therefore, the incorrect batch would likely have to be given at ten times the equivalent dose of clonal vaccine in order to achieve similar immunogenicity. Administering ten times the dose would increase the reactogenicity profile for an equivalent immune response compared to clonal vaccine. While this may have been feasible, previous clinical trials of ChAdOx1-vectored vaccines have given us a good indication of the viral particle dose that results in an acceptable reactogenicity profile. ChAdOx1 RVF was therefore immediately resynthesized for use

in future trials. By this time, a GMP-approved T-REx cell line was available. I resynthesized the vaccine, removing instances of >3 identical base runs and provided the linearised BAC to the Viral-Vector Core Facility to manufacture in T-REx cells. NGS on the resynthesized vaccine showed that it was successfully manufactured without errors. Gn and Gc expression was confirmed by Western blot and the vaccine was subsequently shown to be highly efficacious in a livestock trial [148].

I attempted to understand how growing the virus in T-REx cells, or removing identical base runs in the transgene, affected the genetic stability of the vaccine. It is clear from the NGS results and the PCR covering the GnGc insert, that growing up in HEK293 cells, regardless of the presence or absence of numerous >3 consecutive, identical base runs, rapidly results in genetic errors. The deletion of a cysteine at bp306-311 proving once again the major site of errors. Using T-REx cells on the other hand, and regardless of transgene sequence, resulted in no such issues. Having multiple regions of consecutive, identical bases may increase the risk of acquiring single deletions. Since DNA polymerase slippage can occur commonly in regions like this, preventing transgene expression during manufacture by using T-REx cells, removes any selection pressure on viruses that acquire these deletions. However, even after removal of these regions, when growing in HEK293 cells, the selection pressure is such that it appears to propagate virus that has excised out either the whole insert or large portions of it.

While these data are clear on the necessity of repressing transgene protein expression during manufacture, the consequences of removing identical base runs are less clear. Evidently, removing these bases alone was not sufficient to avoid genetic stability issues. However, it could be argued that after P5 the genetic stability was better in the resynthesized compared to the original virus. While both suffered significant drop off in the number of reads indicating a large portion of the transgene was excised, the resynthesized virus that remained did not contain any major sites of error. The number of reads at each base position can be influenced by various factors including

initial DNA quantity. However, the severe drop in read coverage over the entire transgene compared to the rest of the BAC from the same sequencing run suggests significant portions of these viruses had large parts of the transgene missing.

Differences in the inherent immunogenicity of adenoviral-vectored vaccines may be explained by differences in transgene expression levels which have been demonstrated both in vitro and in vivo [184]. Organisms exhibit biases in the codons they use for a given amino acid [185]. Synonymous mutations that do not result in amino acid changes can still influence protein expression. Therefore, there is a potential risk in modifying codons to avoid consecutive base runs if usage of those codons is otherwise suboptimal. For this to negatively impact on immunogenicity, the transgene insert first must have been optimised for a particular species. For One Health vaccines such as ChAdOx1 RVF, developed for use in multiple species, it is unlikely to have a universal negative impact. Codon usage is well studied in humans and particular other species but there is little information for livestock. Approximately 1.3% of the original transgene sequence was taken up by >3 identical consecutive base runs resulting in 42 codons requiring change. This represents just 3.8% of the transgene's total codons. Biases in codon usage are often subtle, with little difference in the frequencies between two or more codons for a given amino acid. For example, a frequent codon change required for the resynthesized ChAdOx1 RVF involved substituting the codon for proline, CCC (33% frequency in humans) to CCT (28% frequency). As such, the use of marginally sub-optimal codons in such a small percentage of the transgene is perhaps unlikely to have a major negative impact.

These findings, however, may be applicable only to certain transgene inserts. Prior to the availability of a GMP approved T-REx cell line, adenoviral vectored vaccines were routinely expressed in HEK293 cells. It may be the case that in the absence of carrying out NGS on all previous vaccines, small errors were simply not picked up but were present. Or it may be that RVFV Gn and Gc, along with other glycoproteins that have had issues, may be particularly toxic. In any case, when

designing transgenes for inclusion in ChAdOx1-vectored vaccines, manufacture with cell lines that repress protein expression should always be used.

Because the relationship between dose and immune response is not linear, higher doses will increase immunogenicity only up to a point. For this reason, if the dose administered is high enough, reduced vaccine potency may not translate into reduced immunogenicity. Therefore, in order to determine the impact of vaccine storage temperature on in vivo immunogenicity, three different doses were used for each condition. As expected, lower doses tended to elicit lower responses. A year stored at 4°C had no negative impact on immunogenicity compared to vaccine stored at -80°C. This is in line with ChAdOx1-nCoV-19, given emergency use licence, which can be stored up to 6 months at 4°C and possibly longer once additional stability data is available [186]. Storage at higher temperatures for shorter periods of time may also be possible without significant loss of immunogenicity. Immunogenicity induced by lyophilised vaccine compared to storage at the equivalent temperature in liquid formulation tended to be lower, and depending on the dose, sometimes significantly so. Although the comparison is confounded by the different lengths of storage. Lyophilisation was carried out according to a protocol described by Chen *et al* which showed only a very minor drop off in potency of adenovirus vaccines when stored at 25^{o}C for one month [187]. Further optimisation of lyophilisation protocol would be needed for lyophilised material to be stored for periods significantly longer than a year. Vaccination of target species may also be important to ascertain whether reduced vaccine potency translates into lower immunogenicity when given at their recommended doses.

In summary, I have shown that the genetic stability of ChAdOx1 RVF is significantly improved by growing up in T-REx rather than HEK293 cells, likely as a result of negating the pressure that would otherwise select for viral clones not expressing the transgene. The resynthesized vaccine construct that I made during this chapter was subsequently used for the efficacy trial in pregnant sheep and

goats and a large-scale, multi-species field trial in Kenya. These data on the genetic stability have informed subsequent adenovirus vaccine manufacture for a variety of pathogens. Finally, I have provided evidence that immunogenicity in mice is not significantly impacted by long-term storage of ChAdOx1 RVF at 4°C in X48A liquid buffer, and up to 20°C for shorter periods of time.

5

Immunogenicity of ChAdOx1 RVF among adults in Oxford

5.1 Introduction:

ChAdOx1 RVF has been designed from the outset for use in both livestock and humans. Previous livestock trials have shown a single dose is highly effective at preventing RVF viraemia post-challenge [103]. It was also highly effective at preventing RVF disease and foetal loss in pregnant animals [148]. Currently there are no licenced vaccines for human use. This chapter provides the first immunogenicity data of ChAdOx1 RVF in humans.

Human exposure to RVFV predominantly occurs through direct contact with infected animals, so an improved livestock vaccine could be expected to reduce human infections by lowering exposure risk. However, for numerous socioeconomic reasons, uptake of current livestock vaccines is extremely patchy [139]. The direct risk of RVFV to human health, therefore, will remain even when better livestock vaccines are available. As humans can also become infected by mosquito bite, there exists a much larger susceptible population potentially at risk than just those working directly with livestock. For this reason, in addition to improved livestock vaccines, a human vaccine is critically needed with RVF currently appearing on World Health Organisation's (WHO) list of priority pathogens and among the Coalition of Epidemic Preparedness' (CEPI) priority diseases. In 2019, the WHO released a draft target product profile (TPP) for RVF vaccines [188]. ChAdOx1 RVF, a cheap, stable, safe and efficacious, DIVA compliant vaccine ticks many of the boxes as a veterinary vaccine. As a human vaccine, ChAdOx1 RVF has the potential to fulfil these criteria too and provide a vaccine capable of protecting people and their livelihoods from the devastation caused by RVF outbreaks.

The aims of this human clinical trial are to assess the safety and immunogenicity of a single dose of ChAdOx1 RVF in healthy UK volunteers aged 18-50 years old (**Figure 24**) (see Materials and Methods for vaccine and participant information). As a first in human trial, the initial group (*n* = 3) are vaccinated with a low dose of $5x10^9$ vp. If there are no safety concerns, the next group will be vaccinated with $2.5x10^{10}$ vp (*n* = 6) and the last group with $5x10^{10}$ vp (*n* = 6). Due to the ongoing COVID-19 pandemic and large-scale rollout of another ChAdOx1-vectored vaccine (ChAdOx1-

nCoV19), the protocol was amended to only recruit volunteers that have already received a non-ChAdOx1 COVID-19 vaccine (e.g. Pfizer or Moderna). Additionally, volunteers cannot have received any vaccines within the previous 30 days prior to enrolment. Since enrolment for this trial coincided with opening up COVID-19 vaccinations in the UK to similar age ranges required for this trial, the available pool of volunteers has been significantly reduced. Additionally, with several other ChAdOx1-vectored vaccine trials competing for the same reduced volunteer pool, recruitment has been slower than it would have been prior to the pandemic. For this reason, the first volunteer was vaccinated in June 2021, with a total of 12 volunteers being vaccinated to date (group 1, *n* = 3; group 2, *n* = 6, group 3, *n* = 3). All group 1 and 2 volunteers have data up to at least D28 post-vaccination and are included in this chapter. If available, data from volunteers post-D28 are also included. A few ELISA and ELISpot data points from the initial group 3 volunteers have also been included.

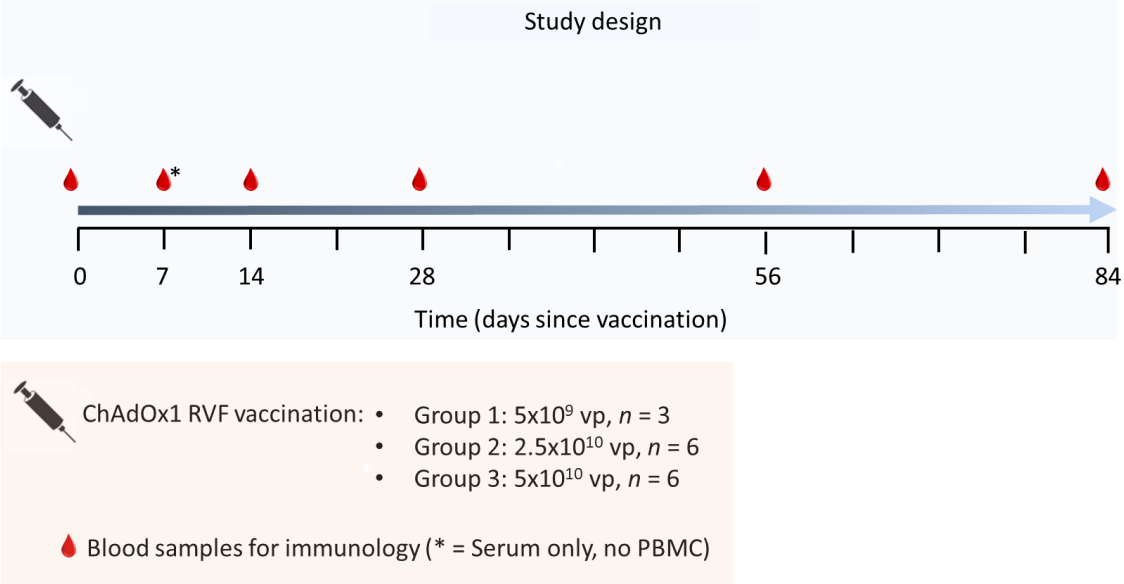


Figure 24. *RVF001 Trial design. Participants were given a single dose of ChAdOx1 RVF at 5x10^9 vp, 2.5x10^{10} vp or 5x10^{10} vp and followed up for 3 months. Immunology bloods were taken at D0 (pre-vaccine) and then D7, D14, D28, D56 and D84 post-vaccine*

I have established the RVF001 clinical trial laboratory analytical plan and here, using the assays previously optimised, provide the first assessment of the immunogenicity elicited by ChAdOx1 RVF in humans, comparing it to some of the Kenyan adults naturally exposed to RVFV from Chapter 3.

5.2 Objectives:

1. To assess the neutralising antibody response elicited after vaccination with ChAdOx1 RVF
2. To assess the total IgG titre induced towards Gn and Gc
3. To compare neutralising and binding IgG titres in vaccinees to titres acquired after RVFV infection
4. Assess the cellular response to RVFV Gn and Gc peptides by IFNγ ELISpot

5.3 Results:

5.3.1 Neutralising antibody response elicited after vaccination with ChAdOx1 RVF

Serum taken pre-vaccine (D0) and at various intervals post-vaccine were assessed for their ability to neutralise RVFV. All except a single group 1 vaccinee had detectable nAb titres at D28 (**Figure 25**). 3 months post-vaccination, a single group 1 volunteer and all group 2 volunteers remained positive (**Figure 25**).

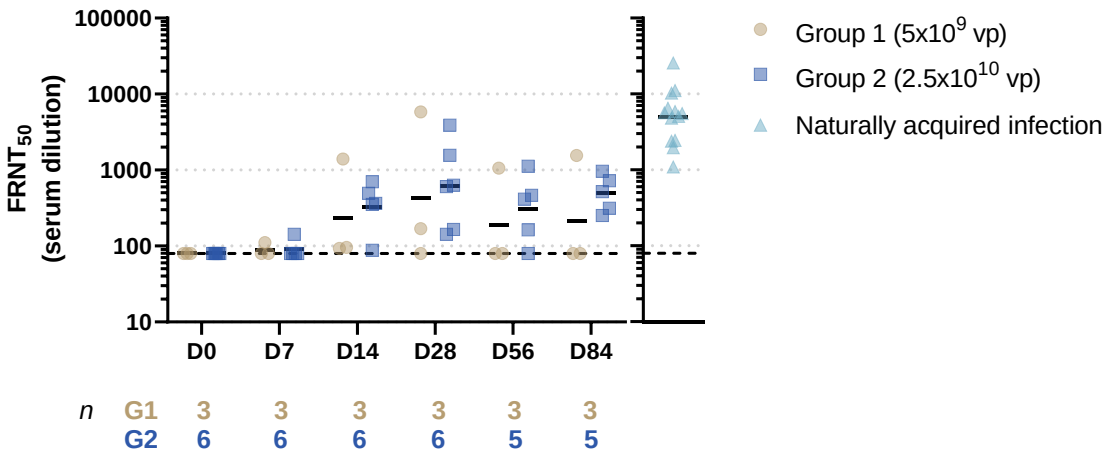


Figure 25. *Neutralising antibody titres in volunteers vaccinated with ChAdOx1 RVF or after naturally acquired infection. Naturally acquired infection samples (n = 13) are from Kenyan adults assayed in chapter 3, part of the 50 samples characterised from Tana River County and represent a mixture of samples with low, medium and high responses. G1 and G2 volunteers were vaccinated with $5x10^9$ (n = 3) or $2.5x10^{10}$ vp (n = 6) ChAdOx1 RVF, respectively. Samples were titrated in duplicate with symbols representing the mean. Bars represent geomeans.*

5.3.2 IgG response targeting Gn and Gc elicited after vaccination with ChAdOx1 RVF

Serum samples were assayed by ELISA to determine binding titres of anti-Gn and anti-Gc IgG. There was no significant increase in antibodies towards Gn in group 1 or 2 (G1, p = 0.24, RM one-way ANOVA test; G2, p = 0.09, mixed-effects analysis) (**Figure 26**). Statistical analysis was not conducted on group 3 data due to low numbers. Anti-Gc IgG titres increased in both groups 1 and 2 post-vaccination, although this was only statistically significant in group 2 (G1, p = 0.21, RM one-way ANOVA test; G2, p = 0.04, Mixed-effects analysis) (**Figure 26**). A selection of individuals naturally exposed to RVFV, encompassing low, medium and high responders from Chapter 3, were repeated on the same assay run. These responses showed significantly higher anti-Gn IgG titres than vaccinees at all timepoints except D84 (natural infection vs G2 D0, p = 0.001; vs G2 D7, p = 0.002; vs G2 D14, p = 0.038; vs G2 D28 p = 0.011; vs G2 D56, p = 0.040; vs G2 D84, p = 0.14, Kruskal Wallis with Dunn's multiple comparison test) (**Figure 26**). In contrast, by D28 post-vaccination, anti-Gc IgG titres were similar in magnitude to those induced by natural exposure and continued rising to D56 (G1 D28 geometric mean of 104 [95%CI 11-947]; G1 D56 200 [70-569]; G2 D28 227 [117-437]; G2 D56 344 [61-1944]; Individuals naturally exposed had a geometric mean titre of 276 [163-467]). Naturally exposed individuals were only significantly higher than group 2 vaccinees at D0 and D7 (natural infection vs D0, p = 0.013; vs D7, p = 0.013; vs D14, p = 0.240; vs D28, p = 0.846; vs D56, p > 0.999; vs D84, p > 0.999, Kruskal Wallis with Dunn's multiple comparison test] (**Figure 26**).

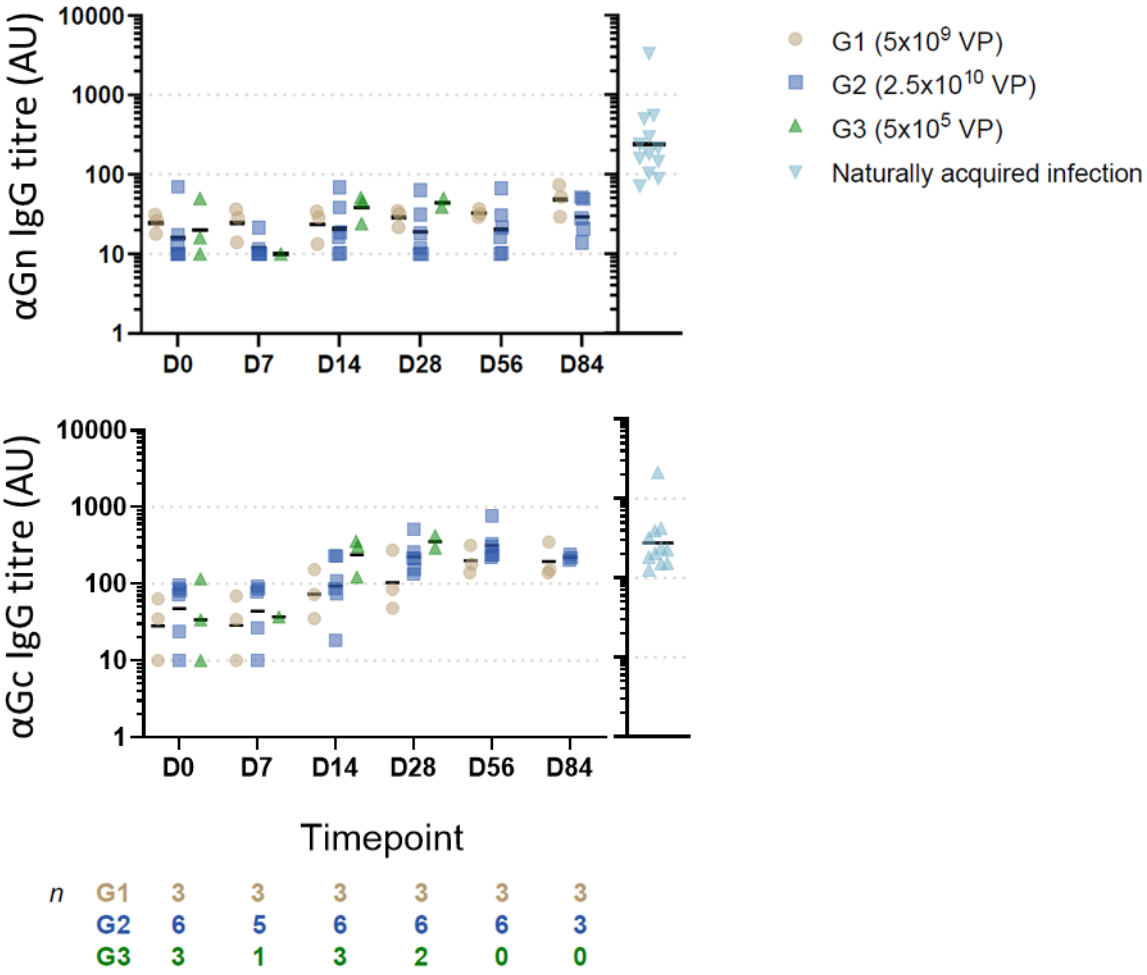


***Figure 26**. Binding IgG titres towards RVFV Gn and Gc over time in volunteers vaccinated with ChAdOx1 RVF or after naturally acquired infection. Top, anti-Gn IgG titres. Bottom, anti-Gc IgG titres. Naturally acquired infection samples are from Kenyan adults assayed in chapter 3, part of the 50 samples characterised from Tana River County and represent a mixture of samples with low, medium and high responses. These samples were repeated on the same assay run as the clinical trial samples. The values below the graph represent the number of samples assayed for each group at each timepoint. Group 1 and 2 volunteers were vaccinated with $5x10^9$ vp (group 1), $2.5x10^{10}$ vp (group 2) or $5x10^{10}$ vp (group 3) ChAdOx1 RVF, respectively.*

5.3.3 IFNγ ELISpot response after vaccination with ChAdOx1 RVF

I assessed the IFNγ ELISpot response after stimulation of PBMC samples, freshly isolated from whole blood, with an overlapping peptide library spanning Gn and Gc. Of the three volunteers in group 1, a single volunteer failed to mount any detectable IFNγ response while the response in the other two peaked at D28 post-vaccine (**Figure 27**). All group 2 and 3 volunteers mounted a response, peaking at D14. While area under the curve analysis up to D84 showed the group 2 response to be larger than group 1, the difference was not significant (G1 AUC = 12,080 vs G2 AUC = 17,743, p = 0.46, unpaired T test). AUC for group 3 was not calculated due to limited data but showed a higher median response than the other groups at D14 and D28 (**Figure 27**).

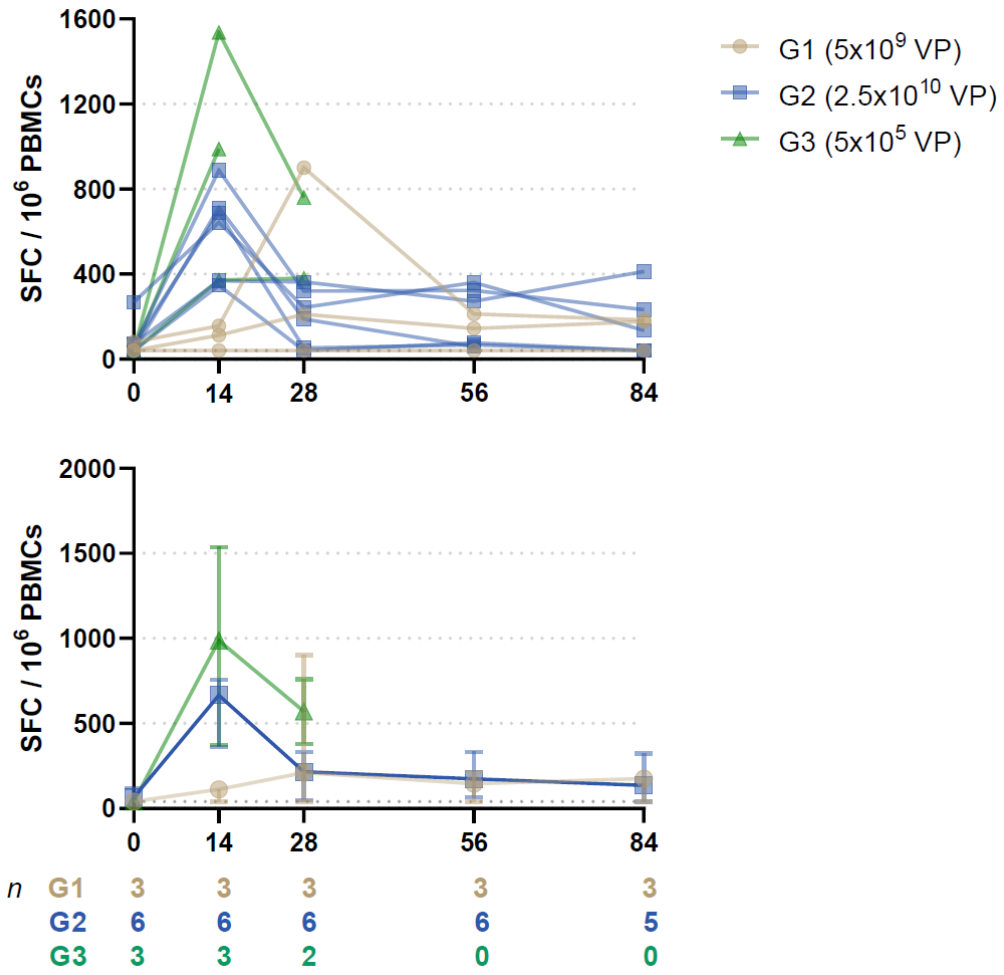


Figure 27. *IFNγ ELISpot response after PBMC stimulation of an overlapping peptide library covering the GnGc polyprotein. Top, time course of individual IFNγ ELISpot responses. Bottom, time course of*

the IFNγ response for groups 1, 2 and 3. Line represents median, with error pars representing IQR. Area under the curve analysis up to D84 shows no significant difference between groups 1 and 2 (G1 AUC = 12080, G2 AUC = 17743, p = 0.46, unpaired T test). AUC not calculated for group 3 due to low numbers. SFC = spot forming cells. Values below graphs indicate the number of individuals sampled at each timepoint per group

I then carried out further peptide pool-specific analysis into the IFNγ response by comparing the fold increase from D0 to their peak response (**Figure 28**). Responses were broad, with all pools showing some level of increase in at least one individual. 4/12 volunteers had their largest increase in response to stimulation with Gn pool 2, starting at amino acid position 105 (**Figure 28**). There was no significant difference in magnitude between individuals' responses towards peptides spanning Gn or Gc (p = 0.06, paired t test) (**Figure 28**).

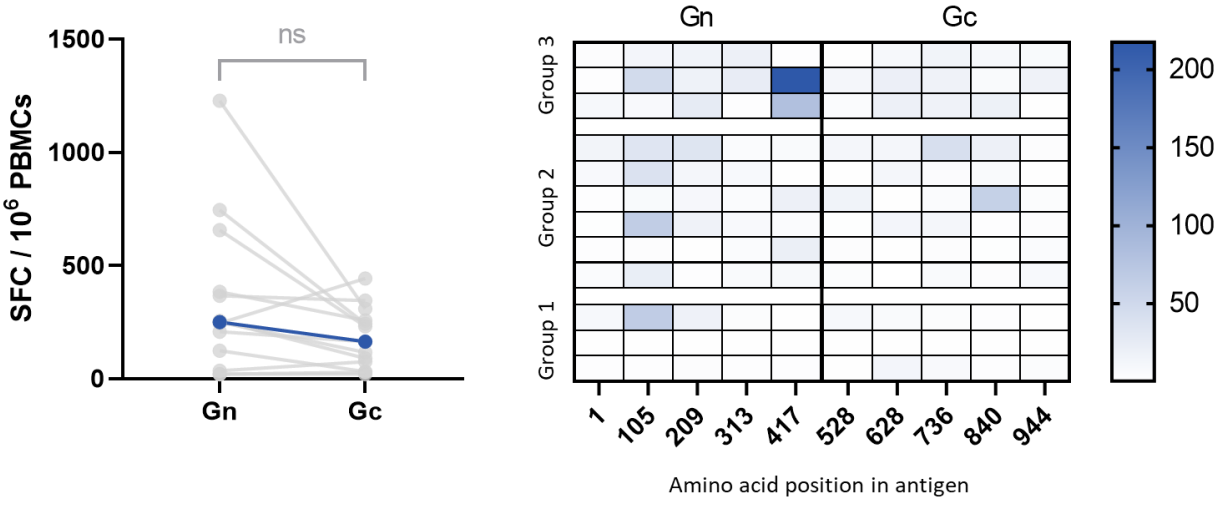


Figure 28. *Further breakdown of IFNγ ELISpot response. Left, comparison of Individual IFNγ ELISpot responses split between Gn and Gc peptides (p = 0.06, paired t test). Grey symbols/lines represent individual data with blue symbol/line representing median. Right, heat map showing the fold change in IFNγ ELISpot response (SFC/10^6 PBMC) from pre-vaccine (D0) to their peak for each peptide pool. Each row represents a single volunteer.*

There was no correlation between nAb titres at D28 and IFNγ ELISpot response or anti-Gn binding IgG titres (**Figure 29**). There was, however, a strong correlation between nAb titres and anti-Gc IgG titres (**Figure 29**).

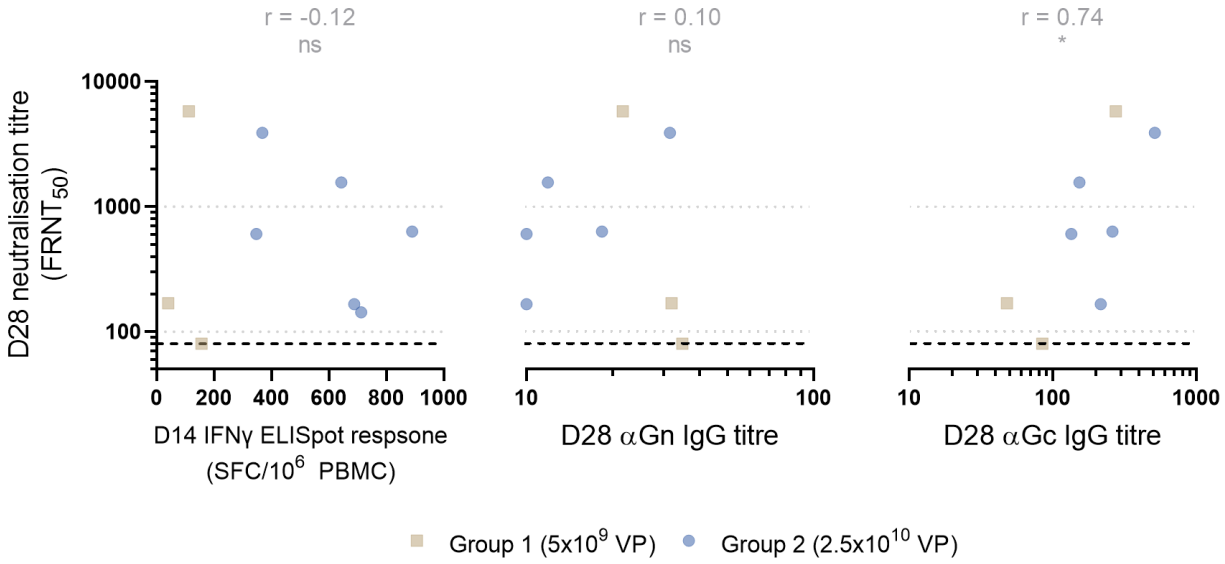


***Figure 29**. nAb titres correlate with binding IgG titres but not IFNγ response. Correlation of neutralisation titres ($FRNT_{50}$) with IFNγ ELISpot response (left), Gn ELISA (middle), and Gc ELISA (right). Spearman's correlation: $FRNT_{50}$ vs IFNγ response r=-0.12, p = 0.78; $FRNT_{50}$ vs Gn ELISA r = 0.10, p = 0.82 ; $FRNT_{50}$ vs Gc ELISA r = 0.74,*. *, p = 0.04.*

5.4 Discussion:

RVF is a particularly attractive target for a One Health approach to vaccine development as isolates collected throughout Africa and the Arabian Peninsula in various species from the 1950s onwards show a high degree of conservation at the nucleotide and amino acid level [89-91]. Indeed a single serotype is responsible for all disease in both livestock and humans [93]. A safe and effective vaccine for use in both livestock and humans would be an extremely useful tool to combat RVF outbreaks. Previous published research by the Warimwe group has shown ChAdOx1 RVF to be safe and highly efficacious in healthy and pregnant livestock [103, 148]. This chapter provides the first data of the human immune response to the same vaccine.

While the primary readout for first-in-human clinical vaccine trials is safety, I have focused on the secondary endpoint of immunogenicity. At the time of writing, only groups 1 and 2 have been fully enrolled. Since these data, in addition to data from previous adenovirus-vectored vaccines, show a dose-dependent response, it is probable that group 3 volunteers (receiving 10x and 2x the doses given to group 1 and 2 volunteers, respectively) will show further increases in immunogenicity. Indeed, data from the first group 3 volunteers shows both an improved IFNγ ELISpot response and higher anti-Gc IgG titres, although no neutralisation assays on group 3 samples have yet been done.

All except one of the group 1 volunteers seroconverted with nAbs by D28. While this was the peak of the nAb response, all except two group 1 volunteers still had detectable titres three months after vaccination. During the peak, there was significant overlap with the titres conferred by RVFV infection. For group 1 volunteers, in contrast to anti-Gn IgG titres, their anti-Gc IgG titres increased post-vaccination, although the increase was not statistically significant. In group 2, there was still no increase in anti-Gn titres post-vaccine, however anti-Gc titres did show significant increases and, at their peak, the median response was even higher than those detected after natural exposure. That naturally exposed humans, considered to have long-lived protection, showed comparable anti-Gc IgG responses is encouraging. Consistent with data from naturally exposed individuals, anti-Gc IgG correlates strongly with nAb titres after ChAdOx1 RVF vaccination. However, while naturally exposed individuals also showed a strong correlation between anti-Gn IgG and nAb titre, this was not present after vaccination due to the extremely low or undetectable titres of Gn antibodies.

In chapter 3, I showed that neutralising antibodies in naturally exposed humans predominantly target Gn over Gc. That there was no significant induction of anti-Gn IgG after ChAdOx1 RVF vaccination is interesting and warrants further study. For example, examination of differences in antigen expression and how the glycoproteins interact after ChAdOx1 RVF vaccination compared

to wildtype RVFV infection may provide insights into the differential presentation of RVFV Gn and Gc to the immune system. Furthermore, a caveat worth exploring is that the recombinant glycoproteins used in the IgG ELISA are soluble fragments and not expected to form the higher-order architectures of RVFV Gn and Gc on the surface of the mature virion [75]. Thus, differences in Gn and Gc antigenicity observed across experiments may also relate to how the elicited immune responses target these isolated proteins (versus higher-order quaternary epitopes), as well as the integrity of the Gn and Gc antigens. Interestingly, however, livestock vaccinated with ChAdOx1 RVF also appear to induce relatively higher titres towards Gc than Gn compared to a live attenuated vaccine (chapter 6), and yet efficacy trials with both vaccines showed ChAdOx1 RVF to be more protective [103]. So while the naturally acquired immune response to RVFV is very robust, with particular importance on antibodies targeting Gn, protective immunity may also be conferred through antibodies targeting Gc or other mechanisms.

As expected, ChAdOx1 RVF elicited a dose-dependent IFNγ ELISpot response between all groups. While not statistically significant, the low numbers so far enrolled make achieving statistical significance in any of the measures more difficult. I found no correlation between IFNγ ELISpot response at D14 and their nAb titres at D28. While the response here is substantially higher than in naturally exposed individuals assayed in chapter 3, at present, it is not possible to directly compare the responses due to different peptide purity, concentration and pooling used. Now we have these clinical trial-grade peptides, PBMC from those naturally exposed samples can be re-run and compared using the identical assay. In this trial, 2/3 group 1 volunteers had their peak IFNγ response at D28 rather than the typical D14. In the case of one volunteer, this response was significantly higher than their D14, reaching the highest level out of everyone. Whether the 2/3 volunteers peaking at D28 is just down to chance or if it reflects the kinetics of giving much lower vaccine doses is not certain. A previous first-in-human trial of a TB candidate vaccine showed that while certain individuals do peak later, the median response of 6 individuals given the same low

dose of $5x10^9$ vp was still D14 [176]. Of all the volunteers tested, the highest response in a third of them came after stimulation with the Gn pool spanning amino acids 105-208. A recent study identifying cellular epitopes in adults vaccinated with up to 6 doses of an inactivated candidate RVF vaccine showed an epitope beginning at amino acid position 109 to induce the highest response over the entire Gn and Gc polyprotein [173]. By stimulating cells with the constituent peptides that made up the pools they responded to here, minimal T cell epitopes can be experimentally identified in the future.

At the time of writing, the COVID-19 vaccine ChAdOx1-nCov19 has been authorised for emergency use in over 160 countries with over 2 billion doses being released [174-176, 189]. There is a legitimate concern that multiple doses of homologous viral-vectors is problematic due to the build-up of anti-vector immunity in the population. Indeed, the use of chimpanzee or rare human adenovirus serotypes as vectors were specifically designed to avoid the issue of pre-existing immunity diminishing vaccine efficacy. With millions of people now having received a ChAdOx1-vectored vaccine, anti-vector immunity may be significantly more prevalent with uncertain consequences for future vaccines using the same vector, should they be rolled out. Fortunately, the large scale roll out of ChAdOx1 nCoV-19 has given us the opportunity to learn more broadly about the immune response that vaccines using these vectors can elicit. We have now seen from those data that a second dose, despite people now having a level of anti-vector immunity from the first dose, was still effective at boosting the antibody response [190, 191]. The anti-vector responses after ChAdOx1-vectored vaccination do not appear to be particularly strong, perhaps in part due to its inability to replicate resulting in the initial dose being the only exposure the immune system sees. 6-9 months post ChAdOx1 85A, a TB candidate vaccine, anti-vector immunity from both T cells and antibodies appear to fall back to pre-vaccine levels, even in volunteers given two doses [176]. While an absence of effector memory T cells and detectable IgG towards ChAdOx1 does not rule out a robust memory response, a lack of these circulating cells and antibodies does

suggest sufficient opportunity for subsequent ChAdOx1-vectored vaccines to be used without significantly impacting upon their efficacy.

In addition to this ChAdOx1 RVF trial in Oxford, a similar trial in Uganda is due to begin imminently. This involves the same three dose escalation groups but with additional volunteers (*n* = 4, 10 and 10 for the three dose groups, respectively). This will provide safety and immunogenicity data in the target adult population. Broad differences in MHC allele frequencies between people from different geographic locations can affect the epitopes they recognise and therefore impact upon the overall immunogenicity. It is therefore critical to evaluate these vaccines in target populations as early as possible.

This chapter provides preliminary clinical trial immunogenicity data in a small number of healthy adults. I have shown that vaccination with a single shot of ChAdOx1 RVF has encouraging immunogenicity in humans. Whether the high anti-Gc IgG titres and comparatively absent anti-Gn IgG titres are capable of protection remains to be seen but the induction of neutralising antibodies bodes well [7]. Predictably, the responses measured so far show a dose effect, with higher doses inducing both stronger T cell responses and binding antibody titres. Full enrolment of the final group, who will receive twice the dose of group 2 will give us a realistic picture of immunogenicity at the dose we would intend to use going forward. Work characterising additional aspects of the cellular and antibody responses is ongoing. If, following these two initial clinical trials in the UK and Uganda, ChAdOx1 RVF continues to show promising immunogenicity and favourable safety data, further phase II studies can investigate optimal regimes.

6

Immunogenicity of ChAdOx1 RVF in livestock

6.1 Introduction:

Due to the drawbacks of current RVF livestock vaccines previously described (e.g. contraindications in pregnancy, reversion to virulence of live attenuated vaccines, lack of DIVA compliance etc.), better vaccines are required. As with humans, protection from RVF appears to be primarily mediated by nAbs targeting the glycoproteins, Gn and Gc [192]. While the use of chimpanzee adenovirus' as a vaccine platform has been used for a variety of human pathogens and shown to elicit potent humoral and cellular responses in clinical trials [193], apart from ChAdOx1 RVF, only one other ChAdOx1 vaccine has been tested in livestock species, ChAdOx1 MERS. Middle East Respiratory Syndrome (MERS) is a zoonotic coronavirus with a camel reservoir, with both camel-to-human and human-to-human transmission observed [194]. ChAdOx1 MERS was tested in dromedary camels and showed a significant reduction in viraemia post-exposure compared to non-vaccinated animals [195].

Considering the potential differences in immune response across different species, the development of a vaccine for multiple species poses unique challenges. However, with only one serotype and passive transfer of convalescent plasma to various naïve animals providing protection, a single vaccine for use in multiple species appears feasible [96, 196].

After showing promising immunogenicity in mice [197], ChAdOx1 RVF was then tested in the target livestock species of sheep, goats and cattle (Trial B, **Table 1**). [103] . This livestock trial compared the efficacy, as measured by the presence of viraemia in the blood post-challenge with live RVFV, in animals vaccinated with ChAdOx1 RVF, Smithburn or placebo. A single dose of ChAdOx1 RVF induced high nAb titres in sheep, goats, and cattle with no safety concerns, showing 100% sterile protection, even outperforming the Smithburn vaccine where two animals failed to seroconvert [103]. Following this success, three further livestock trials have been conducted: 1) a challenge trial in pregnant sheep and goats (WRVB, The Netherlands), which showed extremely high protection

from RVF disease and foetal loss (Trial C, **Table 1** [148]). 2) A dose de-escalation trial in sheep and cattle (Trial D, **Table 1**), and 3) a large non-inferiority field trial comparing ChAdOx1 RVF with Smithburn in multiple species (Trial E, **Table 1**).

The co-development of ChAdOx1 RVF for multiple species allows us to better understand how immune systems of different species respond after the same vaccination, and how it pertains to protection. In this chapter, I have measured the IgG response to Gn and Gc from the initial livestock trial, measured the humoral response from the dose-escalation trial and measured the cellular response from the pregnancy trial. Understanding which RVF epitopes are recognised and the mechanisms of neutralisation have previously arisen through analysis of monoclonal antibodies isolated from convalescent patients and vaccinated animals [94, 131, 198]. ChAdOx1 RVF was sent to Dr Jan Steyaert's lab in Brussels where they vaccinated a single llama with two doses, followed by further boosting with recombinant Gn and Gc proteins. DNA containing the variable regions of these antibodies were cloned into nanobody expression plasmids and shipped to Oxford. As preliminary work for the eventual characterisation of these nanobodies, I expressed and purified a small library of them, assessing their ability to bind Gn and Gc and neutralise RVFV in vitro.

6.2 Objectives:

- To determine the total IgG titre and avidity towards the surface glycoproteins after vaccination with ChAdOx1 RVF in sheep, goats and cattle, and correlate with nAb titre.
- To set-up and harmonize neutralization assays using a new live-attenuated strain of RVFV
- To investigate the immunogenicity of reduced dosing schedules of ChAdOx1 RVF in cattle and sheep.
- To compare the immunogenicity from livestock efficacy trials with immunogenicity from the dose de-escalation study to infer the potential for protection when using lower doses of ChAdOx1 RVF
- To optimize ELISpot assays to provide the first measurements of the cellular response towards RVFV in livestock after ChAdOx1 RVF vaccination.
- To express and purify a small library of nanobodies isolated from a llama vaccinated with ChAdOx1 RVF and recombinant Gn and Gc proteins and assess their ability to bind Gn and Gc and to neutralize live RVFV in vitro.

6.3 Results:

6.3.1 IgG responses in livestock towards both Gn and Gc after vaccination with ChAdOx1 RVF or Smithburn

I used frozen serum samples from the multi-species efficacy trial (trial B, **Table 1**) to provide the first insight into the binding IgG titres elicited in livestock following ChAdOx1 RVF vaccination. Detectable IgG titres towards both glycoproteins in sheep, goats and cattle vaccinated with ChAdOx1 RVF appear by D14 (**Figure 30**). This increase continues to D28 and is boosted following challenge (**Figure 30**).

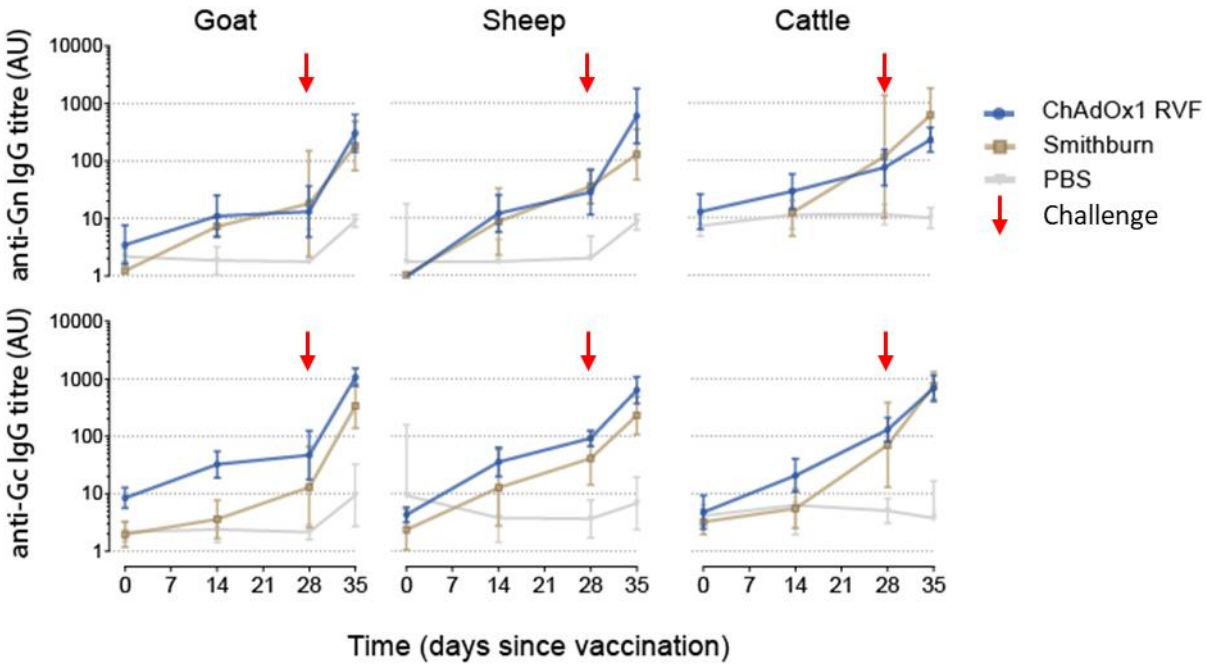


Figure 30. *Timecourse of total IgG titres, as measured by standardised ELISA, towards Gn (top) or Gc (bottom), in livestock vaccinated with ChAdOx1 RVF, Smithburn or PBS (***Table 1***, Trial B). Symbols represent geomeans, error bars represent 95% CI. Arrows denote challenge with live RVFV 28 days post-vaccine. ChAdOx1 RVF administered at 1x10^9 IU, Smithburn dose administered according to instructions. See Materials and methods for ELISA information.*

There was no significant differences between titres towards either glycoprotein after vaccination with either ChAdOx1 RVF or Smithburn at D28, the peak response prior to challenge (Mann-Whitney test, details in figure legend (**Figure 31**).

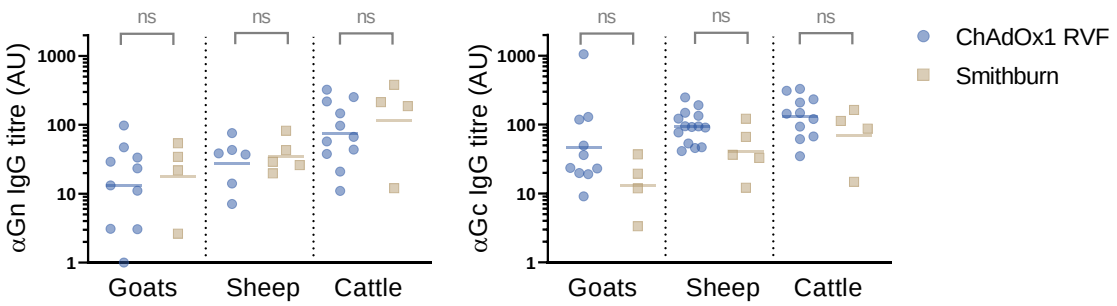


Figure 31*. D28 post-vaccine comparison of anti-Gn (left) and anti-Gc (right) IgG titres 28 days after vaccination with ChAdOx1 RVF or Smithburn. Goats: ChAdOx1 RVF Gn geomean of 13 [95% CI 5-36]*

vs Smithburn 18 [2-150], p = 0.73. ChAdOx1 RVF Gc geomean of 47 [18-125] vs Smithburn 13 [3-66], p = 0.14. D28 sheep: ChAdOx1 RVF Gn geomean of 28 [11-69] vs Smithburn 35 [18-70], p = 0.93. ChAdOx1 RVF Gc geomean of 92 [67-126] vs Smithburn 41 [14-120], p = 0.55. D28 cattle: ChAdOx1 RVF Gn geomean of 74 [36-152] vs Smithburn 116 [10-1355], p = 0.49. ChAdOx1 RVF Gc geomean of 129 [80-209] vs Smithburn 70 [13-383], p = 0.34. Mann-Whitney test was used for all comparisons.

There was a positive association between binding IgG titres targeting either glycoprotein and overall nAb titre after ChAdOx1 RVF vaccination in all three species. Only for Gn antibodies in cattle was the correlation with overall nAb titre not significant (Gn IgG vs VNT_{50} Spearman's correlation: goats r = 0.85,***; sheep r = 0.67,**; cattle r = 0.55,*. Gc IgG vs VNT_{50} Spearman's correlation goats r = 0.70,*; sheep r = 0.62,*; cattle r = 0.38, ns.) (**Figure 32**). Due to the low numbers (*n* = 4 per species), Spearman's correlations were not calculated for Smithburn vaccinated animals.

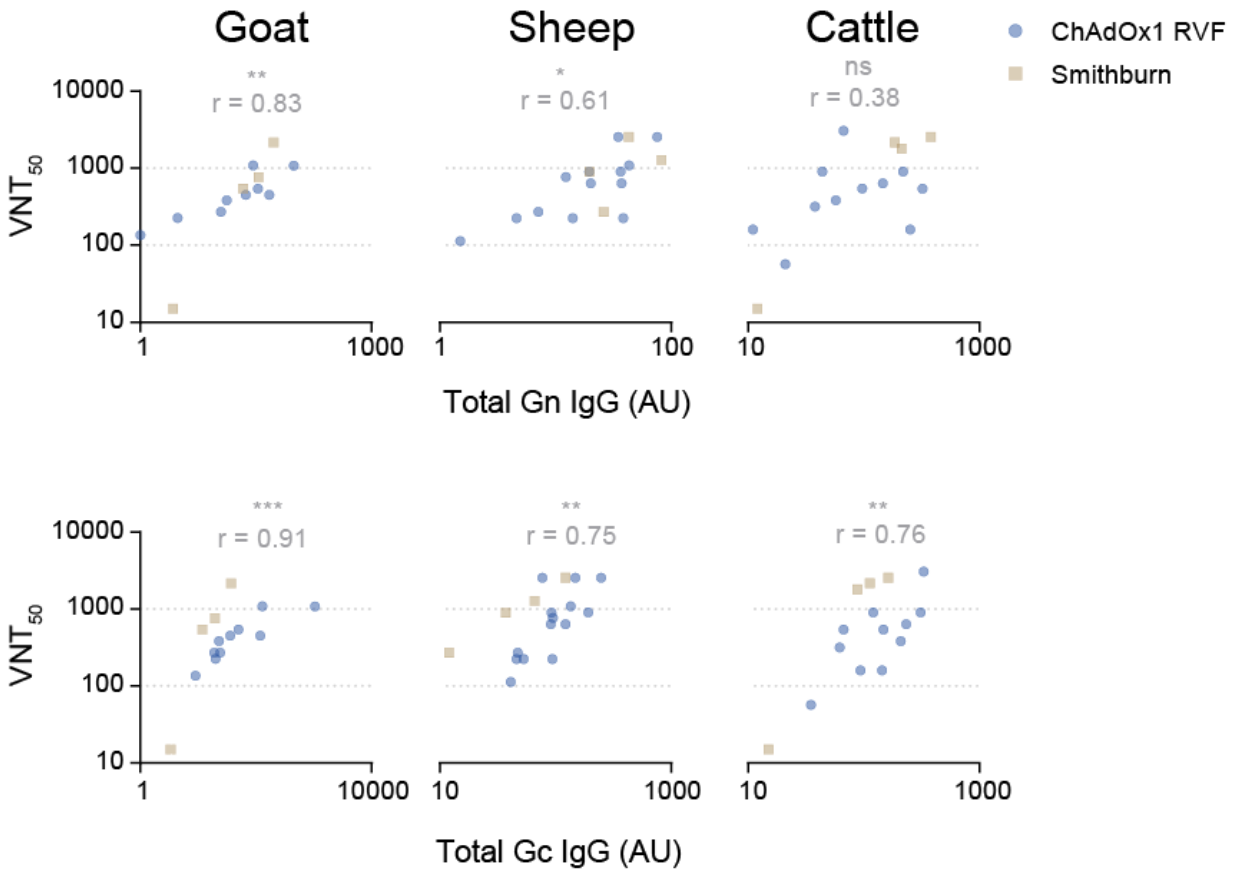


Figure 32**. Correlations between neutralisation titre, as measured by VNT assay, and total IgG titre towards Gn (top row) and Gc (bottom row), as measured by ELISA at D28 post-vaccine using samples (from Trial B, Table 1). Gn IgG vs VNT Spearman's correlation: goats r = 0.83 [unable to calculate 95% CI due to low n],; sheep r = 0.67 [0.07-0.87],**; cattle r = 0.38 [-0.31-0.80], ns. Gc IgG vs VNT Spearman's correlation: Goats r = 0.70 [0.13-0.92],*; sheep r = 0.62 [0.14-0.87],*; cattle r = 0.70 [0.17-0.92], *.*, p <0.05; **, p <0.01; ***, p <0.001; ns, p = 0.25. Due to low number of Smithburn vaccinated animals (n = 4), Spearman's correlations are for ChAdOx1 RVF vaccinated animals only. G.M. carried out the neutralisation assays.*

The association between avidity of IgG binding Gn and Gc and the animal's ability to neutralise is less clear (**Figure 33**). Spearman's correlations between IgG avidity and neutralisation titre were only significant for both Gn and Gc in goats (r = 0.73, p = 0.02 and r= 0.80, p = 0.007, respectively).

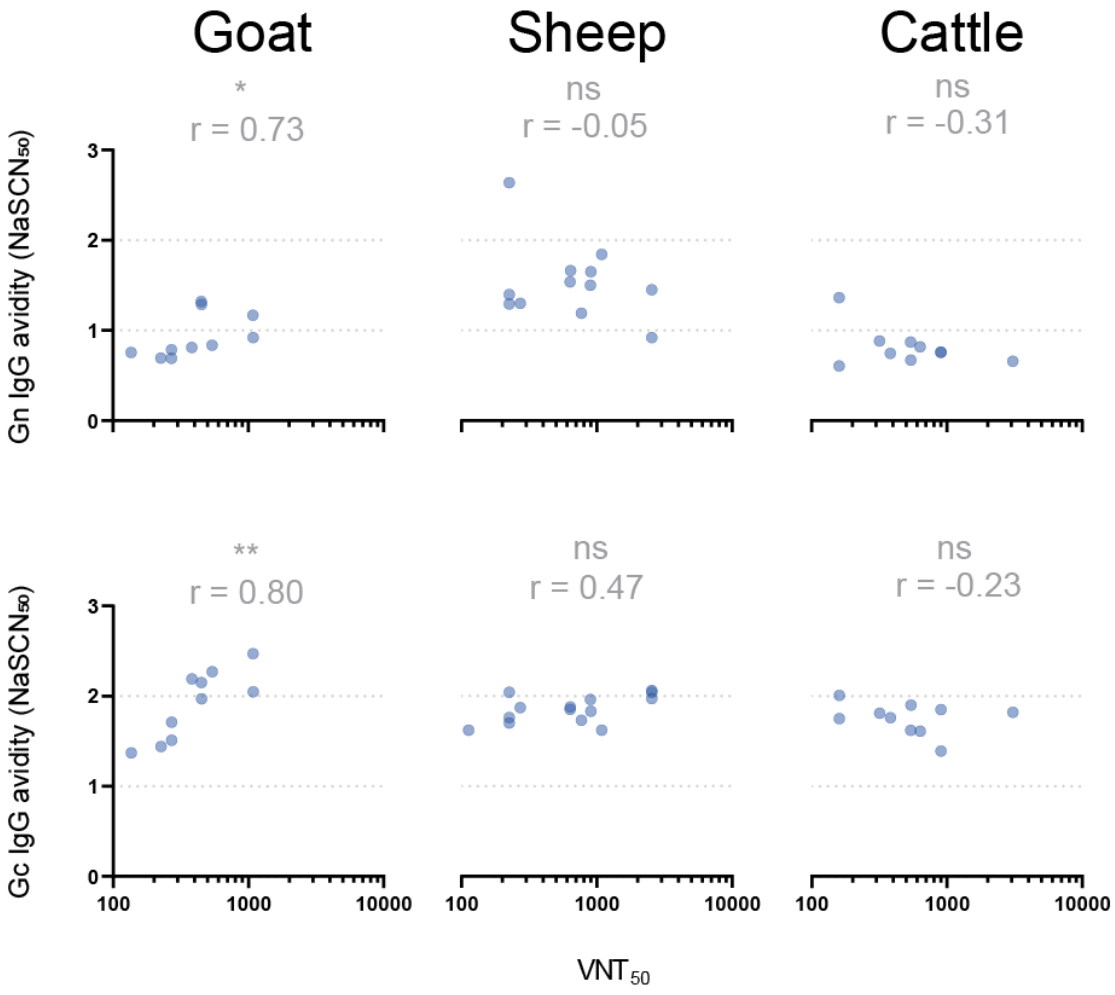


***Figure 33.** Correlations between neutralisation titre, as measured by VNT assay, and IgG avidity towards Gn (top row) and Gc (bottom row), as measured by ELISA at D28 post-vaccine. Gn IgG vs*

*VNT Spearman's correlation: goats r = -0.73 [unable to calculate 95% CI due to low n], **; sheep r = -0.05 [-0.62-0.55], ns; cattle r = -0.31 [-0.78-0.37], ns. Gc IgG vs VNT Spearman's correlation goats r = 0.80 [unable to calculate 95% CI due to low n],**; sheep r = 0.47 [-0.10-0.81], ns; cattle r = -0.23 [-0.74-4.4], ns.*,p <0.05; **,p <0.01; ***, p <0.001; ns, p=0.25. This uses the same neutralisation data as Figure 32, carried out by G.M.*

6.3.2 Harmonizing neutralisation assays using new live-attenuated RVFV strain

Due to diminishing stocks of our live-attenuated MP-12 strain of RVFV and a desire to try and harmonize neutralisation assays between RVF research groups, we received another live-attenuated RVFV strain and a protocol from a collaborator in the Netherlands [199]. This eGFP strain has been attenuated by splitting the M segment in two, resulting in the separation of Gn and Gc. It also lacks the primary virulence factor, the NSs gene. To show that this neutralisation assay is consistent with previous assays used, I compared it with the VNT_{50} assay (used in **Figure 30** and **Figure 32**) as well as the Gn and Gc ELISA response. All showed a significant positive correlation, consistent with previous neutralisation assays (VNT_{80} (eGFP assay) vs VNT_{50} (MP-12 assay) r = 0.72, **; VNT_{80} vs Gn ELISA r = 0.42 [0.07-0.87],*; VNT_{80} vs Gc ELISA r = 0.57 [-0.31-0.80], ***. *, *p* <0.05; **, *p* <0.01; ***, *p* <0.001. Spearman's correlation) (**Figure 34**).

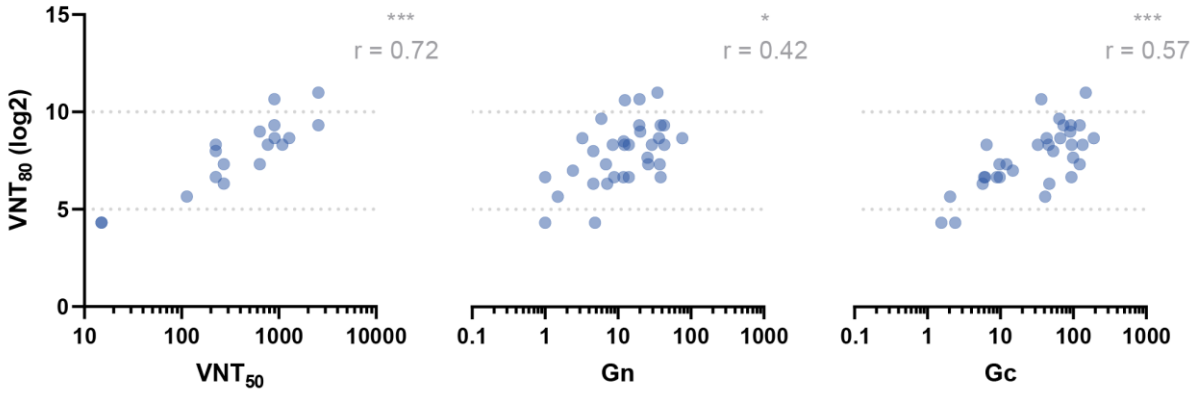


Figure 34. *VNT_{80} is consistent with previous assays. Correlation of neutralisation assay (VNT_{80}) with the previous neutralisation assay used on livestock (left), Gn ELISA (middle) and Gc ELISA (right). Spearman's correlation: VNT_{80} (eGFP assay) vs VNT50 (MP-12 assay) r=-0.72 [95% CI 0.39-0.89], **; VNT_{80} vs Gn ELISA r=-0.42 [0.10-0.66],*; VNT80 vs Gc ELISA r=-0.57 [0.28-0.77], ***.*,p = 0.01; ***, P < 0.0001; This uses the same VNT_{50} data on the left-hand graph as Figure 32, carried out by G.W.*

6.3.3 Investigating the immunogenicity of reduced dosing schedules of ChAdOx1 RVF in cattle and sheep.

In these early ChAdOx1 RVF trials, the first in target livestock species, a dose of 1E9 IU was used for all species. In order to shed light on the optimum dose, a dose-escalation trial carried out in Pirbright vaccinated sheep (*n* = 5 per group) and cattle (*n* = 7 per group) with ChAdOx1 RVF at either 5E6 IU, 5E7 IU or 5E8 IU (trial C, **Table 1**). The animal work in Pirbright was carried out under Bryan Charleston's team. Serum was collected pre- and post-vaccine and shipped to Oxford, where I measured the humoral response.

In sheep, nAbs and binding antibodies towards Gn and Gc show reduced immunogenicity when lower vaccine doses were used but this was statistically significant only for nAb titres and anti-Gc binding IgG titres at D21 (log2 VNT_{80} low dose mean 6.57 [95% CI 5.49-7.66] vs high dose mean 8.39 [6.86-9.92], p = 0.049, Ordinary one-way ANOVA with multiple comparisons; D21 Gc IgG titre low dose geomean 6.67 [2.48-18.07] vs high dose geomean 45.74 [14.74-141.9], p = 0.03, Kruskal Wallis with Dunn's multiple comparisons test) (**Figure 35**). Combining all dose groups, the response was significantly higher at D14 compared to D21 for both nAb titre and anti-Gc IgG but not anti-Gn IgG (D14 vs D21: log2 VNT_{80} p = 0.0002, paired T test; anti-Gn IgG p = 0.10 and anti-Gc IgG p = 0.02, Wilcoxon matched-pairs signed rank test) (**Figure 35**).

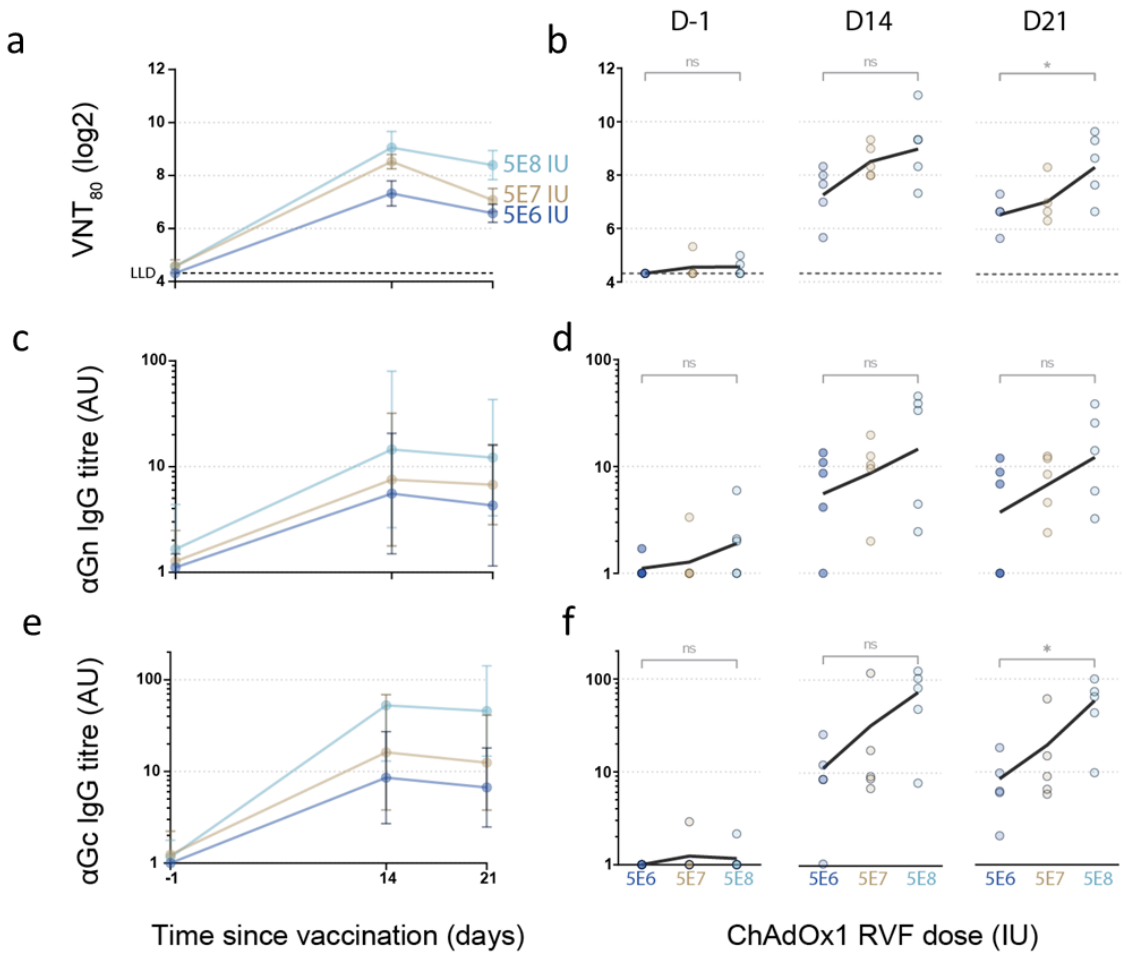


***Figure 35**. Humoral response in sheep after vaccination with different doses of ChAdOx1 RVF. (**a**) Time course of log2 VNT_{80} as measured by neutralisation assay grouped by dose. Symbols represent mean, error bars represent SEM. (**b**) Individual log2 VNT_{80} titres at each timepoint. (**c**) Time course of anti-Gn binding IgG titres and (**d**) Individual anti-Gn titres at each timepoint as measured by ELISA. Symbols represent Geomean, error bars represent 95% CI. (**e**) Time course of anti-Gc binding IgG titres and (**f**) Individual anti-Gn titres at each timepoint as measured by ELISA. Symbols represent Geomean, error bars represent 95% CI. Only D21 showed a significant difference between 5E6 and 5E8 dose groups (VNT_{80}: *, p = 0.049, Ordinary one-way ANOVA with multiple comparisons. Gc IgG titre *, p = 0.03, Kruskal Wallis test with Dunn's multiple comparison test). 5E6, 5E7 and 5E8 refers to a dose of $5x10^6$, $5x10^7$ and $5x10^8$, respectively.*

In cattle, binding IgG towards Gn and Gc both showed reduced titres when lower ChAdOx1 RVF doses were given (**Figure 36**). nAb titres have not yet been assessed but will be shortly.

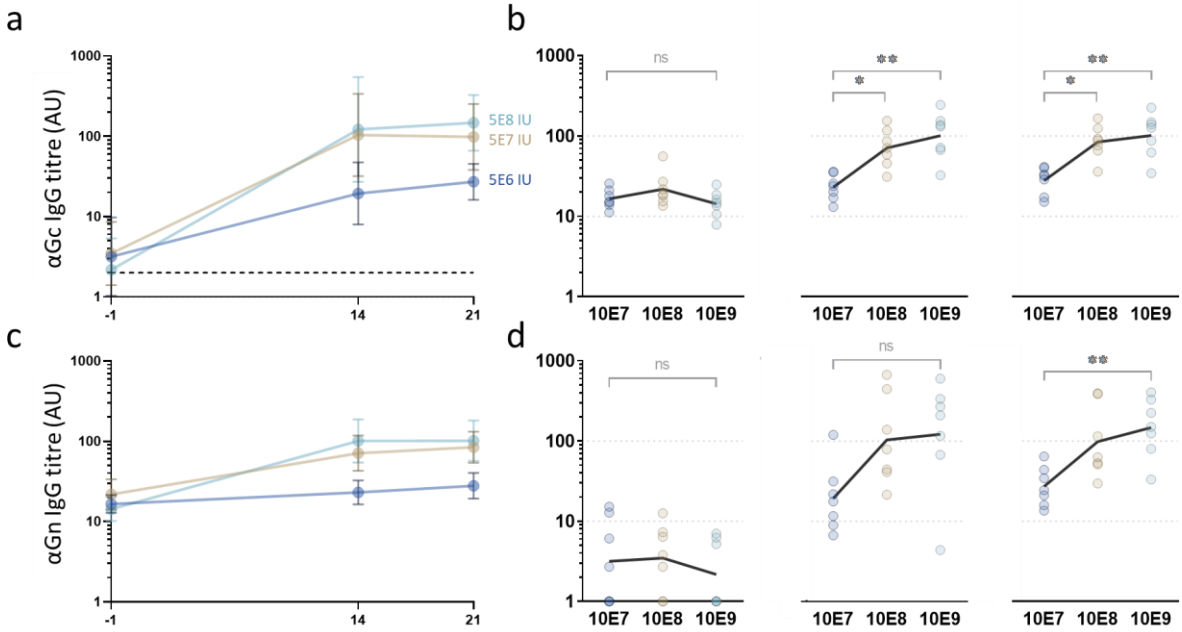


Figure 36. *Humoral response in cattle after vaccination with different doses of ChAdOx1 RVF. (**a**) Time course of anti-Gc binding IgG titres and (**b**) Individual anti-Gc IgG titres at each timepoint as measured by ELISA. (**c**) Time course of anti-Gn binding IgG titres and (**d**) Individual anti-Gn IgG titres at each timepoint as measured by ELISA. Symbols represent Geomean, error bars represent 95% CI. D14 and D21 showed a significant difference in anti-Gc IgG titres between the lowest dose and medium and high doses. Anti-Gn IgG titres were significantly different only between the low and high dose at D21. Gc IgG titre *, p < 0.05; **, p = < 0.01, Kruskal Wallis test with Dunn's multiple comparisons test.*

6.3.4 Comparison of immunogenicity from livestock efficacy trials with immunogenicity from the dose de-escalation study

In order to gauge whether these lower titres may still be protective, I reran sera from the multi-species Kenyan efficacy trial, where we have corresponding efficacy data, and compared to the nAb titres achieved after decreasing doses of ChAdOx1 RVF are administered, using the same neutralisation assay.

Mean log2 VNT_{80} in sheep immediately prior to challenge that subsequently showed 100% sterile protection was 8.30 (95% CI 7.58-9.02) with a minimum of 5.66 (**Figure 37**). None of the animals in the Pirbright dose escalation trial elicited titres lower than 5.66. Mean VNT_{80} at D21 was 6.57 (5.49-7.66), 7.07 (5.68-8.47) and 8.39 (6.86-9.92) after low, medium and high doses, respectively (**Figure**

37). Mean VNT_{80} at D14 was 7.32 (6.02-8.63), 8.52 (7.77-9.27) and 9.05 (7.36-10.75) after low, medium and high dose, respectively (**Figure 37**). The vast majority of naïve animals have a log2 VNT_{80} estimated at 4.32 which is the lower limit of detection (no neutralisation at 1:40 serum dilution). A small portion of animals showed neutralisation in some replicates at the highest serum concentrations, however, none had a titre above 5.66 (D-1, **Figure 35**).

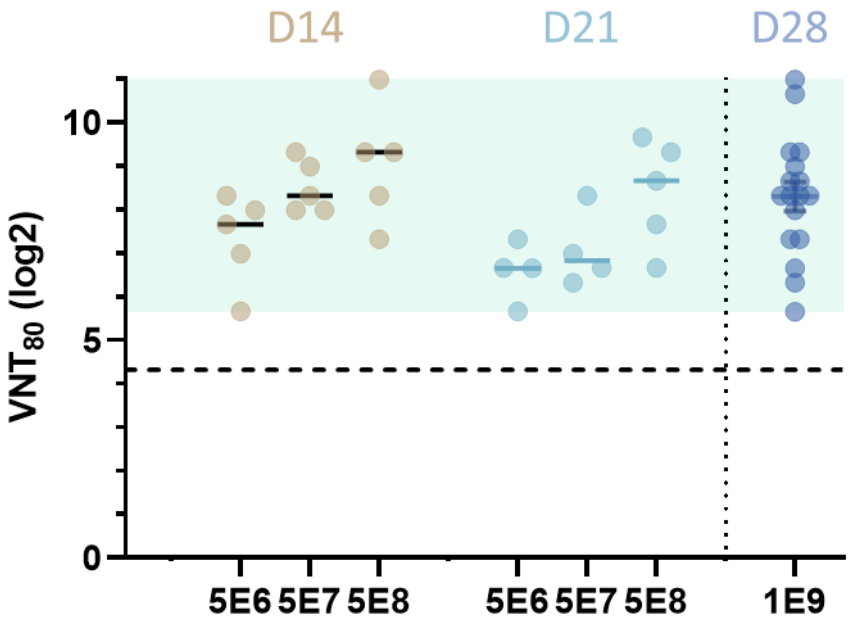


***Figure 37**. Comparison of neutralisation titres between the dose-escalation trial (D, Table 1) and the challenge trial (B, Table 1). Symbols represent individual VNT_{80} titres, with bars representing means. Error bars (where present) represent SEM. Green shaded area represents the range of titres seen in animals that were protected following live RVFV challenge.*

6.3.5 ELISpot optimisation

I have attempted a first look at the cellular response to RVFV antigens in livestock by measuring IFNγ production after stimulating PBMC with an overlapping peptide library spanning the GnGc polyprotein. Originally, peptides with crude purity (>30%) were used, these were combined into six pools. Initially, only a small number of frozen PBMC from cattle vaccinated with ChAdOx1 RVF were available (Trial A, **Table 1**). PBMCs from two cows were tested by ELISpot, using a final peptide

concentration of 10 µg/mL. One of the cows (001) had relatively high background of 139 SFC/10^6 PBMC in the unstimulated wells, however, it had significantly fewer spots in the peptide stimulation wells (**Figure 38a**). It seemed the peptides at the concentration used were inhibiting the response rather than eliciting one. To confirm, I stimulated PBMC from three cows (Trial A, **Table 1**) with a peptide pool along with the Gc protein, which on its own was previously eliciting a response. Peptides added to Gc abrogated the normal Gc response, while reducing the concentration of peptide appeared to increase the response (**Figure 38**).

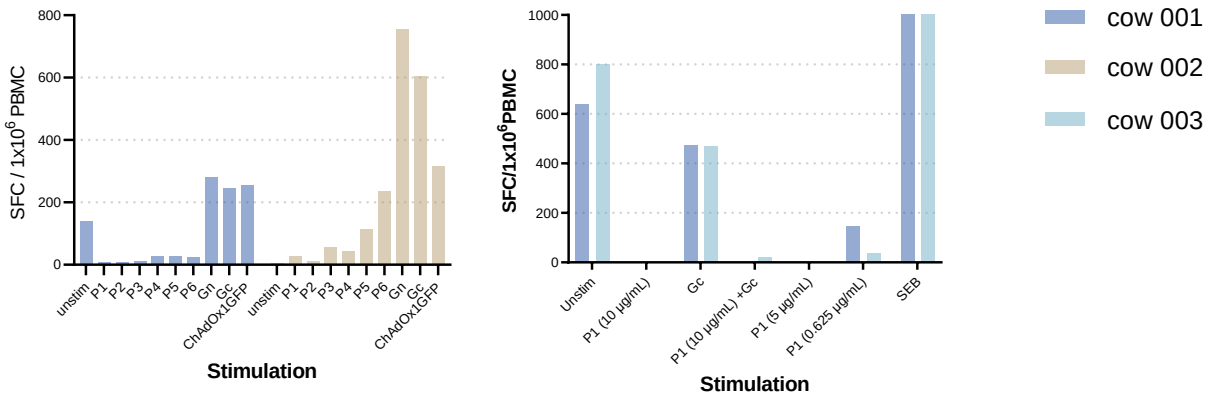


***Figure 38**. Initial test of cattle PBMC by RVF ELISpot. Both samples used PBMC taken 2 weeks after vaccination with 1E9 ChAdOx1 RVF. Unstim = media only; P1-P6 = peptide pools of a library spanning GnGc. Gn and Gc = recombinant protein (1 µg/mL). ChAdOx1 GFP was added at 2 MOI. Confirmation that peptides (Pool 1 in this case) at 10 µg/mL are supressing IFNγ production. Cells were co-stimulated with both Gc (1 µg/mL) and peptides (10 µg/mL). The addition of 10 µg/mL peptides to Gc reduces the signal >97%. 0.625 µg/mL of peptide alone resulted in higher signal than 5 µg/mL or 10 µg/mL.*

By this point, the efficacy trial in pregnant sheep and goats had begun in the Netherlands. I separated and froze PBMC from these animals and shipped them to Oxford. I then carried out a titration of peptide concentration using sheep PBMC (n = 2) from two weeks post-vaccination (**Figure 39**).

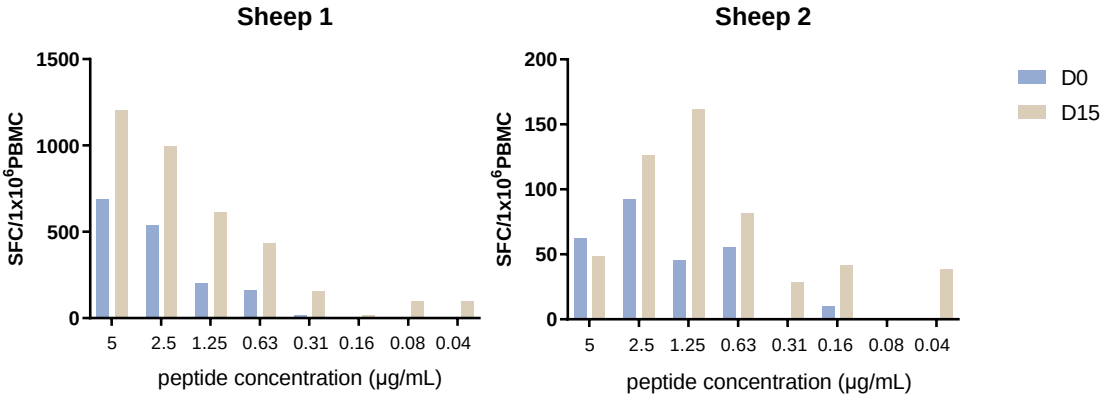


***Figure 39**. ELISpot peptide concentration titration using sheep PBMC pre- and post-ChAdOx1 RVF vaccination.*

While sheep 1 showed a similar pattern to the cattle samples, where the peptide response increased as peptide concentration decreased to 1.25 µg/mL, sheep 2 showed a reduction in response as the concentration reduced. However, the signal-to-noise ratio was highest for both sheep when peptides were used at a concentration of 1.25 µg/mL and this is what was then used for initial ELISpots on pregnant sheep and goats.

6.3.6 Cellular immunity in pregnant sheep and goats

To investigate whether sheep and goats vaccinated with ChAdOx1 RVF elicit detectable IFNγ T cell responses to PBMC stimulation with GnGc peptides, I carried out ELISpots on samples from the pregnancy trial (Trial C, **Table 1**). As expected, there was no significant increase in IFNγ response post-vaccine in the mock-vaccinated groups (goats (n = 8): D0 median 13 SFC/10^6 PBMC vs D15 median of 15 SFC/10^6 PBMC. Sheep (n = 8): D0 median 127 SFC/10^6 PBMC vs D15 median of 101 SFC/10^6 PBMC) (**Figure 40**). While there was an increase in response in 7/8 ChAdOx1 RVF vaccinated goats, overall, this was not significant (D0 median of 35 SFC/10^6 PBMC vs D15 median of 69 SFC/10^6 PBMC, p = 0.11, Wilcoxon matched-pairs signed rank test). There was also no significant increase post-ChAdOx1 RVF vaccination in sheep (D0 median of 74 SFC/10^6 PBMC vs D15 median of 111

SFC/10^6 PBMC, p = 0.84, Wilcoxon matched-pairs signed rank test). In contrast to goats, only 2/8 individual sheep showed an increase of any magnitude.

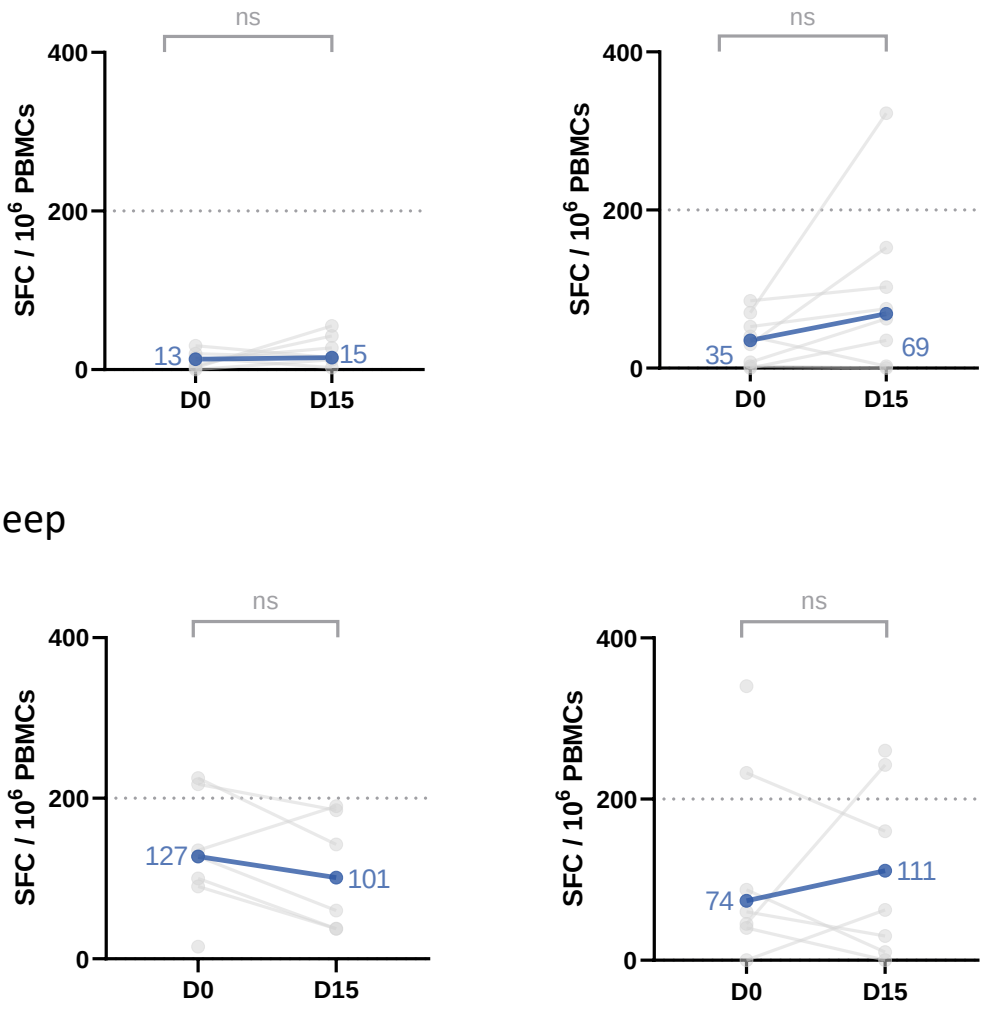


***Figure 40**. IFNγ ELISpot response in pregnant goats and sheep. (left) mock vaccinated, (right) ChAdOx1 RVF vaccinated. Grey symbols represent individual animals with lines connecting the same animals. Blue symbols/lines represent the median response. ns = non-significant difference by Wilcoxon matched-pairs signed rank test.*

Since the ChAdOx1 RVF clinical trial, where higher purity peptides were used (>80%), I reran these samples using the same peptide pools as the clinical trial. In addition to higher purity, due to the larger number of pools, a higher peptide concentration in each pool could be used (final

concentration of 5 µg/mL). Using these peptides increased the signal:noise ratio. All ChAdOx1 RVF vaccinated goats increased their response post-vaccine, with a significant increase of the median response from 90 to 498 SFC/ 10^6 PBMC (**Figure 41**). In addition to GnGc peptides, the anti-vector response was measured by stimulating with ChAdOx1 GFP. The response here was modest in comparison to the peptides but ChAdOx1 RVF vaccinated goats did elicit a significant increase post-vaccine, from 5 to 33 SFC/10^6 PBMC, p = 0.03, Wilcoxon matched-pairs signed rank test) (**Figure 41**).

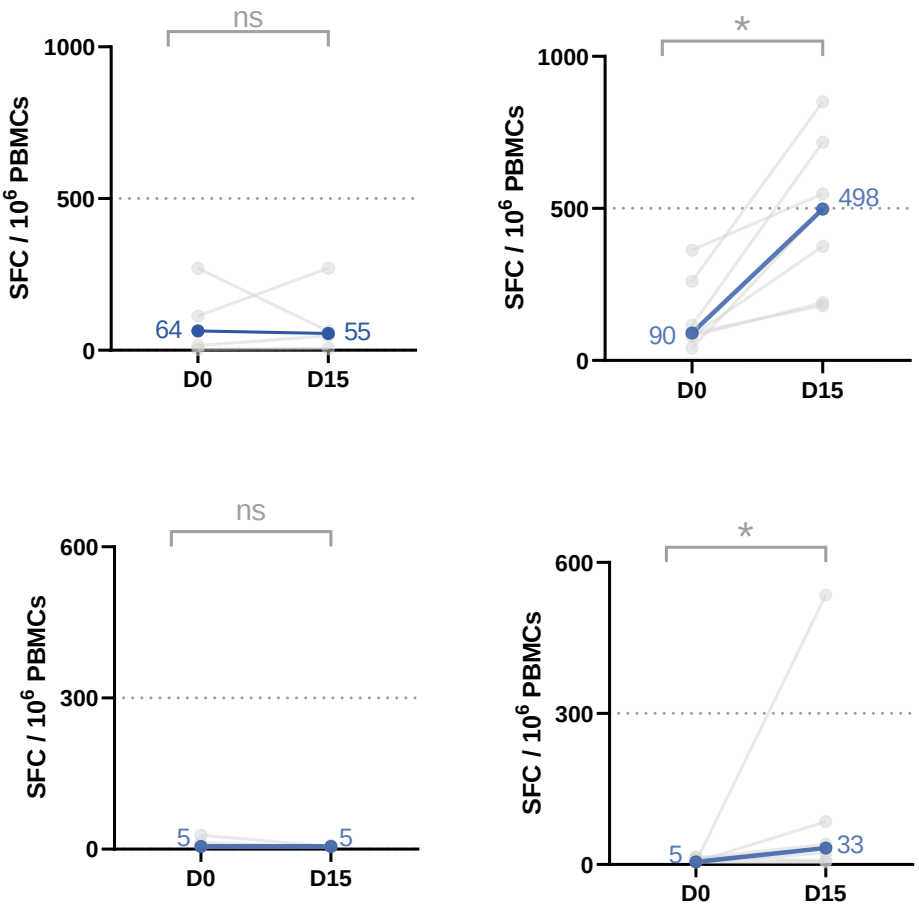


Figure 41. *IFNγ ELISpot response in pregnant goats. (Top) IFNγ response towards an overlapping peptide library covering the GnGc polyprotein after vaccinating with PBS (top left) or ChAdOx1 RVF (top right). (Bottom) IFNγ response towards ChAdOx1 GFP after vaccinating with PBS (bottom left) or ChAdOx1 RVF (bottom right). Grey circles/lines represent individual animals (n = 6-8 per group), blue circles/lines represents the median response at both timepoints. anti GnGc *, p = 0.016; anti-vector *, p = 0.031, Wilcoxon matched-pairs signed rank test.*

In sheep, however, high background remained with no significant increase post-vaccine. Similar to the earlier attempt with crude peptides, just 2/8 sheep showed an increase of any magnitude (D0 median of 138 to D15 median of 286 SFC/10^6 PBMC, p = 0.94, Wilcoxon matched-pairs signed rank test). There was no significant difference in the median anti-vector response in sheep post-vaccine (D0 median of 0 to D15 median of 3 SFC/10^6 PBMC, p = 0.94, Wilcoxon matched-pairs signed rank test), with 4/8 sheep showing an increase of any magnitude (**Figure 42**). Due to the lack of response in vaccinated sheep (**Figure 42**), the mock-vaccinated sheep were not assayed using these peptides. Further optimisation will be required.

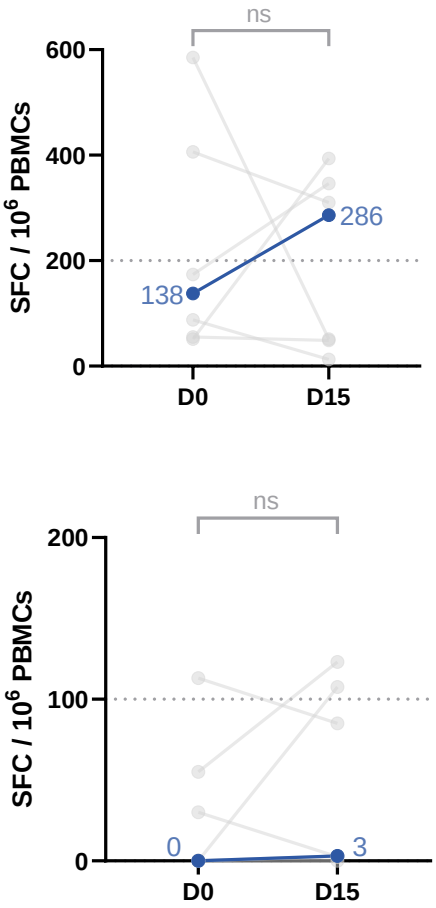


Figure 42. *IFNγ ELISpot response in pregnant sheep. (top) GnGc response two weeks post-ChAdOx1 RVF vaccination. Grey symbols represent individual animals with lines connecting the same animals. Blue symbols/lines represent the median response. ns = non-significant difference by Wilcoxon matched-pairs signed rank test.*

Because there was a significant increase in IFNγ response in goats post-vaccination, I looked at the relationship between VNT and cellular response by comparing the fold change in IFNγ ELISpot response (D15/D0) with their neutralisation titres. While the goat with the highest nAb titre also has the highest cellular response, and the goat with the lowest nAb titre has the lowest cellular response, there was no clear relationship elsewhere resulting in no overall correlation (Spearman's correlation r = 0.36, *p* = 0.42) (**Figure 43**).

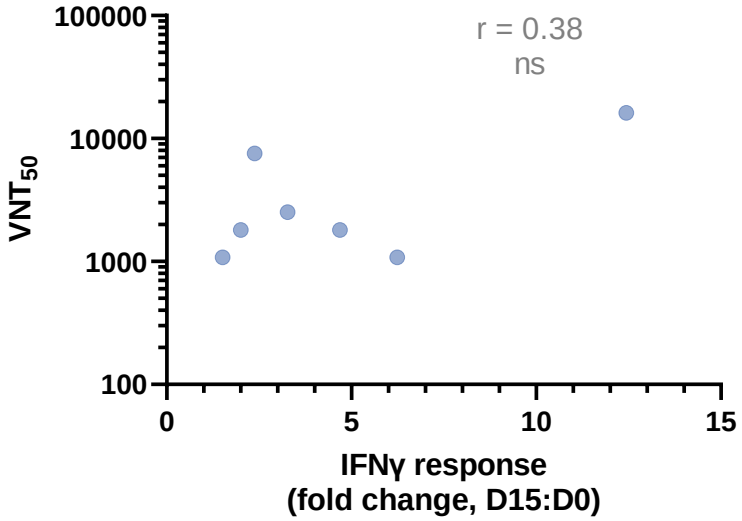


Figure 43. *Correlation between IFNγ response and VNT_{50} in pregnant goats. Samples assayed from Trial C, Table 1. There was no significant correlation between VNT and IFNγ ELISpot response at D21, just prior to challenge. Spearman's correlation r = 0.36, ns, p = 0.42. Neutralisation data carried out by J.K. and P.W from [148].*

6.3.7 Expression of nanobodies from a vaccinated llama

Due to their small size and potentially high affinity, nanobodies can provide useful reagents for structural and molecular biology analyses in addition to possible therapeutic applications [200, 201]. Dr Jan Steyaert's previously vaccinated a single Llama with ChAdOx1 RVF followed by a booster dose 8 months later. Six weeks after this the llama was further boosted with recombinant Gn and Gc protein. Total RNA was purified from the llama's PBMCs after the recombinant protein boost. RT-PCR was then used to clone the nanobody genes into the phage display vector pMESy4 as described [202].

The nanobodies with a poly histidine tag on the C-terminus were previously cloned into expression plasmids by Dr Elizabeth Allen and made into glycerol stocks. I expressed these in *E. coli* and purified by immobilized metal affinity chromatography (IMAC) with nickel beads. A coomassie gel demonstrated the successful expression and purification for each of these constructs (**Figure 44**).

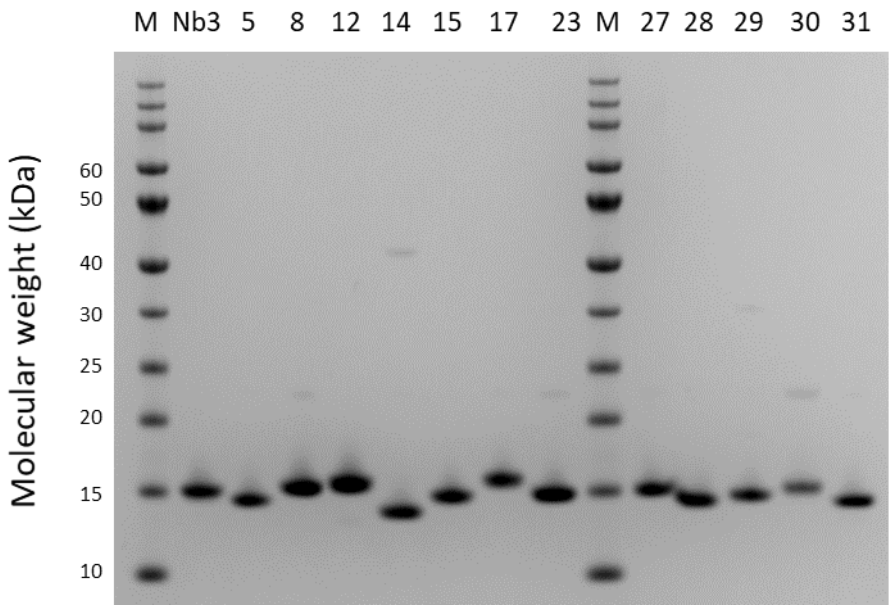


***Figure 44**. SDS-PAGE of recombinant nanobodies expressed in E. coli (HIS-tagged). Samples were loaded with reducing buffer on a NuPAGE 4-12 % Mini poly-acrylamide gel and stained with Quick Coomassie Stain. M = marker, numbers represent the nanobody ID. Each nanobody is approximately 15 kDa*

6.3.8 Assessment of the nanobodies ability to bind Gn and Gc and neutralise RVFV in vitro

I monitored binding of each of the 13 nanobodies to Gn or Gc by ELISA. Nb3-15 bound Gn while Nb17-30 bound Gc (**Figure 45**). Nb12, the strongest binder of Gn, also weakly bound Gc at the highest concentration. This occurred to a lesser extent with a handful of other nanobodies, where they weakly bound the heterologous antigen when added at 10 µM concentration. Nb3, Nb14 and Nb15 had relatively low signal by ELISA, even at 10 µM, possibly due to low affinity or limited access

to epitopes on the immobilised antigen as it is bound on the ELISA plate. The nanobody characteristics, including IC50 as an estimate of binding affinity are included in **Table 2**

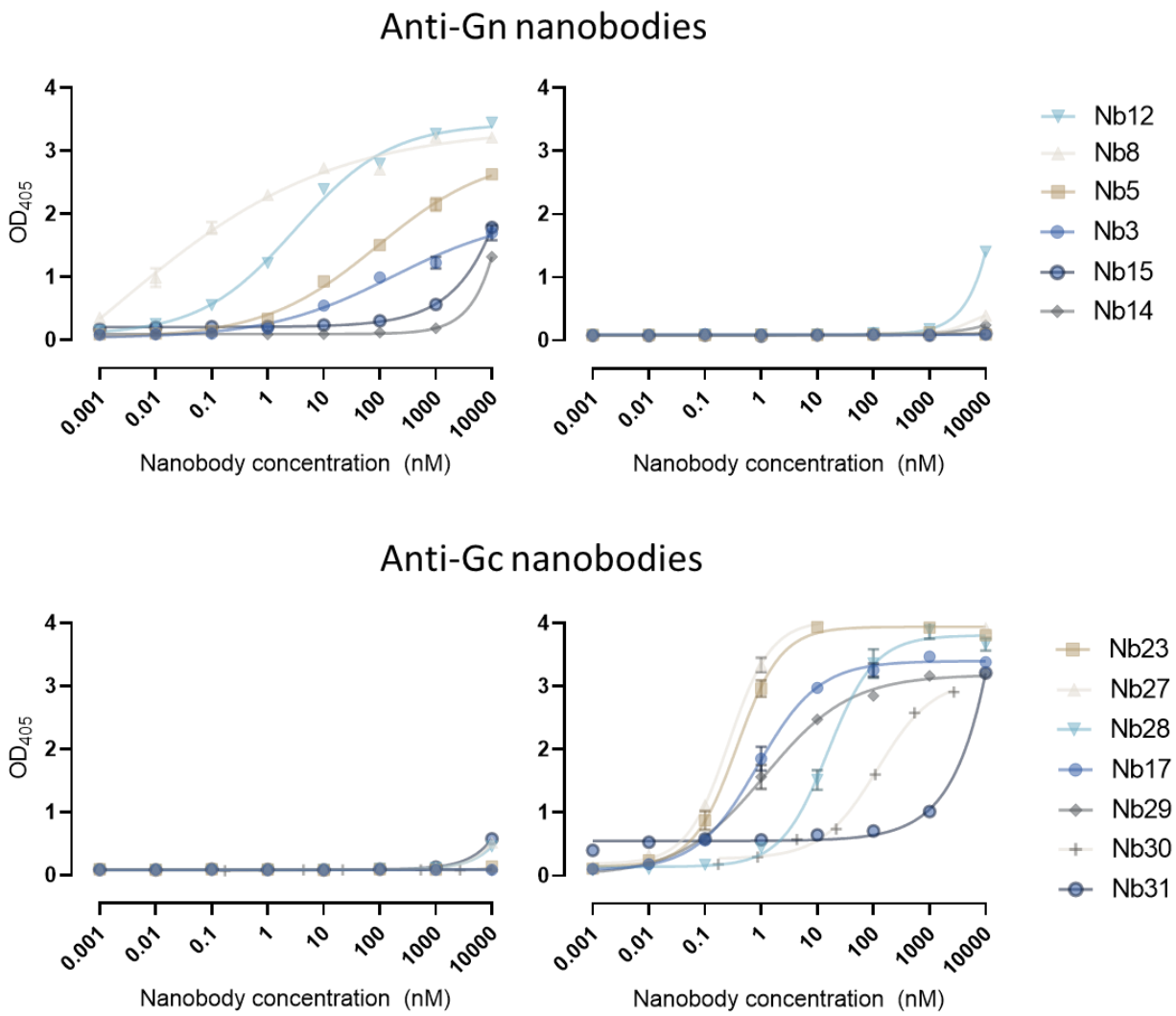


Figure 45. *Optical density (OD) at 405 nm measured by Gn or Gc ELISA for 13 nanobodies. Nanobodies have been separated based on whether they bind predominantly to Gn (top) or Gc (bottom). Graphs on the left are Gn ELISAs and graphs on the right are Gc ELISAs. Nanobodies were purified from a llama vaccinated with two doses of ChAdOx1 RVF followed by a boost with recombinant Gn and Gc proteins in Dr Jan Steyaert's lab. Dr Elizabeth Allen cloned the nanobodies into expression plasmids. Nanobodies were expressed in E. coli and purified using nickel beads. Symbols represent mean and error bars represent range of triplicates. Non-linear regression using a 4-paramter curve was fitted to each nanobody's ELISA data.*

Table 2. *Nanobody binding affinity and neutralisation characteristics*
[1] Binding affinity estimated by ELISA IC50

Antigen	Nanobody ID	Binding affinity[1] (nM)	Neutralisation
Gn	Nb3	73.80	none
	Nb5	51.59	none
	Nb8	0.074	none
	Nb12	2.881	none
	Nb14	4992	none
	Nb15	2681	none
Gc	Nb17	0.807	none
	Nb23	0.325	none
	Nb27	0.234	none
	Nb28	13.48	none
	Nb29	1.190	none
	Nb30	81.23	none
	Nb31	2798	none

All 13 nanobodies were then tested for neutralisation. Even at the top concentration of 10µM, none showed significant neutralising activity (**Figure 46a**). Three of the nanobodies: Nb23, Nb29 and Nb17 showed partial neutralisation but never achieved a measurable VNT_{80} titre, using the same eGFP VNT_{80} assay that was used for the sheep dose escalation trial earlier in the chapter. Due to unexpected GFP issues with the VNT_{80} assay, I then assayed the three partially neutralising antibodies again, individually and as a cocktail containing all three in addition to a cocktail of all 13 nanobodies in equal quantities using the RVFV-4s $FRNT_{50}$ assay (**Figure 46b**). None of the nanobodies showing partial neutralisation achieved a measurable $FRNT_{50}$ titre, including the cocktail of all 3. The cocktail of all 13, however, did show neutralising activity with an $FRNT_{50}$ titre of 2.734 µM (**Figure 46b**).

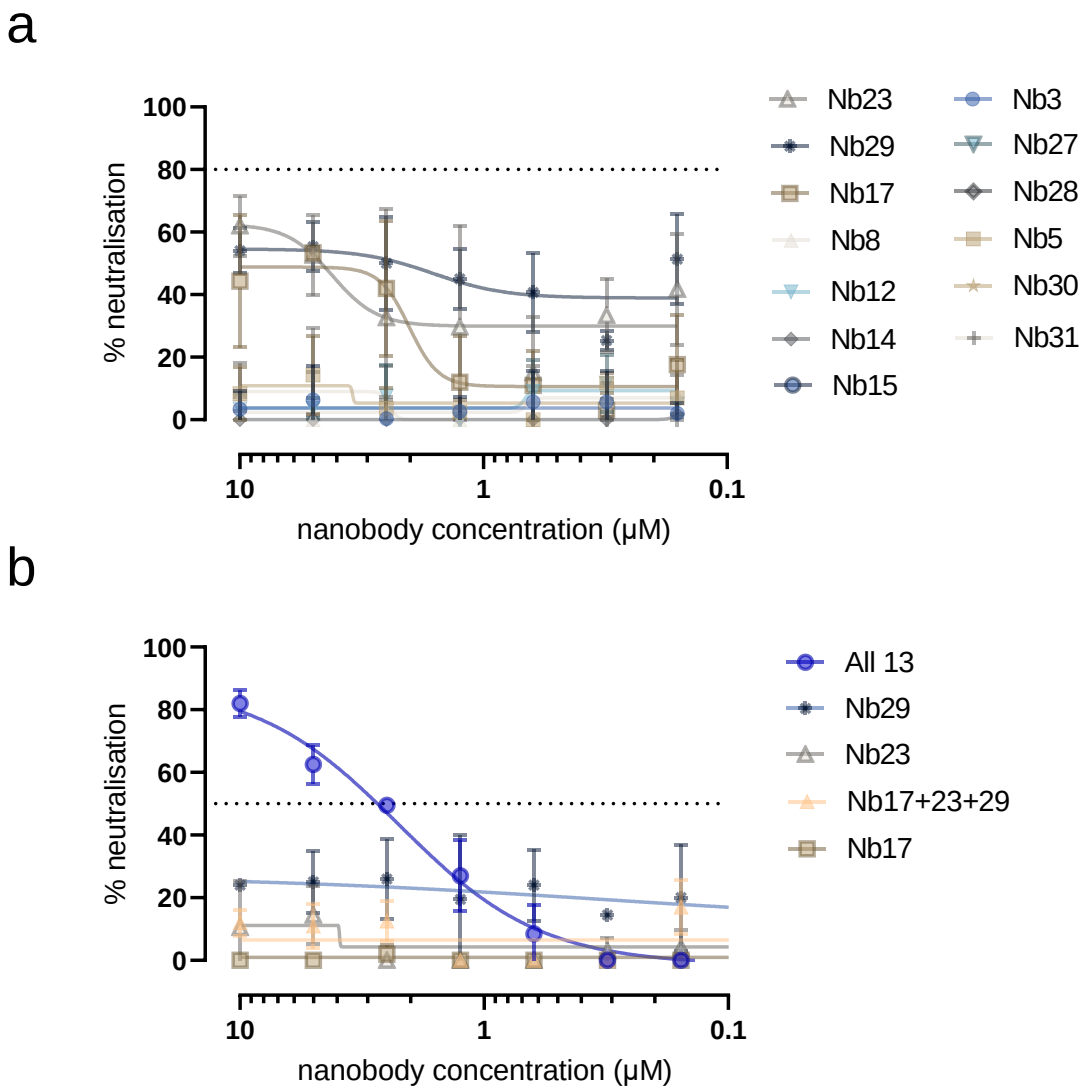


Figure 46. *Viral neutralising titres of 13 nanobodies isolated from a vaccinated llama. (**a**), neutralisation of 13 individual nanobodies using the eGFP VNT_{80} assay. B, neutralisation activity, as measured by $FRNT_{50}$, of 3 nanobodies that showed partial neutralisation in panel a. (**b**), the 3 nanobodies were also assessed in a cocktail, in addition to a cocktail of all 13 nanobodies. The stated concentrations of nanobody cocktails represent the total concentration of all nanobodies together. Symbols represent means and error bars represent standard deviation*

6.4 Discussion:

The ChAdOx1 RVF vaccine has previously shown to confer 100% protection against RVFV infection in healthy sheep, goats and cattle [103]. Following this, it showed extremely high protection against disease and foetal loss in pregnant sheep and goats [148]. Here, I have established assays to

measure the humoral and cellular immune response towards both Gn and Gc in sheep, goats and cattle. With regards to anti-Gc IgG titres, the humoral response in these livestock species is broadly in line with what I have shown in ChAdOx1 RVF vaccinated humans. Namely, that they are induced and strongly correlate with neutralising antibody titres. However, in contrast to vaccinated humans that showed essentially no detectable anti-Gn IgG titres, here they were readily detected in all livestock species. As with naturally exposed humans, the ability of animals to neutralise RVFV in vitro can be better predicted by their total IgG titre towards both glycoproteins, rather than their avidity, except in goats where IgG avidity was highly correlated to nAb titres. As mentioned in chapter 3, neutralisation assays that incubate serum and virus prior to addition of cells may reduce the consequences of lower avidity IgG compared to in vivo, where speed of binding may play a more important role.

While the original livestock efficacy trial has already compared nAb titres between the ChAdOx1 RVF and Smithburn vaccines, finding no significant difference, I have compared the total IgG titres against each glycoprotein. While there was no significant difference in peak titres between vaccines, anti-Gn IgG geomeans were lower in all ChAdOx1 RVF vaccinated species compared to Smithburn. In contrast, anti-Gc IgG geomeans were higher in all ChAdOx1 RVF vaccinated species compared to Smithburn. The lack of statistical significance means this may well be due to chance, however, it may also reflect how Gn and Gc proteins are expressed in both vaccines. Smithburn is a formalin inactivated vaccine. At present is it unknown if the tertiary structure remains intact following inactivation, with Gn as the more membrane distal glycoprotein shielding much of the Gc protein [75]. Exactly how the Gn and Gc expressed by ChAdOx1 RVF assemble and interact is also not yet known. While it is possible they spontaneously form VLPs or at least Gn-Gc heterodimers, monomeric Gc may also provide the immune system increased opportunity to ‘see’ it compared to its native position on the virion surface. The large field trial in Kenya with hundreds of livestock vaccinated with either vaccine can inform us whether this is a real difference between vaccines,

while further studies using cellular cryoET may help to elucidate the confirmation of expressed Gn and Gc proteins by ChAdOx1 RVF, as was recently shown for the spike protein in ChAdOx1 nCoV-19 [203].

Given the important role nAb titres play in protection against RVF, harmonising RVFV neutralisation assays between research groups will allow useful comparisons between vaccines. With RVFV on the WHO list of priority pathogens and the subsequent increased interest in RVFV vaccine development, assay harmonisation is set to become even more relevant.

I have shown there is a drop off in the antibody response as lower doses are administered but it is often not statistically significant. In the dose-escalation trial, it is curious that, for sheep, the response at D14 was significantly higher than D21. From figure 1 we can see the initial ChAdOx1 RVF efficacy trial in livestock (Trial B, **Table 1**) showed an increase in IgG titres from D14 to D28, although with no D21 time point, the kinetics between the two was not measured. The latter trial in pregnant sheep and goats (Trial C, **Table 1**) did measure the D21 response and found a very similar nAb titre from D14 to D21, in both species [148]. Previous experience with the ChAdOx1 platform has shown us that antibodies towards the encoded antigen, regardless of what that antigen is, tend to peak approximately 4 weeks post-vaccination in both humans and animal models. Potentially, the lower response at D21 may be a result of a storage issue with the D21 serum samples themselves, rather than a genuine difference in the animals. While previously, the same dose of 1E9 IU ChAdOx1 RVF has protected both small and large ruminants similarly, lowering the dose may have more marked consequences for larger ruminants. This was reflected in the ELISA data, where there was a larger statistical difference between the low dose and medium/high doses in cattle compared to sheep.

Finding a mechanistic correlate of protection in the target species is extremely beneficial for any disease where vaccines are needed. It allows us to down-select candidates at an earlier stage with greater confidence should they not provide sufficient immunogenicity, with a far better understanding of what sufficient immunity entails. That neutralising antibodies are associated with protection against RVFV is already known [6, 96], but the minimum threshold is not. Here, I have bridged an earlier ChAdOx1 RVF efficacy study in sheep, goats and cattle to a dose escalation study where animals were not challenged. By re-measuring the neutralising titres from that earlier efficacy trial with the same assay, knowing these animals were subsequently protected from RVFV challenge, we can compare those titres associated protection with those achieved after administering lower doses of ChAdOx1 RVF. While I found that lower doses of vaccine induced lower binding and neutralising antibody titres, importantly, even with the low dose of 5E6 IU, all animals induced nAb titres within the range of those associated with being protected. As previously mentioned, nAbs are not the only mechanism of protection and at present, we cannot be certain that other aspects of immunity are comparable with lower doses. Importantly, I have only measured antibodies at 3-4 weeks post vaccination. While having similar nAb titres as animals that were shown to be protected, how long the response lasts is crucial. Increased confidence in a correlate of protection will require demonstrating that it is the nAbs providing the protection and not other antibody mediated mechanisms or non-neutralising antibodies. Additionally, challenge trials in animals with a range of nAb titres to determine at which point protection is reduced by a specified amount would be beneficial.

This finding does, however, suggest that despite reduced immunogenicity, lowering the dose of ChAdOx1 RVF may not have a major detrimental impact on protection against RVF. The ability to give doses lower than 5E9 IU would significantly increase the number of available doses resulting in a reduced cost per dose. At present RVF is primarily a disease of LMICs, reduced production costs could lead to reduced costs to the end user and therefore increase uptake and use in livestock. An

analysis of potentially reducing effectiveness with lower doses would need to be calculated against the potential for lowering the cost and increasing production capacity.

To my knowledge, the cellular response to RVFV has not been previously measured in livestock, whether after vaccination or naturally acquired infection. Initial attempts to measure the vaccine induced response using crude peptides spanning Gn and Gc (>30% purity) resulted in relatively low responses in goats and no clear response in sheep. The peptide library was reconstituted in dimethyl sulfoxide (DMSO), a strong solvent. DMSO can negatively impact cytokine production in cell culture [204], which limits the number of peptides in any given pool to ensure there is no suppression of the response. The crude peptides originally used at 10 μg/mL final concentration resulted in 0.44% final DMSO concentration. While for clinical trials carried out at the Jenner, anything below 0.5% is considered acceptable, these crude peptides appears to have been high enough to supress the IFNγ ELISpot response in the cattle and sheep samples tested. Stimulation with clinical trial grade peptides (>80% purity at 5 μg/mL [0.25% DMSO]), split between 11 pools showed a more than five-fold increase post-vaccination in goats. However, in sheep there remains very high background and no increase post-vaccination in most animals. After a single dose of ChAdOx1 RVF, it is possible sheep just fail to generate a strong IFNγ response. However, there are legitimate questions over how well the assay is able to detect antigen-specific T cells given the very high background response in some sheep. For sheep, further ELISpot optimisation is needed. Once again, a large-scale field trial involving 580 healthy sheep, goats, cattle and camels was recently completed with PBMC taken pre-vaccine and two weeks post-vaccine and will allow a more complete optimisation for each species.

RVFV, like many pathogens, is more dangerous when infection occurs during pregnancy. RVFV is able to replicate extremely efficiently in the placenta [34]. The pregnant goats assayed by ELISpot here were subsequently challenged and all had high neutralising antibodies and significant

protection from disease and foetal loss. Cellular assays carried out on healthy livestock will shed light on differences in immune response between pregnant and non-pregnant animals.

The anti-vector IFNγ response was absent prior to vaccination, as expected. In goats, there was a significant increase at D15 post-vaccination. However, these were modest in magnitude compared to the response towards the GnGc peptides. Anti-vector nAb titres after vaccination may provide a better indicator for the effectiveness of additional doses. However, ChAdOx1 RVF has thus far shown very high efficacy in livestock after a single dose so it seems unlikely that anti-vector immunity will be a major issue if booster doses are not needed. Particularly for livestock, rather than humans, where the economic case for multiple doses may be harder to justify.

In addition to use as potential therapeutics, characterisation of anti-RVFV mAbs can elucidate the nature of antibody-mediated protection. Nanobodies can be extremely useful biomolecules due to their small size and potential for high affinity binding [201]. To obtain RVFV nanobodies, a llama was vaccinated with ChAdOx1 RVF. However, due to limited immunogenicity, nanobodies were not able to be isolated. A previous study in camels, part of the same camelid family, showed neutralising antibodies were elicited after a single dose of ChAdOx1 RVF, although titres were lower than the other livestock species [103]. The llama was then given a second dose of ChAdOx1 RVF followed by further boosting with recombinant Gn and Gc protein. Nanobodies were then successfully purified from the llama, and to investigate the epitopes targeted by vaccine-induced antibodies, I expressed and purified a library of 13 RVFV nanobodies that had been previously isolated and cloned into plasmids by Dr Elizabeth Allen. Unfortunately, while all 13 nanobodies bound their antigenic targets by ELISA, none strongly neutralised RVFV in vitro.

Previous data has shown that cocktails targeting different epitopes can have synergistic effects where the resulting ability to neutralise is better than the sum of the individual antibodies involved

[100]. Indeed, a cocktail of all 13 nanobodies did show partial neutralisation at high concentrations, and while this exhibited more neutralising activity than any individual nanobody, the titre was low in comparison to serum from vaccinated livestock. A sample of post-vaccine serum from the llama was later sent and I was able to confirm it lacked any detectable neutralising activity. The RVFV Gn glycoprotein used as part of this vaccine regime has been used previously to raise a nAb response in rabbits but that was adjuvanted with Adjuplex™ (Sigma Alrich) and given as a 3 dose regime [94]. A previous study characterising a panel of nanobodies raised in a llama against recombinant RVFV Gn also found that none were neutralising individually or when used in pairs [198]. However, by using 'bacterial superglue' (Spy-tag and Snoopcatcher) to create bivalent and bispecific complexes, strong in vitro neutralisation coupled with in vivo protection in rodents was demonstrated [198]. This ability for bispecific/bivalent nanobodies to neutralise RVFV even when their constituent nanobodies on their own cannot may be due to their increased size and/or ability to cross-link glycoproteins. This may improve their ability to inhibit rearrangement of GnGc thus preventing fusion with host cells. I have an expression plasmid coding for the human IgG Fc region and plan to clone in our nanobody VHH regions to create bispecific/bivalent nanobodies which can then be assessed for in vitro neutralising activity. If these exhibit neutralising activity then future structural studies focusing on the epitopes recognised by these can provide insights into their mechanisms.

The work in this chapter has established various assays for measuring the humoral and cellular response towards RVFV Gn and Gc in multiple livestock species. I have provided the first livestock data on the cellular and binding IgG response towards RVFV Gn and Gc, as well as investigated the impact of administering lower vaccine doses on immunogenicity. These studies also provide data for the first time on the immune response elicited in several livestock species after vaccination with the ChAdOx1 platform.

7

Production of monovalent and bivalent vaccines to target an additional livestock disease

7.1 Introduction:

Livestock diseases including Foot and Mouth (FMD), Africa Swine fever (ASF), Contagious caprine pleuropneumonia (CBPP), East Coast fever (ECF), Pest-des-petit ruminants (PPR) and RVF among others have enormous economic costs, devastate livelihoods and significantly impact food security. Effective vaccines, if they exist, can mitigate against this burden. A major component of the overall cost of administering livestock vaccines involves the logistical challenges associated with the transport of animals and physically reaching the target population [205]. The economies of scale associated with sharing these costs to deliver multiple vaccines at the same time, therefore, could result in significant cost savings to the end user, removing one of the barriers towards increased vaccine uptake.

Peste-des-petits ruminants virus (PPRV) is a morbillivirus in the paramoxyvirus family with a geographic range spanning Africa, the Middle East and Asia. It is extremely contagious in small ruminants such as sheep and goats, with a high fatality rate [206]. Larger ruminants, such as cattle, camels and buffalo, can still harbour sub-clinical infections [207-209]. The annual economic burden of PPR has been estimated between $US ~1-2 billion [205]. Due to their similar livestock host range and substantial geographic cross-over throughout Africa, PPRV and RVFV are well suited for attempts to combine a vaccine strategy against them.

Like RVFV, PPRV is a single stranded negative-sense RNA virus. It is closely related to Rinderpest virus (RPV), another member of the morbillivirus genus. In contrast to PPRV, RPV was predominantly a disease of large ruminants such as cattle. Together with smallpox, RPV remains one of only two infectious diseases eradicated from the planet. The eradication of RPV was brought about through widespread use of a highly effective live-attenuated vaccine [210]. Due to the homology between PPRV and RPV, the Rinderpest vaccine also provided protection against PPR [211]. However, as the vaccine succeeded in eliminating RPV, its use was increasingly banned in

regions to aid surveillance and ensure RPV-free areas remained so [212]. Without the use of live-attenuated RPV vaccines to control PPRV, a homologous PPR vaccine was much needed.

Since then, live-attenuated PPR vaccines have been developed and are highly effective. However, there are drawbacks that require the development of better vaccines. Current vaccines, while thermostable when freeze-dried, need to be used quickly to avoid potency loss once reformulated [205]. This is particularly important considering the climate of geographic regions where PPR is endemic. Due to the success of the Rinderpest vaccine programme and the similarities between RPV and PPRV, eradication of PPRV appears feasible. Indeed, this is the aim of the OEI and FAO by 2030 [205]. As was the case with Rinderpest, in order to aid eradication efforts a DIVA compliant vaccine would be extremely beneficial. The ability to distinguish vaccinated and infected animals can significantly aid the latter parts of eradication programmes, where surveillance of outbreaks is critical.

PPRV contains six structural proteins (N, P, M, H, F and L), along with two non-structural proteins [213]. After infection or vaccination with attenuated virus, the nAb response is directed towards the two glycoproteins, H (haemaglutannin) and F (fusion) [214]. Vaccination with recombinant H protein alone has previously been shown to generate a strong nAb and T cell response in goats [215]. Adenovirus-vectored vaccines encoding the H and/or F proteins have since been trialled [216-219]. A human adenovirus (Ad5) encoding only H was shown to fully protect goats from challenge with live PPRV 4 months later [217]. In another study, vaccinating with vectors encoding both antigens showed improved nAb titres over those encoding H or F alone [216]. While this was not the case when combining vaccine constructs that encoded each antigen separately, goats vaccinated with the combination of both constructs appeared to limit viral replication more than those given the same quantity of Ad-H alone. Although both groups showed complete protection from disease [219].

Here, I have attempted to produce a monovalent ChAdOx1 PPR vaccine encoding H, which if protective, would have significant advantages over current PPR vaccines, e.g. DIVA compliance in a stable, cheap and relatively easily manufactured vaccine. H was synthesised in the absence of the F protein so the same antigenic insert could be used in the bivalent vaccine construct without creating too large an insert. A single bivalent vaccine against RVF and PPR could potentially mitigate against two major diseases of small ruminants in a single shot. This would reduce costs compared to individual vaccines, and importantly, could serve to further incentivise livestock owners who may not see RVF vaccination as a priority, particularly during interepidemic periods.

7.2 Objectives:

1. To produce a monovalent ChAdOx1 PPRV H vaccine construct
2. To produce a bivalent ChAdOx1 RVF PPR vaccine, encoding Gn and Gc from RVFV and H from PPRV
3. To use Next-generation sequencing (NGS) to verify sequences of the plasmids and final manufactured virus
4. To confirm and compare expression of RVFV GnGc and PPRV H between the bivalent vaccine and their monovalent equivalents

7.3 Results:

7.3.1 Cloning of monovalent ChAdOx1 PPR and bivalent ChAdOx1 RVF-PPR

In order to make the monovalent ChAdOx1 PPR vaccine, PPRV H was cloned into a shuttle plasmid containing a long CMV promoter as per the Materials and Methods. For the bivalent ChAdOx1 RVF-PPR vaccine, RVFV GnGc and PPRV H were cloned into their respective shuttle plasmids, both containing a short CMV promoter. Five colonies of each transformed shuttle plasmid were digested to check for incorporation of their respective transgenes (**Figure 47a,b**). The vast majority of clones

showed the correct size bands. After confirmation, a single, correct clone of each plasmid was selected [Lanes 5 and 8 (**Figure 47a**) and Lane 2 (**Figure 47b**)]. The GnGc insert was almost identical size to the rest of the shuttle plasmid, leading to the appearance of a single band. The more intense bands suggested the presence of both segments (**Figure 47a**), but additional PCR of the GnGc region was carried out to confirm its incorporation (gel not shown). ChAdOx1 PPR was generated by ligating the shuttle plasmid, containing H under the control of a long CMV promoter into the ChAdOx1 backbone by LR recombination (**Figure 47d**). Bivalent ChAdOx1 RVF-PPR was generated by ligating the two shuttle plasmids, containing RVFV GnGc and PPRV H, both under the control of short CMV promoters, with the ChAdOx1 RVF backbone, again by LR recombination (**Figure 47c**). Clones were then selected with chloramphenicol resistance and without kanamycin (or ampicillin in the case of the bivalent vaccine) resistance. 6 µg each of ChAdOx1 PPR and ChAdOx1 RVF-PPR plasmids were linearised with *Pme*I to remove the bacterial resistance gene and expose the inverted terminal repeats allowing transfection (**Figure 47c-f**).

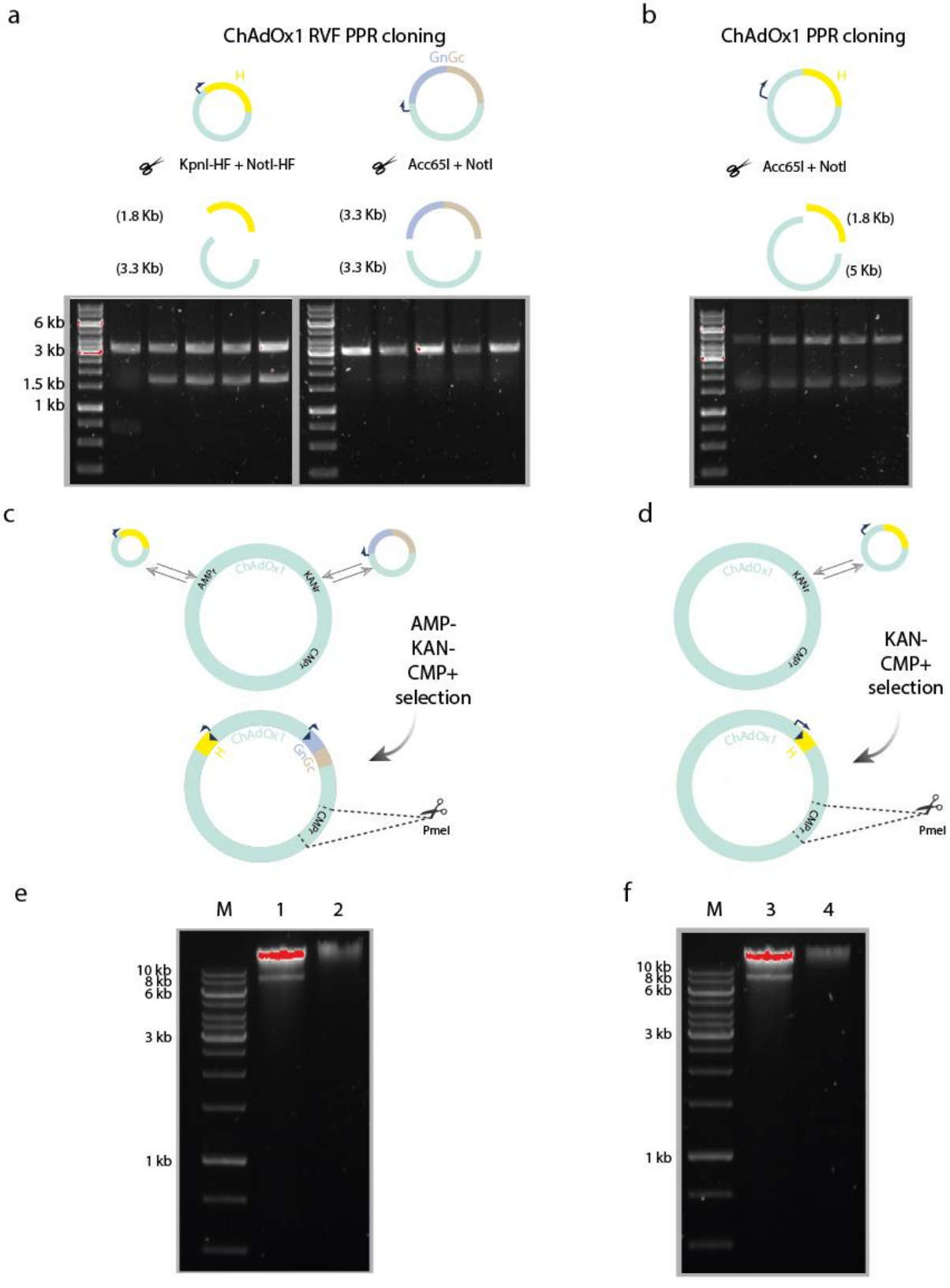


***Figure 47**. Cloning of the bivalent ChAdOx1 RVF-PPR and the monovalent ChAdOx1 PPR vaccine constructs. (**a**), PPRV H and RVFV GnGc were cloned into separate shuttle vectors, each under the control of a short CMV promoter. Restriction digest of five clones each were used to identify one with successful incorporation of their respective antigen. (**b**), PPRV H was cloned into a shuttle*

*vector under the control of a long CMV promoter. Restriction digest of five clones was used to identify one with successful incorporation of the antigen. (**c**), LR clonase recombination of a single correct clone of both shuttle plasmids with the ChAdOx1 backbone. H and GnGc replace ampicillin and kanamycin resistance genes in the E4 and E1 locus of ChAdOx1, respectively. PmeI digest linearises the plasmid, removing the chloramphenicol resistance gene, exposing the inverted terminal repeats allowing transfection and virus bulk-up. (**d**), LR clonase ligation of a single correct clone of the shuttle plasmid with the ChAdOx1 backbone. H replaces the Kanamycin resistance genes in the E1 locus of ChAdOx1. PmeI digest removes chloramphenicol resistance gene and exposes inverted terminal repeats allowing transfection and virus bulk-up. (**e-f**), DNA gels of final bacterial artificial chromosome (BAC) plasmids, M = marker, 1 = PmeI digested ChAdOx1 RVF-PPR, 2 = undigested ChAdOx1 RVF-PPR plasmid, 3 = PmeI digested ChAdOx1 PPR, 4 = undigested ChAdOx1 PPR plasmid.*

Prior to passing onto VVCF to transfect and grow up virus, NGS was carried out on both BAC plasmids to confirm the correct sequence (**Figure 48**). Read coverage was >3000 per base position and error rates across the antigens were low with the highest occurring as a single base pair substitution in 1.8% of reads towards the C-terminus of Gc (**Figure 48b**). There were no significant drop-outs in read coverage over the entire BAC plasmid, suggesting no losses of genome sections (**Figure 48c**)

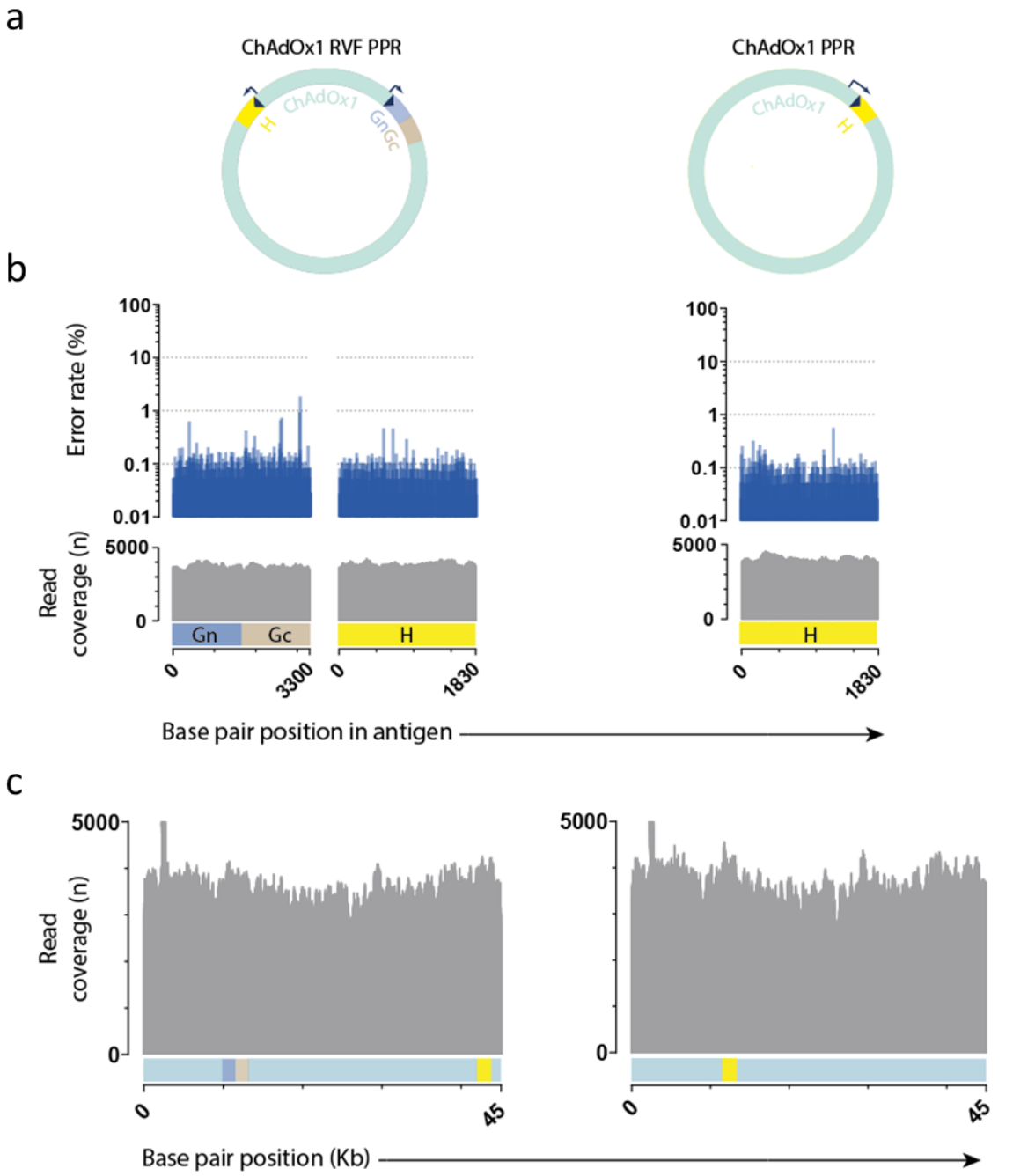


Figure 48. *NGS read coverage and error rate of ChAdOx1 RVF-PPR bivalent and ChAdOx1 PPR monovalent BAC plasmids prior to linearisation and virus bulk-up. (**a**), Schematic of ChAdOx1 RVF-PPR and ChAdOx1 PPR BAC plasmids. (**b**), Error rate and read coverage of the antigen inserts. (**c**), Read coverage of the entire BAC plasmids. NGS carried out by F.J. Analysis carried out by myself.*

Initial production of both vectors by VVCF resulted in low yield. Subsequent QC of the rescued virus showed that while yield was low, both constructs still contained the correct size antigenic inserts.

Both viruses were then re-bulked by VVCF using hyperflasks to increase yield. This re-bulk produced high titres of $9.9x10^{10}$ IU / $1.1x10^{12}$ vp and $2.1x10^{10}$ IU / $1.8x10^{12}$ vp for ChAdOx1 PPR and ChAdOx1 RVF-PPR, respectively. Both were then analysed by NGS again to confirm sequences were still correct (**Figure 49**). As before, there were no major errors at any position in the antigenic inserts with high read coverage throughout (**Figure 49b**). Read coverage of the GnGc insert in the bivalent vaccine was lower than for the H insert, although still maintained >10,000 correct reads per base position (**Figure 49c**).

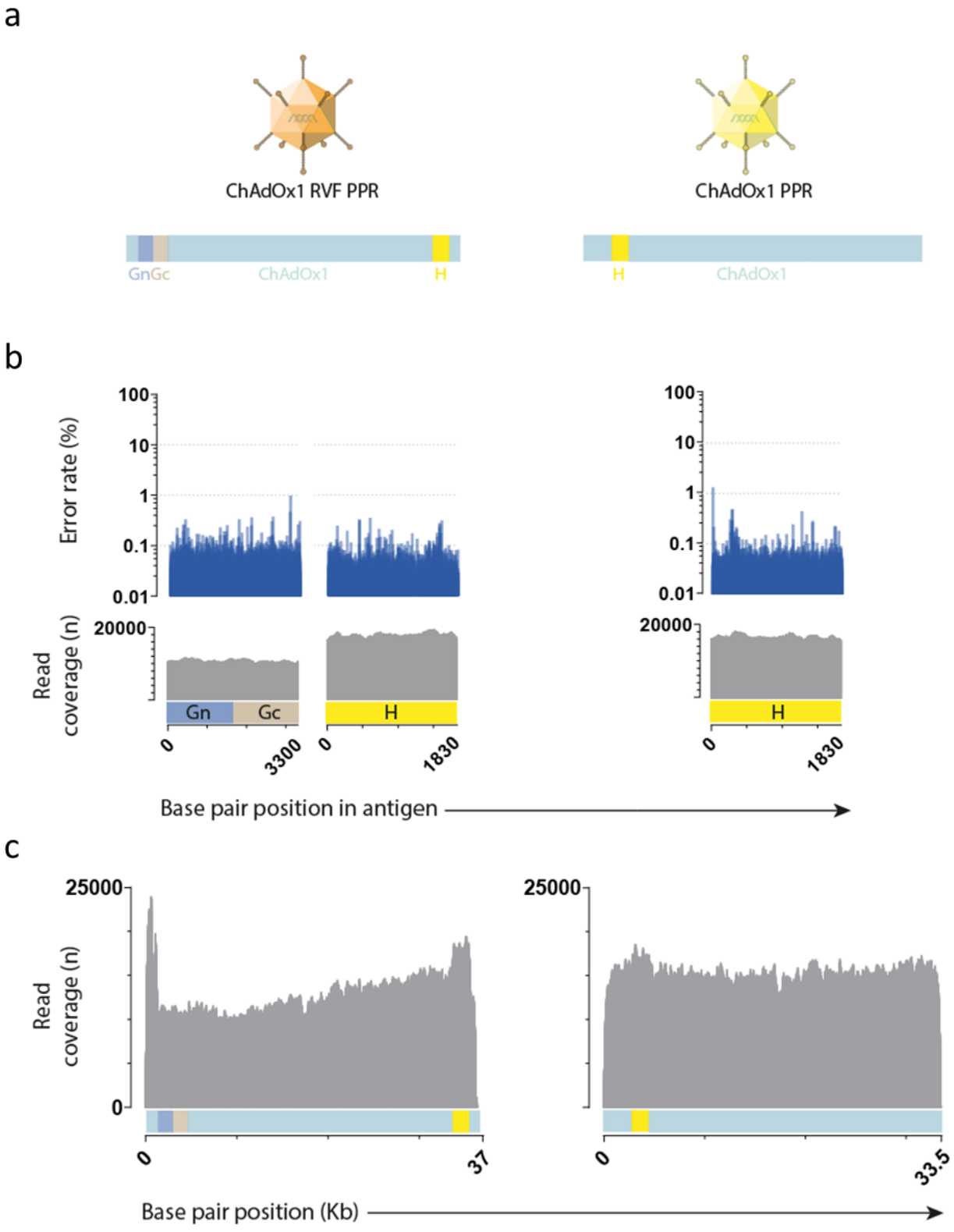


Figure 49. *NGS read coverage and error rate of ChAdOx1 RVF-PPR bivalent and ChAdOx1 PPR monovalent vaccines after virus rescue. (**a**), schematic of ChAdOx1 RVF-PPR and ChAdOx1 PPR genomes. (**b**), Error rate and read coverage of the antigen inserts. (**c**), Read coverage of the entire viral genomes. NGS carried out by F.J. Analysis carried out by myself.*

7.3.2 Confirmation of antigen expression

HeLa cells were infected with ChAdOx1 RVF, ChAdOx1 PPR or ChAdOx1 RVF-PPR along with an uninfected control as per Materials and Methods. 24 h later, cell lysate from each infection was collected and run on a Western blot using anti-Gn (4D4), -Gc (5E2) or -H (C77) mAbs to detect expression (**Figure 50**).

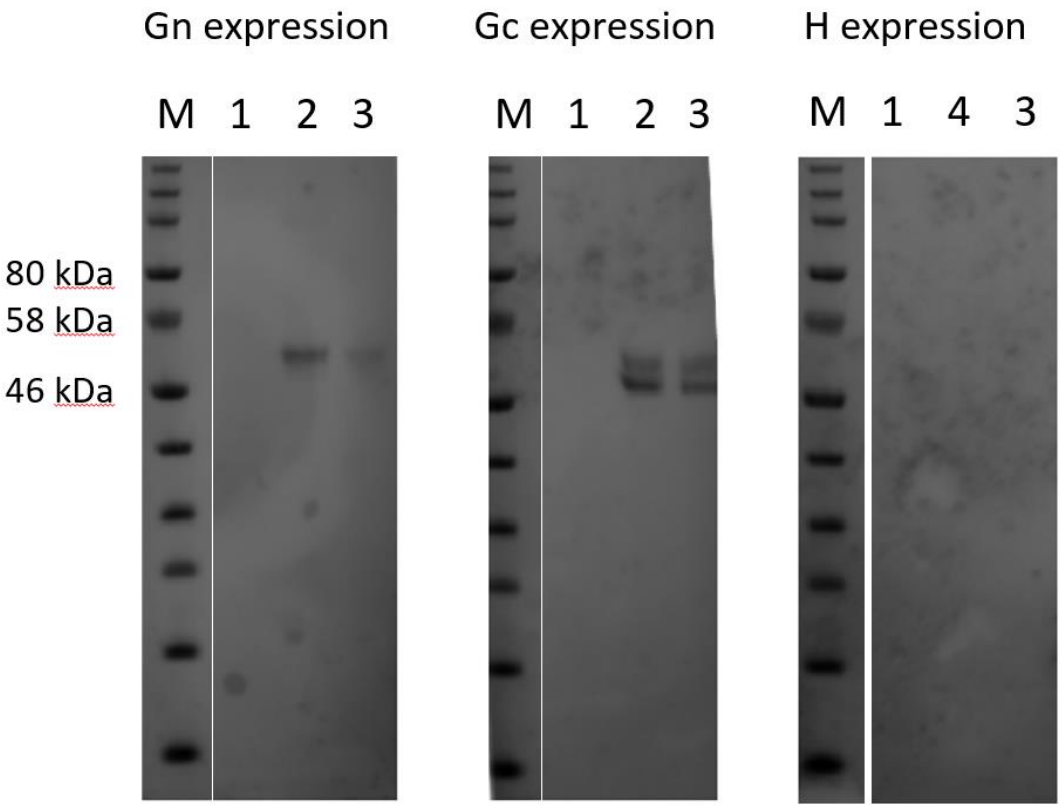


Figure 50. *Western blot on cell lysate from HeLa cells infected with ChAdOx1 RVF, ChAdOx1 RVF-PPR or ChAdOx1 PPR. Left, RVFV Gn expression. Middle, RVFV Gc expression. Right, PPRV H expression. Gels have been cropped after each marker to remove irrelevant wells. (1) Cell lysate from uninfected control. (2) Cell lysate from ChAdOx1 RVF infection. (3) Cell lysate from ChAdOx1 RVF-PPR infection. (4) Cell lysate from ChAdOx1 PPR infection. RVFV Gn and Gc are expressed in both ChAdOx1 RVF and ChAdOx1 RVF-PPR. PPRV H expression was not detected in either ChAdOx1 PPR or ChAdOx1 RVF- PPR. RVFV Gn and Gc expected size is ~58 kDa while PPRV H expected size is approximately ~80 kDa*

RVFV Gn and Gc are clearly expressed in both the monovalent ChAdOx1 RVF and bivalent ChAdOx1 RVF-PPR constructs. However, PPRV H was not detected in either ChAdOx1 PPR or ChAdOx1 RVF-PPR. It is possible that the anti-PPRV H mAb (C77) binds a conformational epitope that is not present after linearisation by SDS-PAGE. I therefore attempted to detect expression by immunofluorescence staining. HeLa cells were again infected with ChAdOx1 RVF, ChAdOx1 PPR and ChAdOx1 RVF-PPR along with an uninfected control. As an additional control for H expression, cells were also infected with the Ad5 H construct previously shown to be efficacious in goats. 24 h later, the same mouse mAbs that bind Gn (4D4) or H (C77) followed by an anti-mouse IgG-FITC secondary antibody were used as detailed in Materials and methods. Slides were examined by fluorescent microscopy for antigen expression (**Figure 51**)

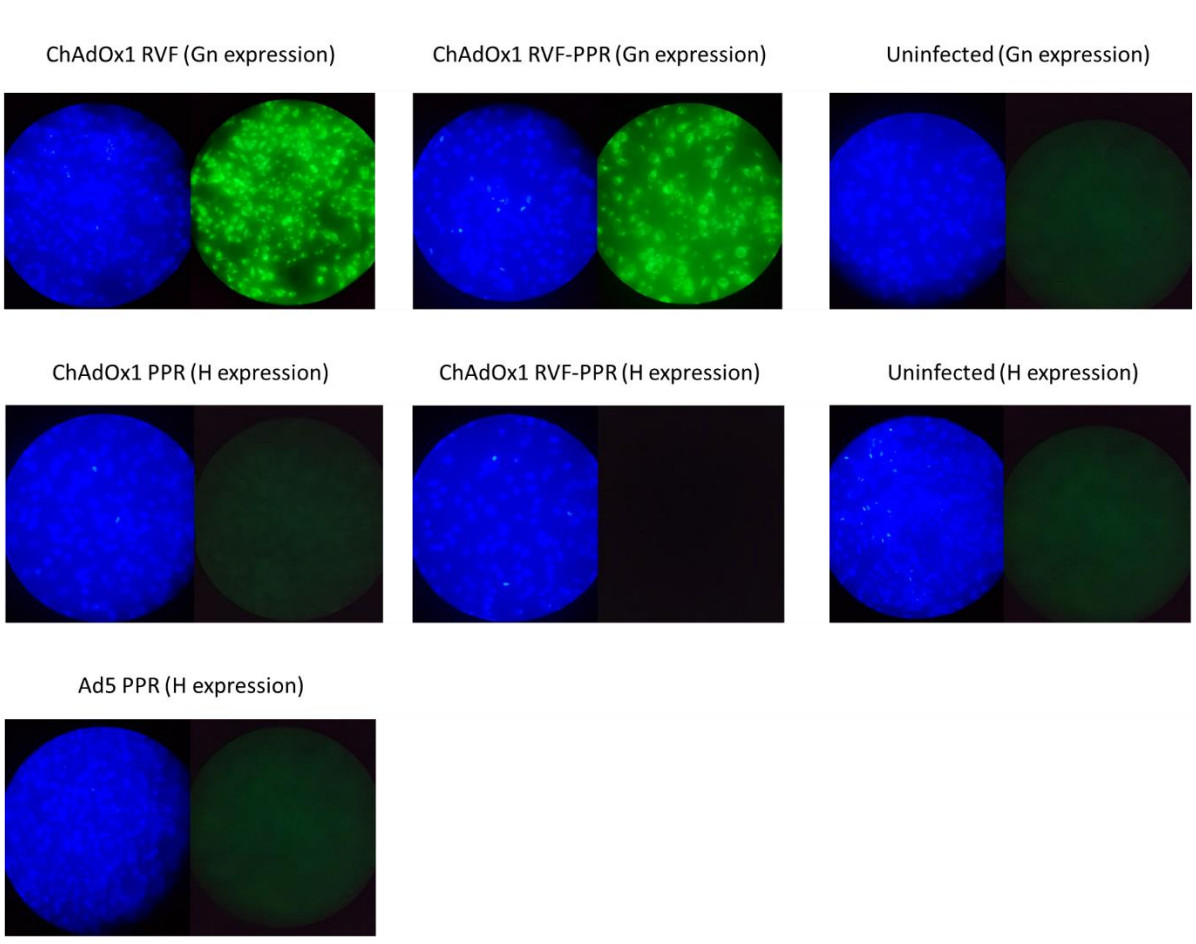


***Figure 51**. Immunofluorescent staining of RVFV Gn and PPRV H in the various constructs. Blue slides on the left of each panel are dapi-stained cell nuclei. GFP slides on the right of each panel show antigen-specific expression (if present). RVFV Gn expression was detected in ChAdOx1 RVF and*

ChAdOx1 RVF-PPR. PPRV H expression was not detected in either ChAdOx1 PPR, ChAdOx1 RVF-PPR or Ad5 H.

Gn staining was used as a general control for the method as it is already known to be expressed in both ChAdOx1 RVF and ChAdOx1 RVF-PPR vaccines and its expression was once again confirmed here. PPRV H expression was still undetectable, even in the Ad5 H construct. A Dot blot using purified PPRV antigens (Pirbright) was tested to ensure C77 could detect H but there was no signal (data not shown). I then tried an ELISA, coating with PPRV purified antigens (or RVFV Gn as a control) and attempted to detect signal using C77 at different concentrations (**Figure 52.**) The signal was relatively low unless C77 was used at 1:100 dilution and the purified PPRV antigens were coated at high concentrations, however, it unmistakably bound PPRV antigen with no significant background signal when added to an irrelevantly coated well (Gn).

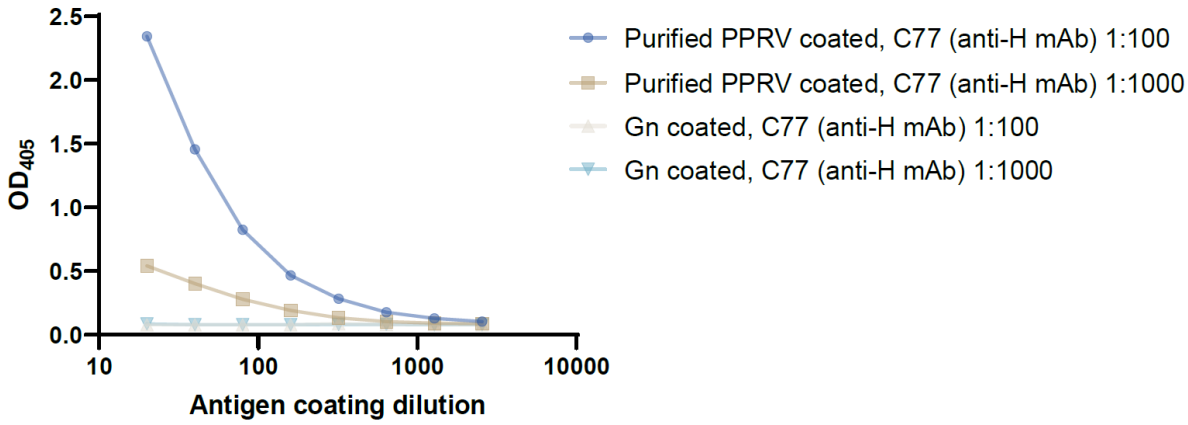


Figure 52. *Test of C77's ability to detect PPRV H by ELISA. Plates were coated with 'purified PPRV antigen' (Pirbright) diluted in PBS to various concentrations ranging from 1:20 to 1:2560 (or Gn coated at 1 µg/mL). C77 was diluted either 1:100 or 1:1000 in casein and added in triplicate, followed by anti-mouse-ALP diluted 1:1000 in casein and developed for 1.5h.*

7.4 Discussion:

Due to the nature of emerging pathogens, where the burden of disease can seem minimal outside of outbreaks, the need for vaccination can be underappreciated by both the public and policy makers. Particularly for RVF, during the often long inter-epidemic periods, the perceived risk can wane in comparison to other diseases [220]. This can result in reduced awareness and lead to lower livestock vaccination rates, fostering some of the conditions that will facilitate future RVF outbreaks. Here, I have cloned two new vaccine constructs; a bivalent ChAdOx1 RVF-PPR vaccine and a monovalent ChAdOx1 PPR vaccine. A successful bivalent vaccine could further incentivise vaccination against RVF if it can maintain the protection seen with ChAdOx1 RVF while also providing protection against PPR. The monovalent ChAdOx1 PPR vaccine, in addition to the potential advantages over current PPR vaccines if it proved to be effective, can serve to compare the immune response towards H generated from the bivalent vaccine, allowing us to investigate the impact on H expression when additional antigens are encoded in the same construct.

While I was able to detect Gn and Gc expression in the bivalent construct, so far I have not been able to detect H expression, either in the bivalent or monovalent constructs. The H antigen cloned into these ChAdOx1 constructs was taken directly from the H antigen encoded in the human Ad5 vaccine tested previously and showing 100% protection in goats [217]. The antigenic insert was resynthesized by GeneArt to remove instances of >3 identical consecutive bases while maintaining the identical amino acid sequence. Additionally, three further synonymous mutations were requested to remove restriction sites incompatible with ChAdOx1 cloning. Otherwise, the H insert from the promoter to the poly-A tail, is identical to the successful Ad5 challenge trial construct, which was originally produced by VVCF with the trial carried out in Pirbright. The antigenic insert of Ad5 H was Sanger sequenced recently and this conforms to the H sequence used in these ChAdOx1 constructs (excluding the changes mentioned above). NGS of both the monovalent and bivalent rescued virus showed the sequence to still be correct. That I was also unable to detect H

expression in the Ad5 construct, which had previously demonstrated efficacy, suggests the issue may be with the detection rather than expression. Herbert et al demonstrated Ad5 H expression using rabbit polyclonal raised against purified H [217]. It may be that the C77 mAb does not bind H encoded in this construct, indeed there are two mutations over the closest wild type PPRV H sequence. I am currently awaiting arrival of anti-PPRV polyclonal serum from Pirbright.

There are various factors to consider when producing multivalent viral-vectored vaccines, encoding two or more antigens. To begin with, the maximum size of transgene inserts that ChAdOx1 can accommodate is thought to be roughly ~7.5kb. While this allows for the possibility of inserts coding for large or multiple antigens, there are limits. The total combined insert size of ChAdOx1 RVF-PPR is ~7.2kb. While both antigens were correctly incorporated, being at the upper limit of what an adenovirus can accommodate can have an impact on the VP:IU ratio, as a larger proportion of viral particles may have packaging issues that inhibit infection. This tends to be the case with all adenovirus-vectored multivalent vaccines compared to their monovalent equivalents and was the same here. Despite this, the yield produced after production in hyperflasks was still high. For a polyprotein like GnGc, there is potential to reduce the transgene size by omitting one of the proteins. I have previously shown that the ability of human sera to neutralising RVFV after naturally acquired immunity comes predominantly from those nAbs that target Gn. However, preliminary clinical trial data suggests that ChAdOx1 RVF induces a better binding antibody response towards Gc than Gn. Understanding the reasons for this could shed light on the possibility of inducing a protective response against RVF from a single protein. Removing Gn or Gc would reduce the antigen insert size of ChAdOx1 RVF-PPR by ~1.5kb. It remains to be seen if this would cause a significant drop in protection. Early studies for DNA vaccines in mice showed that while Gn induced higher immunogenicity than Gc, combining both antigens was better still [101]. Another study in a small number of cattle vaccinated with either a Gn or GnGc protein subunit vaccine showed both

conferred protection, but only two doses of GnGc resulted in no detectable viremia post-challenge [221].

Another consideration for viral-vectored vaccines is how to incorporate the different antigens. Here I have cloned both RVFV GnGc and PPRV H, each under the control of their own separate promoter, into the deleted E1 and E4 locus, respectively. Due to size constraints, I have used short, rather than long, CMV promoters. Use of a long promoter for monovalent ChAdOx1 platform vaccines is generally used (including for ChAdOx1 RVF and ChAdOx1 PPR) as it includes a large intron. This aims to mimic eukaryotic genes and increase expression of the transgene in the vaccinated host.

A potential drawback with this method of bivalent vaccine cloning is the potential for differential expression between antigens. Another possibility would have been to clone both antigens into the E1 locus, immediately downstream of each other and sharing the same promoter but this requires additional gene synthesis and comes with its own risks, in particular the potential negative impact on correct protein folding. Indeed, how multiple encoded antigens interact and how that resembles the quaternary structure of antigens as they appear on the pathogen surface is an important consideration. This method was, however, previously trialled for a ChAdOx1 Flu vaccine encoding bivalent antigens separated by a 2A ribosome skipping sequences to ensure individual protein expression. This vaccine demonstrated no reduction in antigen-specific immunity compared to their monovalent equivalents [222].

Prior to the availability of NGS for routine vaccine construct QC, the antigen inserts would be Sanger sequenced with forward and reverse reads. Now, the ability to have upwards of 5000 reads per base position poses the question of what an acceptable error rate would be. NGS of the resynthesized ChAdOx1 RVF, which we know to be correct by Sanger sequence and Western blot and has been used in challenge trials showing sterile protection has shed light on this. That vaccine

showed no base positions with >3% error, providing a basis for what we might consider an acceptable error rate. The error rate of the constructs made in this chapter also did not exceed 3% at any base position.

In this chapter I have produced a candidate vaccine against PPRV, a livestock disease with significant species and geographic overlap with RVFV. Additionally, by combining a highly effective RVF vaccine with a vaccine for PPRV, the latter perhaps appearing a more pressing issue to end users in the absence of a current RVF outbreak, could further increase uptake. While confirmation of H expression is still pending, I have shown that despite their large combined size, RVFV GnGc and PPRV H can be cloned together into a bivalent ChAdOx1 vaccine and produced without genetic stability issues. Once expression of H is verified, we can compare immunogenicity in mice between the bivalent vaccine and their monovalent equivalents. If that proves successful, we can move on to testing in the target species.

8

Contributions to the pandemic response

Towards the end of March 2020, COVID-19 began to surge in the UK, leading to a 'lockdown' and stopping of all non-Covid labwork at the Jenner Institute. While this took significant time away from my DPhil work, I was fortunate enough to be in a position to contribute towards the pandemic response. From the Start of April 2020 until December 2020, I worked full-time on COVID-19 research. This initially involved bulking up and shipping spike protein expression plasmids to various research institutions, predominantly in the UK. Later, to aid preclinical testing of ChAdOx1 nCoV-19, I developed a standardised ELISA protocol, allowing total anti-spike IgG titres to be assessed in mice [223, 224] and ferrets [225].

Phase I/II clinical trial enrolment then began with a focus on recruiting healthcare workers as they were at greater risk of exposure than the general public. I carried out spike and NP ELISAs on potential volunteers to avoid recruitment of those who had already been exposed to SARS-CoV-2. A large portion of my time was spent as part of the core serology team measuring the humoral immune response after ChAdOx1 nCov-19 vaccination. While this involved some total IgG antibody responses, I was predominantly involved in measuring isotypes and IgG subclasses towards spike. Apart from IgE, IgG2 and IgG4, these were all standardised ELISA assays set-up by Jordan Barret and Sandra Belij-Rammerstorfer, with some minor changes from me. Overall we measured IgG1-4, IgA, IgM and IgE pre-vaccination and at various times post-vaccination. From December 2020 to June 2021 I was involved in QC of all the total IgG ELISA data from the clinical trials.

With few people >65 years old enrolled early on, immunogenicity data showing a similar magnitude of response to younger adults allowed emergency use to be given in all age groups despite lack of proven efficacy in older people. Subsequent efficacy data in clinical trials and real world data confirmed that the vaccine was effective in older adults. Key immunology data published is here [189-191, 226-228].

9

Concluding remarks and future work

Rift Valley fever outbreaks can devastate economies, threaten food security and significantly impact public health. Both animal and human outbreaks have the potential to spread globally. There is an urgent need to counter the threat of RVFV and an effective vaccine that can be used in both livestock and humans would be invaluable. As part of Prof. Warimwe's RVF vaccine programme, I have sought to advance this goal on several fronts. Initially through improving our understanding of RVFV immunology, principally through the characterisation of the naturally acquired and likely protective immune response. I have described for the first time a snapshot of the humoral and cellular immune response in individuals naturally exposed to RVFV. Additionally, I've made use of the invaluable biobank of serum and PBMC samples in KEMRI-Wellcome Trust, Kenya, to screen, identify and characterise for the first time the naturally acquired immune response to RVFV in humans over time.

Humans naturally exposed to RVFV generate long-lived neutralising and binding antibodies targeting Gn and Gc. The half-life of IgG in vivo is roughly three weeks, so to maintain the high titres in the peripheral blood for many years, as seen in chapter 3, requires the presence of long-lived plasma cells, residing in the bone marrow and able to continually secrete large quantities of IgG. Maintaining sterilising immunity to RVFV likely requires these circulating nAbs. However, even if nAb titres wane, protection against RVF may still be present in the form of memory B cells capable of differentiating into plasma cells that again secrete nAbs upon re-exposure. However, considering the incubation period following RVFV infection is around 2-6 days [10], there may not be enough time to allow the memory response to build up sufficient quantities of nAbs to prevent infection or mild illness. Circulating effector memory T cells, detectable in individuals with historical RVFV exposure, that secrete IFNγ upon re-exposure to Gn and Gc peptides may also provide important protection. Future work, where samples are available that link the individual's clinical status post RVFV exposure, will be instrumental in determining minimum thresholds associated with protective immunity.

With improved knowledge of the naturally-acquired immune response to RVFV, I have supported the advancement of ChAdOx1 RVF as a vaccine candidate in livestock and human trials. Initially this involved resynthesizing ChAdOx1 RVF due to earlier genetic instability, resulting in a batch comprised primarily of viral clones with a deletion in the antigenic insert which led to lack of expression. This had been seen previously with adenoviral vectored vaccines containing, for example, Crimean Congo Haemorrhagic fever virus (CCHFV) and HIV inserts, and so required a better understanding of the underlying reasons. In Chapter 4, I resynthesized the vaccine taking two precautions that could plausibly reduce the likelihood of it happening again. Further evaluation then showed one of these, use of T-REx cell line, was likely predominantly responsible for allowing successful manufacture. Although the removal of identical consecutive base runs may provide additional safeguards against the introduction of genetic deletions. This resynthesized vaccine construct was then successfully used in the pregnant livestock efficacy trial showing extremely high protection against disease and foetal loss and is currently being used in ongoing human clinical trials.

The safety and efficacy of vaccines, while critical, are not the only important attributes. In addition to cost, successful rollout of an RVF vaccine requires the ability to manufacture at the required scale to benefit public and animal health. An understanding of the factors associated with manufacture failures is critical to reduce the chances of it happening again. This becomes even more crucial when speed of manufacture is so important, as was the case with the AZ/Oxford COVID-19 vaccine, ChAdOx1 nCoV-19. Some of these lessons learned during early ChAdOx1 RVF manufacture have helped inform subsequent ChAdOx1-vectored vaccine productions.

One silver lining of the devastating COVID-19 pandemic has been the enormous gains in our understanding of immunology and vaccines, in particular, the ChAdOx1 platform due to the

widespread use of ChAdOx1 nCov-19. At the time of writing, more than two billion doses of the AZ/Oxford vaccines have been produced. This has resulted in significant advancement in our understanding and ability to mass produce ChAdOx1-vectored vaccines. The majority of these in LMICs, which at present is where the burden of RVF disease lies. This provides real world proof of the feasibility of rolling out a vaccine like ChAdOx1 RVF to countries and regions that would benefit most.

With ChAdOx1 RVF resynthesized and following successful livestock trials, the vaccine was ready to be trialled for the first time in humans. Chapter 5 describes the characterisation of this immunity. In the absence of a bona fide correlate of protection and the lack of a human challenge model, the assay development and information gleaned from my analysis of the infection-acquired immune response allowed me to compare this to the immunogenicity induced after ChAdOx1 RVF. It is encouraging that the nAb titres induced by volunteers in group 2, given a half dose, overlaps with those elicited after infection. These titres represent the peak post-vaccination response, while the infection-induced immune response is snapshot of their immune response potentially many years post exposure. While these lower doses of vaccine appear to slightly wane from their peak, they remain detectable and significantly above baseline after three months. Half of the group 2 volunteers also had detectable Gn/Gc specific effector memory T cells after 3 months. Additional data looking for the presence of memory B cells and central memory T cells in addition to trials with a longer follow up will shed light on the longer-term immunity induced by ChAdOx1 RVF vaccination.

In both pre-clinical models and humans, reactogenicity of vaccination depends on the number of viral particles given, regardless of infectivity or which antigen is encoded helping to narrow down the range of doses used in future trials of similar vaccines. While ChAdOx1-vectored vaccines encoding antigens from a variety of diseases have previously been trialled in humans, in large part

due to the phase III testing and subsequent rollout of ChAdOx1 nCov-19, this vector has now been given to hundreds of millions of people at a dose of $5x10^{10}$ vp [174-176, 189], providing confidence that future vaccines involving the same dosage of ChAdOx1 are likely to have a similar safety profile. The group 3 dose of $5x10^{10}$ vp is, therefore, likely to elicit improved immunogenicity while maintaining an acceptable safety profile, as has been the case for the limited numbers so far enrolled. Although the safety profile has been favourable overall, in the huge population of AZ/Oxford COVID-19 vaccinees, there have been very rare but serious adverse events involving blood clots with thrombocytopenia, estimated to effect 1 in 100,000 vaccinees, with a fatality rate of <2 per million in Northern Europe [229-231]. However, in Asia and South America, rates were considerably lower and are unlikely to be explained by reporting differences alone [232]. Blood clots with thrombocytopenia was also seen with another COVID-19 vaccine, developed by Johnson and Johnson involving the human Ad26 vector, suggesting that these rare events may be associated with adenoviral vectored vaccines more broadly [233]. Early data points to a role for Platelet Factor 4 and its interaction with adenovirus particles [234-236]. Work is ongoing to further determine the cause of these rare events and how they may be mitigated against for future adenovirus-vectored vaccines.

At present, ChAdOx1 RVF has only been used as a single dose. Given the costs and logistical challenges in rolling out vaccines, and the benefit of quickly inducing protective immunity, particular during outbreaks, a single dose capable of conferring long-lived protection is a major advantage over those requiring multiple boosters. However, it is worth investigating whether a second dose of ChAdOx1 RVF improves immunogenicity in humans. As previously discussed, homologous boosting with the same viral-vectored vaccine has the potential to be hampered by the presence of anti-vector immunity induced after the original dose. We can begin to understand the impact of additional doses of ChAdOx1 RVF by looking at data from previous ChAdOx1-vectored vaccines. The recent ChAdOx1 nCov-19 vaccine trial directly compared a single prime vaccination

with a homologous prime/boost given 28 days apart [237]. Despite the presence of anti-vector nAbs, the second dose was found to significantly boost humoral immunity towards the antigen insert, including neutralisation titres. However, there was a weak, negative correlation between anti-vector neutralising antibodies prior to the second dose and subsequent ELISA response towards the target antigen 28 days later. This contrasts with cellular immunity, where IFNγ response was not boosted following a second dose and there was no correlation between anti-vector nAbs prior to the booster dose and IFNγ ELISpot response to the target antigen 14 days later [237]. A clinical trial of a candidate TB vaccine ChAdOx1 Ag85A also investigated a homologous prime/boost with an interval of 4 weeks and found IFNγ response was also not boosted, however, it did remain above baseline for longer than a single dose alone [176]. Anti-vector immunity following a second ChAdOx1 dose was not boosted, with neutralising antibodies remaining similar in the 4 weeks after peak [189]. Anti-vector IFNγ response did, however, remain above baseline for roughly twice as long following two doses compared to a single dose.

To avoid potential issues of anti-vector immunity, numerous candidate vaccine studies involving adenovirus vectors have been deployed as one part of a heterologous prime/boost regime involving MVA encoding an identical cassette. These studies have significantly increased both the levels of antigen specific T cells and antibodies compared to a single dose [222, 237, 238]. However, the need to test and license a separate vaccine for use as booster would be a significant additional challenge. Increasing the interval between the first and second dose can also result in higher antibody levels post second dose [239]. This may be due to several factors, not least affinity maturation leading to a dwindling pool of higher affinity cells as time passes, boosting these 'better' cells later on is more effective than boosting more numerous cells earlier. A longer interval may also allow the anti-vector response to wane, potentially increasing the immunogenicity of the encoded antigen. A third dose of ChAdOx1 nCov-19, given >70 days after the second dose was still able to significantly boost the humoral response, although not the cellular response [240]. These

data suggest future doses of ChAdOx1 RVF in populations that have largely received two previous ChAdOx1-vectored vaccines are still likely to be immunogenic.

In chapter 6, I have optimised assays allowing the characterisation of the immune response towards RVFV Gn and Gc in livestock. Due to the various efficacy trials undertaken, and subsequent protection from challenge, we know the immune response elicited is a protective one. Broadly, the response is similar to naturally-exposed humans, with nAb titre correlating with binding antibody titres towards Gn and Gc. Livestock Gc responses tended to be higher than Gn, in contrast to livestock vaccinated with Smithburn or naturally exposed humans. Human clinical trial data also appears to elicit higher titres of Gc antibodies, in fact Gn antibodies were not detectable at all. It remains to be seen whether increasing the dose for group 3 will elicit Gn antibody response more in line with those seen in vaccinated livestock or if these are species-specific differences in immune response elicited after administering the same vaccine. The low Gn IgG titres of the first two group 3 samples, 4 weeks post-vaccine, suggest perhaps the latter.

Whether comparable titres in different species results in comparable protection is not yet known. However, the relatively low level of neutralising antibodies required for protection, coupled with a good cellular response, the importance of which is less well understood, is encouraging. The susceptibility of pregnant animals to RVF is well established [6, 34]. While direct evidence of abortions or teratogenic effects in humans following RVF infection is lacking, indirect evidence points to RVF in pregnant humans being particularly dangerous [32, 33, 69]. That ChAdOx1 RVF confers such high protection against foetal loss in sheep and goats bodes well for efficacy in pregnant humans. Because pregnant woman are excluded from early phase ChAdOx1 candidate vaccine trials, there is little data on its use during pregnancy. Although over 100 women became pregnant during participation in the large ChAdOx1 nCov-19 trials and no safety concerns were apparent up to 3 months after birth [241]

There are currently no specific treatments for RVF beyond general care. Effective mAb therapy for a variety of diseases has increased considerably over the past decade with the number of approved mAbs in the US and EU now over 100 [242]. The vast majority of these are widely available only in high income countries [243]. However, the cost of mAb production has dropped significantly over the previous decade increasing the potential for mAb therapies to become more widely available in LMICs [244]. For infectious diseases, identifying the post-exposure window where mAbs are effective is critical to understand. RVF tends to result in febrile illness in the days following infection, severe disease can manifest after initial fever resides and recrudescence occurs [38]. Due to the unspecific nature of febrile illness it is perhaps unlikely that those experiencing it will immediately seek medical attention. When they eventually do seek treatment, the window for effective mAb therapy may already have shut. It is therefore critical to improve our understanding of who is most at risk of severe RVF disease so that, should therapeutics like mAbs become available, it is possible to identify those that are most likely to benefit, facilitating prompt treatment. This is a challenge in itself and requires robust surveillance so RVF outbreaks can be identified early, helping patients to know when to seek treatment should they experience otherwise innocuous symptoms in the early stages post-infection.

Another reason for characterising mAbs and nanobodies, in addition to identifying potential therapeutic candidates, is their ability to identify protective epitopes and elucidate mechanisms of neutralisation. Improving our understanding here can inform future vaccine strategies of critical epitopes to include. Unfortunately, none of the nanobodies identified in chapter 6 from a vaccinated llama, part of the camelid family, showed strong neutralising potential on their own. Linking two of these nanobodies together via a human IgG1 Fc domain may show significantly improved neutralisation activity and, if so, facilitate future analyses into the mechanisms of action.

The complex lifecycle of RVFV in mosquitoes, wildlife, livestock and humans and the myriad ways that control measures targeting certain species can impact on the wider RVFV ecology encourage a holistic, or "One-Health", approach to vaccine development. Additional attributes of RVFV such as encompassing a single serotype and eliciting long-lived immunity post-infection provide optimism that a multi-species vaccine may work. By simultaneously developing the vaccine for livestock and humans we can learn about ChAdOx1 RVF in target species which then also inform human trials. Since we have efficacy data in ChAdOx1 RVF vaccinated target livestock species, future comparison with human trial data can inform us if protective titres in livestock are achieved in humans, then we can attempt to untangle the question of whether the various species have similar protective thresholds.

Taking a wider view of disease control measures and developing vaccines with those in mind is not limited to RVF, indeed it is not limited to a single disease. Numerous diseases impact upon every species and combining control interventions can make economic and scientific sense. By designing a bivalent vaccine in chapter 7, one that targets RVFV and PPRV, another disease of livestock occurring with significant geographic overlap, the impacts can be greater than their individual vaccines. While additional assays are required to confirm expression of the PPRV H antigen, the proof of principal that both antigens can be cloned into ChAdOx1, with no genetic stability issues despite its overall size being at the upper limit of what is possible. RVF vaccination, even in endemic countries such as Kenya, is extremely patchy [139]. This partially reflects the nature of RVF outbreaks, which can have considerable tempo-spatial variability. Convincing someone to vaccinate their livestock if they have never heard of, or experienced any costs associated with, the disease may understandably be difficult. The inclusion of antigens to create bivalent vaccines, potentially providing protection against additional pathogens and therefore increasing the vaccine's utility, is one way that we can overcome this and improve uptake.

A potential limitation of bivalent adenovirus-vectored vaccines are the maximum size of transgene insert that can be successfully cloned. Identifying the antigens or parts of antigens most critical for a protective immune response would allow us to free-up space by removing unnecessary parts. I have provided the first evidence that the neutralising antibody response in humans predominantly targets Gn in comparison to Gc. This ties with more recent evidence from monoclonal antibodies isolated from convalescent human sera which found that Gn antibodies tended to be more potent neutralisers than those targeting Gc [131]. On the other hand, this may not be the case for immunity conferred by ChAdOx1 RVF. Compared to livestock vaccinated with Smithburn, the binding IgG titres targeting Gc were slightly higher while those targeting Gn were slightly lower. The majority of nanobodies isolated from the vaccinated llama tended to show higher affinity in those targeting Gc than Gn, and human clinical trial volunteers too appear to have a more robust humoral response towards Gc. If a similar strategy of creating a bivalent RVF vaccine for humans is pursued, removing Gn or Gc to allow room for an additional antigen from a disease which affect similar demographics, such as CCHF may be necessary. Understanding how the tertiary structure of RVF antigens influences the immune response they elicit may shed light on the differences I have seen between infection-induced and ChAdOx1 RVF-induced immunity.

For understandable reasons, when developing vaccines we tend to desire the most immunogenic response and for numerous diseases that has proved a particularly difficult feature to achieve. However, other attributes such as cost, stability, ease of manufacture and ability to scale-up are also critical when it comes to successful deployment and genuine improvements in public and animal health. Issues with these other attributes, for certain regions, can be similarly as prohibitive as no vaccine at all. Correlates of protection for the vast majority of licenced vaccines are based on the induction of antibodies [245]. A major strength that viral vectors possess over their protein and adjuvant counterparts is their ability to induce strong cytotoxic T cell responses by delivering antigens to intracellular processing pathways, stimulating presentation on MHC class I proteins

[246]. ChAdOx1 vectored candidate vaccines for numerous diseases induce a robust pro-inflammatory cellular response in clinical trials and animal models [197, 237, 238, 247]. Vaccines that elicit robust cytotoxic T cell response, able to destroy infected cells, may offer another strategy towards protection from pathogens that have so far proved very difficult to develop effective vaccines against. For RVF in particular, the importance of cellular immunity is still not very well understood. I have shown that the circulating effector memory response years after RVFV infection in humans is detectable, but perhaps more importantly, so are high titre nAbs. With no correlation between a volunteer's nAb titre and their IFNγ ELISpot response, it is possible that those with no detectable nAb titres may still be afforded some protection against disease through other mechanisms.

For many emerging viral pathogens such as RVFV, that have not yet benefited from decades of vaccine research, eliciting protection may not be the hurdle it is for some other diseases, such as HIV and malaria. Immunogenicity of a single dose vaccine, however, certainly cannot be taken for granted. An inactivated RVF vaccine, TSI-GSD-200, that was previously tested in humans required multiple boosters and still failed to cause reliable seroconversion [123].

The wider attributes of ChAdOx1 as a vaccine platform, and the high-level protection seen in livestock after a single dose, make it an excellent candidate RVF vaccine. However, given the close association between nAbs and protection against RVF and that these responses appear sufficient for protection, then other vaccine technologies may well be effective at eliciting higher titres, such as protein + adjuvant or mRNA. Although it appears that a fairly low threshold of nAb activity is sufficient for protection, so aiming to further increase titres at the expense of stability, cost, scalability or other aspects of immunity may not be a better strategy.

ChAdOx1 RVF as a veterinary vaccine is extremely promising, with proven efficacy in multiple livestock species including pregnant animals [103, 148]. Establishing efficacy for human vaccines, on the other hand, particularly in the absence of a human challenge model or widespread disease in natural settings is a significant challenge faced by all vaccination programmes. A human challenge model for RVF is currently unfeasible due to the lack of therapeutics and the risk debilitating sequelae following infection. Licensure of ChAdOx1 RVF as a human vaccine will ultimately be determined by showing safety and efficacy in human clinical trials. Establishing safety by conducting phase I/II clinical trials involves well-established criteria [248]. For a disease like RVFV, where transmission during intra-epidemic periods (IEP) is poorly understood but likely important, it may be possible to test efficacy in natural settings in the absence of an outbreak. This would involve measuring viremia by PCR as an endpoint and would therefore rely on a vaccine that not only protects against disease but also prevents incidence in order to see efficacy. If transmission is too low during these periods then the number of volunteers required to power the study may prove prohibitive.

Another potential approach to licensure is via the US FDA's 'Animal Rule' whereby safety and immunogenicity in humans is considered alongside efficacy in a relevant animal model [249]. This would require Phase III trials to generate a safety database of several thousand volunteers. Confidence that efficacy in animals will translate to efficacy in humans requires a correlate of protection, and one that can be readily compared between species. Humans experience a wide spectrum of clinical outcomes and different animal models may be relevant depending on which outcome we are evaluating protection against. Animal models such as marmosets and African green monkeys, for example, can replicate similar encephalitis symptoms in humans after aerosol challenge [250]. We could then compare the minimum immune response that protects these NHPs to those induced in humans after vaccination. Although how similar the requirements of protection are between species remains unclear. Setting the human threshold too high can result in protective

vaccines being prematurely dismissed. A threshold that is too low can potentially cause misplaced confidence and continued development of poor vaccines. In chapter 6, I have attempted to bridge nAb data from livestock efficacy trials to dose de-escalation trials, to get a sense of how the reduced immunogenicity seen with lower doses compares to that which is known to be protective. These data suggest we could potentially lower the dose while still conferring protection but it is clearly more informative within the same species. Bridging animal efficacy data to inform estimates of protection in humans will be invaluable.

This thesis has established various assays to measure the immune response towards RVFV in multiple species. Using these assays to characterise the response in vaccinated livestock and infection-exposed humans has allowed me to build a picture of what protective immunity looks like. This provides important context to the clinical trial of ChAdOx1 RVF and the first immunogenicity data in humans. Additionally, I have provided data improving our understanding of ChAdOx1-vectored vaccine construct design, genetic stability and thermostability, which has relevance beyond this RVF construct. The efficacy of ChAdOx1 RVF in livestock, including during pregnancy, and the induction of neutralising antibodies in humans vaccinated with low doses is extremely encouraging. Together with real-world evidence that this type of vaccine can be produced at enormous scale in LMICs, ChAdOx1 RVF has the potential to become an important countermeasure against much larger RVF outbreaks, significantly improving animal and public health.

References

1. Daubney, R., J.R. Hudson, and P.C. Garnham, *Enzootic hepatitis or rift valley fever. An undescribed virus disease of sheep cattle and man from east africa.* The Journal of Pathology and Bacteriology, 1931. **34**(4): p. 545-579.
2. Daubney, R. and J.R. Hudson, *Rift Valley Fever.* East African Medical Journal, 1933. **10**: p. 2-19.
3. Hudso, R.D.a.J.R., *Enzootic hepatitis or Rift Valley fever. An undescribed virus disease of sheep, cattle and man from east africa.* 1931. **576.809.429+616.95+619.31**
4. K. C. Smithburn, A.J.H.a.J.D.G., *Rift valley fever. Isolation of the virus from wild mosquitoes.* Br J Exp Pathol, 1948(29(2): 107–121.).
5. Gear, J., et al., *Rift valley fever in South Africa; a study of the 1953 outbreak in the Orange Free State, with special reference to the vectors and possible reservoir hosts.* S Afr Med J, 1955. **29**(22): p. 514-8.
6. Daubney, R., J.R. Hudson, and P.C. Garnham, *Enzootic hepatitis or Rift Valley fever. An undescribed virus disease of sheep, cattle and man from east africa.* J. Pathol. Bacteriol, 1931. **34**(4): p. 545-79.
7. Easterday, B.C., *Rift valley fever.* Adv Vet Sci, 1965. **10**: p. 65-127.
8. Findlay, G.M., *Rift valley fever or enzootic hepatitis.* Transactions of The Royal Society of Tropical Medicine and Hygiene, 1932. **25**(4): p. 229-262.
9. Dickson, J.L., *Rift Valley fever in the Union.* Journal of the South African Veterinary Medical Association 1951. **22**: p. 110-111.
10. Smithburn, K.C., A.F. Mahaffy, and et al., *Rift Valley fever; accidental infections among laboratory workers.* J Immunol, 1949. **62**(2): p. 213-27.
11. Kitchen, S.F., *Laboratory Infections with the Virus of Rift Valley Fever.* The American Journal of Tropical Medicine and Hygiene, 1934. **s1-14**(6): p. 547-564.
12. Schwentker, F.F. and T.M. Rivers, *RIFT VALLEY FEVER IN MAN : REPORT OF A FATAL LABORATORY INFECTION COMPLICATED BY THROMBOPHLEBITIS.* J Exp Med, 1934. **59**(3): p. 305-13.
13. McMillen, C.M. and A.L. Hartman, *Rift Valley fever in animals and humans: Current perspectives.* Antiviral Res, 2018. **156**: p. 29-37.
14. Linthicum, K.J., et al., *Rift Valley fever virus (family Bunyaviridae, genus Phlebovirus). Isolations from Diptera collected during an inter-epizootic period in Kenya.* J Hyg (Lond), 1985. **95**(1): p. 197-209.
15. Lumley, S., et al., *Rift Valley fever virus: strategies for maintenance, survival and vertical transmission in mosquitoes.* J Gen Virol, 2017. **98**(5): p. 875-887.
16. Evans, A., et al., *Prevalence of antibodies against Rift Valley fever virus in Kenyan wildlife.* Epidemiol Infect, 2008. **136**(9): p. 1261-9.
17. Murithi, R.M., et al., *Rift Valley fever in Kenya: history of epizootics and identification of vulnerable districts.* Epidemiol Infect, 2011. **139**(3): p. 372-80.
18. Rostal, M.K., et al., *Rift Valley Fever: Does Wildlife Play a Role?* Ilar j, 2017. **58**(3): p. 359-370.
19. Wright, D., et al., *Rift Valley fever: biology and epidemiology.* J Gen Virol, 2019. **100**(8): p. 1187-1199.
20. Linthicum, K.J., et al., *Climate and satellite indicators to forecast Rift Valley fever epidemics in Kenya.* Science, 1999. **285**(5426): p. 397-400.

21. Anyamba, A., et al., *Prediction, assessment of the Rift Valley fever activity in East and Southern Africa 2006-2008 and possible vector control strategies.* Am J Trop Med Hyg, 2010. **83**(2 Suppl): p. 43-51.
22. Anyamba, A., et al., *Developing global climate anomalies suggest potential disease risks for 2006-2007.* Int J Health Geogr, 2006. **5**: p. 60.
23. Oyas, H., et al., *Enhanced surveillance for Rift Valley Fever in livestock during El Niño rains and threat of RVF outbreak, Kenya, 2015-2016.* PLoS neglected tropical diseases, 2018. **12**(4): p. e0006353-e0006353.
24. Linthicum, K.J., S.C. Britch, and A. Anyamba, *Rift Valley Fever: An Emerging Mosquito-Borne Disease.* Annu Rev Entomol, 2016. **61**: p. 395-415.
25. Mansfield, K.L., et al., *Rift Valley fever virus: A review of diagnosis and vaccination, and implications for emergence in Europe.* Vaccine, 2015. **33**(42): p. 5520-5531.
26. Pepin, M., et al., *Rift Valley fever virus (Bunyaviridae: Phlebovirus): an update on pathogenesis, molecular epidemiology, vectors, diagnostics and prevention.* Vet Res, 2010. **41**(6): p. 61.
27. Nicholas, D.E., K.H. Jacobsen, and N.M. Waters, *Risk factors associated with human Rift Valley fever infection: systematic review and meta-analysis.* Trop Med Int Health, 2014. **19**(12): p. 1420-9.
28. Meegan, J.M., et al., *Experimental transmission and field isolation studies implicating Culex pipiens as a vector of Rift Valley fever virus in Egypt.* Am J Trop Med Hyg, 1980. **29**(6): p. 1405-10.
29. Liu, J., et al., *The first imported case of Rift Valley fever in China reveals a genetic reassortment of different viral lineages.* Emerg Microbes Infect, 2017. **6**(1): p. e4.
30. Al-Hamdan, N.A., et al., *The Risk of Nosocomial Transmission of Rift Valley Fever.* PLOS Neglected Tropical Diseases, 2015. **9**(12): p. e0004314.
31. Haneche, F., et al., *Rift Valley fever in kidney transplant recipient returning from Mali with viral RNA detected in semen up to four months from symptom onset, France, autumn 2015.* Euro Surveill, 2016. **21**(18).
32. Adam, I. and M.S. Karsany, *Case report: Rift Valley Fever with vertical transmission in a pregnant Sudanese woman.* J Med Virol, 2008. **80**(5): p. 929.
33. Arishi, H.M., A.Y. Aqeel, and M.M. Al Hazmi, *Vertical transmission of fatal Rift Valley fever in a newborn.* Ann Trop Paediatr, 2006. **26**(3): p. 251-3.
34. McMillen, C.M., et al., *Rift Valley fever virus induces fetal demise in Sprague-Dawley rats through direct placental infection.* Science Advances, 2018. **4**(12): p. eaau9812.
35. Wichgers Schreur, P.J., et al., *Co-housing of Rift Valley Fever Virus Infected Lambs with Immunocompetent or Immunosuppressed Lambs Does Not Result in Virus Transmission.* Front Microbiol, 2016. **7**: p. 287.
36. Antonis, A.F., et al., *Vertical transmission of Rift Valley fever virus without detectable maternal viremia.* Vector Borne Zoonotic Dis, 2013. **13**(8): p. 601-6.
37. McIntosh, B.M., et al., *Rift Valley fever in humans in South Africa.* S Afr Med J, 1980. **58**(20): p. 803-6.
38. Laughlin, L.W., et al., *Epidemic Rift Valley fever in Egypt: observations of the spectrum of human illness.* Trans R Soc Trop Med Hyg, 1979. **73**(6): p. 630-3.
39. Digoutte, J.P. and C.J. Peters, *General aspects of the 1987 Rift Valley fever epidemic in Mauritania.* Res Virol, 1989. **140**(1): p. 27-30.
40. Anonymous, *An outbreak of Rift Valley Fever, Eastern Africa, 1997-1998.* EMHJ, 1998. **4**(2): p. 379-381.
41. Madani, T.A., et al., *Rift Valley fever epidemic in Saudi Arabia: epidemiological, clinical, and laboratory characteristics.* Clin Infect Dis, 2003. **37**(8): p. 1084-92.
42. Samy, A.M., A.T. Peterson, and M. Hall, *Phylogeography of Rift Valley Fever Virus in Africa and the Arabian Peninsula.* PLOS Neglected Tropical Diseases, 2017. **11**(1): p. e0005226.

43. Baba, M., et al., *Has Rift Valley fever virus evolved with increasing severity in human populations in East Africa?* Emerging Microbes &Amp; Infections, 2016. **5**: p. e58.
44. FAO. *EMPRES. Transboundary Animal Diseases Bulletin*. 2000; pp. 4–9].
45. Peyre, M., et al., *A Systematic Scoping Study of the Socio-Economic Impact of Rift Valley Fever: Research Gaps and Needs.* Zoonoses Public Health, 2015. **62**(5): p. 309-25.
46. Orinde, A.B., T. Kimani, E. Schelling, J. Omolo, G. M. Kikuvi, and K. M. Njenga, *Estimation of the Rift Valley Fever burden of disease in the 2006/2007 outbreak in Kenya*, in *61st Conference of the American society of Tropical Medicine and Hygiene*. 2012: ILRI, Nairobi.
47. Baba, S., et al., *Effects of livestock importbans imposed by Saudi Arabia on Somaliland for sanitary reasons related to Rift Valley fever.* Outlook on AGRICULTURE, 2006. **35**(No 1): p. 19–24.
48. Orinde, A.B., Kimani, T., Schelling, E., Omolo, J., Kikuvi, G.M. and Njenga, K.M., *Estimation of the Rift Valley Fever Burden of Disease in the 2006/2007 Outbreak in Kenya. Presented at 61st Conference of the American Society of Tropical Medicine and Hygiene, Atlanta, GA, USA, 11 - 15 November 2012. Nairobi: ILRI 2012.*
49. Clark, M.H.A., et al., *Systematic literature review of Rift Valley fever virus seroprevalence in livestock, wildlife and humans in Africa from 1968 to 2016.* PLoS neglected tropical diseases, 2018. **12**(7): p. e0006627-e0006627.
50. LaBeaud, A.D., et al., *Factors associated with severe human Rift Valley fever in Sangailu, Garissa County, Kenya.* PLoS Negl Trop Dis, 2015. **9**(3): p. e0003548.
51. Woods, C.W., et al., *An outbreak of Rift Valley fever in Northeastern Kenya, 1997-98.* Emerg Infect Dis, 2002. **8**(2): p. 138-44.
52. Grossi-Soyster, E.N., et al., *Rift Valley Fever Seroprevalence in Coastal Kenya.* Am J Trop Med Hyg, 2017. **97**(1): p. 115-120.
53. CDC. *Rift Valley Fever (RVF) Centers for Disease Control and Prevention*. 2018 April 3, 2019]; Available from: https://wwwnc.cdc.gov/travel/diseases/rift-river-valley.
54. Mohamed, M., et al., *Epidemiologic and clinical aspects of a Rift Valley fever outbreak in humans in Tanzania, 2007.* Am J Trop Med Hyg, 2010. **83**(2 Suppl): p. 22-7.
55. Dodd, K.A., et al., *Rift Valley fever virus clearance and protection from neurologic disease are dependent on CD4+ T cell and virus-specific antibody responses.* J Virol, 2013. **87**(11): p. 6161-71.
56. McElroy, A.K. and S.T. Nichol, *Rift Valley fever virus inhibits a pro-inflammatory response in experimentally infected human monocyte derived macrophages and a pro-inflammatory cytokine response may be associated with patient survival during natural infection.* Virology, 2012. **422**(1): p. 6-12.
57. Hise, A.G., et al., *Association of symptoms and severity of rift valley fever with genetic polymorphisms in human innate immune pathways.* PLoS Negl Trop Dis, 2015. **9**(3): p. e0003584.
58. Rostal, M.K., et al., *Identification of potential vectors of and detection of antibodies against Rift Valley fever virus in livestock during interepizootic periods.* Am J Vet Res, 2010. **71**(5): p. 522-6.
59. Blomström, A.-L., et al., *Seroprevalence of Rift Valley fever virus in sheep and goats in Zambézia, Mozambique.* Infection Ecology & Epidemiology, 2016. **6**(1): p. 31343.
60. Lichoti, J.K., et al., *Detection of Rift Valley Fever Virus Interepidemic Activity in Some Hotspot Areas of Kenya by Sentinel Animal Surveillance, 2009–2012.* Veterinary Medicine International, 2014. **2014**: p. 9.
61. Lernout, T., et al., *Rift Valley Fever in Humans and Animals in Mayotte, an Endemic Situation?* PLOS ONE, 2013. **8**(9): p. e74192.
62. Smithburn, K.C., et al., *Rift Valley fever; accidental infections among laboratory workers.* J Immunol, 1949. **62**(2): p. 213-27.

63. Ikegami, T. and S. Makino, *The pathogenesis of Rift Valley fever.* Viruses, 2011. **3**(5): p. 493-519.
64. Meegan, J.M., R.H. Watten, and L.W. Laughlin, *Clinical experience with Rift Valley fever in humans during the 1977 Egyptian epizootic.* Contrib Epidemiol Biostat, 1981. **3**: p. 114-123.
65. Arthur, R.R., et al., *Recurrence of Rift Valley fever in Egypt.* Lancet, 1993. **342**(8880): p. 1149-50.
66. Al-Hazmi, A., et al., *Ocular complications of Rift Valley fever outbreak in Saudi Arabia.* Ophthalmology, 2005. **112**(2): p. 313-8.
67. Freed, I., *Rift valley fever in man, complicated by retinal changes and loss of vision.* South African Medical Journal, 1951. **25**(50): p. 930-932.
68. Abdel-Aziz, A.A., J.M. Meegan, and L.W. Laughlin, *Rift Valley fever as a possible cause of human abortions.* Transactions of the Royal Society of Tropical Medicine and Hygiene, 1980. **74**(5): p. 685-686.
69. Baudin, M., et al., *Association of Rift Valley fever virus infection with miscarriage in Sudanese women: a cross-sectional study.* Lancet Glob Health, 2016. **4**(11): p. e864-e871.
70. Swartz T.A., et al., eds. *The symptomatology and pathology of Rift Valley fever in domestic animals*. Contributions to epidemiology and biostatistics: Rift Valley fever. 1981. 77-82.
71. Hartman, A., *Rift Valley Fever.* Clin Lab Med, 2017. **37**(2): p. 285-301.
72. Faburay, B., et al., *Development of a sheep challenge model for Rift Valley fever.* Virology, 2016. **489**: p. 128-40.
73. Wilson, W.C., et al., *Experimental Infection of Calves by Two Genetically-Distinct Strains of Rift Valley Fever Virus.* Viruses, 2016. **8**(5).
74. El Mamy, A.B., et al., *Unexpected Rift Valley fever outbreak, northern Mauritania.* Emerg Infect Dis, 2011. **17**(10): p. 1894-6.
75. Halldorsson, S., et al., *Shielding and activation of a viral membrane fusion protein.* Nat Commun, 2018. **9**(1): p. 349.
76. Freiberg, A.N., et al., *Three-dimensional organization of Rift Valley fever virus revealed by cryoelectron tomography.* J. Virol., 2008. **82**(21): p. 10341-13048.
77. Sherman, M.B., et al., *Single-particle cryo-electron microscopy of Rift Valley fever virus.* Virology, 2009. **387**(1): p. 11-15.
78. Huiskonen, J.T., et al., *Electron cryo-microscopy and single-particle averaging of Rift Valley fever virus: evidence for GN-GC glycoprotein heterodimers.* J. Virol., 2009. **83**(8): p. 3762-3769.
79. Weingartl, H.M., et al., *Rift Valley fever virus incorporates the 78 kDa glycoprotein into virions matured in mosquito C6/36 cells.* PLoS One, 2014. **9**(1): p. e87385.
80. Kreher, F., et al., *The Rift Valley fever accessory proteins NSm and P78/NSm-GN are distinct determinants of virus propagation in vertebrate and invertebrate hosts.* Emerging Microbes & Infections, 2014. **3**(1): p. 1-12.
81. Wright, D., et al., *Naturally Acquired Rift Valley Fever Virus Neutralizing Antibodies Predominantly Target the Gn Glycoprotein.* iScience, 2020. **23**(11).
82. Lozach, P.-Y., et al., *DC-SIGN as a Receptor for Phleboviruses.* Cell Host & Microbe, 2011. **10**(1): p. 75-88.
83. Phoenix, I., et al., *N-Glycans on the Rift Valley Fever Virus Envelope Glycoproteins Gn and Gc Redundantly Support Viral Infection via DC-SIGN.* Viruses, 2016. **8**(5).
84. Leger, P., et al., *Differential Use of the C-Type Lectins L-SIGN and DC-SIGN for Phlebovirus Endocytosis.* Traffic, 2016. **17**(6): p. 639-56.
85. Riblett, A.M., et al., *A Haploid Genetic Screen Identifies Heparan Sulfate Proteoglycans Supporting Rift Valley Fever Virus Infection.* Journal of Virology, 2016. **90**(3): p. 1414-1423.
86. de Boer, S.M., et al., *Heparan sulfate facilitates Rift Valley fever virus entry into the cell.* J Virol, 2012. **86**(24): p. 13767-71.

87. Ganaie, S.S., et al., *Lrp1 is a host entry factor for Rift Valley fever virus.* Cell, 2021. **184**(20): p. 5163-5178.e24.
88. Knipe, D.M., et al., eds. *Fields Virology*. 6 ed. 2013, Lippincot Williams & Wilkins. 1254.
89. Grobbelaar, A.A., et al., *Molecular epidemiology of Rift Valley fever virus.* Emerg Infect Dis, 2011. **17**(12): p. 2270-6.
90. Bird, B.H., et al., *Complete genome analysis of 33 ecologically and biologically diverse Rift Valley fever virus strains reveals widespread virus movement and low genetic diversity due to recent common ancestry.* J Virol, 2007. **81**(6): p. 2805-16.
91. Battles, J.K. and J.M. Dalrymple, *Genetic variation among geographic isolates of Rift Valley fever virus.* Am J Trop Med Hyg, 1988. **39**(6): p. 617-31.
92. Nanyingi, M.O., et al., *A systematic review of Rift Valley Fever epidemiology 1931-2014.* Infect Ecol Epidemiol, 2015. **5**: p. 28024.
93. FAO. *The last hurdles towards Rift Valley Fever control. Report on the Ad hoc workshop on the Current State of Rift Valley Fever Vaccine And Diagnostics Development*. in *FAO Animal Production and Health Report, No. 9.* 2015. Rome, Italy.
94. Allen, E.R., et al., *A Protective Monoclonal Antibody Targets a Site of Vulnerability on the Surface of Rift Valley Fever Virus.* Cell Rep, 2018. **25**(13): p. 3750-3758.e4.
95. *Contributions to epidemiology and biostatistics: Rift Valley fever*. 1981.
96. Peters, C.J., et al., *Experimental Rift Valley fever in rhesus macaques.* Arch Virol, 1988. **99**(1-2): p. 31-44.
97. LaBeaud, D., *Towards a safe, effective vaccine for Rift Valley fever virus.* Future virology, 2010. **5**(6): p. 675-678.
98. Brown, R.D., G.R. Scott, and T. Dalling, *Persistence of antibodies to Rift Valley fever in man.* The Lancet, 1957. **270**(6990): p. 345.
99. Besselaar, T.G. and N.K. Blackburn, *Topological mapping of antigenic sites on the Rift Valley fever virus envelope glycoproteins using monoclonal antibodies.* Arch Virol, 1991. **121**(1-4): p. 111-24.
100. Besselaar-Blackburn, *The synergistic neutralization of Rift Valley fever virus by monoclonal antibodies to the envelope glycoproteins.* 1992.
101. Lagerqvist, N., et al., *Characterisation of immune responses and protective efficacy in mice after immunisation with Rift Valley Fever virus cDNA constructs.* Virol J, 2009. **6**: p. 6.
102. Wallace, D.B., et al., *Protective immune responses induced by different recombinant vaccine regimes to Rift Valley fever.* Vaccine, 2006. **24**(49-50): p. 7181-9.
103. Warimwe, G.M., et al., *Chimpanzee Adenovirus Vaccine Provides Multispecies Protection against Rift Valley Fever.* Sci Rep, 2016. **6**: p. 20617.
104. Lopez-Gil, E., et al., *A single immunization with MVA expressing GnGc glycoproteins promotes epitope-specific CD8+-T cell activation and protects immune-competent mice against a lethal RVFV infection.* PLoS Negl Trop Dis, 2013. **7**(7): p. e2309.
105. McElroy, A.K., C.G. Albarino, and S.T. Nichol, *Development of a RVFV ELISA that can distinguish infected from vaccinated animals.* Virology Journal, 2009. **6**.
106. Fafetine, J.M., et al., *Cloning and expression of Rift Valley fever virus nucleocapsid (N) protein and evaluation of a N-protein based indirect ELISA for the detection of specific IgG and IgM antibodies in domestic ruminants.* Veterinary Microbiology, 2007. **121**(1): p. 29-38.
107. Hamers-Casterman, C., et al., *Naturally occurring antibodies devoid of light chains.* Nature, 1993. **363**(6428): p. 446-8.
108. Wang, F., et al., *Reshaping antibody diversity.* Cell, 2013. **153**(6): p. 1379-93.
109. Oscherwitz, J., *The promise and challenge of epitope-focused vaccines.* Human vaccines & immunotherapeutics, 2016. **12**(8): p. 2113-2116.
110. Terasaki, K. and S. Makino, *Interplay between the Virus and Host in Rift Valley Fever Pathogenesis.* J Innate Immun, 2015. **7**(5): p. 450-8.

111. Lozach, P.Y., et al., *DC-SIGN as a receptor for phleboviruses.* Cell Host Microbe, 2011. **10**(1): p. 75-88.
112. Wonderlich, E.R., et al., *Peripheral Blood Biomarkers of Disease Outcome in a Monkey Model of Rift Valley Fever Encephalitis.* Journal of Virology, 2018. **92**(3): p. e01662-17.
113. Dungu, B., et al., *Evaluation of the efficacy and safety of the Rift Valley Fever Clone 13 vaccine in sheep.* Vaccine, 2010. **28**(29): p. 4581-7.
114. von Teichman, B., et al., *Safety and efficacy of Rift Valley fever Smithburn and Clone 13 vaccines in calves.* Vaccine, 2011. **29**(34): p. 5771-7.
115. Bouloy, M., et al., *Genetic evidence for an interferon-antagonistic function of rift valley fever virus nonstructural protein NSs.* J Virol, 2001. **75**(3): p. 1371-7.
116. Njenga, M.K., et al., *Randomized controlled field trial to assess the immunogenicity and safety of rift valley fever clone 13 vaccine in livestock.* PLoS Negl Trop Dis, 2015. **9**(3): p. e0003550.
117. Ly, H.J. and T. Ikegami, *Rift Valley fever virus NSs protein functions and the similarity to other bunyavirus NSs proteins.* Virology journal, 2016. **13**: p. 118-118.
118. Le May, N., et al., *A SAP30 complex inhibits IFN-beta expression in Rift Valley fever virus infected cells.* PLoS Pathog, 2008. **4**(1): p. e13.
119. Le May, N., et al., *TFIIH transcription factor, a target for the Rift Valley hemorrhagic fever virus.* Cell, 2004. **116**(4): p. 541-50.
120. Swanepoel, R. and N.K. Blackburn, *Demonstration of nuclear immunofluorescence in Rift Valley fever infected cells.* J Gen Virol, 1977. **34**(3): p. 557-61.
121. Ikegami, T., et al., *Rift Valley fever virus NSs protein promotes post-transcriptional downregulation of protein kinase PKR and inhibits eIF2alpha phosphorylation.* PLoS Pathog, 2009. **5**(2): p. e1000287.
122. Ikegami, T., *Rift Valley fever vaccines: an overview of the safety and efficacy of the live-attenuated MP-12 vaccine candidate.* Expert Rev Vaccines, 2017. **16**(6): p. 601-611.
123. Pittman, P.R., et al., *Immunogenicity of an inactivated Rift Valley fever vaccine in humans: a 12-year experience.* Vaccine, 1999. **18**(1): p. 181-189.
124. von Teichman, B., et al., *Safety and efficacy of Rift Valley fever Smithburn and Clone 13 vaccines in calves.* Vaccine, 2011. **29**(34): p. 5771-5777.
125. Wilson, W.C., et al., *Evaluation of lamb and calf responses to Rift Valley fever MP-12 vaccination.* Vet Microbiol, 2014. **172**(1-2): p. 44-50.
126. Mroz, C., et al., *Rift Valley fever virus infections in Egyptian cattle and their prevention.* Transbound Emerg Dis, 2017. **64**(6): p. 2049-2058.
127. Zidan, S., et al., *Some associated risk Factors with Occurrence of Rift Valley Fever in Some Animals and Man in Certain localities of Nile Delta, Egypt*. 2015.
128. Dungu, B., M. Donadeu, and M. Bouloy, *Vaccination for the control of Rift Valley fever in enzootic and epizootic situations.* Dev Biol (Basel), 2013. **135**: p. 61-72.
129. Jansen van Vuren, P., C.T. Tiemessen, and J.T. Paweska, *Anti-nucleocapsid protein immune responses counteract pathogenic effects of Rift Valley fever virus infection in mice.* PLoS One, 2011. **6**(9): p. e25027.
130. Xu, W., et al., *The Nucleocapsid Protein of Rift Valley Fever Virus Is a Potent Human CD8+ T Cell Antigen and Elicits Memory Responses.* PLOS ONE, 2013. **8**(3): p. e59210.
131. Wang, Q., et al., *Neutralization mechanism of human monoclonal antibodies against Rift Valley fever virus.* Nature Microbiology, 2019.
132. Chapman, N.S., et al., *Potent neutralization of Rift Valley fever virus by human monoclonal antibodies through fusion inhibition.* Proceedings of the National Academy of Sciences, 2021. **118**(14): p. e2025642118.
133. Keegan, K. and M.S. Collett, *Use of bacterial expression cloning to define the amino acid sequences of antigenic determinants on the G2 glycoprotein of Rift Valley fever virus.* J Virol, 1986. **58**(2): p. 263-70.

134. Williams, R., et al., *Validation of an IgM antibody capture ELISA based on a recombinant nucleoprotein for identification of domestic ruminants infected with Rift Valley fever virus.* Journal of Virological Methods, 2011. **177**(2): p. 140-146.
135. Pawęska, J.T., et al., *Rift Valley Fever Virus Seroprevalence among Humans, Northern KwaZulu-Natal Province, South Africa, 2018-2019.* Emerging infectious diseases, 2021. **27**(12): p. 3159-3162.
136. Meegan, J.M., *The Rift Valley fever epizootic in Egypt 1977–1978 1. Description of the epizootic and virological studies.* Transactions of The Royal Society of Tropical Medicine and Hygiene, 1979. **73**(6): p. 618-623.
137. Atkins, C. and A.N. Freiberg, *Recent advances in the development of antiviral therapeutics for Rift Valley fever virus infection.* Future Virol, 2017. **12**(11): p. 651-665.
138. Faburay, B., et al., *Current Status of Rift Valley Fever Vaccine Development.* Vaccines (Basel), 2017. **5**(3).
139. Dungu, B., B.A. Lubisi, and T. Ikegami, *Rift Valley fever vaccines: current and future needs.* Curr Opin Virol, 2018. **29**: p. 8-15.
140. Ikegami, T., et al., *Rift Valley Fever Virus MP-12 Vaccine Is Fully Attenuated by a Combination of Partial Attenuations in the S, M, and L Segments.* J Virol, 2015. **89**(14): p. 7262-76.
141. Botros, B., et al., *Adverse response of non-indigenous cattle of European breeds to live attenuated Smithburn Rift Valley fever vaccine.* J Med Virol, 2006. **78**(6): p. 787-91.
142. Ahmed Kamal, S., *Observations on rift valley fever virus and vaccines in Egypt.* Virol J, 2011. **8**: p. 532.
143. Muller, R., et al., *Characterization of clone 13, a naturally attenuated avirulent isolate of Rift Valley fever virus, which is altered in the small segment.* Am J Trop Med Hyg, 1995. **53**(4): p. 405-11.
144. Makoschey, B., et al., *Rift Valley Fever Vaccine Virus Clone 13 Is Able to Cross the Ovine Placental Barrier Associated with Foetal Infections, Malformations, and Stillbirths.* PLOS Neglected Tropical Diseases, 2016. **10**(3): p. e0004550.
145. Faburay, B., et al., *A Recombinant Rift Valley Fever Virus Glycoprotein Subunit Vaccine Confers Full Protection against Rift Valley Fever Challenge in Sheep.* Sci Rep, 2016. **6**: p. 27719.
146. Wichgers Schreur, P.J., et al., *Four-segmented Rift Valley fever virus induces sterile immunity in sheep after a single vaccination.* Vaccine, 2015. **33**(12): p. 1459-64.
147. Wichgers Schreur, P.J., et al., *Four-segmented Rift Valley fever virus-based vaccines can be applied safely in ewes during pregnancy.* Vaccine, 2017. **35**(23): p. 3123-3128.
148. Stedman, A., et al., *Safety and efficacy of ChAdOx1 RVF vaccine against Rift Valley fever in pregnant sheep and goats.* npj Vaccines, 2019. **4**(1): p. 44.
149. Dulal, P., et al., *Potency of a thermostabilised chimpanzee adenovirus Rift Valley Fever vaccine in cattle.* Vaccine, 2016. **34**(20): p. 2296-8.
150. Aricescu, A.R., W. Lu, and E.Y. Jones, *A time- and cost-efficient system for high-level protein production in mammalian cells.* Acta Crystallogr D Biol Crystallogr, 2006. **62**(Pt 10): p. 1243-50.
151. Seiradake, E., et al., *Production of cell surface and secreted glycoproteins in mammalian cells.* Methods Mol Biol, 2015. **1261**: p. 115-27.
152. Biswas, S., et al., *Assessment of humoral immune responses to blood-stage malaria antigens following ChAd63-MVA immunization, controlled human malaria infection and natural exposure.* PLoS One, 2014. **9**(9): p. e107903.
153. Barsosio, H.C., et al., *Congenital microcephaly unrelated to flavivirus exposure in coastal Kenya.* Wellcome Open Res, 2019. **4**(179): p. 179.

154. Bett, B., et al., *Association between Rift Valley fever virus seroprevalences in livestock and humans and their respective intra-cluster correlation coefficients, Tana River County, Kenya.* Epidemiol Infect, 2018: p. 1-9.
155. Paweska, J.T., et al., *An inhibition enzyme-linked immunosorbent assay for the detection of antibody to Rift Valley fever virus in humans, domestic and wild ruminants.* Journal of Virological Methods, 2005. **127**(1): p. 10-18.
156. Illingworth, J., et al., *Chronic exposure to Plasmodium falciparum is associated with phenotypic evidence of B and T cell exhaustion.* Journal of immunology (Baltimore, Md. : 1950), 2013. **190**(3): p. 1038-1047.
157. Kimani, D., et al., *Translating the immunogenicity of prime-boost immunization with ChAd63 and MVA ME-TRAP from malaria naive to malaria-endemic populations.* Mol Ther, 2014. **22**(11): p. 1992-2003.
158. Plotkin, S.A. and P.B. Gilbert, *Nomenclature for immune correlates of protection after vaccination.* Clin Infect Dis, 2012. **54**(11): p. 1615-7.
159. Sabin, A.B. and R.W. Blumberg, *Human infection with Rift Valley fever virus and immunity twelve years after single attack.* Proc Soc Exp Biol Med, 1947. **64**(4): p. 385-9.
160. Scott, J.A.G., et al., *Profile: The Kilifi Health and Demographic Surveillance System (KHDSS).* International Journal of Epidemiology, 2012. **41**(3): p. 650-657.
161. Munyua, P., et al., *Rift Valley Fever Outbreak in Livestock in Kenya, 2006–2007.* The American Journal of Tropical Medicine and Hygiene, 2010. **83**(2_Suppl): p. 58-64.
162. Niklasson, B.S., G.F. Meadors, and C.J. Peters, *Active and passive immunization against Rift Valley fever virus infection in Syrian hamsters.* Acta Pathol Microbiol Immunol Scand C, 1984. **92**(4): p. 197-200.
163. Pittman, P.R., et al., *Rift Valley fever MP-12 vaccine Phase 2 clinical trial: Safety, immunogenicity, and genetic characterization of virus isolates.* Vaccine, 2016. **34**(4): p. 523-530.
164. Ellgaard, L. and A. Helenius, *Quality control in the endoplasmic reticulum.* Nat Rev Mol Cell Biol, 2003. **4**(3): p. 181-91.
165. Halldorsson, S., et al., *Structure of a phleboviral envelope glycoprotein reveals a consolidated model of membrane fusion.* Proc Natl Acad Sci U S A, 2016. **113**(26): p. 7154-9.
166. Li, S., et al., *A Molecular-Level Account of the Antigenic Hantaviral Surface.* Cell reports, 2016. **15**(5): p. 959-967.
167. Rissanen, I., et al., *Structural Transitions of the Conserved and Metastable Hantaviral Glycoprotein Envelope.* J Virol, 2017. **91**(21).
168. Rissanen, I., et al., *Molecular rationale for antibody-mediated targeting of the hantavirus fusion glycoprotein.* eLife, 2020. **9**: p. e58242.
169. Gutjahr, B., et al., *Two monoclonal antibodies against glycoprotein Gn protect mice from Rift Valley Fever challenge by cooperative effects.* PLoS Negl Trop Dis, 2020. **14**(3): p. e0008143.
170. Lopez-Gil, E., et al., *MVA Vectored Vaccines Encoding Rift Valley Fever Virus Glycoproteins Protect Mice against Lethal Challenge in the Absence of Neutralizing Antibody Responses.* Vaccines (Basel), 2020. **8**(1).
171. Vidarsson, G., G. Dekkers, and T. Rispens, *IgG subclasses and allotypes: from structure to effector functions.* Frontiers in immunology, 2014. **5**: p. 520-520.
172. Calarota, S.A. and F. Baldanti, *Enumeration and characterization of human memory T cells by enzyme-linked immunospot assays.* Clinical & developmental immunology, 2013. **2013**: p. 637649-637649.
173. Harmon, J.R., et al., *Rift Valley fever virus vaccination induces long-lived, antigen-specific human T cell responses.* NPJ Vaccines, 2020. **5**: p. 17.

174. Antrobus, R.D., et al., *Clinical assessment of a novel recombinant simian adenovirus ChAdOx1 as a vectored vaccine expressing conserved Influenza A antigens.* Mol Ther, 2014. **22**(3): p. 668-674.
175. Folegatti, P.M., et al., *Safety and immunogenicity of a candidate Middle East respiratory syndrome coronavirus viral-vectored vaccine: a dose-escalation, open-label, non-randomised, uncontrolled, phase 1 trial.* Lancet Infect Dis, 2020.
176. Wilkie, M., et al., *A phase I trial evaluating the safety and immunogenicity of a candidate tuberculosis vaccination regimen, ChAdOx1 85A prime - MVA85A boost in healthy UK adults.* Vaccine, 2020. **38**(4): p. 779-789.
177. Dicks, M.D., et al., *A novel chimpanzee adenovirus vector with low human seroprevalence: improved systems for vector derivation and comparative immunogenicity.* PLoS One, 2012. **7**(7): p. e40385.
178. Gerrard, S.R. and S.T. Nichol, *Synthesis, proteolytic processing and complex formation of N-terminally nested precursor proteins of the Rift Valley fever virus glycoproteins.* Virology, 2007. **357**(2): p. 124-33.
179. Viguera, E., D. Canceill, and S.D. Ehrlich, *Replication slippage involves DNA polymerase pausing and dissociation.* The EMBO journal, 2001. **20**(10): p. 2587-2595.
180. Berg, A., et al., *Stability of Chimpanzee Adenovirus Vectored Vaccines (ChAdOx1 and ChAdOx2) in Liquid and Lyophilised Formulations.* Vaccines, 2021. **9**(11): p. 1249.
181. Kortekaas, J., *One Health approach to Rift Valley fever vaccine development.* Antiviral Research, 2014. **106**: p. 24-32.
182. Bosaeed, M., et al., *Safety and immunogenicity of ChAdOx1 MERS vaccine candidate in healthy Middle Eastern adults (MERS002): an open-label, non-randomised, dose-escalation, phase 1b trial.* The Lancet Microbe.
183. Tatsis, N., et al., *Chimpanzee-origin adenovirus vectors as vaccine carriers.* Gene Ther, 2006. **13**(5): p. 421-9.
184. Quinn, K.M., et al., *Antigen expression determines adenoviral vaccine potency independent of IFN and STING signaling.* J Clin Invest, 2015. **125**(3): p. 1129-46.
185. Ikemura, T., *Codon usage and tRNA content in unicellular and multicellular organisms.* Molecular Biology and Evolution, 1985. **2**(1): p. 13-34.
186. *Health and Social Care and the Medicines & Healthcare products Regulatory Agency. COVID-19 vaccine AstraZeneca UK: Reg 174 information for UK healthcare professionals*, H.a.S.C.a.t.M.H.p.R. Agency, Editor. 2021. p. 10.
187. Chen, Y., et al., *Freeze-Drying Formulations Increased the Adenovirus and Poxvirus Vaccine Storage Times and Antigen Stabilities.* Virologica Sinica, 2020.
188. *WHO Target Product Profiles for Rift Valley Fever Virus Vaccines*. 2019 [cited 2021 11th October]; Available from: https://www.who.int/docs/default-source/blue-print/call-for-comments/tpp-rift-valley-fever-vaccines-draft3-0pc.pdf?sfvrsn=f2f3b314_2.
189. Ramasamy, M.N., et al., *Safety and immunogenicity of ChAdOx1 nCoV-19 vaccine administered in a prime-boost regimen in young and old adults (COV002): a single-blind, randomised, controlled, phase 2/3 trial.* Lancet, 2021. **396**(10267): p. 1979-1993.
190. Folegatti, P.M., et al., *Safety and immunogenicity of the ChAdOx1 nCoV-19 vaccine against SARS-CoV-2: a preliminary report of a phase 1/2, single-blind, randomised controlled trial.* The Lancet, 2020.
191. Barrett, J.R., et al., *Phase 1/2 trial of SARS-CoV-2 vaccine ChAdOx1 nCoV-19 with a booster dose induces multifunctional antibody responses.* Nature Medicine, 2020.
192. Pepin, M., et al., *Rift Valley fever virus(Bunyaviridae: Phlebovirus): an update on pathogenesis, molecular epidemiology, vectors, diagnostics and prevention.* Vet Res, 2010. **41**(6): p. 61.
193. Ewer, K.J., et al., *Viral vectors as vaccine platforms: from immunogenicity to impact.* Curr Opin Immunol, 2016. **41**: p. 47-54.

194. Memish, Z.A., et al., *Middle East respiratory syndrome.* The Lancet, 2020. **395**(10229): p. 1063-1077.
195. Alharbi, N.K., et al., *Humoral Immunogenicity and Efficacy of a Single Dose of ChAdOx1 MERS Vaccine Candidate in Dromedary Camels.* Sci Rep, 2019. **9**(1): p. 16292.
196. R., D.R.a.H.J., *Enzootic hepatitis or Rift Valley fever. An undescribed virus disease of sheep, cattle and man from east africa.* 1931. **576.809.429+616.95+619.31**.
197. Warimwe, G.M., et al., *Immunogenicity and efficacy of a chimpanzee adenovirus-vectored Rift Valley fever vaccine in mice.* Virol J, 2013. **10**: p. 349.
198. Wichgers Schreur, P.J., et al., *Multimeric single-domain antibody complexes protect against bunyavirus infections.* eLife, 2020. **9**: p. e52716.
199. Wichgers Schreur, P.J., et al., *A novel highly sensitive, rapid and safe Rift Valley fever virus neutralization test.* J Virol Methods, 2017. **248**: p. 26-30.
200. Arbabi-Ghahroudi, M., *Camelid Single-Domain Antibodies: Historical Perspective and Future Outlook.* Frontiers in immunology, 2017. **8**: p. 1589-1589.
201. Harmsen, M.M. and H.J. De Haard, *Properties, production, and applications of camelid single-domain antibody fragments.* Appl Microbiol Biotechnol, 2007. **77**(1): p. 13-22.
202. Pardon, E., et al., *A general protocol for the generation of Nanobodies for structural biology.* Nature Protocols, 2014. **9**(3): p. 674-693.
203. Watanabe, Y., et al., *Native-like SARS-CoV-2 Spike Glycoprotein Expressed by ChAdOx1 nCoV-19/AZD1222 Vaccine.* ACS Central Science, 2021. **7**(4): p. 594-602.
204. Elisia, I., et al., *DMSO Represses Inflammatory Cytokine Production from Human Blood Cells and Reduces Autoimmune Arthritis.* PloS one, 2016. **11**(3): p. e0152538-e0152538.
205. *Food and Agriculture Organization of the United Nations World Organisation for Animal Health. Global Strategy for the Control and Eradication of PPR. (2015)*. [cited 2021 10th September]; Available from: http://www.oie.int/eng/PPR2015/doc/PPR-Global-Strategy-avecAnnexes_2015-03-28.pdf.
206. Taylor, W.P., *The distribution and epidemiology of peste des petits ruminants.* Preventive Veterinary Medicine, 1984. **2**(1): p. 157-166.
207. Sen, A., et al., *Detection of subclinical peste des petits ruminants virus infection in experimental cattle.* Virusdisease, 2014. **25**(3): p. 408-11.
208. Abubakar, M., et al., *Serological Detection of Antibodies to Peste des Petits Ruminants Virus in Large Ruminants.* Transboundary and Emerging Diseases, 2017. **64**(2): p. 513-519.
209. Woma, T.Y., et al., *Serological evidence of camel exposure to peste des petits ruminants virus (PPRV) in Nigeria.* Tropical Animal Health and Production, 2015. **47**(3): p. 603-606.
210. Horzinek, M.C., *Rinderpest: The second viral disease eradicated.* Veterinary Microbiology, 2011. **149**(3-4): p. 295-297.
211. Roeder, P., J. Mariner, and R. Kock, *Rinderpest: the veterinary perspective on eradication.* Philosophical Transactions of the Royal Society B: Biological Sciences, 2013. **368**(1623): p. 20120139.
212. Jia, X.-X., et al., *Development of vaccines for prevention of peste-des-petits-ruminants virus infection.* Microbial Pathogenesis, 2020. **142**: p. 104045.
213. Diallo, A., *Morbillivirus group: genome organisation and proteins.* Veterinary Microbiology, 1990. **23**(1): p. 155-163.
214. Sinnathamby, G., et al., *Immune responses in goats to recombinant hemagglutinin-neuraminidase glycoprotein of Peste des petits ruminants virus: Identification of a T cell determinant.* Vaccine, 2001. **19**: p. 4816-23.
215. Sinnathamby, G., et al., *Immune responses in goats to recombinant hemagglutinin-neuraminidase glycoprotein of Peste des petits ruminants virus: identification of a T cell determinant.* Vaccine, 2001. **19**(32): p. 4816-23.

216. Wang, Y., et al., *Recombinant adenovirus expressing F and H fusion proteins of peste des petits ruminants virus induces both humoral and cell-mediated immune responses in goats.* Vet Immunol Immunopathol, 2013. **154**(1-2): p. 1-7.
217. Herbert, R., et al., *Recombinant adenovirus expressing the haemagglutinin of peste des petits ruminants virus (PPRV) protects goats against challenge with pathogenic virus; A DIVA vaccine for PPR.* Veterinary Research, 2014. **45**(1).
218. Rojas, J.M., et al., *Vaccination with recombinant adenovirus expressing peste des petits ruminants virus-F or -H proteins elicits T cell responses to epitopes that arises during PPRV infection.* Veterinary Research, 2017. **48**(1): p. 79.
219. Holzer, B., et al., *Determination of the minimum fully protective dose of adenovirus-based DIVA vaccine against peste des petits ruminants virus challenge in East African goats.* Veterinary Research, 2016. **47**(1): p. 20.
220. Bett, B. *Introducing English and Swahili Instructional Videos on the Patterns, Signs, Symptoms and Control of Rift Valley Fever*. 2018 [cited 2021 21st September 2021]; Available from: https://ilvac.net/2018/06/22/introducing-english-and-swahili-instructional-videos-on-the-patterns-signs-symptoms-and-control-of-rift-valley-fever/.
221. Wilson, W.C., et al., *Preliminary Evaluation of a Recombinant Rift Valley Fever Virus Glycoprotein Subunit Vaccine Providing Full Protection against Heterologous Virulent Challenge in Cattle.* Vaccines, 2021. **9**(7): p. 748.
222. McMahon, M., et al., *Vaccination With Viral Vectors Expressing Chimeric Hemagglutinin, NP and M1 Antigens Protects Ferrets Against Influenza Virus Challenge.* Front Immunol, 2019. **10**: p. 2005.
223. Graham, S.P., et al., *Evaluation of the immunogenicity of prime-boost vaccination with the replication-deficient viral vectored COVID-19 vaccine candidate ChAdOx1 nCoV-19.* npj Vaccines, 2020. **5**(1): p. 69.
224. van Doremalen, N., et al., *ChAdOx1 nCoV-19 vaccine prevents SARS-CoV-2 pneumonia in rhesus macaques.* Nature, 2020.
225. Lambe, T., et al., *ChAdOx1 nCoV-19 protection against SARS-CoV-2 in rhesus macaque and ferret challenge models.* Communications biology, 2021. **4**(1): p. 915-915.
226. Voysey, M., et al., *Safety and efficacy of the ChAdOx1 nCoV-19 vaccine (AZD1222) against SARS-CoV-2: an interim analysis of four randomised controlled trials in Brazil, South Africa, and the UK.* Lancet, 2020.
227. Silva-Cayetano, A., et al., *A booster dose enhances immunogenicity of the COVID-19 vaccine candidate ChAdOx1 nCoV-19 in aged mice.* Med, 2020.
228. Ewer, K.J., et al., *T cell and antibody responses induced by a single dose of ChAdOx1 nCoV-19 (AZD1222) vaccine in a phase 1/2 clinical trial.* Nature Medicine, 2020.
229. Simpson, C.R., et al., *First-dose ChAdOx1 and BNT162b2 COVID-19 vaccines and thrombocytopenic, thromboembolic and hemorrhagic events in Scotland.* Nature Medicine, 2021. **27**(7): p. 1290-1297.
230. Greinacher, A., et al., *Thrombotic Thrombocytopenia after ChAdOx1 nCov-19 Vaccination.* New England Journal of Medicine, 2021. **384**(22): p. 2092-2101.
231. Schultz, N.H., et al., *Thrombosis and Thrombocytopenia after ChAdOx1 nCoV-19 Vaccination.* New England Journal of Medicine, 2021. **384**(22): p. 2124-2130.
232. Soboleva, K., et al., *Geographical distribution of TTS cases following AZD1222 (ChAdOx1 nCoV-19) vaccination.* The Lancet Global Health, 2022. **10**(1): p. e33-e34.
233. Sadoff, J., K. Davis, and M. Douoguih, *Thrombotic Thrombocytopenia after Ad26.COV2.S Vaccination — Response from the Manufacturer.* New England Journal of Medicine, 2021. **384**(20): p. 1965-1966.
234. Baker, A.T., et al., *ChAdOx1 interacts with CAR and PF4 with implications for thrombosis with thrombocytopenia syndrome.* Science Advances, 2021. **7**(49): p. eabl8213.

235. Greinacher, A., et al., *Insights in ChAdOx1 nCoV-19 vaccine-induced immune thrombotic thrombocytopenia.* Blood, 2021. **138**(22): p. 2256-2268.
236. Othman, M., et al., *To clot or not to clot? Ad is the question-Insights on mechanisms related to vaccine-induced thrombotic thrombocytopenia.* J Thromb Haemost, 2021. **19**(11): p. 2845-2856.
237. Stylianou, E., et al., *Improvement of BCG protective efficacy with a novel chimpanzee adenovirus and a modified vaccinia Ankara virus both expressing Ag85A.* Vaccine, 2015. **33**(48): p. 6800-8.
238. Lopez-Camacho, C., et al., *Assessment of Immunogenicity and Neutralisation Efficacy of Viral-Vectored Vaccines Against Chikungunya Virus.* Viruses, 2019. **11**(4).
239. Flaxman, A., et al., *Reactogenicity and immunogenicity after a late second dose or a third dose of ChAdOx1 nCoV-19 in the UK: a substudy of two randomised controlled trials (COV001 and COV002).* The Lancet, 2021. **398**(10304): p. 981-990.
240. Munro, A.P.S., et al., *Safety and immunogenicity of seven COVID-19 vaccines as a third dose (booster) following two doses of ChAdOx1 nCov-19 or BNT162b2 in the UK (COV-BOOST): a blinded, multicentre, randomised, controlled, phase 2 trial.* The Lancet.
241. Hillson, K., et al., *Fertility rates and birth outcomes after ChAdOx1 nCoV-19 (AZD1222) vaccination.* The Lancet, 2021. **398**(10312): p. 1683-1684.
242. *The Antibody Society. Therapeutic monoclonal antibodies approved or in review in the EU or US.* [cited 2021 7th Dec]; Available from: www.antibodysociety.org.
243. *IAVI/Wellcome., Expanding access to monoclonal antibody-based products: A global call to action*. 2020.
244. Hooft van Huijsduijnen, R., et al., *Reassessing therapeutic antibodies for neglected and tropical diseases.* PLOS Neglected Tropical Diseases, 2020. **14**(1): p. e0007860.
245. Plotkin, S.A., *Correlates of protection induced by vaccination.* Clinical and vaccine immunology : CVI, 2010. **17**(7): p. 1055-1065.
246. Liu, M.A., *Immunologic Basis of Vaccine Vectors.* Immunity, 2010. **33**(4): p. 504-515.
247. Alharbi, N.K., et al., *ChAdOx1 and MVA based vaccine candidates against MERS-CoV elicit neutralising antibodies and cellular immune responses in mice.* Vaccine, 2017. **35**(30): p. 3780-3788.
248. WHO. *Guidelines on clinical evaluation of vaccines: regulatory expectations*. 2016 2016; Available from: https://www.who.int/biologicals/BS2287_Clinical_guidelines_final_LINE_NOs_20_July_2016.pdf.
249. Beasley, D.W.C., T.L. Brasel, and J.E. Comer, *First vaccine approval under the FDA Animal Rule.* npj Vaccines, 2016. **1**(1): p. 16013.
250. Hartman, A.L., et al., *Aerosolized rift valley fever virus causes fatal encephalitis in african green monkeys and common marmosets.* J Virol, 2014. **88**(4): p. 2235-45.

Appendix

Nanobody sequences:

Nanobody ID	Amino acid sequence
>Nb3	QVQLVESGGGLVQAGGSLTLACAASGHSLTSYVTGWFRQAPGKEREILATMSWIGDSGYY ADSVKGRFTMSRGSADNMVSLQMGSLEPEDTAVYYCAAGRRSTGRNYLSASAYDYWGQGT QVTVSSHHHHHHHEPEA
>Nb5	QVQLVESGGGLVQAGGSLSLSCAASGGSFSPYVVGWFRQAPGKEREFVSVINWGGDSTSY GDSVKGRFTLSRDNAKRTVTLQMNSLKPEDTAVYFCAASRIYIADATFYDYWGQGTQVTV SSHHHHHHEPEA
>Nb8	QVQLVESGGGLVQPGGSLRLSCTASGLFSGDMITTMHWNRQAPGLQRELVALVMREGSTK YVDSVKGRFTISMDKTKNTVYLQMNSLRPDDTAVYNCNAQVVRSGTTYHYWGQGTQVTVS SHHHHHHEPEA
>Nb14	QVQLVESGGGSVQAGGSLRLSCTASGLISGDMVMTMHWNRQAPGKQRELVALVSRDGSTK YEDSVKGRFTISMDNAKNTVYLQMNSLKPDDTAVYNCNAQVVRSGTTYYYWGQGTQVTVS SHHHHHHEPEA
>Nb15	QVQLVESGGGLVQPGGSLRLTCAASGNIVNLIDMAWYRQVPGKEREQVASLTSYGAADYA DFVKGRFTISKDNAKNTVYLQMNNLRPEDTAVYVCNVFAHTRESGTTASSLAHYWGQGTQ VTVSSHHHHHHEPEA
>Nb17	QVQLVESGGGLEQPGGSLRLSCAASGFIFKNYPMSWVRQAPGKGPEWVSTIYAHDNTTHY ADSVKGRFTISRDNAKNMLYLQMNSLKPEDTAVYYCARGGYVSNPRQRANDWGPGTQVTV SSHHHHHHEPEA
>Nb23	QVQLVESGGGLVQPGGSLRLSCAASGFSFSTTAMSWVRQAPGKGPEWVSSIYNSADNTRY ADSVKGRFTISRDNAKNTLYLQMNTLEPEDTAMYYCTRGAYSSNPRQRTPDWGPGTQVTV SSHHHHHHEPEA
> Nb27	QVQLVESGGGLEQSGGSLRLSCLASGFTFRDYPMSWVRQAPGKGPEWVSTIYKDGTTDYP NSMKGRFTISRDNAKNTVFLQMNNLKPDDTAVYSCARGGYRSDPRLRANDWGPGTQVTVS SHHHHHHEPEA
> Nb28	QVQLVESGGGLVQPGGSLRLSCAASGMIFSDNAMAWYRQAPGKQRELLAVITSGGVANYL DSVKGRFAISRDNAKNTLYLQMNSLKPEDTAVYYCHAGSFPNVLHGTARYWGQGTQVTVS SHHHHHHEPEA
> Nb29	QVQLVESGGGLVQPGGSLRLSCQASGSIYNNHMGWYRQAPGKQREFVAVVTSGDTTSYAD SAKGRFTISRDNEKNTVYLQMNSLKPEDTAAYYCNTWPANWYWGQGTQVTVSSHHHHHHE PEA

> Nb30 QVQLVESGGGLVQPGESLRLSCAVSGRISRIEAMGWYRQAPGKQRDFVALLTAGGSTTYA
DSVKGRFTISKDNAKSYLYLQMNSLKPEDTAVYYCYGNLTIYRGAYYTDNYWGQGTQVTV
SSHHHHHHEPEA

> Nb31 QVQLVESGGGLVQAGGSLRLACAASGGGFSIDGMGWYRQAPGKQRELVAFMDQNLNTNYT
DSVKGRFTISRSEAGDTLYLQMNALKTEDTAVYYCSAAVRLTRYASPTIYWGQGTQVTVS
SHHHHHHEPEA